Modelling effects of ionising radiation

Fuaada Mohd Siam

Department of Mathematics and Statistics

University of Strathclyde

Glasgow, UK

February 2014

This thesis is submitted to the University of Strathclyde for the degree of Doctor of Philosophy in the Faculty of Science.

This thesis is the result of the author's original research. It has been composed by the author and has not been previously submitted for examination which has led to the award of a degree.

Signed: Date:

Acknowledgements

I must express my gratitude to the Ministry of Higher Education (MOHE), Malaysia and Universiti Teknologi Malaysia (UTM) for the funding which allowed me to undertake this research.

I would like to express my deep and sincere gratitude to my supervisor, Dr Michael Grinfeld, for his patience, encouragement and personal guidance throughout my PhD. I would have been lost without his support. I am also grateful to Dr David Pritchard for his constructive comments and support throughout this work.

I would also like to thank my examiners, Dr Eliezer Shochat and Dr Steven Webb, who provided encouraging and constructive feedback. It is no easy task, reviewing a thesis, and I am grateful for their thoughtful and detailed comments. My appreciation is also expressed to Dr Gabriel Barrenechea, as a viva convenor, for his support and guidance. One person who always been ready to help me was our postgraduate secretary Irene Spencer. She took care of all non-scientific works including official procedure of PhD promotie. Thank you Irene for all your support!

I warmly thank Professor Alastair Munro, a radiotherapist from Ninewells Hospital and Medical School, Dundee, for his valuable advice and guidance in radiotherapy studies. I also thank Dr Kirk D Dolan from Michigan State University for providing me with several useful matlab codes especially for bootstrapping.

This thesis is dedicated to my beloved husband Nor Saidi Mohamed Nasir and my children Danish, Atirah, Ahmad, and Akram for their endless support, love and understanding during the preparation of this thesis. I owe my utmost thanks to my family, in particular, my parents Hj Mohd Siam and Hjh Siti Eshah and my parent-in-law Hj Mohamed Nasir and Hjh Hapsah for their unfailing love and constant prayers over my years of study. Lastly, and most importantly, I wish to thank to all my friends; Farhana, Yaza, Meetu, Wafa, Chanpen, Martin and everyone in the department for helping me get through the difficult times. In particular, I warmly thank Maymona Al-Husari and Norhaiza Ahmad for not hesitating to proofread my thesis and provide me with useful comments.

Abstract

In this thesis, we are concerned with the molecular biology processes of ionising radiation (IR) damage and its repair. In particular, we develop a mechanistic model of high dose irradiation damage to DNA in mammalian cells by considering a population of cells structured by the number of double strand breaks and mis-repairs. This framework allows us to construct a mechanistic explanation for the Linear-Quadratic (LQ) formalism. Other contributions of this thesis are a model of ataxia telangiectasia mutated (ATM) dynamics in DNA damage repair, and a discussion of bistability, an important ingredient in the construction of a general theory of non-targeted radiation effects.

Contents

List of Figures

Chapter 1

Introduction

It is important to be able to account for the effects of radiation on living tissues. In radiation oncology, ionising radiation (IR) is used as a therapeutic weapon against cancer. During the treatment, one needs simultaneously to maximise damage to the tumour by directly killing tumour cells, and to minimise the damage and the exposure of normal tissue to radiation. Radiation not only can be directly dangerous to sensitive tissue such as the spinal cord, but its non-targeted effects can lead to secondary cancers.

In radiation treatment, one of the tools that are routinely used in prescribing the radiation dose is the linear-quadratic (LQ) relation, which relates irradiated cell survival rates to the radiation dose. However, the LQ formula raises three questions:

1. Is the LQ formula true? It is not a priori clear how and why the LQ formula arises.

2. What is the mechanistic basis for the LQ relation?

3. What biological parameters account for the LQ parameters? For example, how do radiation sensitivity and radiation damage repair efficiency of a cell enter these parameters?

To find the answers of all those questions we will develop a mechanistic model of high dose irradiation damage. We will see the analysis and the results in chapter 4. While the LQ formalism correctly describes cell survival of high radiation doses, at low radiation doses do other effects [57, p. 17], such as the bystander effects, come into play, and a different theory is needed.

It is known that DNA damage formation induces the damage repair pathways and signal transduction pathways that can lead to cell cycle arrest and to apoptosis (see chapter 2 for further details). One of the important kinases which are involved in the DNA damage bystander response pathways as well as in the targeted radiation effects is ATM (ataxia telangiectasia mutated), a DNA damage sensor. Thus, our goal in chapter 5 is to create a biologically realistic model of the role of ATM species in the response to the DNA damage following IR.

An important aspect of bystander response is bistable behaviour (see section 2.7), a very important property in biology which has been implicated in pathology [165]. Therefore, there is a need to develop an understanding of bistable systems. There are several models of bistable systems that have neglected the importance of protein turnover such as [4, 98]. However, [59] discovered that the bistable system of [98] is sensitive to protein turnover. There is a region where bistability in an autophosphorylating kinase system can disappear for very small values of protein turnover. The question is, can the structural instability phenomenon be found in other bistable systems if protein turnover is taken into account in the system? To answer this question, we will analyse the structural stability of the bistable system of [4] in chapter 6.

The outline of the thesis is as follows. In chapter 2, we discuss processes involved in the molecular biology of IR damage. We also introduce the LQ formalism used to analyse direct large dose radiation effects and also the non-targeted radiation effects mechanisms. The goal is to define the terms that we are going to use in the subsequent chapters. We will also propose a framework for bystander response based on our own understanding. We suggest a bistability mechanism for the concentration of active ATM concentration as a function of the strength of feedback loops between double strand breaks (DSBs) and ATM. The disbalance between the positive and negative feedback loops will switch the bistable system from a state of healthy low activated ATM concentration into a state of chronically high activated ATM concentration. In chapter 3, we will discuss some of the methodologies used to model and analyse the effect of IR in cell populations.

The original contribution in the thesis is contained in chapters 4 to 6. In chapter 4, we will develop a mechanistic model of high dose irradiation damage to DNA in mammalian cells. We will consider a population of cells structured by the number of DNA DSBs (double strand breaks) and the misrepairs (see chapter 4) due to IR. We will separate the work into three parts. Firstly, we will focus on the effect of a single dose of radiation, while in the second part, we will work on the model parameter estimation using Nelder-Mead simplex and simulated annealing algorithms which allow us to relate the clinically useful parameters of the LQ relation to aspects of cellular activity that can be manipulated experimentally. In the third part, we will deal with cell killing effects of fractionated doses of radiation.

In chapter 5, we will construct a mathematical framework to model the dynamics of ATM upon the DNA damage induction. Initially, our intention was to develop a mechanistic model of radiation-induced bystander response, but due to the complexity of the processes involved in the bystander response system, here we limit ourselves by assuming that ATM can be activated only by the DNA damage (see chapter 5 for further details). We will model the full bystander response system in future.

Finally, to explore whether the structural instability phenomena in bistable system can occur in a cell cycle model proposed by [4], we will extend that work by incorporating the protein turnover. This will be done in chapter 6.

Chapter 2

Ionising radiation effects

2.1 Introduction

In this chapter, we describe the molecular biology of ionising radiation damage. We start with a brief explanation of the important components in a cell in section 2.2. In sections 2.3 to 2.5, we survey the main factors concerning radiation induced DNA (deoxyribonucleic acid) lesions, their repair, and the consequence of their misrepair. Next, in sections 2.6 to 2.8 we describe approaches to modelling direct and indirect radiation effects, and in particular, the LQ formalism used to analyse direct large dose radiation effects. Note that in section 2.7 we survey the radiation induced bystander effect mechanism and propose a new framework for its operation.

2.2 Biological facts

In this section, we start with a description of several important components of the mammalian cell.

2.2.1 Cells

All living things are made up of tiny cells: a small compartment and the basic unit of life. There are roughly a hundred million cells of 200 different types in our body [107]. Cells form tissues that make up organs such as the heart, liver, and bladder. Eukaryotic cells such as mammalian cells are composed of three main regions: cell membrane, nucleus, and cytoplasm [49].

The **cell membrane** is a thin envelope that surrounds the cell contents and its job is to control the passage of dissolved substances into and out of the cell. The **cytoplasm** is the contents of the cells (except for the nucleus). It is a jelly-like material which consists of about 80% water and is usually clear in color and contains macromolecules such as carbohydrates, lipids, proteins, and nucleic acids. The **nucleus** is the control centre of the cell. It contains the genetic material DNA.

The **mitochondria** , another organelle found in eukaryotic cells which have a role in generating ATP (adenosine triphosphate), which carries high energy to power most cellular processes [26].

Cells can communicate with their adjacent cells through intercellular channels called gap junctions: the process is called gap junctions intercellular communication (GJIC) . Gap junctions facilitate the transfer of small molecules (up to 1 kDa [122]) between the cytoplasm of adjacent cells.

2.2.2 Proteins

Proteins are very important molecules in human cells. A protein consists of a sequence of amino acids that make up a chain [26]. There are many different proteins with different functions, such as **enzymes** , also called catalysts, which can speed up biochemical reactions. Enzyme-catalysed reactions can be described by the Michaelis-Menten equation (section 2.2.3) [93]. Protein **kinases** are enzymes that modify other proteins by chemically adding phosphate groups to them (phosphorylation). Protein phosphorylation is reversed by protein **phosphatase** , an enzyme that removes phosphate groups from phosphorylated amino acid residues (dephosphorylation). **Receptors** are protein molecules embedded in either the plasma membrane or cytoplasm of a cell to which a signal molecule may attach [26].

There is a number of proteins which have an important role in mediating non-targeted ionising radiation effects; this is explained in more detail in subsection 2.7. Mitogen-activated protein kinases (**MAPKs**) are kinases that phosphorylate the transcription factors and regulate different cellular activities such as mitosis, apoptosis, etc. in response to extracellular stimuli (environmental stresses such as oxidant stress and ionising radiation) [36]. Cyclooxygenase-2 (**COX-2**) is an enzyme involved in cytoplasmic radiation-induced mutagenesis. Its role is to synthesise prostaglandin in response to the extracellular stimuli [73]. Superoxide dismutase (**SOD**) is an important enzyme which acts as an antioxidant. It is involved in cellular defence against reactive oxygen or nitrogen species (ROS/RNS) which can lead to DNA damage in the cells [65, 69]. Inducible nitric oxide synthase (**iNOS**) , is an important enzyme in generating nitric oxide (NO), an RNS (which is a highly reactive free radical) from amino acids. iNOS can produce large amounts of NO in tumour cells [97].

Protein molecules are known to be continuously synthesised and degraded in all living organisms (the process called **turnover**) . Proteins are constantly degraded into their amino acid constituents, a process termed **proteolysis** . For protein mass to remain constant, new proteins must be synthesised to replace the degraded proteins [154]. The turnover of proteins plays an important role in cell cycle and in signal transduction [108, 160] and can also destroy unnecessary proteins.

2.2.3 The Hill equation

This equation was introduced by the biochemist Archibald Hill in 1910. He used it to study the properties of hemoglobin [106]. The Hill equation is commonly used to describe the binding of a substrate (a molecule upon which an enzyme acts) to an enzyme to produce a functional effect. In enzyme-substrate interaction, the Hill equation is generally given by,

$$V = \frac{V_{max} S^n}{(K_M)^n + S^n}, \tag{2.1}$$

where V is the reaction velocity, V_{max} is the maximum reaction velocity, and S is the substrate concentration. The constant K_M is the Michaelis-Menten constant (the substrate concentration at half-maximal velocity) and n is the Hill coefficient. The Hill coefficient n describes the degree of cooperativity which can measure how steeply sigmoidal the response is. By cooperative binding we mean that when an enzyme has several sites to which a substrate can bind, the binding at one substrate can change the binding affinities of other substrates [80, 103].

According to [103], if $n = 1$, then (2.1) is a hyperbolic curve response (no cooperativity), and this is called the **Michaelis-Menten** equation. If $n > 1$, then (2.1) is a sigmoid curve response (also called ultrasensitive response) and describes positive cooperativity: when one molecule of substrate binds to an enzyme, the binding affinities of other substrate molecules increase. In contrast, if $n < 1$, the substrate's binding affinity for the enzyme will decrease (negative cooperativity).

2.2.4 Genes

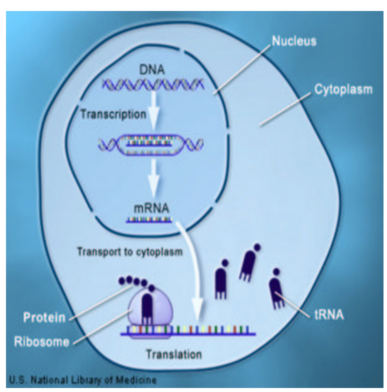

Figure 2.1: The central dogma of molecular biology. Source: `http://ghr.nlm.nih.gov/handbook/howgeneswork/makingprotein`.

"Gene" is very hard to define. Roughly, a gene is a sequence of bases in DNA that codes for the synthesis of a specific protein. This protein then will play a functional role in the body. Since DNA is located in the nucleus of eukaryotic cells (see figure 2.1) while protein synthesis is carried out in the cytoplasm, RNA (ribonucleic acid) is required to convey genetic information from DNA to a **ribosome** (the site of protein synthesis). **RNA** is a single-stranded chain rather than double-stranded which makes it different from DNA. According to the **central dogma of molecular biology**, RNA molecules are synthesised from DNA templates (a process called **transcription**) and proteins are synthesised from RNA templates (a process called **translation**) [58, 125].

The gene expression process starts when the information in the DNA is transcribed into **hnRNA** (heterogeneous nuclear RNA), also called pre-MRNA (pre messenger RNA), by a process of transcription which takes place in the nucleus. Here hnRNA is considered as the intermediate product of transcription which then is transformed into mRNAs in the transcription process. **mRNAs** are RNA molecules that act as templates for protein synthesis and are created in the nucleus. The mRNA then is moved to the cytoplasm and attached to ribosomes. Note that the transcription and RNA processing are followed by translation (which is carried out on ribosomes) of mRNA to **tRNAs** (transfer RNAs), which serve as adaptors between the mRNA template and amino acids that are incorporated into protein. For further details, see [23, 26, 92].

2.2.5 DNA

Every cell in the human body (except for mature red blood cells, which have no nucleus) has the same DNA, most of which is found in the nucleus, but some in mitochondria. A DNA molecule is made up of nucleotides and its structure is a **double helix**: that is, two long, thin strands twisted around each other like a spiral staircase (figure 2.2). The sides of DNA are sugar and phosphate molecules while the rungs are pairs of chemicals called "nitrogenous bases", or "bases" for

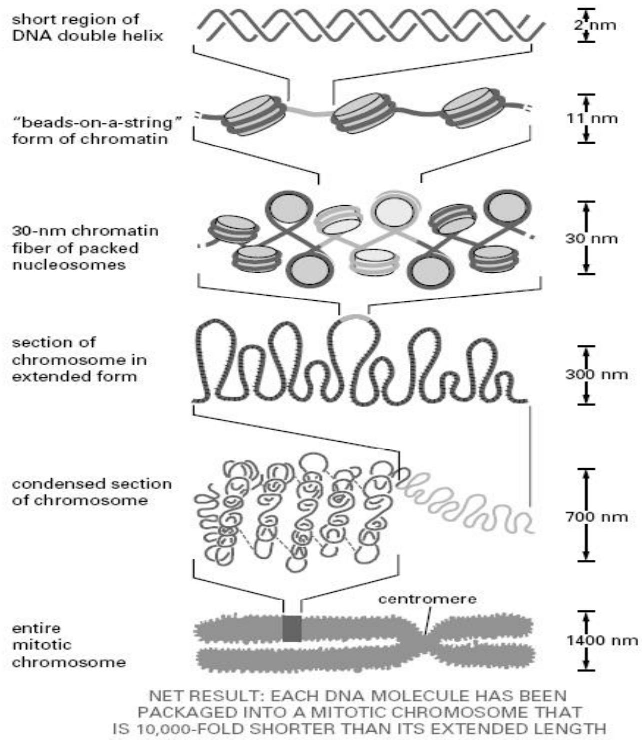

Figure 2.2: Organisation of DNA structure in a cell nucleus. Source: `http://www.accessexcellence.org/RC/VL/GG/structure.php`.

short. **Nucleotides** contain three different components: a deoxyribose sugar, a phosphate, and a base. There are four nucleic acid **bases** in DNA; adenine(**A**), guanine(**G**), cytosine(**C**), and thymine(**T**). **A** forms a base pair with **T** while **G** forms a base pair with **C** by hydrogen bonds that hold the two strands together. The four bases can be categorised in two groups: purine and pyrimidine bases. A and G are purine bases, which are larger than pyrimidine bases (C and T) [26, 64, 95].

2.2.6 Chromosomes

A **chromosome** is an organised structure of DNA that contains many genes. Human cells have 46 chromosomes in their nucleus, 23 that come from the person's mother, and 23 from their father. In a cell nucleus, DNA is packed into a chromosome to allow the very long DNA molecules to fit into the cell nucleus (figure 2.3). **Histone** proteins are essential for the packaging of DNA as the proteins are to be wrapped around by the DNA to form "beads" in a nucleosome (a subunit of chromatin consisting of 147 bp of DNA and histone proteins [26, p.168]). **H2A** is a type of histone that is involved in nucleosome formation. **Chromatin** is the combination of histone, DNA and other proteins that condensed to make up chromosomes. A chromosome has a centromere. The **centromere** is a small region which plays an important role in ensuring that chromosomes are correctly distributed between daughter cells during cell division. It also serves as the site where the two identical chromatids (also called sister chromatids) are connected and it is typically located in the centre of the chromosome. **Sister chromatids** are formed by a replication of one chromosome during interphase of the cell cycle while a **chromatid** is one of the two identical sister chromatids that are joined by a centromere (figure 2.3). A chromosome also has **telomeres** , the important structures at each end of a chromosome which protects the ends from being damaged. If cells divided without telomeres, they would lose the end of their chromosome [13].

2.2.7 Cell cycle

The main process of cellular proliferation is the cell division cycle or simply the **cell cycle**, which is a sequence of events that a cell goes through to produce progeny. During the cell cycle, the cell grows, replicates the DNA and then divides to produce two daughter cells. The cell cycle can be divided in two brief periods. The first phase is termed the **interphase**; in this phase the cell grows in size and synthesises a new copy of DNA including preparation for cell division [26, 111]. There are three stages of interphase:

1. The $\boldsymbol{G1}$ (Gap 1) phase represents the time between the end of mitosis and the beginning of the S phase.
2. The Synthesis ($\boldsymbol{S}$) phase is the time during which the cell duplicates its

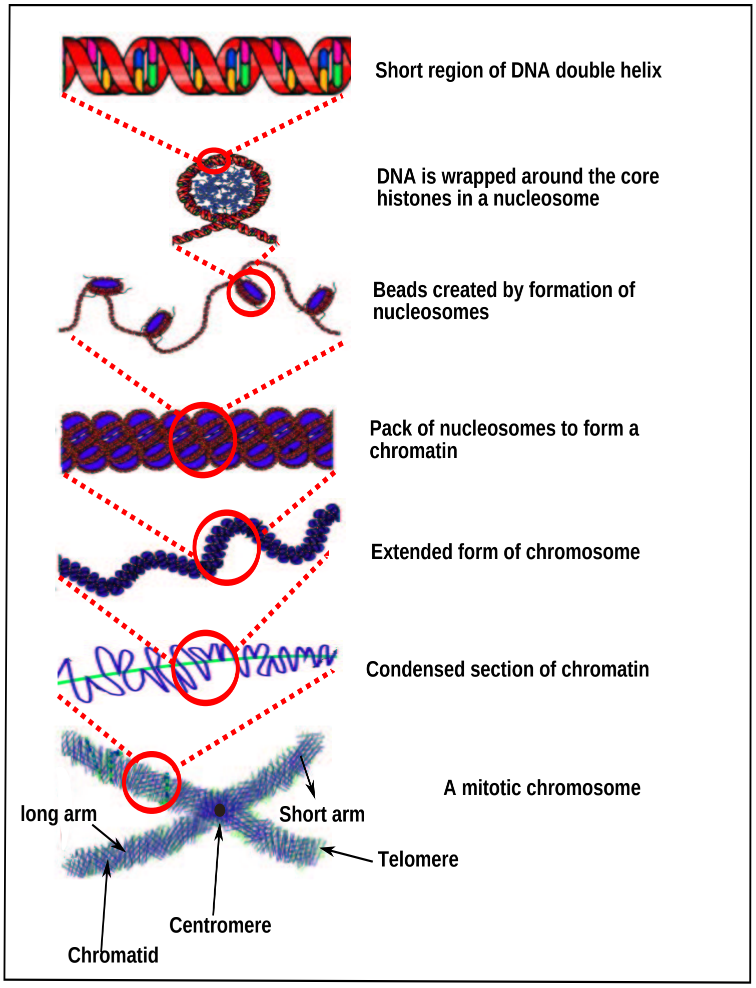

Figure 2.3: Hierarchical folding of chromatin makes up the chromosome. Source: `http://themedicalbiochemistrypage.org/dna.html`.

DNA. The cells in the S phase have a content of DNA intermediate between those of cells in $G1$ and $G2$.

3. The ***G2*** (Gap 2) phase represents the time between the end of the S phase and the next mitosis during which the cell resumes its growth in preparation for mitosis. The DNA content is double that of cells in $G1$ [26, p.656].

The second phase in the cell cycle is the **M-phase**. When $G2$ is completed the cell enters a relatively brief period of nuclear and cytoplasmic division, mitosis and cytokinesis, respectively. After the successful completion of mitosis and cytokinesis both resulting daughter cells re-enter $G1$ of interphase. There is a **restriction point** (a point at which the cell determines whether it has sufficient nutrients to support progression for rest of the cell cycle), in late $G1$. If appropriate growth factors are not available in $G1$, the cell cycle stops at the restriction point. These arrested cells then enter **G0** phase (a phase where the cell is neither dividing nor preparing to divide): cells in this phase are said to be quiescent and can remain non-proliferating for long periods of time [26, 111]. Cells such as skin fibroblasts are arrested in $G0$. They remain in this phase until they are stimulated to divide in order to repair skin damage resulting from a wound [26, 41, 111]. A diagram of the cell cycle is shown in figure 2.4.

The duration of a cell cycle depends on cell types. For example, early frog embryo cells can divide every 30 minutes whereas human liver cells take 1 year to divide [11].

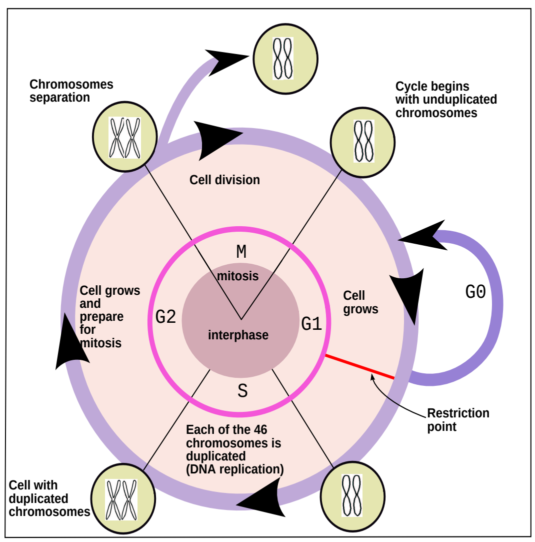

Figure 2.4: Illustration of the cell cycle for a cell with chromosomes in the nucleus. (After `http://drhdmcdowell.com/mitosis_and_cell_cycle.html`).

2.2.8 Cell cycle control

Cell cycle is regulated by the **cell cycle control system**: a corrected process activity of regulatory proteins to ensure the correct progression through the cell cycle. For example, the system ensures that the cell division does not start before DNA replication is complete.

The main components in the cell cycle control system are cyclin-dependent protein kinases (Cdks) and their regulatory subunits (cyclins). **Cyclin-CDK** complexes control the transition from one cell cycle phase to next [53, 111]. In eukaryotes, different types of cyclins and Cdks are activated and required at different cell cycle phases. Therefore cyclin-Cdk complexes can be categorised into three classes that initiate different cell cycle events:

1. $G1$ cyclin-Cdk complexes : important for progression through $G1$ phase and transition to S phase.

2. S cyclin-Cdk complexes : responsible for initiating and completing DNA replication.

3. M cyclin-Cdk complexes : trigger the cell into mitosis.

(For further details, see [111, 117]).

The cell cycle control system consists of a set of cell cycle checkpoints [41, 53, 64, 111]. **Growth arrest** is a process in the cell cycle control which occurs when a cell does not proceed through the cell cycle. If cell DNA is damaged, the cycle of the cell is arrested at one of the **checkpoints** in the cell cycle: 1) $G1/S$ checkpoint, 2) S phase checkpoint, and 3) $G2/M$ checkpoint.

The **G1/S checkpoint** prevents the cell from entering S phase if there is damage to the DNA by inhibiting the initiation of replication. The phosphorylation of cell cycle checkpoint kinase 2 (Chk2) or cell cycle checkpoint kinase 1 (Chk1) by ATM initiates the G_1/S arrest through p53 (see section 2.5.2 for details). Phosphorylated Chk2 in turn is inactivated by phosphorylation cell division cycle 25A phosphatase (Cdc25A).

The **S phase checkpoint** monitors cell cycle progression and reduces the rate of DNA synthesis following DNA damage. A cell which re-entered the cell cycle from $G1/S$ checkpoint may also arrest later at the S phase checkpoint due to incomplete DNA replication or DNA damage.

The **G2/M checkpoint** prevents the cell for entering mitosis (M phase) if DNA is damaged. The $G2$ to M-phase transition in eukaryotes is regulated by mitosis-promoting factor (**MPF**), a complex of **Cdc2** (cell division control protein 2 homolog) also known as Cdk1 (cell division kinase 1) and Cyclin B. Figure 2.5 shows the schematic diagram of Cdc2 and **Wee1** (a kinase that inhibits the transition from $G2$ to mitosis by phosphorylating Cdc2 and thus inactivating it) in eukaryotes. In general, during the mitotic entry process (or the $G2$ to M phase transition), the activity of Wee1 is decreased while Cdc2 activity is increased and it is activated by Cdc25 through dephosphorylation. Cdc2 and Cyclin B combine to produce a complex, the MPF (mitosis-promoting factor) which triggers the initiation of mitosis. In contrast, the inhibition process of Cdc2-cyclinB is triggered by the phosphorylation of Cdc2 by Wee1. This means that Wee1 phosphorylates Cdc2, which keeps the kinase activity of Cdc2 low and prevents entry into mitosis. This results in a mitotic delay. It is important to note that the relationship between Wee1 and Cdc2 described in this subsection will particularly be employed in chapter 6.

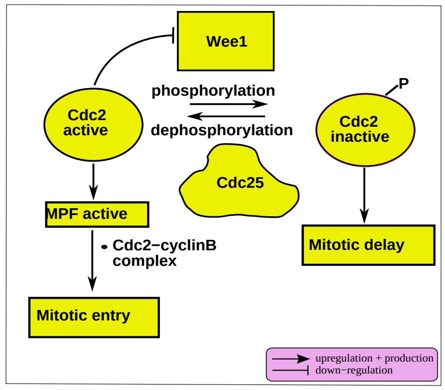

Figure 2.5: Regulation of Wee1 and Cdc2. Source: `http://www.thefullwiki.org/Wee1`.

2.3 Ionising radiation

We are always surrounded by radiation. In general, radiation is a process in which energetic particles or waves travel through a medium or space. There are two types of radiation: non-ionising radiation and ionising radiation.

Ionising radiation (IR) is the process in which an individual particle such as a photon or electron has sufficient energy to **ionise** an atom or molecule, ie. to eject one or more electrons from an atom or molecule along its path (track) of ionising particles. The most commonly known types of ionising radiation are alpha-particle radiation, beta-particle radiation, neutrons, gamma-rays and x-rays [64].

In contrast, **non-ionising radiation** does not contain high-energy particles, thus there is no ionisation process involved. Microwaves, visible light, radio waves, TV waves and ultraviolet (UV) light are classed as non-ionising radiation. These non-ionising forms of radiation are much less harmful to humans or other living things than ionising radiation [64]. This kind of radiation can damage tissue if we are exposed to too much. For example, overexposure to the sun's UV rays can cause skin cancer. A laser, a device that can emit UV rays, is useful in medicine: for example it is used for cataract treatment [76, p.367].

The intensity of IR is measured by the amount of energy deposited per unit mass [101]. The standard unit of absorbed dose is the Gray (Gy): 1 Gy = 1 $\frac{J}{kg}$ (joule per kilogram). The measurement of the energy transferred to the material as an ionising particle travels through it is called **linear energy transfer** (LET). Formally, it is defined as the amount of energy transferred per unit length of the radiation track and is expressed in units of $\frac{keV}{\mu m}$ (kiloelectron volt per micrometer). Gamma-rays, x-rays and electrons are considered as low-LET radiation, while neutrons, alpha particles and protons are high-LET radiation. High-LET radiation has higher biological effects than low-LET radiation [64, p.34].

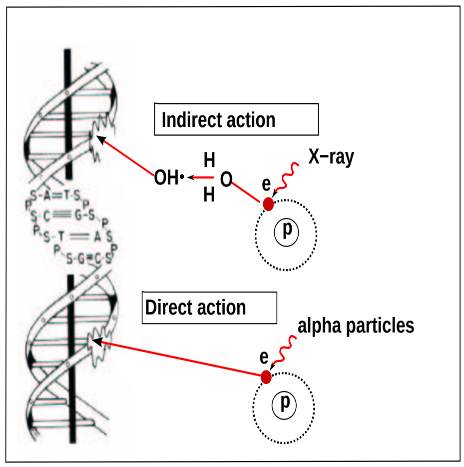

Figure 2.6: Illustrating the direct and indirect actions of radiation. The letters S, P, A, T, G and C represent sugar, phosphate, adenine, thymidine, guanine and cytosine, respectively. The backbone of DNA molecules are made of the alternating units of sugar and phosphate. Direct action: an electron produced by alpha particles interacts directly with the DNA to produce damage in DNA. Indirect action: an electron produced by x-ray or gamma-ray interacts with another molecule such as water molecule (H_2O) to generate radicals such as hydroxyl radical (OH·) [64].

Direct and indirect action of radiation

In general, IR consists of **charged particles**, particles with an electric charge (protons and electrons), or **uncharged particles**, particles with zero net electric charge (atoms and neutrons). All charged-particles radiation such as alpha-particles and beta-particles have sufficient energy to disrupt directly the atomic structure and produce chemical and biological charges. This is also called the **direct action** of radiation (see Figure 2.6). It is the dominant effect of radiation with high-LET (also referred to as densely ionising radiation).

Alternatively, electromagnetic (uncharged particle) radiation or low-LET (also referred to as sparsely ionising) radiation has an indirect ionising effect as the particles do not produce chemical and biological damage themselves. Uncharged particle radiation will first generate charged particles which then produce the ionising effect [64]. The **indirect action** of radiation occurs through the formation of **free radicals** (an atom or molecule with an unpaired number of electrons) which are highly reactive. As we know, 80% of human cells is composed of water. After radiation interacts with a water molecule, the water may be ionised due to the result of the ejection of an electron from the water molecule (H_2O). If the ionised water molecule interacts with another water molecule, it reacts to produce the highly reactive hydroxyl radical, one of the **ROS**. ROS are strong oxidants that can damage cells' metabolism. Examples include hydrogen peroxide (H_2O_2), superoxide (O_2^-), and hydroxyl radical ($OH\cdot$). The interaction of DNA and ROS creates oxidative damage in DNA which causes structural alterations in DNA such as base pair mutations, rearrangements, and deletions [64]. There is considerable evidence suggesting that DNA is the primary target for cell damage from IR.

2.4 Targeted radiation damage

Radiation damage can be classified into two groups; targeted and non-targeted radiation damage. Radiation damage can occur in the cell IR is directed against.

This is what we call targeted radiation damage. Non-targeted radiation damage occur in cells which are not exposed to IR.

2.4.1 Types of DNA damage/lesions

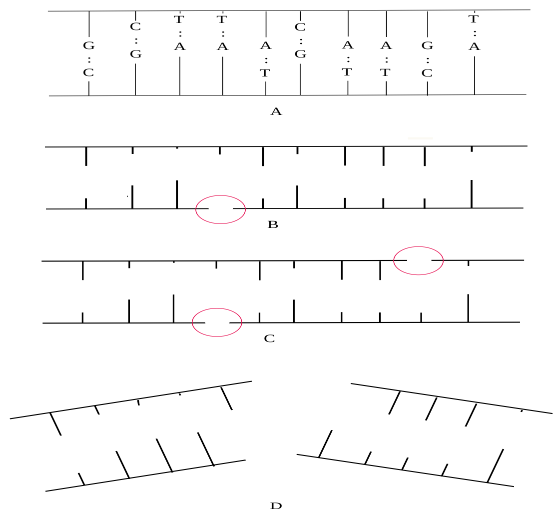

Figure 2.7: Illustrations of DNA SSB and DNA DSB following irradiation. Breaks can be seen in the red circles. **A**: Normal DNA double helix in two-dimensional representation, **B**: DNA SSB (a break in one strand), **C**: DNA SSBs (breaks on each strand, but not opposite one another), **D**: DNA DSB (breaks in both strands; breaks are opposite one another) [64].

Hall [64] reported that there are various types of damage produced in DNA following IR. Typically, the major problem caused by IR in the DNA double helix is DNA breaks: single strand breaks (SSBs) and double strand breaks (DSBs). These consequently will lead to chromosome damage which then can cause cell death.

A **SSB** will be created if the cell is exposed to a moderate dose of radiation. This means that only one of the two strands of a double helix has a defect (figure 2.7B). These SSBs are not really harmful to the cells as they are repaired using the opposite strand. A SSB is not involved in cell killing [64], but it can cause a mutation (a misrepaired SSB).

A **DSB** on the other hand, will be produced if the breaks in the two strands are opposite one another (figure 2.7D). DSBs are considered the most biologically damaging lesions produced by IR [81, p.47]. [64, p.21] reported that the interaction of two DSBs can result in cell death, chromosome aberrations, carcinogenesis, and mutation.

2.4.2 Chromosome effects

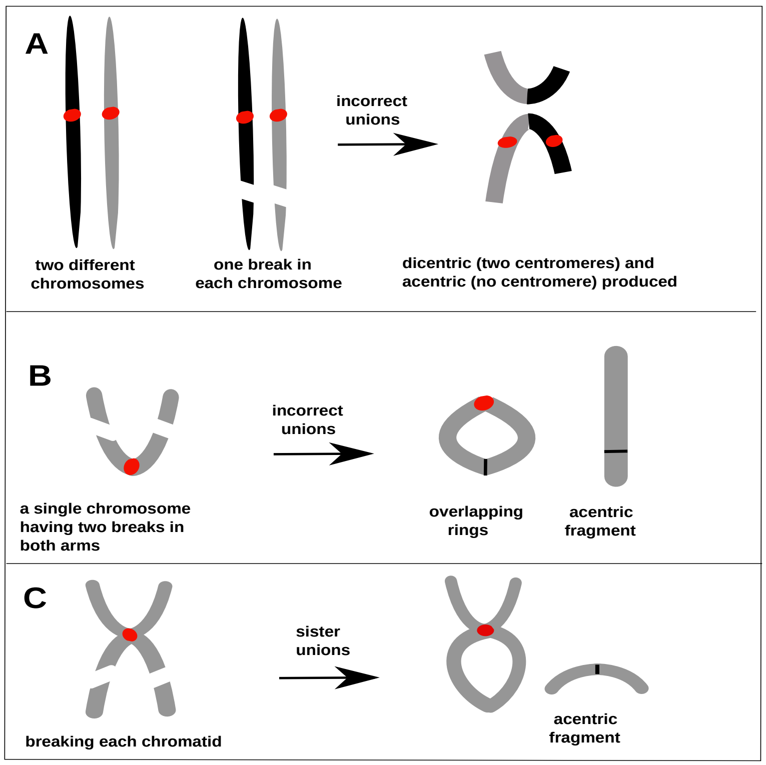

Figure 2.8: The formation of lethal chromosome aberrations: (*A*) dicentric, (*B*) ring, and (*C*) anaphase bridge. [64, p.23]

IR exposure can usually create DSBs in the arms of chromosomes. If several breaks are produced, incorrect rejoining of the ends can take place leading to a **chromosome aberration**. In general, chromosome aberrations can be categorised as lethal or non lethal.

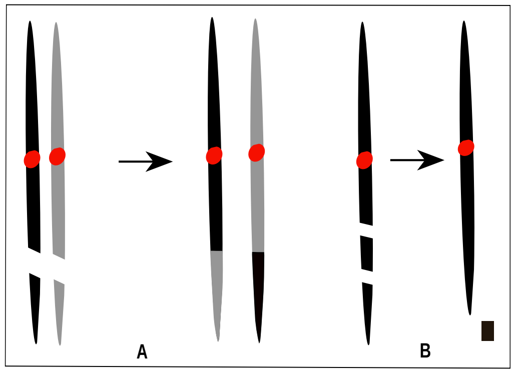

Figure 2.9: The formation of nonlethal chromosome aberrations: (A) symmetric translocation and (B) small deletion. [64, p.27]

There are three types of chromosome aberrations which are lethal to the cell. These aberrations include the dicentric and the ring chromosome which are produced by irradiation early in the cell cycle and before the chromosomes have replicated. The other lethal aberration is the anaphase bridge which is formed in the $G2$ phase (after chromosomes are duplicated).

Dicentric aberration results from an exchange of material between two separate damaged chromosomes. The formation of a dicentric chromosome is depicted in diagrammatic form in figure 2.8. The **ring** is produced by DSBs due to radiation in each arm of the same chromosome. An **anaphase bridge** results from breaks that occur in each chromatid of the same chromosome. This consequently leads to the sticky ends rejoining inappropriately.

There are also types of chromosome aberrations which are non-lethal. These include symmetric translocations and small deletions. As shown in figure 2.9(A), **symmetric translocation** is produced by two damaged chromosomes with the broken end being exchanged between the two chromosomes, while **small deletion** in figure 2.9(B) describes the loss of a small piece of a chromosome that contains genetic information [64, p.27].

2.4.3 Reason for cell lethality following large doses of radiation

Cell death can be measured in various ways. One measure of cell death is called **non-clonogenic** cell (or **reproductive cell death**); the loss of the ability to divide and make colonies [64]. This definition is particularly relevant in the context of radiobiology and cancer therapy since any tumour cell which has an ability to produce progeny results in the failure of tumour control.

In the recent literature, the major mechanisms of mammalian cell death are thought to be apoptosis and necrosis [75]. There is evidence that senescence of cells also can be observed after antitumour therapy [128].

Apoptosis (also known as **programmed cell death**) represents death by suicide. It is an important process to remove unwanted or damaged cells in order to maintain a tissue homeostasis. Alteration in the apoptosis control is responsible for many human diseases, including cancer. Since apoptosis does not require cell division, it is sometimes called an **interphase death** by the process of apoptosis [64]. There are two known apoptotic pathways: intrinsic and extrinsic. The **extrinsic pathway** is triggered from outside the cell, whereas the **intrinsic pathway**, which is relevant for radiation, is triggered from inside the cell. (The reader is referred to [52] for further details). Apoptosis is cell-type dependent. E.g. apoptosis is observed rapidly in tumour cells of lymphoid descent before cell division takes place, while in contrast, tumour cells of epithelial origin show delayed apoptosis during or after mitosis [42]. This delayed apoptosis which occurs after mitosis can be regarded as mitotic death , which will be discussed briefly in the following paragraphs. During apoptosis, cells shrink and the mitochondria and nucleus contents are destroyed. The cell then disintegrates into small membrane-bound particles [64].

The other mammalian cell death mechanism is necrosis. **Necrosis** is unprogrammed cell death due to unexpected cell damage. In contrast to apoptosis, necrosis represents death by injury. During necrosis, the cell swells and disruption of plasma membrane will cause a tissue injury. (The interested reader is referred to [75] for further details).

Senescence is a natural process of aging by which normal and tumour cells loss the ability to divide after irradiation exposure. When cells undergo senescence, the telomeres shorten with every cell division because DNA in those cells cannot be replicated. As a result, the cell division is blocked. (See [128] for further details).

There is evidence that **mitotic cell death** can also be induced by ionising radiation [72, 128]. Mitotic death (also termed **mitotic catastrophe**) is death occurring during or after mitosis due to the failure of cells to divide because of damaged chromosomes [64]. If the IR damage repair is incomplete or imperfect, this repair process leads to lethal chromosome aberration and a cell is allowed to proceed with the cell cycle and go through mitosis. Improper cell division will lead to nonviable cell formation with multiple micronuclei [128]. Some cells that pass through mitosis with large chromosome aberration may then die by apoptosis, necrosis or senescence [128]. Hence the boundary between mitotic catastrophe and other forms of cell death is not well defined.

2.5 Molecular biology of DNA damage repair

DSB formation induces two separate but interrelated responses; the DSB repair processes pathway and signal transduction processes that can lead to cell cycle arrest and to apoptosis.

2.5.1 Damage sensing

There is a group of proteins that recognise radiation-induced DNA DSBs. There is evidence that γ-H2AX foci which can be visualised by using fluorescence microscopy technique, is a biomarker for DNA DSBs [132]. γ-H2AX is a phosphorylated form of histone H2AX which belongs to the H2A histone family (see

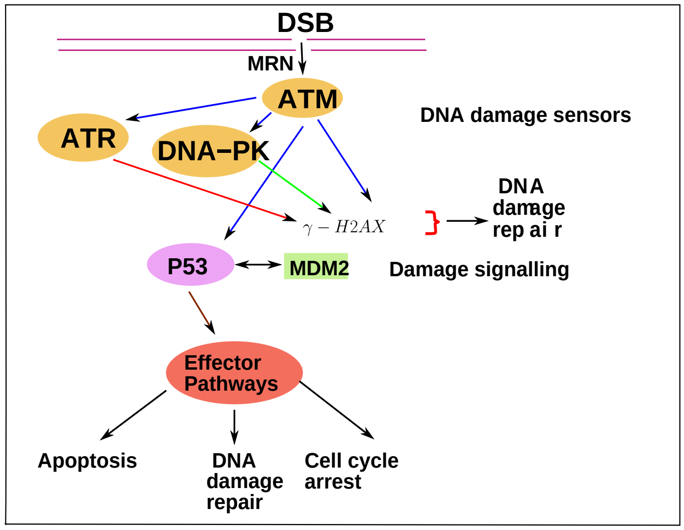

Figure 2.10: The DNA damage response pathways can be divided into three main components: damage sensors, signal transducer, and effectors (see text).

section 2.2.6). After DSBs formation, histone H2AX is phosphorylated by **PIKK** (phosphoinositide-3-kinase-related protein kinase) family proteins which include **ATM** (ataxia telangiectasia mutated), **ATR** (ataxia telangiectasia and Rad3-related protein) and **DNA-PK** (DNA-dependent protein kinase) at the sites of DSBs [50], which are important in cellular response to DNA damage. There is evidence that ATM plays a role as a key regulator of the checkpoint pathways in the DNA damage response (DDR) [35]: which mutation in the ATM gene results in ataxia-telangiectasia and increased risk of cancers such as breast cancer. For the sake of simplicity, in this present thesis, we only deal with the DNA damage signal transducer ATM.

ATM involvement in the DDR can be described as follows: When there is no DNA damage, ATM is sequestered as an inactive dimer as inactive ATMs tend to form dimeric units [168]. Upon DSBs induction, MRN complex is the first factor which binds to the DNA DSBs site to form MRN-DSB complex [10]. An **MRN complex** is a protein complex which contains three proteins which are important in DSBs repair: MRE11 (a protein that is important in DSBs repair), RAD50 (a protein which can directly bind to DNA), and NBS1 (a protein that is required for binding of ATM to the DSB site). The process of activation of ATM starts by the interaction of an inactive ATM dimer with the MRN complex. [10] reported that the activation of ATM involves three important steps at or around the DNA DSBs in chromatin. MRN complex enhances the binding of ATM to the site of DNA damage. The activation of ATM requires the acetylation of ATM by Tip60 acetyltransferase at the damage site. In addition to the acetylation of ATM, the activation of ATM involves autophosphorylation of ATM on S1981, S367, and S1893 by promoting inactive ATM dimer dissociation into active ATM monomers. Once activated, the active ATM monomer can phosphorylate downstream targets that initiate cell cycle checkpoint, DNA repair, apoptosis [35], and also phosphorylates ATM substrate such as histone H2AX [10].

In DNA damage response pathways which includes the ATM activation, the mechanism of active ATM dephosphorylation by phosphatase also plays an important role in the response pathways. The dephosphorylation of active ATM which leads to its inactivation can be induced by phosphatases WIP1 (wild-type p53-induced phosphatase 1), PP5, and PP2A [10]. However, it is worth mentioning that in this thesis, we do not specify which phosphatase is doing the dephosphorylation process. The active ATM protein is not only dephosphorylated, it is also presumably proteolitically degraded [158].

DNA DSBs are not the only initiator of the ATM activation. Recently, in [170], the authors demonstrate that ATM also can be directly activated by hydrogen peroxide (H_2O_2), which is one of ROS (section 2.3) indicating that ATM also plays a role as a sensor of oxidative stress (see section 2.7). It is worthwhile mentioning that the activation of ATM without the DNA DSBs signal is not part of the ATM model that we develop in chapter 5.

2.5.2 Down-stream effects

In response to DSBs, several downstream target substrates are phosphorylated by ATM. Three of the ATM downstream targets are p53, MDM2 (Murine Double Minute 2), and NF-κB (nuclear factor κB). **P53** is a tumour suppressor protein. Activated p53 can induce cell cycle arrest (to allow DNA damage repair) and apoptosis (see figure 2.10) [50]. **MDM2** is a protein that functions to bind p53 and block the subsequent steps (such as transcription activation function of p53) in the activation of p53. In unstressed normal cells, the p53 protein is bound to MDM2. However, in cells with DSB, p53 and MDM2 are phosphorylated, and this disrupts the p53-MDM2 interaction. This disruption enhances the activity of p53 as a **transcription factor** which can regulate cell cycle arrest by the activation of p21 (a protein that is involved in growth arrest), then followed by the repair of DNA damage, or apoptosis by the activation of Bax and PUMA genes (pro-apoptotic genes) [26]. In response to DNA damage, NF-κB is rapidly activated leading to an activation of target genes such as the genes for iNOS and COX-2 [110, 145].

2.5.3 Damage repair

In mammalian cells, there are two major types of DSB repair pathways: non-homologous end joining (**NHEJ**) repair which represents end-to-end joining, and homologous recombination repair (**HRR**), also known as template-assisted repair [64].

2.5.3.1 Homologous recombination repair (HRR)

HRR requires a template which is identical or nearly identical to undamaged DNA strands for repair to occur. It is a common pathway in eukaryotes and is error-free. DNA-PK and the RAD50 complexes play important roles in this repair pathway. For the details of the process, see [26, p.20].

2.5.3.2 Nonhomologous end joining (NHEJ)

NHEJ is a repair mechanism in which the break ends are directly ligated without the need for a homologous template, in contrast to HRR. This is the dominant repair mechanism in many mammalian cells. DNA-PK is crucial to initiate the NHEJ repair mechanism [50]. Through this mechanism, ends of DNA DSBs are brought together, processed and then directly joined together. NHEJ is an error-prone process. The RAD50 complex is needed in this repair pathway. For the details of the process, see [26, p.22].

It is worth to note that HRR and NHEJ processes cannot be performed simultaneously. Which repair option is chosen in a particular cell depends on the phase in the cell cycle. HRR is found mainly in the late S/G_2 phase of the cell cycle where an undamaged sister chromatid is available to serve as a template, while in contrast, NHEJ takes place in the G_1 phase where no template exists [64, p.62].

2.6 Modelling targeted radiation effects (TREs)

As explained in the previous sections, it is of vital important to understand IR damage to mammalian cells.

2.6.1 Linear quadratic (LQ) formalism

A frequently used experimental design for quantifying the effects of radiation is to irradiate a colony of cells in a Petri dish and then to plate them out after some time T to determine what proportion of the cells are able to proliferate (in other words, we use reproductive death as a proxy for cell death). If we denote the number of proliferating cells after irradiation by N_s, with the initial population being N_0, set $S = \dfrac{N_s}{N_0}$ to be the surviving fraction of cells.

Cell survival curves

A cell survival curve is a dose-response curve which represents graphically the relationship between the fraction of surviving cells in logarithmic scale ($\ln S$) and the dose D (in Grays) of radiation in linear scale. We typically obtain a cell survival diagram such as the stars in figure 2.11.

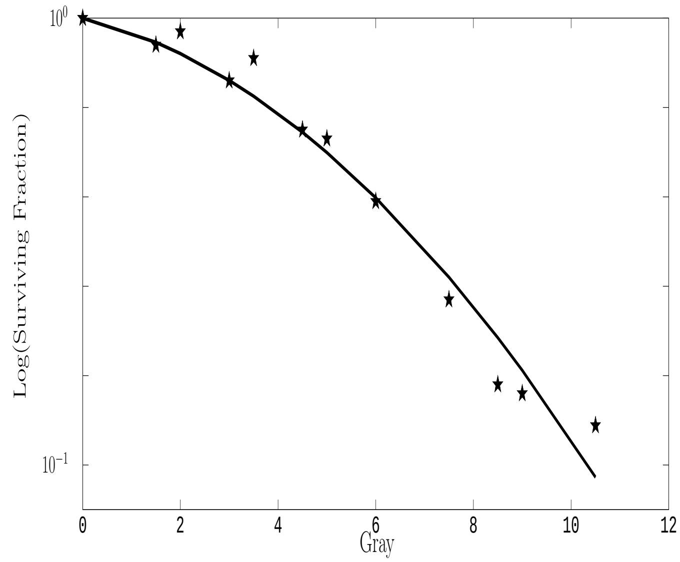

Figure 2.11: Reconstruction of a survival curve for data taken from Yang et al. [164] (mouse embryonic cells ($C3H10T1/2$), $T = 24\ h$, x-rays irradiation. The experimental data ($\star$)) is fitted to an LQ equation (solid curve) $\ln S = -0.0597D - 0.0158D^2$ with $\alpha = 0.0597\ Gy^{-1}$ and $\beta = 0.0158\ Gy^{-2}$.

The dependence of $\ln \dfrac{N_s}{N_0}$ on D seems roughly quadratic for low LET radiation (e.g. x-rays). Most irradiated mammalian cell survival data (including the stars in figure 2.11) can be well approximated by a curve of the form

$$\ln S = -\alpha D - \beta D^2. \tag{2.2}$$

Thus, for small D the dependence of $\ln S$ on the dose D is approximately linear, while for the larger doses it is continuously bending downward quadratically. Relation (2.2) is therefore called the **Linear-Quadratic** (LQ) relation and it is only applicable for mammalian cell populations with surviving fractions larger than 10^{-3} [137].

LQ was first obtained by Kellerer and Rossi in 1972 from the theory of dual radiation action (TDRA) [7] . In this theory, the damage coefficient (LQ parameter) α (Gy^{-1}), the initial slope of the cell survival curve, describes the lethal lesions produced by one-track action; whereas the damage coefficient (LQ parameter) β (Gy^{-2}) describes lethal lesions made by two-track action (quadratic component of cell killing) [137].

An insightful way to characterise survival curves is by the alpha/beta ($\frac{\alpha}{\beta}$) **ratio**. This is the dose at which the linear contribution to damage in (2.2) equals the quadratic contribution, i.e. when $\alpha D = \beta D^2$.

For very high values of the ratio (typical of high-LET radiation), the curve is more linear than for lower values of the ratio (typical of low-LET radiation) which exhibits a more nonlinear curve (see figure 2.12) [64]. It is known that the alpha/beta ratio also depends on the type of cell and typically most tumour cells have a higher alpha/beta ratio than normal cells.

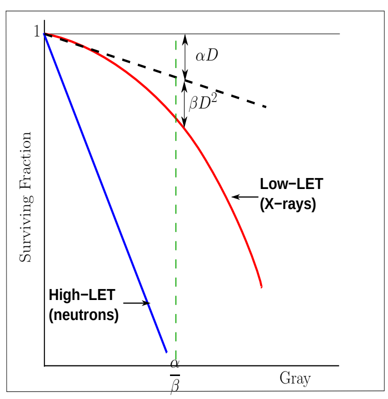

Figure 2.12: Typical shape of radiation cell survival curves for most mammalian cells for low doses of high-LET and low-LET radiation. The $\frac{\alpha}{\beta}$ in the figure is for the low-LET radiation.

Parameters α and β have been fitted to experimental data for a wide variety of tissues and types of ionising radiation and the LQ relation forms the basis of dosimetry planning of radiotherapy regimes. For a detailed account of how it is used in practice, see [64, p.391].

It is not a priori clear how and why (2.2) arises, and what the parameters α and β correspond to on the cellular level. Thus formulating a mechanistic model leading to the LQ relation is one of our aims in the present thesis, and this work is presented in chapter 4.

2.6.2 Models leading to the LQ relation

Over the past 50 years, several models of varying degrees of complexity have been developed to analyse ionising radiation damage to DNA and to mammalian cells. All are based on the concept of the random nature of energy deposition by radiation. The main assumptions adopted in these models can be summarised as follows: 1) the DNA in the cell is the most important cell component for preserving the cell reproductive capacity; 2) ionising radiation inflicts damage mainly by breaking molecular bonds in the DNA, causing DSBs; 3) such lesions can be repaired or be misrepaired.

The models that have been developed can be classified into two different groups: averaged (non individual-based) cell population models and non-averaged (individual-based) cell population models.

2.6.2.1 Averaged (non individual-based) cell population model

In averaged cell population models, the entire irradiated cell population is represented by only one kind of cell (an “average” cell). These models neglect the difference between cells within the population after being exposed to irradiation, and thus the cell population is considered homogeneous and treated as if all the cells have the same level of DNA damage and respond in the same way.

Lea’s [7] target theory of cell killing is one of the earliest radiobiological models, and was proposed in 1946. Target theory considered the biological effects of one or more energy transfers (known as hits) by irradiation to one or more targets. A "target" in this theory is thought of as a specific location on the cell DNA (which is critical in maintaining the cell reproductive capacity): if this target is hit, this will inactivate the cell and thus the cell dies. Various models have been proposed. One of the models of target theory which provides a more general version of the target theory model is the single-hit, multitarget model. "Single-hit, multitarget" means that following irradiation, there is a specific target on the cell's DNA. To inactivate the cell, this target requires two events (hits). "Hits" can be regarded as ionising radiation events that cause the cell inactivation (inability to replicate). For more details, see [7].

By 1960s, experimental data accumulated which could not be fitted well to target theory [167]. To overcome the inadequacy of target theory, it had been replaced by several models whose survival curves can be well approximated by the LQ formula (equation (2.2)).

A number of mechanistic models that directly "lead" to the LQ formula have been proposed. The term "mechanistic" means these are models based on physical and chemical laws, which include parameters with physical, chemical and biological meaning. The first model developed after the target model used the TDRA approach as mentioned in section 2.6.1. The theory assumes that the number of IR-induced sublesions (DSBs) in eukaryotes is proportional to the dose of radiation [87]. Two DSBs in a sensitive site (DNA) will then interact and produce a lesion (which can be thought of as a lethal chromosome aberration). TDRA is based on concepts of microdosimetry for the energy deposition by IR. **Microdosimetry** is an important tool in radiobiology that can be used to measure the microscopic distribution of the energy in order to determine the biological effectiveness for different types of IR. According to TDRA, this model indicates that the average number of lethal lesions within a DNA after a dose D is proportional to the square of the specific energy concentration z, which is a random variable. Using probability theory, the expectation value of number of lethal lesions produced can be estimated by its mean value. This means over a population of cells, the average number of lethal lesions per cell $E(D)$ after a dose D can be expressed as

$$E(D) = k\langle z^2 \rangle. \tag{2.3}$$

where k depends on the system while $\langle z^2 \rangle$ is the average value of the square of the specific energy deposited in a single hit. For details, see [86]. According to [87], $\langle z^2 \rangle$ is given by

$$\langle z^2 \rangle = D(\zeta + D), \tag{2.4}$$

where ζ is the dose-mean specific energy from single events. (2.4) says that the average number of lethal lesions produced is proportional to the number of sub-lesions (DSBs) times the mean energy concentration around the individual DSBs. Kellerer and Rossi [87] assume that the number of DSBs is proportional to the dose D, while the mean energy concentration around the individual DSBs is proportional to $(\zeta + D)$. Of the two components in the bracket, ζ represents the energy concentration produced by the same particle track, and D represents the energy concentration from other particle tracks.

According to (2.3) and (2.4), $E(D)$ can be expressed as $E(D) = k(\zeta D + D^2)$. With the assumption that a surviving cell has no DSBs, and assuming that the number of DSBs follows a Poisson distribution with intensity $k(\zeta D + D^2)$, the probability of cell survival is (see [87] for details)

$$S = \exp[-k(\zeta D + D^2)]. \tag{2.5}$$

In 1973, Chadwick and Leenhout [19] developed a molecular theory of cell survival to replace the TDRA model since the theory proposed by Kellerer and Rossi assumed only the presence of lesions and sublesions without considering the damage repair in detail. Chadwick and Leenhout assume that SSBs are produced linearly with the dose whereas DSB formation is proportional to the square of the dose of radiation, i.e. that DSBs are produced if there are two SSBs located close together. The molecular theory is derived from the assumption that the primary action of irradiation on cells can cause molecular bond breaks in the DNA strands. The theory also assumes that damage repair processes may occur after the breaks are produced. The authors postulate that the solution of the molecular theory can be well approximated by the LQ relation. For details, see [19].

In 1985, Tobias [151] formulated a kinetic model, the Repair-Misrepair (RMR) model, which takes into account DSB formation, repair and misrepair through linear and quadratic processes. It assumes that DSBs can interact pairwise to form a lethal lesion (quadratic misrepair) or that DSBs can be misrepaired on their own (linear misrepair). The model employs equations of ordinary chemical kinetics in order to estimate the evolution of average number of DSBs per cell per Gy produced by low LET radiation. The solution of the RMR model is shown to be well approximated by the LQ formalism.

In 1986, Curtis [29] formulated the lethal-potentially lethal (LPL) model which combines the approaches in TDRA and RMR formulations and was presented as a unified repair theory. This model considers two different kinds of lesions: irreparable (lethal) lesions formed linearly with dose (direct formation of lethal damage), and repairable (potentially lethal) lesions that depend on a **binary misrepair** process (the production of lethal aberration by the interaction between two DSBs), which give rise to the quadratic component in the LQ formula. As in the RMR model, LPL model assumes that potentially lethal lesions are DSBs. In this model, the DSB formation, repair and misrepair processes are modeled by first order nonlinear differential equations. As shown by Curtis, at low doses, the solution of LPL model can be approximated by the LQ relation. TDRA, RMR and LPL models are also called binary lesion interaction models. Those models have in common the assumptions that two lesions may interact to form an aberration and that these lesions may be produced by either a single track or two tracks of radiation.

Another mathematical model which purports to explain the appearance of the LQ shape of survival curves was proposed by Sachs et al. [139] in 2001. This model consists of two ODEs, one for the average number $U(t)$ of DSBs per cell and one for $\overline{N}(t)$, the population density. There are two curious properties of this model. First, they assume that radiation is deposited continuously, which makes this model inapplicable in the usual experimental setup. In the standard experimental procedure, the number of cells surviving ionising radiation is determined after the radiation processes have stopped. Secondly, this model decouples the evolution of $U(t)$, which has to take into account cell death as well as repair, from the evolution of $\overline{N}(t)$. In ODEs (8) and (9) in [139], $U(t)$ would evolve even if there were no cells present.

In 2001, Stewart [148] developed a Two Lesions Kinetics (TLK) model which extends and refines the LPL and RMR models. It provides a description of the DSB rejoining process to obtain a better link between the biochemical processing of DSBs and cell killing. An important aspect of the TLK model is that DSB configurations can be divided into simple and complex DSB types. A simple DSB corresponds to a section of the DNA with length of 10-20 bp that contains a break in each strand. Complex DSBs are simple DSBs that contain additional damage such as damaged bases within the same section of DNA in a cell. Those two groups of DSBs are allowed to interact in pairwise action to produce lethal and nonlethal damage.

There are also various repair saturation models [14, 30, 137, 146] which consider saturable enzymatic repair systems to describe the cell killing effect of ionising radiation, with the assumption that the cell survival is computed after radiation, repair and misrepair processes have been completed. These models are in contrast to binary lesion interaction models which assume that there is direct interaction between DSBs pairs, i.e. a binary misrepair process. By saturable repair one means the decrease of repair rate per lesion as the dose increases, indicating that the number of lesions produced will eventually exceed the number of repair complexes which are available to remove the damage. So that the repair rate tends to a constant. It is found that these models can be well approximated by the LQ relation if the dose or dose rate of the radiation delivered is not very high [137].

In 2004, Guerrero and Li [61] proposed a modified LQ (MLQ) relation in order to improve the formula at large doses per fraction. There is evidence that some cell survival data have a poor fit to LQ formula at high doses [61]. In their work, the authors have shown that the LPL and LQ model were fitted to cell survival data very well at low doses, but when the doses were higher, their predictions were quite different. At high doses, there was more cell killing in the LQ curve than the LPL curve, with the LQ curve continuously bending downward, while the LPL curve has a constant slope. Guerrero and Li introduced a parameter in order for the LQ curve to reproduce the LPL curve. Therefore, the MLQ model has three parameters while the LQ formalism has two parameters. In 2005, Carlone [18] renamed the MLQ model a linear-quadratic-linear (LQL) model, to provide a more physical meaning for the model; Carlone also made some changes in the MLQ model by suggesting a derivation using a compartmental approach to provide a possible mechanistic justification.

2.6.2.2 Non-averaged (individual-based) cell population models

In contrast to the averaged models discussed above, individual-based cell population models consider the effect of statistical fluctuations in DSBs produced in a cell population.

In 2010, Hanin and Zaider [67] developed a statistically-based model of cell survival which takes microdosimetric effects into consideration (see page 30 for a brief explanation of microdosimetry). This model is applicable to both low and high doses of low and high LET and provides a better explanation of the cellular dose response at large doses. By using probability theory, the authors compute survival probability under the assumption that any two sublesions (DSBs) produce a lethal lesion with probability p. The authors claim that their model is free from the assumption that the number of lethal lesions is Poisson distributed, and also showed that for high doses, the probability distribution of specific energy z in DNA can be approximated by a Gaussian distribution. Using this model, the survival probability depends on three adjustable parameters: p is the probability that two sublesions interact to form a lethal lesion, q denotes the probability that an unrepaired or misrepaired sublesion becomes lethal, and λ denotes the Poissonian rate of sublesion formation per unit specific energy.

In addition, there are a number of works modelling radiation cell killing using Markov processes [2, 63, 136, 138]. A Markov process is a stochastic process with the Markov property [2], i.e. that only the present state gives any information about the future behaviour of the process. The master equations of the Markov process approach are broadly equivalent to the equations of structured population dynamics (chapter 4). During our work (in December 2010), we realised that the model proposed by Albright [2] in 1989 is very close in spirit to the model that we have been developing. To discover the differences between [2] and our model, Albright's model will now be considered in detail in the following section.

2.6.3 The Albright model

In 1989, Albright [2] converted the repair-misrepair (RMR) model [151] from a lumped model into a more accurate one which describes how individual cells evolve in time. We describe this model in detail, as in chapter 4 we will present an alternative (population) model which has many similarities to the Albright's model. The aim of Albright's model was to calculate the probability that a cell will survive using a Markov process approach. Albright's model describes DSBs repair dynamics and the production of initial lesions more systematically than the original RMR model. Albright suggests that each cell can be either in "survival state" (S-state), "lethal state" (L-state), or "uncommitted state" (U-state). S-state is a state in which all the initial lesions which were produced immediately after irradiation have been successfully repaired. L-state is the state contains one or more lethal lesion misrepairs, and U-state is the state where not all lesions have been repaired and lethal misrepairs have not yet occurred. Immediately after irradiation and before the repair processes have started, each cell could be either in a U-state or in a S-state. From U-state, the cell can move to L-state (if there are lethal lesion misrepairs) or another U-state (if one or more lesions are correctly repaired) while if it is in an L-state, the cell can no longer move to a U-state but only to another L-state. Once S-state is reached, no more further transition is needed.

Albright suggests that the fraction of surviving cells can be determined by the initial distribution of the number of lesions produced immediately once the radiation process has stopped and the probabilities of repair events in a cell. He makes the following assumptions:

(1) Just before time $t = 0$, irradiation of dose D is given. At time $t = 0$, the irradiation process is completed and all the initial lesions have been produced. Thus the radiation dose D is incorporated into the formulation of initial distribution of the radiation-induced lesions. At this time, repair processes have not yet started.

(2) The production of radiation-induced lesions is assumed to be an instantaneous event. There were three stochastic processes involved in the lesion formation: i) Energy deposition process from an ionising particle. This process completed in 10^{-12} s. ii) Free radical chemical reaction that produced the DNA damage. This damage process will be taken about 10^{-5} s. iii) DSB repair which requires $1 - 10$ h. Processes in (i) and (ii) are considered in the initial condition of the model, while process in (iii) is referred to the assumption in (3).

(3) Repair processes are described as probability of transition from one state to another and occur at random time.

Some remarks on Albright's model:

1. All the biological assumptions of the original RMR model were applied except the two statistical assumptions. In the original RMR model, Tobias [151] assumed that the stochastic effect in the lesions repair process was not important and also assumed that the final radiation-induced distribution of lesions from cell to cell was Poisson.

2. The model does not assume that the initial distribution of the lesion is always Poisson.

3. All lesions due to misrepair are always lethal. This assumption has led the author always to consider that in S-state, the number of misrepairs is zero, which means that cells with nonzero misrepairs are ignored in Albright's discussion.

4. Albright's results are well approximated by the LQ relation if the dose of irradiation given not too large [137].

Albright considers $P(n, m, t|D)$, the probability that a cell has n unrepaired lesions and m lethal misrepairs at time t if dose D is given before time $t = 0$. According to [2], this quantity evolves as follows:

$$\frac{dP(n,m,t|D)}{dt} = -\alpha_n P(n,m,t|D)+\beta_{n+1}P(n+1,m,t|D)+(\alpha_{n+1}-\beta_{n+1})P(n+1,m-1,t|D) \tag{2.6}$$

where the repair transition coefficients α_n and β_n are functions of n (number of unrepaired lesions), given that

$$\alpha_n = \lambda n + \kappa n(n-1), \tag{2.7}$$

and

$$\beta_n = \phi\lambda n + \psi\kappa n(n-1), \tag{2.8}$$

where α_n is always larger than β_n, and λ, κ, ϕ and ψ are constants. α_n is the repair rate for repair processes while β_n is the repair rate for viable (correct) repair processes. α_n and β_n functions are taken from the RMR model which assumes that linear terms (λn and $\phi\lambda n$) correspond to linear repair. The second term in both functions corresponds to quadratic repair which is proportional to the number of distinct pairs of n lesions, $\frac{n(n-1)}{2}$.

The first term on the right side in (2.6) corresponds to transition due to all repair processes, while the second term is for viable repair process from cells that have $n+1$ lesions and m misrepairs. The third term describes the contribution from cells with $n+1$ lesions and $m-1$ misrepairs.

However, Albright was only interested in the state without lethal misrepairs. If $m = 0$, thus we have $P(n,t|D) = P(n,0,t|D)$. (2.6) can be rewritten as:

$$\frac{dP(n,t|D)}{dt} = -\alpha_n P(n,t|D) + \beta_{n+1} P(n+1,t|D). \tag{2.9}$$

To solve the ODEs in (2.9), one needs to specify the initial condition of the system. If k is the number of initial lesions, the initial condition of Albright's model is $P(k,0|D)$, the initial distribution for the number of lesions (the probability that the nucleus will have k lesions at time $t = 0$ if dose D is given).

For the initial distribution of lesions, Albright assumed that $P(r|D)$ (the probability that r energy deposition events will occur if dose D) is given, z_i (the probability that the specific energy deposited in ith event), and $P(k|z_1, \cdots, z_r)$ (the probability that k lesions will be produced if energy depositions $z_1, \cdots, z_r$ occur) are Poissonian. He shows that these independent Poisson distributions that are critically involved in the initial lesions formation, result in a mixture of Poisson distributions, a compound Poisson distribution (CPD) with the variance of CPD larger than for the Poisson distribution (see [60] in detail). This result has led Albright to suggest that the initial distribution of lesions was not necessarily Poisson. He shows that initial lesions distribution is Poisson only for low-LET radiation.

In 1990, Sachs et al. [138] improved the Albright's model by incorporating dose-rate effects. In contrast to Albright's assumption which considered radiation as an instantaneous process, Sachs and his colleagues proposed that the radiation is delivered during a finite time interval. The authors found that by introducing a dose rate parameter into Albright's model, the cell survival fraction was increased for low-dose rate and higher dose rate compared to the original RMR model using the same parameters. Other models which improve on the Albright's model are due to Hahnfeldt et al. [63] and Sachs et al. [136]. [63] considered saturable repair processes while [136] focused on low-dose rate and used partial differential equations to study spatial dependence of DSB interactions.

The probabilistic approach used in Markov models can be linked to non-probabilistic models under the law of large numbers (LLN) equivalence; the probability of a cell being in a particular state is equivalent to the expected/averaged number of cells in that state in a large enough population [44]. This is the approach we will take in chapter 4.

2.7 Nontargeted radiation effects (NTREs)

Apart from direct effects of exposure to ionising radiation that include cell killing and mutations that may lead to the induction of malignant transformation in target cells, ionising radiation can also enhance the frequency of secondary effects in non-irradiated cells, which has been referred to the **radiation-induced bystander effect** (RIBE) . RIBE is a complex of effects that include mutations, chromosomal aberrations, cell death and micronuclei formation. These phenomena indicate that at low doses, cell signaling is more important than direct DNA damage [113]. Both ionising radiation (IR) and non-IR may induce bystander damage in non-targeted cells. In [36], it is shown that exposure to ultraviolet (UV) radiation leads to increase in apoptosis in the bystander population.

There is ample evidence that RIBE involves direct cell-cell communication through GJIC (see subsection 2.2.1) or via soluble factors released by irradiated cells [9].

A number of candidates of the soluble signaling molecules have been identified. These include ROS [163], NO [65], IL6 (interleukin-6)[22], IL8 (interleukin-8)[43] and TGF-β (transforming growth factor-β)[171]. After irradiation, levels of these molecules are found to be increased in the growth medium of irradiated cells. Recently, Dieriks and his co-workers [38] have demonstrated that three cytokines, IL6, IL8, and RANTES (Regulated on Activation, Normal T Expressed and Secreted, which is a family of small cytokines) have been associated with radiation-induced bystander effect.

In [36], it was found that media conditioned on cells targeted with either IR or non-IR, and also with undamaged tumour and senescent cells, contained high level of TGF-β and NO. These signal molecules result in an elevated level of DSBs in non-targeted cells. NO synthase inhibitors, TGF-β blocking antibodies, and antioxidants, led to a decrease in TGF-β level. This result indicates that reactive species and pro-inflammatory cytokines mediate the bystander effect in non-targeted cells. [36] also showed that genomic instability can be produced in cells without irradiation either by direct contact or through shared media with undamaged malignant cells.

The bystander response mechanism

In the present thesis, we suggest a mechanism of bystander response of IR presented in figure 2.13. Due to time constraints a full mathematical analysis of this mechanism is left to future work. The mechanism involves five processes that mediate the response.

1. The establishment of the bystander response starts when MAPK family kinases (such as extracellular signal-regulated kinases (ERK), c-Jun N-terminal Kinase (JNK), and P38) receive some signal S mediated by soluble signaling molecules produced by irradiated cells [129]. Activation of MAPK (see

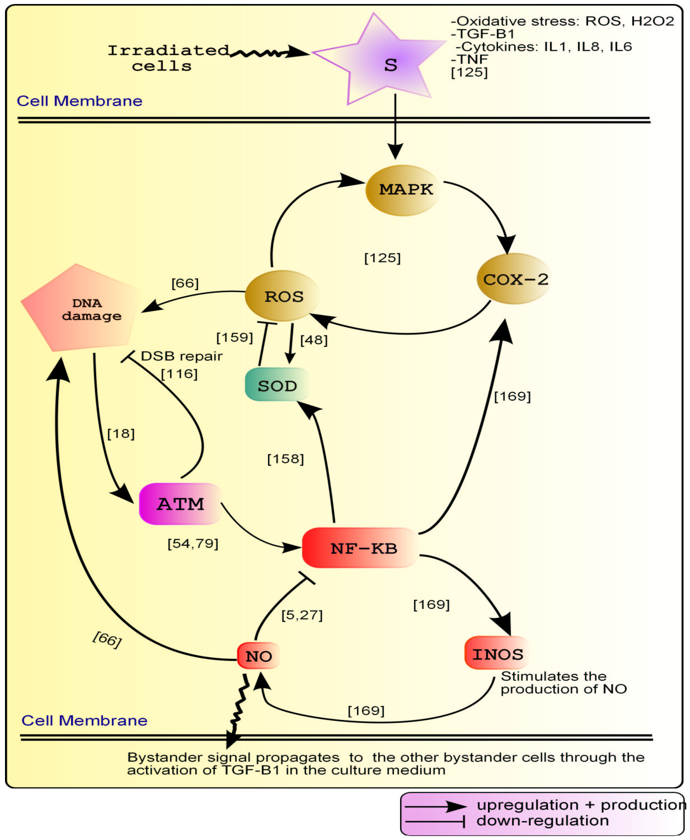

Figure 2.13: The mechanistic scheme of the model of radiation-induced bystander effect. The figure is based on [5, 17, 25, 48, 54, 65, 79, 110, 119, 129, 162, 163, 173]. See text for details.

subsection 2.2.2) upregulates the expression of COX-2 (see subsection 2.2.2) thus leading to a significant increase of ROS. For evidence that ROS can activate MAPK see [129]. [68, 172] show that ERK activation is an important upstream event which leads to COX-2 expression. This can be demonstrated by using ERK inhibitor, PD 98059, and COX-2 inhibitor, NS-398. Treatment of bystander cells with PD 98059 or NS-398 significantly reduced bystander effects. The closed loop between MAPK, COX-2, and ROS (as shown in figure 2.13) is a positive feedback loop, a structure called a vicious circle.

2. Raised level of ROS lead to upregulate of SOD, an antioxidant enzyme [48]. Thus, sufficiently high expression of SOD will reduce the level of ROS and

break the vicious circle [163]. At the same time, high level of ROS initiates another positive feedback loop by producing DSBs [65].

3. DSBs quickly activate ATM (see section 2.5.1) [17]. The negative feedback loop between DNA damage and ATM can reduce the intensity of DNA damage due to the damage repair processes. This consequently will decrease the level of activated ATM. Phosphorylated ATM can also activate its downstream effectors such as NF-κB or p53. [54, 79] show that ATM–p53 pathway is not important in modulating bystander responses. In [79], it is demonstrated that by using p53-independent cells (human skin fibroblasts (HSF) immortalised by SV40 T-antigen), the bystander effect is observed in the cells even though p53 downstream is blocked. As shown in figure 2.13, ATM–NF-κB pathway seems likely the most critical pathway in regulating bystander response.

4. As in the other components of the proposed mechanism, NF-κB initiates a negative feedback mechanism by inducing the production of SOD. At the same time, NF-κB upregulates COX-2 and activates the iNOS–NO pathway [173].

5. Upregulation of iNOS by NF-κB then stimulates the production of NO, which then leads to NF-κB inhibition [173]. However, like ROS, NO also plays an important role in DSB creation [65], thus contributing to the ATM–NF-κB part of the mechanism. Yet again, we see the initiator of both a positive and negative feedback.

   Thus, ROS and NO in our view are important mediators of the bystander response. It is known that treatment of cells with ROS scavengers, such as dimethyl sulfoxide (DMSO) or NO inhibitors, such as C-PTI0, effectively reduces DSB formation. This supports an important role of the reactive species in mediating bystander effects [65].

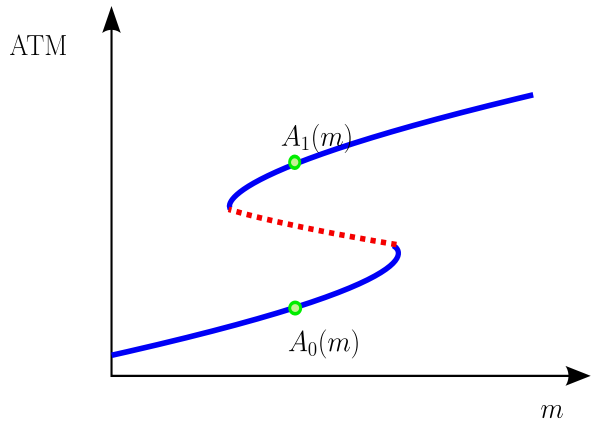

Figure 2.14: The bistable curve. $A_0(m)$ and $A_1(m)$ in the figure represent the lower level (a healthy low activated ATM concentration) and the upper level (a chronically high activated ATM concentration) of the activated ATM, respectively. m measures the strength of feedback loops between DSBs and ATM. The solid line corresponds to a stable state, while the dotted line represents an unstable state.

To summarise, cells have finely tuned stress response. A cell that cannot resolve a stress insult in vivo by its actions attracts components of immune system (e.g. by overproducing NO). In vitro a disbalance between negative and positive feedback loops (presumably caused by the signal S which can modify the strength of these loops) will switch the bistable system described in figure 2.14 into a state of chronically high ROS and chronically high DSB formation. We also claim that this state will be characterised by a chronically high activated ATM concentration, which can be verified experimentally [6].

2.8 Radiotherapy: making use of radiation

Radiotherapy is a treatment that uses a high energy radiation such as gamma-rays, x-rays or charged particles to kill cancer cells. It has been in use for the last 100 years [150].

In general, the goal of radiotherapy is to maximise the dose to abnormal cells and minimise exposure to normal cells. A common form of therapy is external beam radiation therapy (EBRT), in which energy is transferred from an external source of radiation, usually electrons or photons generated by a linear accelerator that points to a particular part of the body. Unlike EBRT, brachytherapy is an internal radiotherapy in which radioactive seeds or sources are placed inside or very close to the tumour itself. See [81, p.164] for details of brachytherapy.

Using the LQ formalism in practice

Mathematical and statistical modelling have played a crucial role to give vital information to determine the optimal radiotherapy schedule for a patient. The LQ formalism (section 2.6.1) is widely used for analysing cell survival in vitro and in vivo in both experimental and clinical radiobiology [81].

To predict the outcome of a given treatment schedule, one can use tumour control probability (TCP). **TCP** is defined as the probability that no malignant cells are left in a specified location after irradiation [71]. The LQ relation provides a formula for the cell survival fraction that can be used for the prediction of TCP. The standard model of local tumour control is given as:

$$TCP = \exp[-N_0 \exp(-\alpha D - \beta D^2)], \tag{2.10}$$

where N_0 is the total number of clonogens per tumour before irradiation and the second exponent comes from LQ relation [71].

TCP determines the optimal treatment strategy at which the dose to the tumour is increased and more malignant cells will die without increasing the cell killing effect to normal cells. For details about TCP, the interested reader is referred to [34, 71, 121, 166].

Another important component in the LQ relation that is involved in treatment protocols is the $\frac{\alpha}{\beta}$ ratio (see (2.2)). $\frac{\alpha}{\beta}$ ratio is a dose in Gray which is used to describe the effect of radiation dose and fractionation. Elkind and Sutton in 1959 first reported the response of a population of cells in vitro to fractionated irradiation and this was later confirmed in vivo as well as in vitro [152]. In fractionated EBRT, a total dose of radiotherapy is broken into smaller amounts and administered over a period of time, rather than a single larger dose. In [62, 156, 157], the authors demonstrate that the irradiation in number of fractions n produces a smaller degree of cell killing than when the same total of dose D is delivered in a single fraction. One of the fractionation schemes that is commonly used in radiotherapy protocol is conventional fractionation radiotherapy. The dose fractionation schedule in conventional fractionation typically 1.8 to 2 Gy per day, usually five days a week [81, p.367]. Other fractionation schemes which can also improve the radiation treatment strategy are hyperfractionation, hypofractionation, etc. See [81, p.136] for details.

The $\frac{\alpha}{\beta}$ ratio describes the tissue's response to dose fractionation (namely fractionation sensitivity). There is evidence that tissues with low $\frac{\alpha}{\beta}$ ratio $(0.5-6$ Gy) (which are usually characterised as late responding tissues) show high sensitivity to fractionation changes, in contrast for tissues with high $\frac{\alpha}{\beta}$ ratio $(7-20$ Gy) (which usually characterised as early responding tissues).

The $\frac{\alpha}{\beta}$ ratio is also used for calculating isoeffective radiotherapy schedules. To compare different fractionation schedules, consisting of different total dose and dose per fraction, one can convert each schedule into an equivalent schedule in 2 Gy fractions (which is commonly used dose per fraction clinically) [81, p.109]. The formula to convert a total dose D Gy given with a fraction size of d Gy into the isoeffective dose in 2 Gy is given by

$$EQD_2 = D\frac{d + \frac{\alpha}{\beta}}{2 + \frac{\alpha}{\beta}}, \tag{2.11}$$

where EQD_2 is equivalent dose in 2 Gy fractions. Example can be found in [81, p.123]. Fractionation allows normal damaged cells time to **recover/repair** the sublethal damage between dose fractions, while tumour cells are less efficient in

DNA repair between fractions. Fractionation also leads tumour cells which are in a radio-resistant cell cycle phase during one treatment into a **radiosensitive** phase of the cell cycle through **reoxygenation**, a process by which oxygen is allowed to reach surviving hypoxic clonogenic cells, so the cells become better oxygenated before the next fraction given. Reoxygenation between fractions improves the tumour cells kill. The **repopulation** of cells also takes place while receiving fractionated doses of radiation. The cell survival will increase resulting from cell division. During fractionation, **redistribution or reassortment** occurs in proliferating cell populations throughout the cell cycle phases. This process allows more cells to die.

All the five Rs processes: radiosensitivity, repair, repopulation, redistribution, and reoxygenation are the basis of fractionation of radiotherapy. A balance is achieved between the dose response of tumour and normal tissues from five Rs processes; repair and repopulation between dose fractions involved in normal tissue sparing, while the increase in tumour damage results from reoxygenation and reassortment of tumour cells. Fractionation of dose depends on types of cancer cell, prolongation of the fraction schedule over too long period can allow for the tumour to begin repopulating.

It is worth noting that in chapter 4, we develop a model that allows dose fractionation.

2.9 Conclusions

Mechanisms of mammalian cell killing effects produced by ionising radiation are complex processes. In order to develop a mathematical modelling of the effect of ionising radiation, one should first understand the whole story of how radiation damage occurs in cells and how the damage is repaired. In chapters 4 and 7 we employ all the biological concepts explained in this chapter and transform them into mathematical language in order to obtain a model of cell population response to irradiation.

Chapter 3

Modelling methodologies

3.1 Introduction

In this chapter we will briefly explain a number of mathematical techniques and concepts that are used in the present thesis. We will discuss the Poisson distribution, least squares and curve fitting, and simulated annealing. We also discuss multistability concept which is an important property of the model that we analyse in chapter 6. A brief explanation of the method used in multivariate polynomials such as the resultant, the discriminant, the Sturm's theorem and Cauchy's Bound for real roots are also provided.

3.2 The Poisson distribution

In 1837, the Poisson distribution which describes discrete events was introduced by a French mathematician, Simeon-Denis Poisson. The probability distribution of a Poisson random variable X representing the number of events occurring in a given time interval or specific region of space is given by the probability function as follows:

$$P(X = x) = \frac{\lambda^x e^{-\lambda}}{x!}, \qquad x = 0, 1, 2, ... \tag{3.1}$$

where $e \approx 2.7183$ and λ is the average number of events in the given time interval or region of space. The mean and variance of the Poisson distribution are $E(X) = \lambda$ and $Var(X) = \lambda$, respectively [82]. In chapter 4, we assume that DSBs (chapter 2) are produced immediately on irradiation following a Poisson distribution.

3.3 Curve fitting and parameter estimation

Estimating values for the parameters of mathematical models is a common issue and an important step in computational and system biology especially for parameters which cannot be directly measured in experiments. For example, a death rate coefficient of model species can be quantified by parameter estimation techniques which give a value of parameters (also known as fit parameters) that produce the best fit of the model simulation to a set of experimental data. There are two general parameter estimation techniques: maximum likelihood and least squares. In this thesis, we are only interested in the least squares method since we do not specify what is the probability distribution of the experimental data that we have.

3.3.1 Least square criterion

The method assumes that the "best fit" line for the experimental data is the curve that has the minimal value of the least square error (or sum of the squares of the deviations) ϕ from the given data. Suppose that we are given a data set (x_1, y_1), (x_2, y_2), ..., (x_n, y_n) where x is the independent variable while y is the dependent variable.

In chapter 4 if $f_i(x_i, \boldsymbol{\theta})$, $i = 1, 2, \cdots, n$ are the data along the fitting curve which contains six adjustable parameters $\boldsymbol{\theta} = (\delta, \alpha_1, \alpha_2, p, V_{max}, K_M)$, then the deviation d of each data point is given by $d_1 = y_1 - f_1(x_1, \boldsymbol{\theta})$, $d_2 = y_2 - f_2(x_2, \boldsymbol{\theta})$, ..., $d_n = y_n - f_n(x_n, \boldsymbol{\theta})$ [12]. The formula known as the least square criterion, which determines the "best fit" curve which has the minimal value of $\phi(\boldsymbol{\theta})$ is given by

$$\begin{aligned}\underset{\boldsymbol{\theta}}{\text{minimize}} \quad \phi(\boldsymbol{\theta}) &= d_1^2 + d_2^2 + \ldots + d_n^2 \\ &= \sum_{i=1}^{n} d_i^2 \\ &= \sum_{i=1}^{n} \left[y_i - f_i(x_i, \boldsymbol{\theta})\right]^2. \qquad (3.2)\end{aligned}$$

Using the least square criterion in (3.2), y_i is fitted to $f(x_2, \boldsymbol{\theta})$ with the estimated value of model parameters $\boldsymbol{\theta}$. In chapter 4, x_i and y_i are dosages and surviving fractions, respectively from experimental work and

$$f_i(x_i, \boldsymbol{\theta}) = \ln \frac{N_i(T, x_i, \boldsymbol{\theta})}{N(0)}$$

are surviving fractions in logarithmic scale (after time T, for doses x_i, and parameters $\boldsymbol{\theta}$).

In general, there are two ways of searching for the minimum of $\phi(\boldsymbol{\theta})$ (the objective function). Firstly, if the objective function is differentiable with respect to the parameters $\boldsymbol{\theta}$, one can employ a gradient-based approach (the interested reader is referred to [143] for further details). Alternatively, if the derivative of the objective function is impossible to find, one can use a direct search method which does not require any derivative information such as the Nelder-Mead simplex method (see section 3.3.2), as we do in chapter 4.

There are two general approaches to optimization problems; seeking local optima and seeking global optima (see figure 3.1).

The simulation data obtained from the model that we propose in chapter 4 is fitted to the LQ equation (2.2). To estimate the LQ parameters α and β (see chapter 4) using the least square criterion, we use a local optimization toolbox in MATLAB *fminsearch*.

The algorithm of *fminsearch* uses a direct search method which does not require any gradient or Hessian (second order partial derivatives of a function) evaluations.

It solves nonlinear unconstrained multivariable optimization problems and is based on the Nelder-Mead sequential simplex algorithm (see section 3.3.2). However, if the objective function provided is too complicated and has a large number of parameters to be estimated, then the optimizer may be sensitive to the user-supplied starting values of the parameters that are to be estimated.

The *fminsearch* syntax for finding the minimum of an objective function named "fun" with $\boldsymbol{x_0}$ as an initial guess for the minimum is $\boldsymbol{x} = \text{fminsearch}(fun, \boldsymbol{x_0})$ and it will return $\boldsymbol{x}$, the estimated value of the fit parameters. The reader is referred to [105] for the background of *fminsearch*.

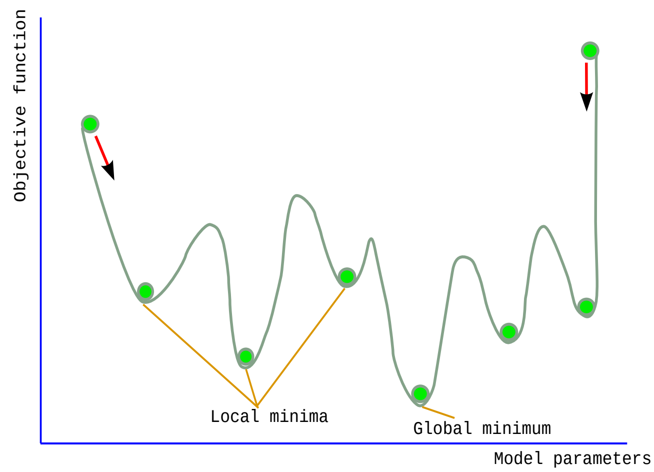

Figure 3.1: Local and global maxima and minima

3.3.2 Nelder-Mead simplex algorithm

For the last 40 years, the Nelder-Mead simplex algorithm has been used to solve parameter estimation problems [32]. This method is applicable for non-smooth objective functions where function values are noisy and random.

The "simplex" refers to a shape with $j + 1$ points where j is the number of fit parameters $\boldsymbol{\theta}$ that are to be estimated. This algorithm works with several rules: Reflection (R), Expansion (E), Contraction (C), and Shrink (S).

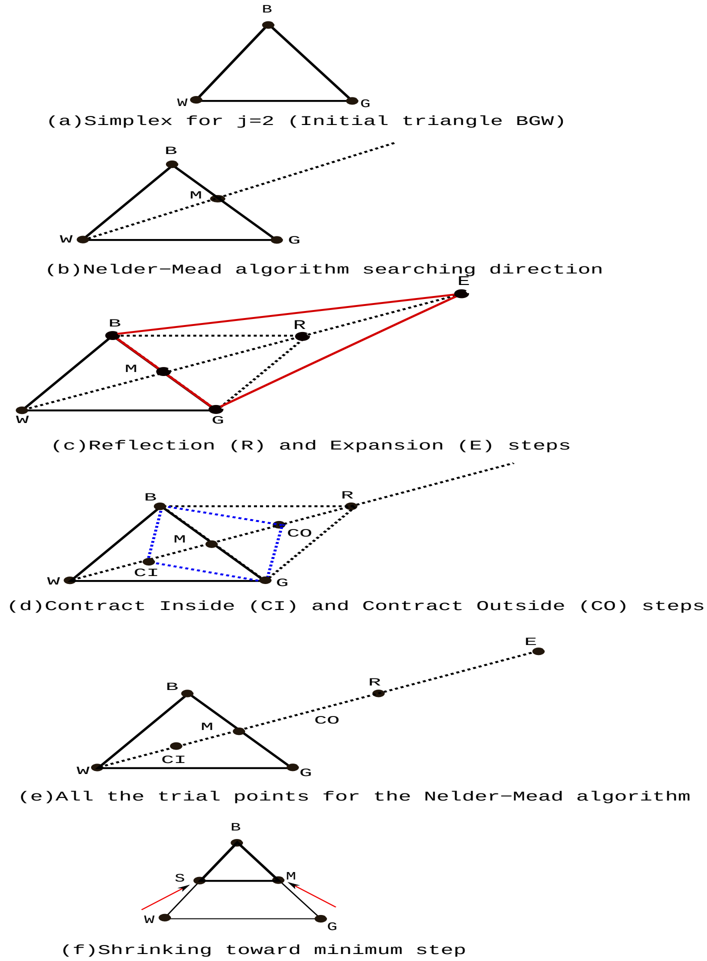

Figure 3.2: The three basic movements in the Nelder-Mead simplex algorithm. See text for details.

Suppose we have an objective function $f(x, y)$ to be minimized. Here we have a 2-simplex, a triangle with vertices: $V_k = (x_k, y_k)$, $k = 1, 2, 3$. Next, according to [104], we need to

1. Evaluate $z_k = f(x_k, y_k)$ for $k = 1, 2, 3$ and reorder $z_1 \leq z_2 \leq z_3$.

   In this example we use $B = z_1$, $G = z_2$ and $W = z_3$ indicating that B is the best vertex, G is good and W is the worst vertex. See figure 3.2(a).

2. Evaluate the midpoint of the good side (line from B to G). See figure 3.2(b).

Consider the midpoint M of a good line segment BG given by the averaging the coordinates: $M = \frac{B+G}{2}$ or $M(\frac{x_1+x_2}{2}, \frac{y_1+y_2}{2})$

3. Update the triangle using the best of the transformations as shown in figure 3.2. Below is the logical decision tree for the Nelder-Mead algorithm.

   - Compute $R = M + (M - W)$ and $f(R)$,
   - **If** $f(R) < f(G)$, **then** perform **Case** (i) (either reflect or extend).
   - **Else** perform **Case** (ii) (either contract or shrink).
   - **Case** (i)
     - **If** $f(B) < f(R)$, **then** replace W with R and reorder $B \le G \le W$.
     - **Else** compute $E = R + (R - M)$ and $f(E)$,
       * **If** $f(E) < f(B)$, **then** replace W with E and reorder $B \le G \le W$.
       * **Else** replace W with R and reorder $B \le G \le W$.
   - **Case** (ii)
     - **If** $f(R) < f(W)$, **then** replace W with R and reorder $B \le G \le W$.
     - **Else** compute the two midpoints: Contract Inside $CI = \frac{W+M}{2}$, Contract Outside $CO = \frac{M+R}{2}$, $f(CI)$ and $f(CO)$. The point with smaller function value is called C,
       * **If** $f(C) < f(W)$, **then** replace W with C and reorder $B \le G \le W$.
       * **Else** G and W must be shrunk toward B. Then compute $S = \frac{W+B}{2}$ and $f(S)$ and replace W with S and replace G with M and reorder $B \le G \le W$.

4. Stopping Criterion: $f(B)$, $f(G)$ and $f(W)$ did not change (flat to the minimum value).

However, in order to estimate the six mechanistic parameters $\boldsymbol{\theta}$ of the model in chapter 4 which is using more complicated objective function $\phi(\boldsymbol{\theta})$, we implement both optimizer; the local optimizer (i.e the Nelder-Mead simplex method) and the global optimizer. There are several techniques in global optimization, but we restrict ourselves to using the simulated annealing technique to estimate the six parameters of the model in chapter 4.

3.3.3 Simulated annealing

Simulated annealing as a global optimization algorithm was first introduced in the early 1980s by Kirkpatrick. According to [83], the simulated annealing algorithm mimics the annealing process: a process by which a solid in a heat bath melts when the temperature of the heat bath is increased to a maximum value. At high temperature, all particles in the liquid-phase move randomly in high energy. The temperature of the heat bath is then decreased slowly until the particles arrange themselves in the low energy state of the solid. Simulated annealing is a powerful technique in minimizing or maximizing an objective function [83] which has been applied in many different disciplines, for example in model parameter estimation [1].

The simulated annealing algorithm accepts all points that lower the objective function and it also accepts all points that make the objective function go up with probability P. The probability of accepting downhill/uphill moves is given by

$$P = \begin{cases} 1 & \text{if } \Delta\phi < 0, \\ \exp(\dfrac{-\Delta\phi}{\Theta}) & \text{if } \Delta\phi > 0, \end{cases} \tag{3.3}$$

where $\Delta\phi$ is the increase in objective function ϕ at temperature Θ. In this way, the algorithm does not get stuck in local minima, which is a major advantage of simulated annealing over other methods [83].

We use the *simulannealbnd* routine in MATLAB. This is a built-in package in the Global Optimization Toolbox. The steps of simulated annealing procedures for parameter estimation that are applied in section 4.8 (chapter 4) are explained below.

1. Initialise: Temperature $\Theta_0 = 100$, random starting point $\boldsymbol{\theta_0} = (\theta_{10}, \theta_{20}, \theta_{30}, \theta_{40}, \theta_{50}, \theta_{60})$.

2. Set $\Theta = \Theta_0$,$\boldsymbol{\theta} = \boldsymbol{\theta_0}$.

3. Compute SSE function $\phi(\boldsymbol{\theta_0})$.

4. While the stopping criterion is not reached:

   for $i = 1$ to L (reanneal interval,$L = 100$)

   - Generate neighboring point $\boldsymbol{\theta_i}$ for $\boldsymbol{\theta_{i-1}}$.
   - Compute SSE function $(\phi(\boldsymbol{\theta_i}))$.
   - Parameter evaluation
     - If $\phi(\boldsymbol{\theta_i}) < \phi(\boldsymbol{\theta})$ then $\boldsymbol{\theta} = \boldsymbol{\theta_i}$ and $\phi(\boldsymbol{\theta}) = \phi(\boldsymbol{\theta_i})$.

       Else

       Generate a random probability of acceptance $P^* \in (0, 1)$

       - If $P^* < P$ then accept $\boldsymbol{\theta} = \boldsymbol{\theta_i}$ and $\phi(\boldsymbol{\theta}) = \phi(\boldsymbol{\theta_i})$.

       - Else keep $\boldsymbol{\theta}$ unchanged
   - Temperature reduction : The temperature is adjusted according to a given annealing schedule (often also called cooling schedule). There are several schemes to reduce the temperature such as

     - Geometric cooling schedule : $\Theta_i = C\Theta_{i-1}$ [74].

     - Exponential cooling schedule : $\Theta_i = \Theta_0 C^i$ [116].

     - Boltzman cooling schedule : $\Theta_i = \dfrac{\Theta_0}{\ln i}$ [78].

     - Fast Cauchy cooling schedule : $\Theta_i = \dfrac{\Theta_0}{i}$[141].

     where C is the cooling rate and $0 < C < 1$.

5. Algorithm stops when TolFun criteria is met (at which the minimum value of SSE is reached) (please refer to [105] for further details).

6. Optimal solution is obtained : $\boldsymbol{\theta_{opt}} = (\theta_{1opt}, \theta_{2opt}, \theta_{3opt}, \theta_{4opt}, \theta_{5opt}, \theta_{6opt})$ estimates of $(\delta, \alpha_1, \alpha_2, p, V_{max}, K_M)$.

In step 4, L is a number of accepted points before reannealing. According to [131], the cooling rate C is typically chosen between 0.8 and 0.99. If C is large, this leads the temperature of the annealing process to decrease slowly to avoid the algorithm getting trapped in a local minimum. In step 6, the TolFun criteria is met if the average change in the objective function value is less than TolFun. We set TolFun$= 10^{-7}$, and MaxFunEval$= 9000$. These values are chosen due to the limited computer memory.

3.3.4 Bootstrap confidence interval for parameters

After we perform the parameter estimation procedure (see section 4.8), we calculate the interval of the individual values of all of the six parameters in the model. This can be obtained by using the method of bootstrapping confidence interval (CI) on the estimated parameters. Bootstrap was introduced by Bradley Efron in 1979 (see the details of the method in [40, 109]). This is a powerful technique for estimating the CI of the parameters when we do not know the distribution of the sample data. This method allows randomized resampling of the original data to construct a new set of data. Bootstrap do not generate new data but resamples all the original data with replacement. Here we deal with a 95% bootstrap confidence interval of the model parameters. This means that we are 95% sure that the true parameter value is within the range. The bootstrap method used in section 4.8.1 is discussed in the following steps:

1. For the data points $y_1, y_2, \cdots, y_n$ an estimate of parameter set $\boldsymbol{\theta}$ can be obtained using the algorithm of Nelder-Mead simplex

$$\boldsymbol{\theta} = T(y_1, y_2, \cdots, y_n),$$

where T is the *fminsearch* in MATLAB (see section 3.3.1 for details).

2. A new data set called bootstrap data is constructed by sampling n points with replacement from the y_n original data. These bootstrap data consist of $y_1^*, y_2^*, \cdots, y_n^*$ points where each y_i^* is drawn at random from the original data. The bootstrap data sets are used to estimate the new set of parameters

$$\boldsymbol{\theta^*} = T(y_1^*, y_2^*, \cdots, y_n^*).$$

3. Step in 2 is repeated many times to obtain a set of values of the estimated parameters $\boldsymbol{\theta^*}$. Since the distribution of the sample data is unknown, the 95% bootstrap CI on the parameters are calculated based on the upper and lower $100(1-\alpha)$ percentiles of the estimated parameters $\boldsymbol{\theta^*}$ when $\alpha = 0.05$. The 95% CI for the six estimated parameters can be obtained by

$$(\boldsymbol{\theta}_{lower}, \boldsymbol{\theta}_{upper}) = (\boldsymbol{\theta}^{*(\frac{\alpha}{2})th}, \boldsymbol{\theta}^{*(1-\frac{\alpha}{2})th}).$$

For example, in section 4.8.1 there are 1000 bootstrap iterations. Then each of the parameter in $\boldsymbol{\theta^*} = (\delta^*, \alpha_1^*, \alpha_2^*, p^*, V_{max}^*, K_M^*)$ is ranked from bottom $(\boldsymbol{\theta^*})^{1st}$ to top $(\boldsymbol{\theta^*})^{1000th}$. The lower $(\boldsymbol{\theta}_{lower})$ and the upper $(\boldsymbol{\theta}_{upper})$ 95% confidence intervals for the six estimated parameters in the model are $(\delta^*, \alpha_1^*, \alpha_2^*, p^*, V_{max}^*, K_M^*)^{25th}$ and $(\delta^*, \alpha_1^*, \alpha_2^*, p^*, V_{max}^*, K_M^*)^{975th}$, respectively.

3.4 Elasticity

Elasticity or sensitivity is a measure of responsiveness of one variable to another. Elasticity of the dependent variable (y) with respect to independent variable (x) is the ratio of the percentage change in y to the corresponding percentage change in x [8]. That is

$$\frac{\%\Delta y}{\%\Delta x} = \left(\frac{x}{y}\right)\frac{\text{change in } y}{\text{change in } x}. \tag{3.4}$$

When an elasticity is small (between 0 and 1 in absolute value), we can describe the x elasticity of y is inelastic. Inelastic y means that the y is not very sensitive to x. In contrast, when an elasticity is large (greater than 1 in absolute value), the x elasticity of y is elastic (y is sensitive to x). Elasticity of y is unitary if x elasticity of y is equal to 1.

In section 4.9, elasticity is implemented to measure the sensitivity of the linear-quadratic (LQ) parameters α and β with respect to δ and p as these (radiosensitivity and replication fidelity rates, respectively) can be manipulated. See chapter 4 for details.

3.5 Multistability

An important property of biological networks is bistability (or more generally, multistability). This is the property of coexistence of two or more stable steady states [47]. Multistability is of particular relevance to biological systems that have to switch between discrete states. Parameter perturbations or small changes in initial conditions can lead the system to jump between stable states [126].

The first example of bistability in lactose operon of Escherichia Coli was demonstrated by Novick and Weiner [118] and Cohn and Horibata [24] in the 1950s. More recent examples of bistability were found in mitogen-activated protein kinase (MAPK) cascades in animal cells [46, 94, 130, 159] and in cell cycle regulatory circuits [4, 46, 47, 165].

There is evidence that bistable responses are to be expected in biochemical reaction systems which contain positive feedback loops (e.g. where the phosphorylated substrate enhances the activation of the kinase) [46, 47, 149]. Bistability also occurs in mutually inhibitory double-negative-feedback loop systems [4, 28, 39, 85].

Bistable response curves are sigmoidal and have two important properties (see figure 3.3 for an example). The first one is hysteresis [127]. A system with hysteresis has memory. In a signalling process, once a stimulus (signal) has reached a sufficient level to switch the system to the "on" state, the system will remain on even if the stimulus is lowered back below the threshold [47]. Thus, a bistable system has the potential to remember a stimulus long after the stimulus has been removed. Second, in a bistable system, there is a discontinuity in the stimulus response curve and an intermediate response does not exist [20].

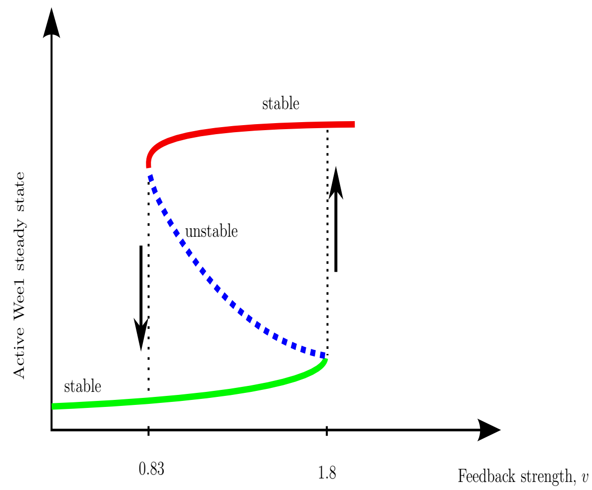

Figure 3.3: Bistable response for the Cdc2-CyclinB/Wee1 system for some range of feedback strength (after [4], figure 3d).

In chapter 6, we will extend the work of [4]. The authors show that there are parameter regimes in Cdc2-cyclin B/Wee1 system without kinase turnover for which the system exhibits bistability (see figure 3.3). We will investigate the structural stability of the system with respect to bistability if the protein turnover is taken into account. The equations of [4] are given in section 3.5.1. To modify [4], we incorporate turnover of one of the kinases. Here we explain their model.

3.5.1 The Angeli et al. model (the case of zero protein turnover)

The main idea of the work in [4] is illustrated through two examples drawn from experimental studies: the Cdc2-cyclin B/Wee1 system and the Mos/MAPK kinase p42 MAPK cascade. In this thesis, we are only interested in the simplest example, the Cdc2-cyclin B/Wee1 system. This is a four-variable system, and it can be reduced to a two-variable system without turnover. The simplified Cdc2-cyclin B/Wee1 system of [4] is shown in figure 3.4.

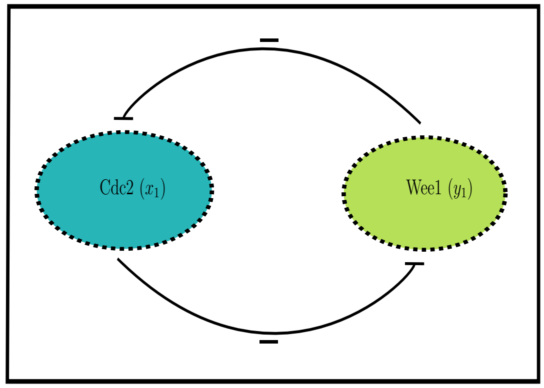

Figure 3.4: A Cdc2-cyclin B/Wee1 system: a two-component, mutually inhibitory feedback loop which one of the feedback systems that may exhibit bistability

The authors assume that there are only active and inactive forms of Cdc2-cyclinB and Wee1 (rather than multiple forms of both proteins as in reality). The authors in [4] use variables x_1 and x_2 to denote the active and inactive Cdc2, respectively, and y_1 and y_2 to denote the active and inactive Wee1, respectively. They also assume that the dephosphorylation of Cdc2 and Wee1 is caused by some unspecified phosphatase. In [4], the contribution of Cdc25 to the bistability of the Cdc2 system is neglected. See section 2.2.8 in chapter 2 for details about Cdc2 and Wee1.

Moreover, they assume that the inhibition of each kinase by the other is described by a Hill equation [45] (see section 2.2.3). Using a Hill equation with high Hill exponent assumes that inactivation of Wee1 is ultrasensitive to Cdc2 levels, and likewise inactivation of Cdc2 is ultrasensitive to Wee1. Kim and Ferrell [89] suggest that the Hill coefficient γ is 3.5 by fitting experimental data to the Hill equation.

Using all the above assumptions, the equations proposed in [4] are,

$$\dot{x}_1 = \alpha_1 x_2 - \frac{\beta_1 x_1 (\nu y_1)^{\gamma_1}}{K_1 + (\nu y_1)^{\gamma_1}} \tag{3.5}$$

$$\dot{x}_2 = -\alpha_1 x_2 + \frac{\beta_1 x_1 (\nu y_1)^{\gamma_1}}{K_1 + (\nu y_1)^{\gamma_1}} \tag{3.6}$$

$$\dot{y}_1 = \alpha_2 y_2 - \frac{\beta_2 y_1 (x_1)^{\gamma_2}}{K_2 + (x_1)^{\gamma_2}} \tag{3.7}$$

$$\dot{y}_2 = -\alpha_2 y_2 + \frac{\beta_2 y_1 (x_1)^{\gamma_2}}{K_2 + (x_1)^{\gamma_2}} \tag{3.8}$$

where α_1 and α_2 are the rate of phosphorylation which are constants, K_1 and K_2 are Michaelis constants, γ_1 and γ_2 are Hill coefficients and ν measures the strength of the influence of Wee1 on Cdc2-cyclinB (alternatively, this measure provides a sense of the strength of the inhibition of Cdc2 by Wee1).

Without protein turnover the total concentrations of Wee1 and Cdc2-cyclinB are unchanging, thus the sum of (3.5) and (3.6) gives $\dot{x}_1 + \dot{x}_2 = 0$ and the sum of (3.7) and (3.8) gives $\dot{y}_1 + \dot{y}_2 = 0$.

Let S and T be the total concentrations of Cdc2-cyclinB and Wee1, respectively. Then, without kinase turnover for all time $S(t)$ and $T(t)$ are constant, so that $S(t) = S$ and $T(t) = T$. If we substitute

$$x_2 = S - x_1$$

and

$$y_2 = T - y_1,$$

into the model equations in (3.5)-(3.8), and non-dimensionalise the variables x_1 and y_1, we obtain

$$\dot{x}_1 = \alpha_1 (1 - x_1) - \frac{\beta_1 x_1 (\nu y_1)^{\gamma_1}}{K_1 + (\nu y_1)^{\gamma_1}}, \tag{3.9}$$

$$\dot{y}_1 = \alpha_2 (1 - y_1) - \frac{\beta_2 y_1 (x_1)^{\gamma_2}}{K_2 + (x_1)^{\gamma_2}}. \tag{3.10}$$

The authors of [4] demonstrate the dynamic behavior of x_1 and y_1 for some specific values of parameters (see table 6.1 in chapter 6). This system exhibits bistability, with two attracting steady states: one corresponding to mitosis (a high concentration of Cdc2-cyclinB) and one to interphase (a high concentration of Wee1) for feedback strength $0.83 < \nu < 1.8$. See [4] for further details.

3.5.2 Method for dealing with multivariate polynomials

From (3.9)-(3.10), we have multivariate polynomials. Next, we will discuss some methods which are important in these kind of polynomials.

3.5.2.1 Resultant of two-variable polynomials, R

Suppose that

$$g(x,y) = a_n(x)y^n + a_{n-1}(x)y^{n-1} + a_{n-2}(x)y^{n-2} + .. + a_1(x)y + a_0(x) \tag{3.11}$$

and

$$h(x,y) = b_m(x)y^m + b_{m-1}(x)y^{m-1} + b_{m-2}(x)y^{m-2} + .. + b_1(x)y + b_0(x). \tag{3.12}$$

Then the resultant $R(g,h)$ of g and h with respect to y is the determinant of the $(m+n)\times(m+n)$ Sylvester matrix of g and h [21]:

$$R(g,h) = \begin{vmatrix} a_n(x) & a_{n-1}(x) & a_{n-2}(x) & \cdots & a_1(x) & a_0(x) & \cdots & 0 \\ \vdots & \vdots & \ddots & \vdots & \vdots & \vdots & \ddots & \vdots \\ 0 & 0 & \cdots & a_n(x) & a_{n-1}(x) & \cdots & \cdots & a_0(x) \\ b_m(x) & b_{m-1}(x) & \cdots & b_1(x) & b_0(x) & 0 & \cdots & \cdots \\ \vdots & \vdots & \ddots & \cdots & \vdots & \vdots & \ddots & \vdots \\ 0 & 0 & \cdots & \cdots & b_m(x) & b_{m-1}(x) & \cdots & b_0(x) \end{vmatrix}. \tag{3.13}$$

From (3.13), we get a polynomial in terms of x. Resultants are applied for solving simultaneous systems of polynomial equations and allow one to eliminate a variable from a system of equations. This is why resultants are also known as eliminants.

In chapter 6, we will be interested in the properties of a polynomial in one variable as the parameters change. To investigate these properties we will consider the discriminant of the polynomial (the discriminant of the polynomial is the resultant between this polynomial and its derivative). See next section for details.

3.5.2.2 Discriminant of a polynomial, Δ

Suppose that $Q(x)$ is a one-variable polynomial given by

$$Q(x) = c_r x^r + c_{r-1}x^{r-1} + c_{r-2}x^{r-2} + .. + c_1 x + c_0. \tag{3.14}$$

The discriminant Δ of $Q(x)$ is given by [21]

$$\Delta = (-1)^{\frac{1}{2}r(r-1)} \frac{1}{c_r} R(Q, Q'), \tag{3.15}$$

where $R(Q, Q')$ is known as the resultant of $Q(x)$ and the derivative of Q with respect to x, $Q'(x)$ which can be obtained by the determinant of the $(2r-1)\times(2r-1)$ Sylvester matrix in (3.13). (See section 3.5.2.1 for the details of the resultant R).

3.5.2.3 Sturm's theorem and Cauchy's bound for real roots

This is a very useful theorem for working with polynomials. It gives an algebraic procedure for determining the number of distinct real roots of a polynomial. As we noticed that polynomial characteristics are always of interest in the analysis of differential equations in mathematical modelling, the Sturm theorem [70] can be a great tool for counting the real zeroes of the equations.

To apply the Sturm theorem, we need a Sturm chain. Let the polynomial

$$P(x) = a_n x^n + a_{n-1}x^{n-1} + \cdots + a_1 x + a_0. \tag{3.16}$$

Definition 1. *A Sturm chain or Sturm sequence is a finite sequence of polynomials $P_0, P_1, \cdots, P_n$ such that*

$$\begin{aligned}
&P_0(x) = P(x),\\
&P_1(x) = P'(x),\\
&P_2(x) = -rem(P_0, P_1) = P_1(x)q_2(x) - P_0(x),\\
&P_3(x) = -rem(P_1, P_2) = P_2(x)q_3(x) - P_1(x),\\
&\vdots\\
&P_{n-1}(x) = -rem(P_{n-3}, P_{n-2}) = P_{n-2}(x)q_{n-1}(x) - P_{n-3}(x),\\
&P_n(x) = -rem(P_{n-2}, P_{n-1}) = P_{n-1}(x)q_n(x) - P_{n-2}(x),\\
&0 = -rem(P_{n-1}, P_n).
\end{aligned} \tag{3.17}$$

where $P(x)$ is a polynomial in one variable x with real coefficients having no repeated roots, while $rem(P_0, P_1)$ and $q_2(x)$ are the remainder and the quotient, respectively when dividing the polynomial P_0 by P_1. Note that this chain is terminated when a zero remainder is obtained.

Theorem 3.5.1. *Suppose $P(x)$ has the Sturm chain $P_0(x)$, $P_1(x)$,..., $P_n(x)$ as above. For all $t \in \mathbb{R}$, let $N(t)$ be the number of sign changes in the sequence $P_0(t)$, $P_1(t)$,...,. Then for any interval $J = [a, b]$, the number of real roots of $P(x)$ in J is $N(a) - N(b)$.*

Sturm's theorem can be used to calculate the total number of real roots of polynomials by choosing a and b appropriately. One can use the Cauchy Criterion to determine a and b [90]. The Cauchy Criterion states that all real roots of a polynomial (3.16) are in the interval $[-M, M]$, where:

$$M = 1 + \frac{max_{0 \le i \le n-1}|a_i|}{|a_n|}. \tag{3.18}$$

3.5.2.4 An example of cubic polynomial

Suppose we are given a system of two differential equations given by:

$$\begin{aligned} \frac{dx}{dt} &= f_1(x, y, p, q) \\ \frac{dy}{dt} &= f_2(x, y, p, q). \end{aligned} \tag{3.19}$$

f_1 and f_2 are polynomials in two variables x and y, and in parameters p and q. To obtain the equilibrium points of (3.19), we set

$$\begin{aligned} f_1(x, y, p, q) &= 0 \\ f_2(x, y, p, q) &= 0. \end{aligned} \tag{3.20}$$

Using resultant (section 3.5.2.1), we can eliminate y from (3.20), thus we obtain a polynomial $P(x, p, q)$, the zeros of which are the $x-$coordinates of the equilibria (x^*, y^*).

In chapter 6, we deal with the roots of an odd-degree polynomial, that is a 17−degree polynomials to analyse the equilibrium points of the Cdc2-cyclinB/Wee1 system with protein turnover parameters a and d. To develop an understanding of the relationship between the roots of a polynomial and its coefficients, we present the simplest example of an odd-degree polynomial that has more that one root. Here we consider a cubic function given by:

$$P(x, p, q) = -x^3 - px + q, \tag{3.21}$$

in parameters p and q. Thus, by setting $P(x) = 0$ or $-x^3 - px + q = 0$, we can find the roots of the polynomial equation as p and q vary. Figure 3.5 and figure 3.6 show where the roots are located on the x-axis.

We now pose the question: What is the condition for (3.21) to have one, two and three roots?. We can distinguish several possible cases depending on the discriminant Δ (section 3.5.2.2) [37]:

1. If $\Delta < 0$, then the equation has one real root and a pair of complex conjugate roots.

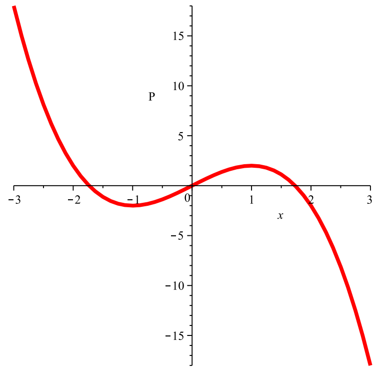

Figure 3.5: Three roots of a cubic equation with $p = -3$ and $q = 0$ in (3.21).

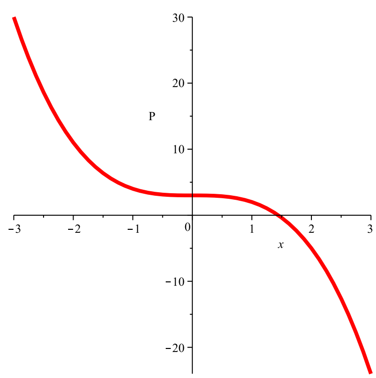

Figure 3.6: One root cubic equation with $p = 0$ and $q = 3$ in (3.21).

2. If $\Delta > 0$, then all roots (three roots) are real and unequal.

3. If $\Delta = 0$, then the equation has three real roots and at least two are equal.

To obtain the resultant of the cubic polynomial in (3.21), the first derivative of $P(x)$ is given by

$$P'(x) = -3x^2 - p. \tag{3.22}$$

Therefore, using MAPLE 12 the discriminant of P is

$$\Delta = -27q^2 - 4p^3. \tag{3.23}$$

In order to distinguish several possible cases which are based on the number of roots or equilibrium points, we need to plot $\Delta = 0$ (3.23). This defines a curve in the (p, q) parameter space (see figure 3.7).

From the figure, it is shown that the number of equilibrium point of system in (3.21) depends on p and q. Consequently, one may ask : For what range of (p, q) does the equation have three roots, two roots and one root? Hence, we have

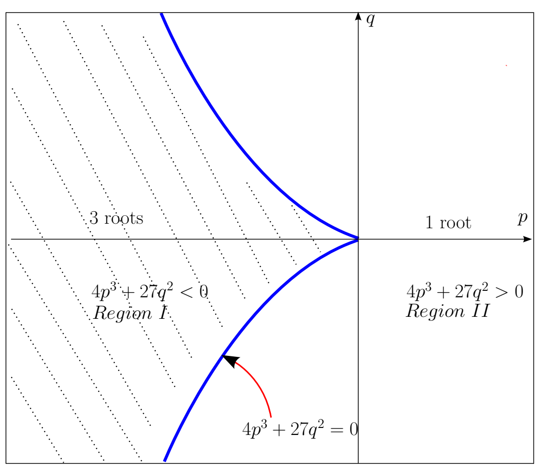

Figure 3.7: The domain of the equation having three real roots (*Region* 1) and one real root (*Region II*).

1. If $-4p^3 - 27q^2 < 0$ the equation has one real root and a pair of complex conjugate roots.

2. If $-4p^3 - 27q^2 > 0$ all the roots are real and unequal.

3. If $-4p^3 - 27q^2 = 0$ the equation has three real roots and at least two are equal.

3.6 Conclusion

In this chapter we have briefly described several mathematical concepts that are used to develop the cell population model in chapter 4, the modelling of ATM dynamics in chapter 5, and the example of a structurally unstable bistable system in chapter 6.

Chapter 4

A mechanistic model of high dose irradiation damage

4.1 Introduction

It is of vital importance to understand ionising radiation damage to mammalian cells. In this chapter, we suggest a framework to model cell population evolution following high dose irradiation. Our model, under certain assumptions, easily leads to the popular LQ relation which is reviewed in chapter 2.

4.2 Issues with Albright's model

It is worthwhile to note that the model of Albright [2] looks very close to the model that we develop. For Albright's notation, see section 2.6.3. We start by clarifying the differences between our model and [2]:

1. Albright assumed that all misrepairs are lethal and any misrepaired lesion causes immediate removal of the cell from the population. However, there is evidence that misrepaired lesions can be nonlethal [64]. Thus, we believe that the population should be structured according to the number of DSBs

and the number of misrepairs.

2. The quadratic repair process that is proposed in [2] does not have a mechanistic basis.

3. Albright does not discuss the effect of dose fractionation.

4. In Albright's model, there is no discussion of parameter estimation. This is certainly an important issue in mathematical modeling as we want to know what is information that we can get from the model that we developed, since some of the information that we got from modeling cannot be found through experimental results. For an example, the cells' radiosensitivity. This study also will be part of our main objective. This will be explained in detail in section 4.8 in this chapter.

Based on Albright's assumptions and some remarks on his model, we can conclude that there are some differences between our model and [2]. The reader will please bear in mind that initially we developed our model in complete ignorance of Albright's work as we mentioned in section 2.6.3. Without using the Markov process approach, the model that we develop here is definitely independent from the model proposed by Albright. The aim of our work is to develop a better and more realistic model that would be able to describe the survival of mammalian cells after being exposed to ionising radiation.

4.3 Model assumptions

As in most work on cell survival under radiation, we make the following three assumptions: (1) The integrity of the DNA in the cell is responsible for preserving the cell's reproductive capacity; (2) Ionising radiation can break molecular bonds in the double helix, causing double strand breaks (DSBs); (3) Such lesions can be repaired or misrepaired; we also assume that not all misrepairs are lethal damage [124].

For truly realistic models [66], one should also assume that the cell dies only as it attempts mitosis. At this stage we do not make this assumption, but when repopulation is introduced into the model, it will have to be made, with the consequence that cell cycle dynamics will have to be incorporated explicitly. Thus below we are assuming that the most significant contribution to death rate of cells is interphase death. However, some evidence shows that apoptosis may not be the dominant mode of cell death following ionising radiation [15, 64, 77].

4.4 Limitations of the model

There are four limitations that need to be acknowledged regarding the present model. The first limitation is that the model does not allow repopulation as already mentioned in section 4.3. The second limitation is that the model does not incorporate any representation of the cell cycle. The third limitation is that the model does not allow cells to become quiescent, and the forth limitation is that the model has very simplified "models" of DSB repair and cell death. For truly realistic and more complex model, one should incorporate all these effects into the model. At this stage, we wanted to construct not so much a final model (because many things are unknown), but a "modeling framework" that can be built upon.

4.5 A structured population modeling approach

According to [31, 153], a population is structured if every individual is assigned by a particular class or cohort. The categorisation of individuals can be based on chronological age, life cycle stages, size, etc. In contrast, in unstructured populations, individuals within the population are assumed to be identical and thus only population averages are considered.

Structured population models are more realistic model since they are derived from the individual-based models by taking into account events from birth till death. The state of a population is no longer described by a single number, but by the distribution of the individuals among cohorts.

There are several formalisms used to model structured population (see [153] for details). One of them is matrix models. In the 1940's, matrix models for structured populations were discovered by Leslie [153]: these are used in discrete time, describing projection of a population from time t to $t+1$. Since we are not focusing on discrete models, we refer the reader to [31, 153] for details.

In this chapter, we suggest using the framework of structured population theory [31, 153]. This means that we are saying that the population of cells can be structured into cohorts, and that a cell can travel between these cohorts under the influence of radiation or as a result of radiation damage repair attempts. Usually one structures populations according to size, age, or developmental stage. In our case it makes sense to structure a population according to the radiation damage incurred after a dose of radiation. Any structuring criterion that could be directly related to irradiation, damage repair and cell death would be acceptable. On the other hand, just taking the number of DSBs as the proxy of radiation damage does not seem to us sufficient, misrepairs also must be taken into consideration as already discussed in section 2.6.3.

We proceed as follows. We use a two-dimensional vector (k, m) to structure a population, where k is the number of DSBs a cell has and m is the number of misrepaired lesions. Making the death rate function in our model dependent on the number of misrepairs seems to us much more realistic than Albright's [2] approach. The only stochastic element in our model is the initial conditions of the ODE system. All the rest is deterministic: if the initial condition is known, one may know the state of the system for any subsequent time.

In a subsequent section, we extend the model by studying the effect of dividing the dose D in two fractions, separated by a time interval T. This is followed by a discussion of parameter estimation. We use MATLAB to simulate the model, to quantify the dose fractionation effect, and also to estimate model parameters.

We consider an initial population of $N(0)$ ($N_0 = N(0)$) cells being subjected to a dose of radiation D which results in $N_{k,0}(0)$ cells having k DSBs. Thus the total cell population $N(t)$ satisfies

$$N(0) = \sum_{k=0}^{k_{max}} N_{k,0}(0), \tag{4.1}$$

k_{max} is the maximum number of DSBs produced in the cell population just after being exposed to irradiation. The average DSB load is

$$U(0) = \frac{\sum_{k=0}^{k_{max}} kN_{k,0}(0)}{\sum_{k=0}^{k_{max}} N_{k,0}(0)}. \tag{4.2}$$

We will discuss k_{max} and the method for generating $N_{k,0}(0)$ in the following section.

We want to specify the laws for the evolution of $N_{k,m}(t)$. If Δt is an increment of time,

$$N_{k,m}(t+\Delta t) = N_{k,m}(t) - \Delta t\beta(k,m)N_{k,m}(t) - \Delta t\sum_{l=1}^{k}\gamma(k,m,l)N_{k,m}(t)$$
$$+\Delta t\sum_{j=0}^{m}\sum_{i=0}^{k_{max}-k-m} p(k+i+j,m-j,i,j)\gamma(k+i+j,m-j,i+j)N_{k+i+j,m-j}(t).$$

Let us explain the notation we are using:

- $\beta(k,m)$ is the death rate of cells with k DSBs and m misrepaired lesions.
- $\gamma(k,m,l)$, $k \geq l$ is the rate at which a cell with k DSBs and m misrepaired lesions repairs simultaneously l of them.
- $p(k+i+j,m-j,i,j)$, $0 < i+j \leq k$, $i+j = l$ is the probability that a cell with k DSBs and m misrepaired lesions will repair i correctly and j incorrectly in a unit of time.

There is evidence that DSBs can be repaired more than one at a time [115]. However due to time constraints, at this stage we only consider the case for $l =$

1 (DSBs are repaired one-at-a-time). The formulation of model of DSB repair queueing system as suggested by [115] should be made once a queueing DSB repair term is added into the model that we develop. Thus consequently we assume that $\gamma(k,m,l) = 0$ if $l > 1$ and we will put $\gamma(k,m,1) \equiv \gamma(k,m)$. If $l = 1$, then $i + j = 1$. This means the model contains two populations; one has $i = 1, j = 0$, and the other has $i = 0, j = 1$ after DNA repair process. For $i = 1, j = 0$, we put $p(k+1,m,1,0)$, whereas for $i = 0, j = 1$, we put $p(k+1,m-1,0,1)$. Hence by passing to the limit $\Delta t \to 0$ we obtain:

$$\begin{aligned}\frac{dN_{k,m}}{dt} = &- \beta(k,m)N_{k,m} - \gamma(k,m)N_{k,m} + p(k+1,m,1,0)\gamma(k+1,m)N_{k+1,m} \\ &+ p(k+1,m-1,0,1)\gamma(k+1,m-1)N_{k+1,m-1}. \qquad (4.3)\end{aligned}$$

Now we want to argue on biological grounds that some of the dependencies of the functions β, γ and p on the variables k or m can be safely neglected.

The rate of repair depends only on the availability of the repair machinery [100] and the number of DSBs [140]. In [100], it is demonstrated that cells lacking signalling protein show DSB repair defect. Hence it makes sense to put $\gamma(k,m) \equiv \gamma(k)$ and

$$p(k,m,1,0) = p(k,1,0) = 1 - p(k,0,1), \qquad (4.4)$$

with all the other probabilities being zero. We will thus denote for simplicity the probability of a successful repair of a DSB given that the cell has k DSBs by $p(k)$.

Finally, all the indications in the literature are that $\beta(k,m)$ depends both on k and on m, the number of unrepaired and of misrepaired lesions, respectively. (See section 4.5.2). This means that the final form of the equations we are investigating is

$$\begin{aligned}\frac{dN_{k,m}}{dt} = &- \beta(k,m)N_{k,m} - \gamma(k)N_{k,m} + p(k+1)\gamma(k+1)N_{k+1,m} \\ &+ (1-p(k+1))\gamma(k+1)N_{k+1,m-1}, \qquad (4.5)\end{aligned}$$

for $k = 0, 1, 2, \cdots, k_{max}$ and $m = 0, 1, 2, \cdots, k_{max}$ with $k + m \leq k_{max}$. The brief schematic description of the cell survival model is shown in figure 4.1.

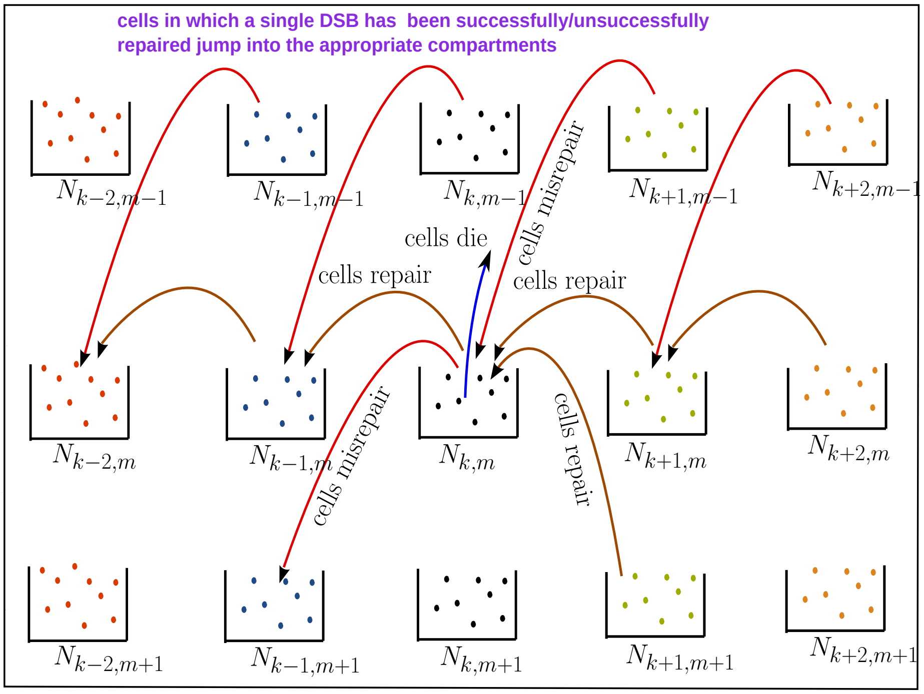

Figure 4.1: The figure shows the brief schematic description of the cell survival model determined by the value of k and m.

We note that it is impossible to structure the population simply by the number k of DSBs since the death rate depends on the number m of misrepairs.

Below we shall assume for simplicity that in simulations we always put $p(k)$ is just a constant, say $p(k) = \eta$. In [151], the author also makes the same assumption. $p(k)$ is very important in both tumour and normal tissues. In particular, decreasing repair fidelity is a possible strategy for increasing tumour radiosensitivity.

Next we need to consider in detail a reasonable form of the repair rate function $\gamma(k)$ and death rate function $\beta(k, m)$.

4.5.1 Repair rates

The repair rate $\gamma(k)$ describes the rate of single DSB repair for a cell having k DSBs. [14, 146, 147] argue for a saturable lesion repair process. Sontag [146] suggests that the repair process can be described by Michaelis-Menten kinetics. Thus,

$$\gamma(k) = \frac{V_{max}k}{K_M + k}, \qquad k = 0, 1, 2, \ldots \tag{4.6}$$

where V_{max} is the maximum repair rate and K_M, the Michaelis-Menten constant, is the number of DSBs at which the repair rate is half of V_{max}. The Michaelis-Menten plot of the repair rate γ is shown in figure 4.2.

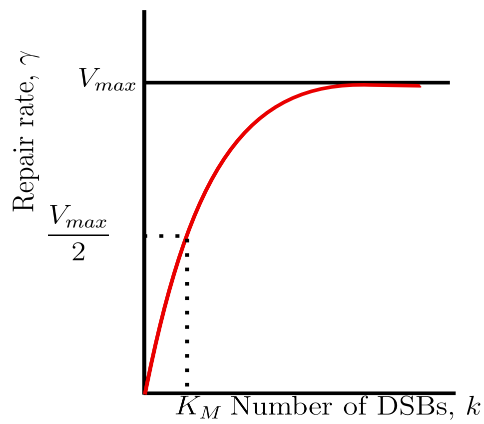

Figure 4.2: Michaelis - Menten plot of the repair rate γ against the number of DSBs k.

4.5.2 Death rates

We consider two reasons for interphase death. First, a cell can die due to misrepair of a DSB. Clearly, the probability of such an event is proportional to m [84]. Second, the cell also can die if there are two DSBs located in spatial proximity, which can interact to produce a lethal chromosome aberration. The probability of such an event is proportional to k^2. In [148], the author notes that cell lethality is proportional to the square of the number of unrepaired DSBs in a cell. Hence the form of death rate we adopt in the present thesis is

$$\beta(k, m) = \alpha_1 m + \alpha_2 k^2. \tag{4.7}$$

where α_1 is a misrepair rate constant while α_2 is a lethal binary misrepair rate constant. It is clear that in this modelling framework all the functional dependencies (of cell death, DSB repair rates, fidelity of repair) can be easily modified as new experimental data becomes available.

4.6 Initial condition

We assume that new DSBs are produced immediately on irradiation. Following the experimental work of [124, 134, 135], who measure γ-H2AX phosphorylation foci, a direct biomarker of DSBs, we assume that the probability of a cell acquiring k DSBs follows a Poisson distribution with mean

$$\lambda = \delta D, \tag{4.8}$$

where D is the radiation dose (in Grays) and δ is a measure of the radiosensitivity of cells. [148] suggests $\delta = 25$ per Gray per cell for Chinese hamster cells, while [99] sets $\delta = 40$ per Gray per cell for human cells. Thus the probability of a particular cell acquiring $k \geq 0$ DSBs is given by

$$P(\text{no. DSBs} = k) = \frac{\lambda^k e^{-\lambda}}{k!}. \tag{4.9}$$

Note that in radiation oncology δ is a *priori* unknown, and has to be estimated from cell survival data, together with the rest of the kinetic parameters of the model.

In our MATLAB simulations, given a total number N_0 of cells, in each run we sample the Poisson distribution randomly using the `poissrnd()` function, to create the array $\{N_{k,0}(0)\}$, with k_{max} being the maximum number of DSBs in the sample. As an example, we use population of 10000 cells and the results are then averaged over 20 runs.

4.7 Solving the system of ODEs

The model that we discussed in the last section contains M ODEs where M depends on k_{max}, that is

$$M = \frac{(k_{max}+1)(k_{max}+2)}{2}. \tag{4.10}$$

The system can be written as

$$\frac{d\mathbf{N}}{dt} = A\mathbf{N}, \tag{4.11}$$

where the $M \times M$ matrix A is defined by the equations in (4.5). The solution of (4.11) is given by

$$\mathbf{N}(t) = \mathbf{N}(0)e^{At}. \tag{4.12}$$

We discussed the generation of the (random) initial conditions $\mathbf{N}(0)$ in section 4.6. Note that, $N_{k,m}(0) = 0$ if $m > 0$ $\forall k \in \{0, k_{max}\}$.

To solve the system (4.11), we use MATLAB. The code can be found in appendix A.2 at the end of the thesis. The algorithm contains five steps in order to compute the survival fraction of cells. The algorithm proceeds as follows:

(1) Generate random initial conditions, $\mathbf{N}(0)$ (see section 4.6). As in section 4.6, the dose D is incorporated into the system through the initial conditions. At this step, we fix a dose D (see equation (4.8)), so that the value of mean λ can be computed to generate the initial conditions.

(2) Solve the system (4.11) up to time $t = T$ for $T = 24$ hours. This number is chosen just to make sure that the repair processes are completed. There

is evidence that the cell's repair process is almost completed 24 hours after irradiation [99]. In addition, results in [133] suggest that more than 80 % of the DSBs are repaired at repair time $T = 12$ hours.

(3) Compute the fraction of surviving cells $S = \dfrac{\sum_{k,m} N_{k,m}(T)}{\sum_{k,m} N_{k,m}(0)}$.

(4) Plot $\ln S$ versus the dose D. Due to the randomness of the initial conditions, steps (1)-(3) are repeated for twenty runs in order to get an averaged value of $\ln S$. At this step, the loop for a single dose D is completed which corresponds to a single data point. To generate several data points on a survival curve, steps (1)-(3) as well as the averaged value of $\ln S$ need to be repeated for each dose D.

(5) Fit the generated data to the LQ relation (see (2.2) in chapter 2) using *fminsearch* (chapter 3) in MATLAB.

In the present thesis, we generate 31 simulation data points for the value of parameters: $\delta = 2$ Gy^{-1} cell^{-1}, $\alpha_1 = 1.5\ h^{-1}$, $\alpha_2 = 0.001\ h^{-1}$, $p = 0.95$, $V_{max} = 1$ h^{-1}, and $K_M = 3\ \mu M$. These values and total number of data are chosen only as an example, with the values of parameters that we choose lying in the range suggested by [137, 146, 148] (see table 4.1). [137] points out that a convenient value of δ is $\approx 2 - 40$ per Gy per cell depending on the type of cells. To estimate the value of α_2, [148] used survival data for CHO cells and suggest that α_2 lies between 0 per hour and 0.001 per hour, while $\alpha_1 \approx 0.0277 - 20.79$ per hour. As listed in the table, [146] estimate the range of the value of V_{max} and K_M by using 11 experimental survival data sets obtained with different cells lines and different types of radiation.

parameter	lower bound	upper bound
δ	2 Gy^{-1} cell^{-1}	40 Gy^{-1} cell^{-1} [137]
α_1	0.0277 h^{-1}	20.79 h^{-1}[148]
α_2	0 h^{-1}	0.005 h^{-1} [148]
p	0	1
V_{max}	0.1 h^{-1}	3 h^{-1} [146]
K_M	0 μM	5 μM [146]

Table 4.1: The parameter space is restricted to the range of values which are taken from the literature. Units of all the parameters that used in this chapter are as stated in the table.

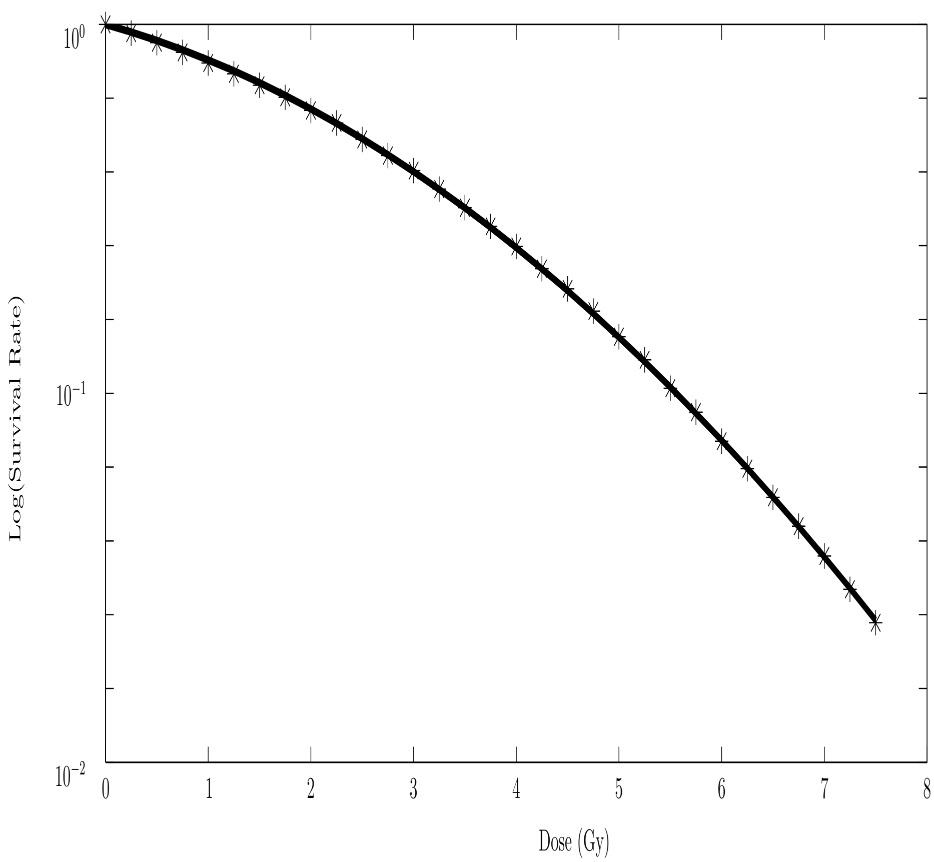

Figure 4.3: The simulation result for single dose D (asterisks) at $t = 24$ hours for $\delta = 2$ Gy^{-1} cell^{-1}, $\alpha_1 = 1.5\ h^{-1}$, $\alpha_2 = 0.001\ h^{-1}$, $p = 0.95$, $V_{max} = 1\ h^{-1}$, and $K_M = 3\ \mu M$. The simulation data is then fitted to LQ relation $\ln S = -0.0896D - 0.0211D^2$ (solid line).

In figure 4.3 we show the survival data ($*$) averaged over 20 runs of the model, and fit them to an LQ relation (2.2) (solid curve). The fit is very good, which indicates that the biological assumptions we have made concerning repair, misrepair, and cell death processes are adequate to account for the LQ relation.

Figure 4.4 plots several survival curves as parameters are varied. The figures 4.4(a), (b), (c), and (f) show that the fraction of cells surviving decreases when δ, α_1, α_2 and K_M are increased, while figure 4.4(d) and (e) show that the cell survival fraction increases as p and V_{max} increase. Figure 4.4(a) illustrates that the more radiosensitive the cells are, the more cells die, while figure 4.4(d) shows that more cells will survive if the damage repair fidelity is increased.

A model such as the one proposed in this section can be used in therapy protocols as we shall explain in section 4.9.

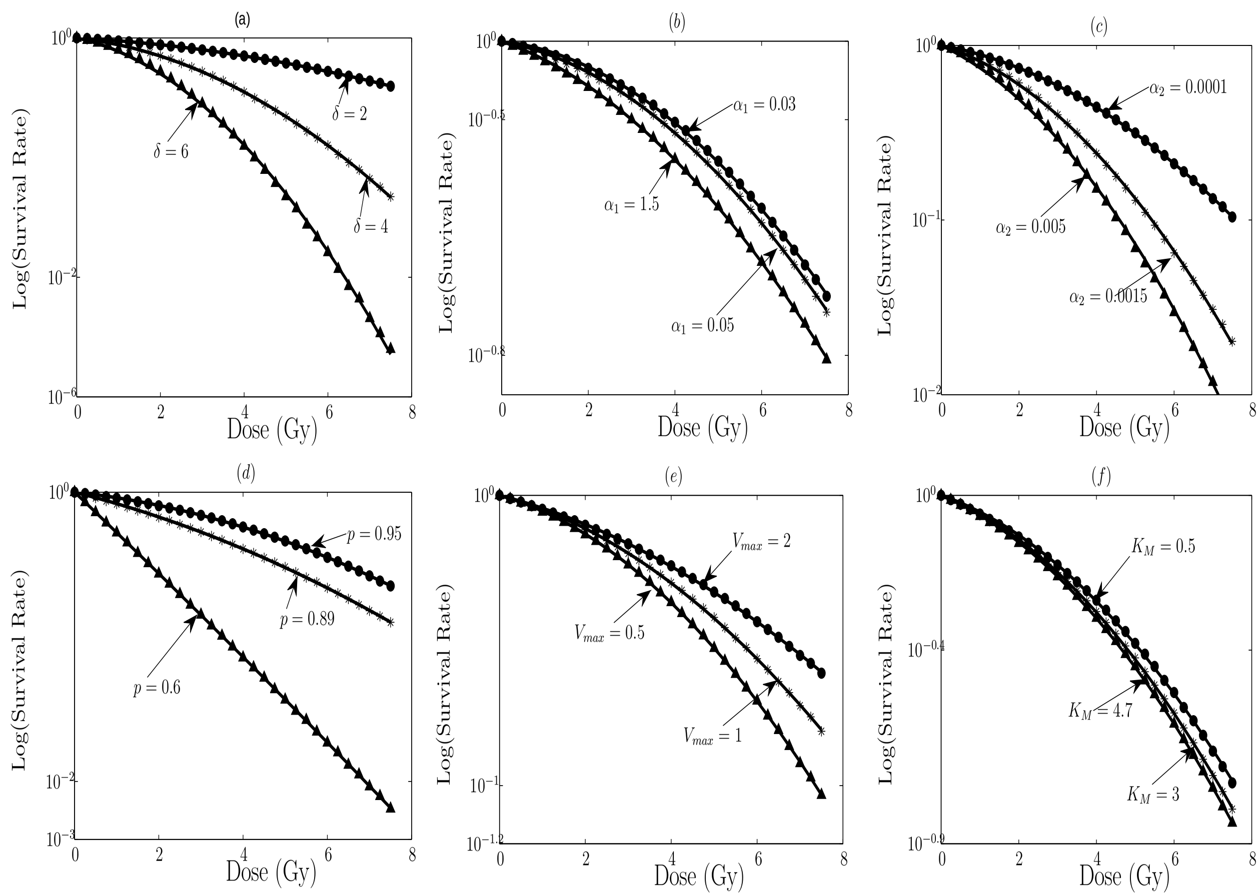

Figure 4.4: The simulation results at $T = 24$ hours and for the parameter values $\delta = 2$ Gy^{-1} cell^{-1}, $\alpha_1 = 1.5\ h^{-1}$, $\alpha_2 = 0.001\ h^{-1}$, $p = 0.95$, $V_{max} = 1\ h^{-1}$, and $K_M = 3\ \mu M$. Subfigures (a)-(f) contain survival curves for different values of each parameter.

4.8 Model parameter estimation

In this section, the main goal is to estimate a parameter set $\boldsymbol{\theta} = (\delta, \alpha_1, \alpha_2, p, V_{max}, K_M)$ in the model (equation 4.5) that minimise the sum of squared errors (SSE), $\phi(\boldsymbol{\theta})$ between n number of survival data and the model data (see section 3.3 in chapter 3). We estimate the six model parameters using two different types of optimisation methods; i.e a local and a global optimisation techniques namely: Nelder-Mead (NM) simplex algorithm (see section 3.3.2) and Simulated Annealing (SA) algorithm (see section 3.3.3), respectively. Performance of both optimisation methods are evaluated based on the value of the objective function (SSE), computational time and number of iteration.

In addition, we compute the confidence interval of each estimated parameters to obtain the estimated interval of the true parameter values. See section 3.3.4 for details about confidence interval (CI). We use a 95% confidence interval for our analysis which means that we are 95% sure that the true parameter value lies within the range. Then, we check the reliability of the algorithms by estimating the six parameters in the model again using the same SA and NM simplex algorithms when some of the value of parameters are known exactly. In this case, performance of both optimisation methods are evaluated based on the percentage difference between the mean of true values and the estimated values of parameters and also the value of the objective function (SSE) for both algorithms.

4.8.1 Parameter estimation by NM simplex and SA algorithms

In this section, we use two experimental data sets from the tissue which has been irradiated by IR with different LET. These are the experimental cell survival data for mouse embryonic cells, $C3H10T1/2$, and human melanoma cell line, Mel202. The mouse embryonic cells population were irradiated with different doses of iron particles (high LET) taken from [164], while the human melanoma cell line was irradiated with different doses of x-rays (low LET) taken from [156]. The mouse embryonic cells were incubated for 5 to 6 weeks, while the human melanoma cell lines were incubated for 14 days for colony formation. The experimental data points are plotted in figure 4.5. For notation, α_{exp} and β_{exp} refer to the LQ parameters for experimental data. See chapter 2 for details about LQ relation. These parameters are obtained by fitting the experimental data in figure 4.5 to the LQ relation.

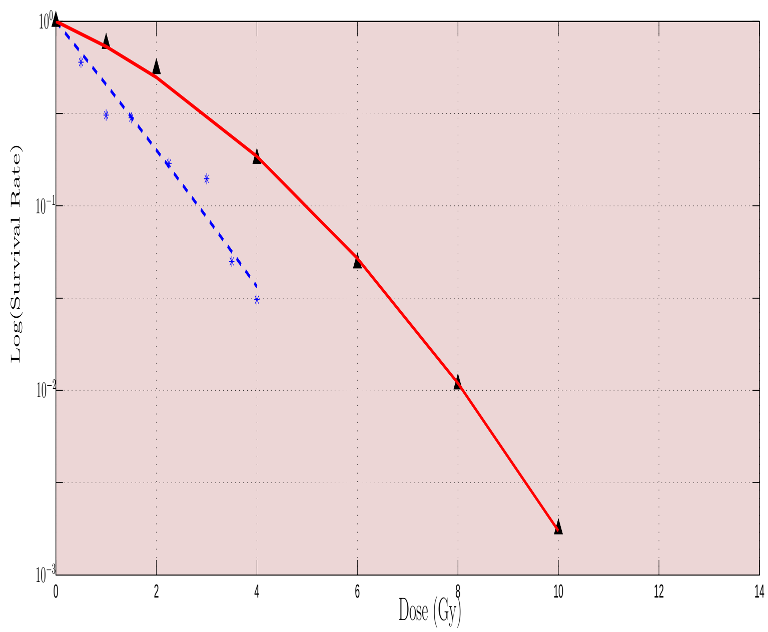

Figure 4.5: The survival data of human melanoma cell lines Mel202 (triangles) and mouse embryonic cells C3H10T1/2 (asterisks). Both of the data sets are fitted to LQ relation $\ln S = -0.2790D - 0.0357D^2$ where $\alpha_{exp} = 0.279\ Gy^{-1}$ and $\beta_{exp} = 0.0357\ Gy^{-2}$ for Mel202 (solid line for low LET) and $\ln S = -0.8D - 0.01D^2$ where $\alpha_{exp} = 0.8\ Gy^{-1}$ and $\beta_{exp} = 0.01\ Gy^{-2}$ for C3H10T1/2 (dashed line for high LET) using NM simplex algorithm.

To begin the parameter estimation procedure, the NM simplex and the SA algorithms require an initial point $\boldsymbol{\theta_0} = (\theta_{10}, \theta_{20}, \theta_{30}, \theta_{40}, \theta_{50}, \theta_{60})$. This is chosen randomly within the parameters range as listed in table 4.1. We use the built-in functions in MATLAB *fminsearch* routine and *simulannealbnd* routine, which perform the Nelder-Mead simplex algorithm and the simulated annealing algorithm, respectively. The steps of the Nelder-Mead simplex and SA procedures that are applied here are explained in section 3.3.2 and section 3.3.3, respectively. See appendix A.4.1 and A.5.1 for the MATLAB codes.

Table 4.2 presents the parameter estimation results for 150 random initial points $\boldsymbol{\theta_0}$ (ie corresponds to 150 rounds of parameter estimation algorithm). The results in the table show that NM simplex algorithm is more superior than SA algorithm for both low and high LET survival data. In particular, the value of the objective function (SSE) is much smaller than provided by SA method. In addition the value of the correlation between estimated survival data and experimental data r^2 are close to 1 which correspond to an excellent fit. Furthermore, the good fit between estimated survival data and experimental data can also be seen from the value of the LQ parameters for estimated survival data α_{model} and β_{model} which are close to α_{exp} and β_{exp}. See appendix A.4.2 and A.4.3 for the list of the estimated parameter values of low and high LET IR, respectively. The values of sample mean $\bar{x}$ and sample standard deviation s of each parameter which corresponds to the results in table 4.2 are also provided in table 4.3.

It should be noted that computational time of the optimisation runs till convergence using NM simplex technique are shorter (i.e < 1 minute) than using the SA algorithm (i.e > 1 hours).

For a single run of both algorithms, figure 4.6 (for low LET) and figure 4.7 (for high LET) describe the objective function (SSE) for both of the algorithms. The figures show that the NM method provides a fewer number of iterations than the SA simplex method to converge to the minimum value of SSE.

Type of IR	Algorithm name	Estimated parameter values (mean)						SSE (mean)	r^2 (mean)	LQ parameters (mean)	
		δ	α_1	α_2	p	V_{max}	K_M			α_{model}	β_{model}
Low LET	NM simplex	2.0036	8.4955	0.0056	0.8812	1.4802	4.2021	0.0016	0.9998	0.2771	0.0359
	SA	2.0001	11.6092	0.0061	0.9993	2.9897	0.0123	35.9961	0	1.2256	0.0335
High LET	NM simplex	3.7092	6.4476	0.0017	0.7368	2.554	1.0664	0.0784	0.9572	0.7377	0.0246
	SA	2.0037	10.3327	0.0050	0.989	2.8604	0.1924	2.5483	0	1.0853	0.0788

Table 4.2: The summary of optimisation results for 150 rounds of NM simplex and SA algorithms using low and high LET IR cell survival curve. The LQ parameters of the estimated survival data α_{model} and β_{model} are computed using the model simulation data which are obtained by the six estimated parameters. The estimated survival data is then fitted to the LQ relation to get α_{model} and β_{model}. For low LET, $\alpha_{exp} = 0.2790$ and $\beta_{exp} = 0.0357$, while for high LET, $\alpha_{exp} = 0.8$ and $\beta_{exp} = 0.01$.

Algorithm	**Parameter**	**Sample mean, $\bar{x}$**		**Sample standard deviation, s**	
		Low LET	High LET	Low LET	High LET
NM Simplex	δ	2.0036	3.7092	0.0141	0.7435
	α_1	8.4955	7.7148	7.4806	7.3445
	α_2	0.0056	0.0015	0.0028	0.0014
	p	0.8812	0.7368	0.0507	0.1322
	V_{max}	1.4802	2.5540	0.8248	0.7134
	K_M	4.2021	1.587	1.3790	1.53
SA	δ	2.0001	2.0037	0.0004	0.0171
	α_1	11.6092	10.3327	6.3235	6.2980
	α_2	0.0061	0.005	0.0038	0.0036
	p	0.9993	0.9890	0.0036	0.0246
	V_{max}	2.9897	2.8604	0.0482	0.1868
	K_M	0.0004	0.1260	0.0004	0.1249

Table 4.3: The sample mean $\bar{x}$ and the sample standard deviation s of the estimated value of each parameter for low and high LET data using the NM simplex and the SA algorithms. See text for details.

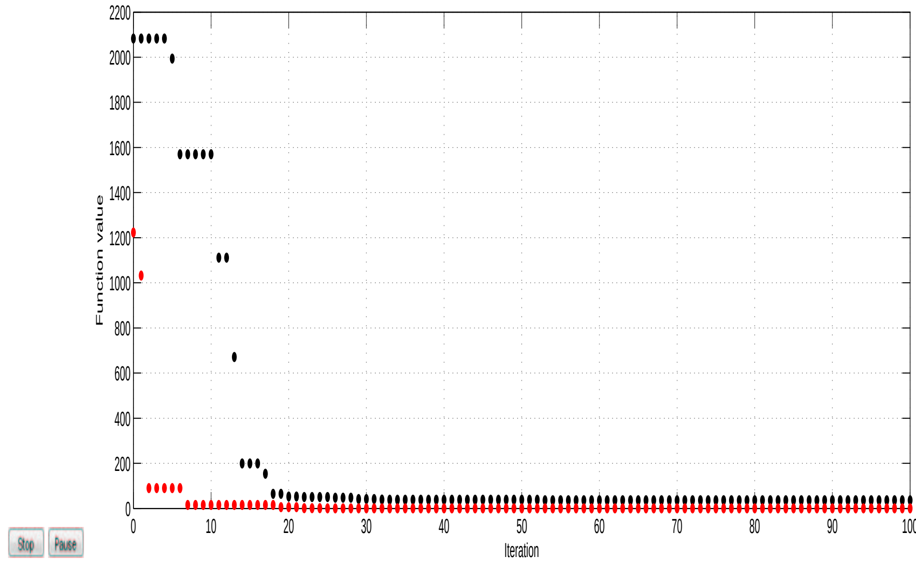

Figure 4.6: Plot of the objective function with iteration for SA algorithm (black dotted line) and NM simplex algorithm (red dotted line) for low LET IR.

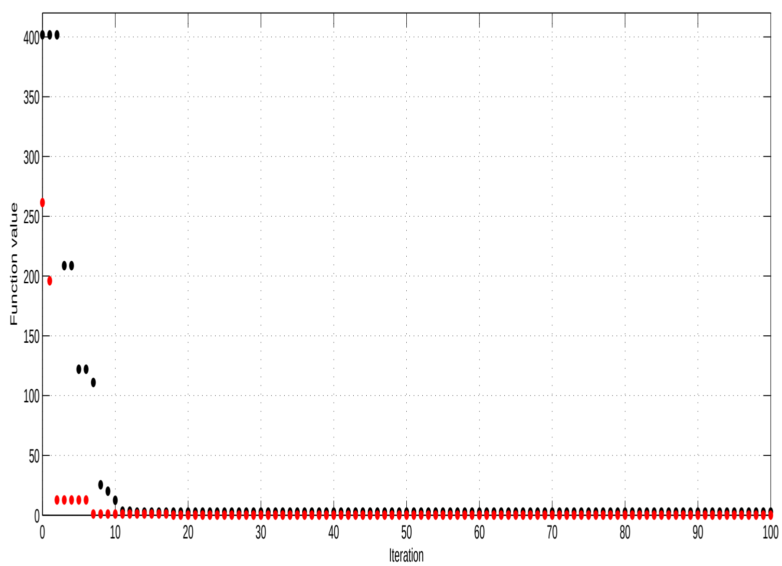

Figure 4.7: Plot of the objective function with iteration for SA algorithm (black dotted line) and NM simplex algorithm (red dotted line) for high LET IR.

It should be noted that for this analysis, we have used a geometric cooling schedule in the SA algorithm. Similar analysis using the SA method done on different cooling schedules as explained in section 3.3.3 show no significant difference in the results.

Next, we compute 95% confidence intervals (CIs) on the six estimated parameters for both low and high LET data (details about the CI can be found in section 3.3.4). Here, since the sampling distribution is unknown, we apply the 95% bootstrap confidence interval. Table 4.4 and table 4.5 present the 95% bootstrap confidence intervals for the six parameters of the model for high LET and low LET survival data, respectively. These confidence limits are computed based on the estimated parameters obtained using 1000 bootstrap data sets. See appendix A.3 and A.4 for the list of the estimated parameter values of low and high LET IR, respectively using 1000 bootstrap data set. The bootstrap CI computation is only on the estimation result obtained by the NM simplex technique since in our case the NM simplex is a superior optimiser.

Parameter	Parameter estimates	Standard error	95% bootstrap CI
δ	2.000000000409338	0.3331	$(2.000000000000074, 2.000000000984723)$
α_1	20.1999	6.5971	$(0.545, 20.6075)$
α_2	0.001000000000004	3.483×10^{-7}	$(0.001, 0.001000000000738)$
p	0.999999999998499	0.0041	$(0.99999999999, 1)$
V_{max}	2.999999999882046	5.717×10^{-5}	$(2.999999998567619, 2.000000000000845)$
K_M	5.57×10^{-11}	7.07×10^{-5}	$(4.7 \times 10^{-14}, 2.5334 \times 10^{-9})$

Table 4.4: The bootstrap 95 % confidence intervals for the six parameters of the model for high LET survival data. See text for details.

Parameter	Parameter estimates	Standard error	95% bootstrap CI
δ	2.3663	0.3114	$(2, 3.1856)$
α_1	18.5595	5.7163	$(0.0277, 20.2853)$
α_2	0.001000000000655	0.0002	$(0.001, 0.0010025)$
p	0.9295	0.1414	$(0.4102, 1)$
V_{max}	2.9999	0.4807	$(0.4805, 3)$
K_M	8.57×10^{-11}	0.6074	$(1.24 \times 10^{-12}, 1.3141)$

Table 4.5: The bootstrap 95 % confidence intervals for the six parameters of the model for low LET survival data. See text for details.

As a summary, when the parameter values are unknown, the NM simplex technique provides the lowest value of the objective function (SSE). In addition the value of the correlation between estimated survival data and experimental data r^2 are close to 1 which correspond to an excellent fit. The algorithm also performs the shortest computational time of the optimisation runs till convergence and obtains a fewer number of iteration to converge to the minimum value of the objective function.

Therefore, all the results shown in this section indicate that the NM simplex algorithm gave a reasonable estimates of all of the parameters. We also 95% confident that the value of each parameter lies within the estimate range covered by the confidence interval which are presented in table 4.4 and table 4.5.

In next section, we check the consistency of the proposed parameter estimation algorithms in this section. This can be done when some of the values of the six parameters of the model are known exactly.

4.8.2 Reliability of the parameter estimation algorithms

In this section we investigate the reliability of the algorithms of the NM simplex and the SA by using the performance of the algorithms to estimate the parameter values of δ, K_M, α_2, p, V_{max} and α_1. This is carried out by generating two sets of model survival data using ODEs in section 4.5 with known parameter values obtained in the previous section. These known values are considered the nominated parameter values. The generated data are shown in figure 4.8 for low LET IR and figure 4.9 for high LET IR.

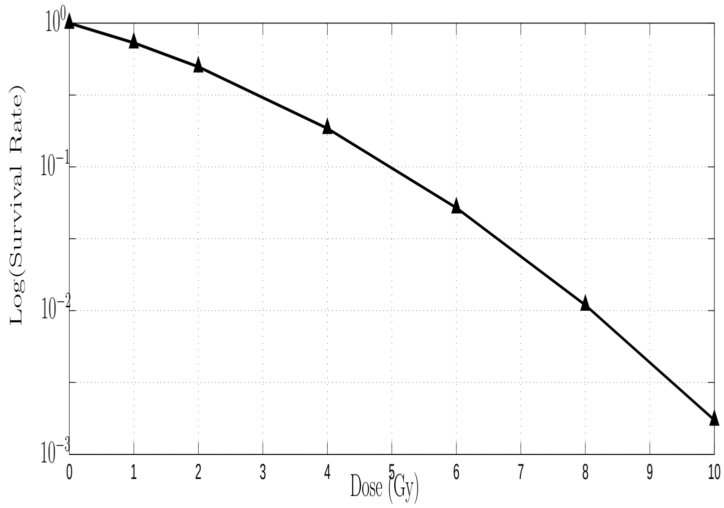

Figure 4.8: The simulation data for low LET IR are plotted (triangles) and fitted (solid line) to the LQ relation. The estimated value of LQ parameters $\alpha = 0.2789$ Gy^{-1} and $\beta = 0.0357$ Gy^{-2} for nominated parameters $\delta = 2$ Gy^{-1} cell^{-1}, $\alpha_1 = 11.4775$ h^{-1}, $\alpha_2 = 0.0082$ h^{-1}, $p = 0.9011$, $V_{max} = 2.3076$ h^{-1}, and $K_M = 5$ μM at $T = 24$ h.

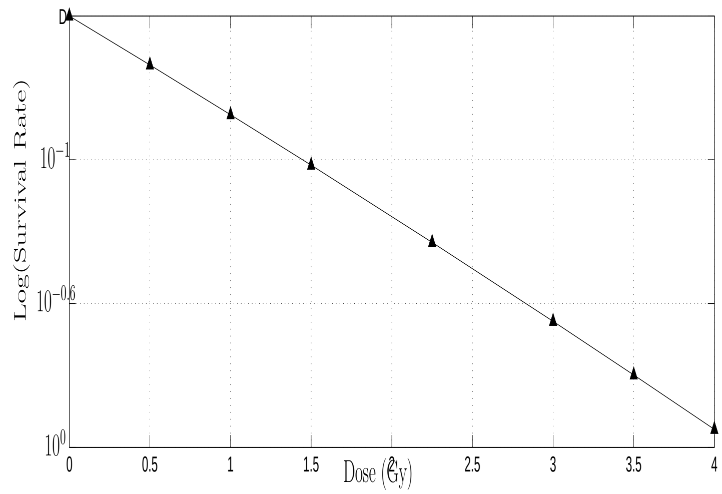

Figure 4.9: The simulation data are plotted (triangles) and fitted (solid line) to the LQ relation. The estimated value of LQ parameters $\alpha = 0.7777\ Gy^{-1}$ and $\beta = 0.0125\ Gy^{-2}$ for nominated parameters $\delta = 3.6703\ Gy^{-1}$ cell^{-1}, $\alpha_1 = 18.9733$ h^{-1}, $\alpha_2 = 0.001\ h^{-1}$, $p = 0.7942$, $V_{max} = 2.9387\ h^{-1}$, and $K_M = 3.7560\ \mu M$ at $T = 24\ h$.

We apply the algorithms to the generated data to obtain a set of estimated parameter values of δ, K_M, α_2, p, V_{max} and α_1 for low and high LET ionising radiation. The performance evaluations of the algorithms are based on the percentage difference between the nominated parameter values and the estimated parameter values and also the value of the objective function (SSE).

Using random start values for parameters, we calculate the mean and the standard deviation of the estimated value of the parameters δ, K_M, α_2, p, V_{max} and α_1 based on 150 optimisation runs for each parameters. The percentage difference between the nominated and the estimated parameter values and also the value of the objective function (SSE) for each parameter are summarized in table 4.6 for low and high LET IR.

Type of IR	Parameter	Nominal value	Estimated values (mean)		Standard deviation of estimated parameters		SSE (mean)		% difference	
			NM	SA	NM	SA	NM	SA	NM	SA
Low LET	δ	2	2.0017	2.0010	0.0401×10^{-13}	0.0003	1×10^{-8}	0.0014	0.085%	0.05%
	α_1	11.4775	20.79	14.9257	0.2495×10^{-13}	2.8736	1×10^{-8}	0.0014	44.7932%	23.1024%
	α_2	0.0082	0.0082	0.0082	0.0001×10^{-13}	0.0001	1×10^{-8}	0.0014	0%	0.1382%
	p	0.9011	0.9003	0.9015	0.0045×10^{-13}	0.0055	1×10^{-8}	0.0014	0.0888%	0.0444%
	V_{max}	2.3076	2.3001	2.3030	0.0842×10^{-13}	0.0124	1×10^{-8}	0.0014	0.325%	0.1989%
	K_M	5	5	4.9995	0	0.0015	1×10^{-8}	0.0014	0%	0.0104%
High LET	δ	3.6703	3.6717	3.6735	0.1745×10^{-3}	0.0210	1×10^{-8}	0.0005	0.0381%	0.0871%
	α_1	18.9733	0.3974	20.3656	0.0699×10^{-3}	0.2674	1×10^{-8}	0.0005	97.91%	6.8365%
	α_2	0.001	0.001	0.001	0	0	1×10^{-8}	0.0005	0%	0%
	p	0.7942	0.794	0.7942	0.014×10^{-3}	0.0078	1×10^{-8}	0.0005	0.0252%	0%
	V_{max}	2.9387	3	2.9887	0	0.0013	1×10^{-8}	0.0005	2.0433%	1.6730%
	K_M	3.756	3.641	3.6963	0.065×10^{-3}	0.0229	1×10^{-8}	0.0005	3.0618%	1.5895%

Table 4.6: Performance evaluation of parameter estimation on the model for low LET IR and high LET IR with random starting values of parameters. The statistic results over 150 runs at each parameter.

In general, table 4.6 shows all parameters for both algorithms seemed to be in a good agreement with very little difference between both algorithms except for α_1. The result found here for α_1 is consistent with the result shown in the previous section where the standard deviation of α_1 is larger than other parameters (see table 4.3). The significant difference between the nominal value and the estimated value of α_1 might suggest the insensitivity of the model to α_1. For both algorithms, the objective function for each parameter also present that the SSE is close to 0 which correspond to an excellent fit.

As a summary, for low and high LET model survival data, the NM simplex and the SA algorithms gave reasonably reliable estimates of all the parameters due to its ability to estimate value of parameters.

4.9 The model and therapy implication

We can relate the LQ bulk parameters α and β to the mechanistic parameters δ, α_1, α_2, p, V_{max}, and K_M using the parameter estimation algorithms proposed in section 4.8. It is of interest to understand the elasticity of α and β with respect to δ and p as these (radiosensitivity and replication fidelity rates, respectively) can be manipulated. See chapter 3 for details about the elasticity.

Using sets of estimated value of parameters obtained in section 4.8, we can compute the elasticity of α with respect to p for low and high LET data, respectively. We assume that p rises by 1 %, while the rest of five model parameters are fixed. With the changes of p, we determine the new value of α by using the model that we propose in (4.5). Using the formula in (3.4) in section 3.4 where the LQ parameters α be y, while p is x, we can evaluate the elasticity.

We apply the same procedure as explained in the last paragraph to determine the elasticity of α with respect to δ, β with respect to p, and β with respect to δ when p and δ are rise by 1 %. The mean of elasticity for low and high LET IR data are presented in table 4.7, which are associated with the estimated values of parameters in table 4.2 provided by the NM simplex method.

Type of IR	Statistic	α_{model}		β_{model}	
		δ	p	δ	p
Low LET	sample mean, $\bar{x}$	1.3881	-5.3967	1.6331	1.5715
	sample standard deviation, s	0.3926	1.0647	0.2916	0.3721
High LET	sample mean, $\bar{x}$	0.9167	-3.9965	2.9916	2.925
	sample standard deviation, s	0.0494	1.6879	0.6032	0.9546

Table 4.7: The sample mean and the sample standard deviation of the elasticity of α_{model} and β_{model} with respect to δ and p for low and high LET data. See text for details.

For low-LET data, it is clearly seen in table 4.7 that in most of the runs of the

SA algorithm, both p and δ give larger than 1 in absolute values of elasticities of α and β. These indicate that the LQ parameters α_{model} and β_{model} are sensitive to both mechanistic parameters p and δ. Using the result in table 4.7, the elasticities of α and β can be interpreted as follows. When p rises by 1 %, the value of α_{model} drops by 5.4 % while β_{model} increases by 1.6 %. When δ rises by 1 %, the value of α_{model} and β_{model} increase by 1.4 % and 1.6 %, respectively. It is found that α_{model} and β_{model} are sensitive to δ, thus we immediately have a treatment recommendation, to try to increase tumour tissue aeration (which correlates positively with radiosensitivity) prior to irradiation.

For high-LET data, the elasticities are presented in table 4.7. In all runs we found that only β is sensitive to δ, but α is not. Using the result in table 4.7, the elasticities of α and β can be interpreted as follows. When p rises by 1 %, the value of α_{model} falls by 4 %, while β_{model} increases by 3 %. When δ rises by 1 %, the value of α_{model} and β_{model} increase by 0.92 % and 3 %, respectively. It is found that β is more sensitive to δ than α. Since β is sensitive to δ, we immediately have a treatment recommendation, to try to increase tumour tissue aeration (which correlates positively with radiosensitivity) prior to irradiation.

Table 4.8 presents the 95% confidence interval of the elasticities for low and high LET data.

Type of IR	α_{model}		β_{model}	
	δ	p	δ	p
Low LET	$(1.3255, 1.4507)$	$(-5.5665, -5.2269)$	$(1.5866, 1.6796)$	$(1.5122, 1.6309)$
High LET	$(0.9087, 0.9247)$	$(-4.2694, -3.7237)$	$(2.894, 3.0891)$	$(2.7707, 3.0793)$

Table 4.8: The 95% confidence interval of the elasticity of α_{model} and β_{model} with respect to δ and p for low and high LET data. See text for details.

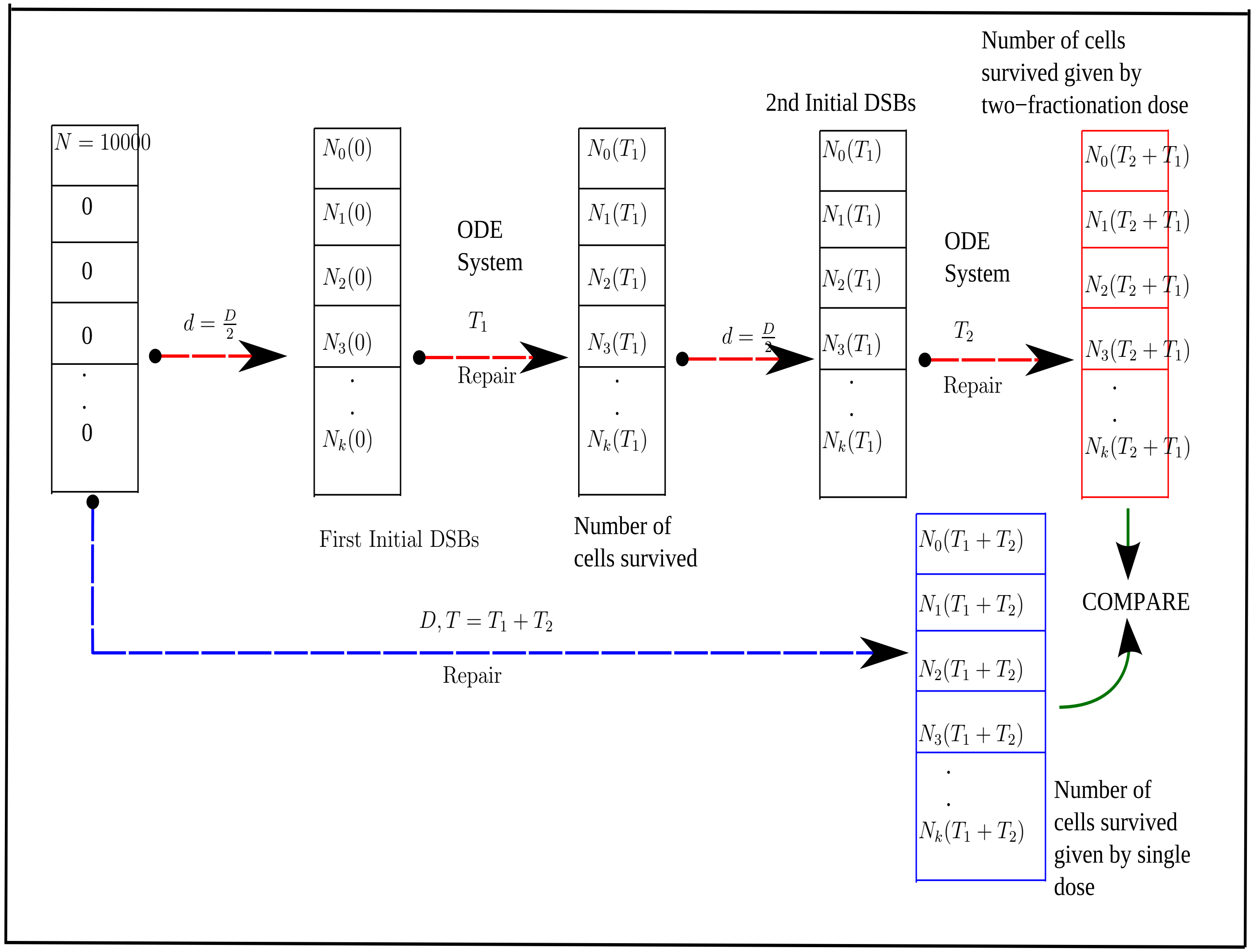

Figure 4.10: The fractionation algorithm of the model

4.10 Dose fractionation

In the previous section, we developed a model which described the cell killing effects of radiation for a single dose D of radiation. It is well known that if a dose D is given in time-separated fractions, the cumulative effect is lower than that of the dose administered all at once (see chapter 2). In this section we implement a version of the model that allows dose fractionation. For simplicity, we study the effect of dividing the dose D in two fractions, separated by a time interval T. Being able to predict the effect of dose fractionation is of paramount importance in radiation oncology treatment planning, as radiation regimens have to be adjusted depending on the well-being of the patients and their ability to continue with the course of treatment.

An algorithm for administering a fractionated dose and following the evolution of a cell population in such a radiation regime is explained diagrammatically in figure 4.10. The blue broken line shows the single-dose treatment algorithm, the results of which were discussed in section 4.7.

The red broken line arrow in figure 4.10 describes the case of two-dose fractionation treatment, which means that the total dose of radiation D is divided into two equal fractions d with interval times $T_1 = T_2 = 24$ hours between the doses. We sample the Poisson distribution with mean $\lambda = \delta\frac{D}{2}$ to obtain the initial conditions, integrate the resulting equations up to time T_1, i.e. allow cells to repair the radiation damage for time T_1, then sample the same Poisson distribution and adjust the number of DSBs for each cell, integrate the equations for another interval of length T_2, and compare the results to subjecting the population to a single dose D of radiation and allowing it $T = T_1 + T_2$ repair time.

We used MATLAB to compute the fraction of surviving cells of the two-dose fractionation treatment. The MATLAB code for two-dose fractionation algorithm of low LET data can be found in appendix A.3 and this code can be extended to any number n of fractions ($D = nd$). The survival curve for two-dose fractionation of low LET and high LET data are shown by circles in figure 4.11 and figure 4.12, respectively.

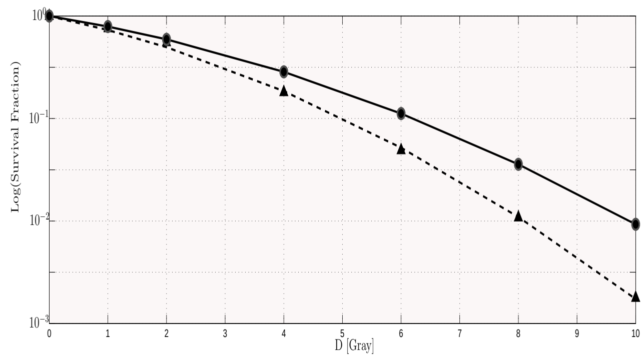

Figure 4.11: The survival data of single-dose treatment (triangles) and two-dose fractionation treatment (circles) for low LET survival data with total repair time $T = 48$ hours are obtained with $\delta = 2$ Gy^{-1} cell^{-1}, $\alpha_1 = 11.5\ h^{-1}$, $\alpha_2 = 0.0082\ h^{-1}$, $p = 0.9011$, $V_{max} = 2.3076\ h^{-1}$ and $K_M = 5\ \mu M$. Both the single-dose treatment and two-dose fractionation treatment simulation data are fitted to LQ equations $\ln S = -0.279D - 0.0357D^2$ with $\alpha_s = 0.279\ Gy^{-1}$ and $\beta_s = 0.0357\ Gy^{-2}$ (dashed line) and $\ln S = -0.211D - 0.0257D^2$ with $\alpha_f = 0.211\ Gy^{-1}$ and $\beta_f = 0.0257$ Gy^{-2} (solid line) respectively.

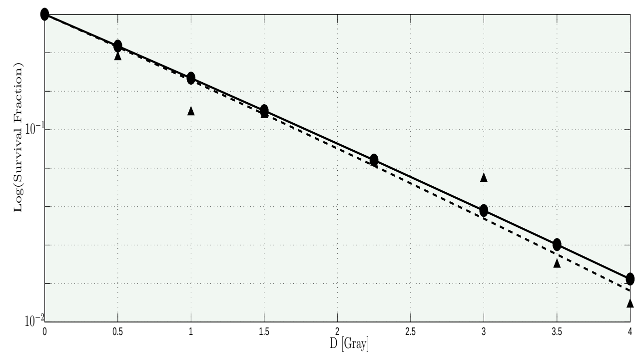

Figure 4.12: The survival data of single-dose treatment (triangles) and two-dose fractionation treatment (asterisks) for high LET survival data with total repair time $T = 48$ hours are obtained with $\delta = 3.67$ Gy^{-1} cell^{-1}, $\alpha_1 = 18.97\ h^{-1}$, $\alpha_2 = 0.001\ h^{-1}$, $p = 0.79$, $V_{max} = 2.94\ h^{-1}$ and $K_M = 3.76\ \mu M$. Both the single-dose treatment and two-dose fractionation treatment simulation data are fitted to LQ equations $\ln S = -0.8D - 0.01D^2$ with $\alpha_s = 0.8\ Gy^{-1}$ and $\beta_s = 0.01$ Gy^{-2} (dashed line) and $\ln S = -0.7549D - 0.0094D^2$ with $\alpha_f = 0.7549\ Gy^{-1}$ and $\beta_f = 0.0094\ Gy^{-2}$ (solid line) respectively.

To show the effect of fractionation on the cell population of low and high LET, we compare the cell surviving fraction given by single-dose treatment with the cell surviving fraction given by two-dose fractionation treatment. Figure 4.11 and figure 4.12 present the comparison between curves of cell surviving fraction between single dose D (dashed line) and two dose fractionation (solid line) with total replating time $T = 48$ hours for low and high LET data cell population, respectively.

Survival curves of both of the single-dose and the split dose irradiations of low and high LET are averaged from $\xi = 150$ repeated runs of the fractionation algorithm using the six parameter values which are listed in the caption of figure 4.11 and 4.12, respectively. As seen in both figures, the fractional survival data as a function of the radiation dose for low and high LET are plotted and fitted by the linear quadratic equation, respectively. It is clearly seen that the two-dose fractionation survival data for both of data sets (low and high LET) fit very well to the LQ relation (given by the solid curve in the figures).

After single-dose irradiation, from the average of $\xi = 150$ repeated runs, for survival data of low and high LET, we obtain the 95% confidence interval of the mean of alpha-beta ratio are the intervals $(7.8114, 7.8286)$ for low LET, and $(79.55, 80.45)$ for high LET.

As expected, after split-dose irradiation, the LQ parameter α_f remains very similar to α_s which is obtained after single-dose irradiation with only deviation $< 7\%$. The results indicate that the $\alpha-$coefficient is not influenced by dose fractionation.

From both of the figures of low and high LET (figure 4.11 and figure 4.12, respectively), we found that the width of shoulder and the slope of the fractional survival curve is decreased and increased, respectively. These results are in agreement with the experimental work done by [156], who suggested that these effects are due to the larger capacity for repair of sublethal DNA damage between fractions.

4.11 Conclusions

In this chapter, we have developed a mechanistic realistic model of the effect of ionising radiation on DNA in mammalian cells. We considered a population of cells structured by the number of DSBs and misrepairs incurred after a dose of low LET radiation. The ODE model describes the evolution of the irradiated population of cells in time. The work is in three parts.

First, we considered the effect of a single dose D of radiation treatment. We observe that the fraction of surviving cells can be well approximated by the linear quadratic relation (see figure 4.3).

Second, in section 4.8 we estimated the six parameter values in the model proposed in section 4.5. We started with the works in section 4.8.1 where we assume that the value of all parameters are totally unknown. We estimated the LQ parameters $\alpha_{exp} = 0.279\ Gy^{-1}$ and $\beta_{exp} = 0.0357\ Gy^{-2}$ of the experimental data of low LET IR and $\alpha_{exp} = 0.8\ Gy^{-1}$ and $\beta_{exp} = 0.01\ Gy^{-2}$ of the experimental data of high LET IR which are plotted in figure 4.5. The estimation of the LQ parameters is done by fitting the experimental data to the LQ relation (see (2.2)). The fitting which is using *fminsearch* routine, the built-in functions in MATLAB which performs Nelder-Mead simplex algorithm (chapter 3), gave us the $\frac{\alpha}{\beta} = 7.81$ Gy^{-1} and $\frac{\alpha}{\beta} = 80\ Gy^{-1}$ for low and high LET IR survival data, respectively. It is known that the higher the alpha-beta ratio, the more linear the cell survival curve. In contrast, the lower the alpha-beta ratio, the more curved the cell survival curve will be [81] (see figure 4.5).

We then used the estimated values of the LQ parameters α_{exp} and β_{exp} of both of the experimental data of low and high LET IR in order to analyse the estimation of the six parameters (δ, α_1, α_2, p, V_{max}, and K_M) of the model that minimise the objective function (i.e the sum of squared errors (SSE) between n number of survival data and the model survival data). We implemented Simulated Annealing (SA) algorithm, and Nelder-Mead (NM) simplex algorithm in the parameter estimation algorithm for both low LET IR and high LET IR survival data. We then compared the performance of both algorithms. For a fair comparison all of the computations are performed using an Intel Pentium 4 CPU 2.80 GHz machine running Windows 7.

The performance evaluations of both optimizer; the NM simplex and the SA are based on the value of the objective function (SSE), computational time and number of iteration. By comparison, we found that the NM simplex algorithm using the model that we propose is more efficient optimiser than the SA algorithm in terms of providing the lowest value of the objective function (SSE). In addition the value of the correlation between estimated survival data and experimental data r^2 are close to 1 which correspond to an excellent fit. The algorithm also performed the shortest computational time of the optimisation runs till convergence and obtains a fewer number of iteration to converge to the minimum value of the objective function.

To determine reliability of the parameter estimation algorithms introduced in section 4.8, in section 4.8.2 two sets of model data are generated using chosen (or nominal) sets of parameters (δ, α_1, α_2, p, V_{max}, and K_M) value for low and high LET cell survival model data. Using the generated model data with some of the parameter values are known, we compared the performance of the NM simplex method and the SA algorithm in terms of the percentage difference between the nominal values and the estimated values and also the value of the objective function (SSE). We observed that for low and high LET model survival data, the NM simplex and the SA algorithms are reliable method of estimation of the parameters of the model when these algorithms returned the same value of the model parameters that we have chosen. It is worth to note that the parameter estimation algorithms which using the model in section 4.5 are applicable and based on the two data sets that we use, the results indicate that there is no restriction in the type of LET to which our model applied.

We can relate the LQ bulk parameters α and β to the mechanistic parameters δ, α_1, α_2, p, V_{max}, and K_M using the proposed parameter estimation algorithm discussed in section 4.8. In section 4.9, we measure the sensitivity (or the elasticity) of α_{model} and β_{model} to parameters δ, α_1, α_2, p, V_{max}, and K_M for both of the survival data (low and high LET IR). Based on the cell survival data of low LET IR that we used, we found that both α_{model} and β_{model} are sensitive to mechanistic parameters δ and p, radiosensitivity and repair fidelity, respectively, which can be experimentally manipulated. In this case, we immediately have a treatment recommendation: to try to increase tumor tissue aeration (which correlates with radiosensitivity) and decrease tumour DNA repair fidelity during pre-radiation treatment.

Using the cell survival data of high LET IR however, only LQ parameter β is sensitive to δ. In this case, we also have a treatment recommendation, which is to try to increase tumour tissue aeration prior to irradiation.

In the last section, we dealt with cell killing effects of fractionated doses of radiation. Using the algorithm that we proposed, we observed that the main effect of fractionation is the increment of cell surviving fraction (which is the reflection of repair of sublethal DNA damage between fractions), with very little influence on the $\alpha-$component. It is worth to note that alpha-beta ratio (which is a tissue property) for low and high LET remain unchanged due to fractionation.

The model proposed in the present study is close in spirit to that of [2], although there are some small differences in assumptions. More importantly, we extend Albright's work both by analysing the effect of dose fractionation effect on cell killing and by developing a method of parameter estimation: neither of these important issues was considered in the previous work.

For further developments, it is clear that the ODE model can be replaced by a continuum (linear) PDE limit, but the two most promising extensions are by making the model more biologically plausible. One direction would be to allow less restrictive repair mechanisms, in which DSBs are repaired in parallel and not sequentially as in the present version, while the other is to allow a structuring also in respect of the position the cell occupies in the cell cycle, a discrete variable c with values in the set of cell cycle phase: G_1-phase, S-phase, G_2-phase, and M-phase, and allow for both interphase and mitotic death.

Chapter 5

Modelling the ATM DNA damage sensor mechanism

5.1 Introduction

In chapter 4, we developed a mechanistic model of high dose irradiation damage. While the LQ formalism correctly describes cell survival of high radiation doses, low radiation doses produce other effects, such as the bystander effect. In section 2.7, we suggested a mechanism of radiation-induced bystander effects presented in figure 2.13. As mentioned in that section, there are several kinases involved in the mechanism (the interested reader is referred to section 2.7).

One of the important kinases which are involved in the DNA damage bystander response pathways as well as in the targeted radiation effects (see section 2.6) is ataxia telangiectaxia mutated, ATM, a DNA damage sensor (see section 2.5.1 and 2.5.2 for further details about ATM in the DNA damage response pathways). It is known that defects ATM gene can cause disregulation DNA damage-induced checkpoint control (see section 2.2.8) as well as in DNA damage repair. Many cancer cells which have a high alpha beta ratio contain ATM gene mutation [33, 120] (see section 2.6.1).

In section 2.7, we also suggested a bistability mechanism (figure 2.14) for the concentration of active ATM concentration as a function of the strength of feedback loops between double strand breaks (DSBs) and ATM. The disbalance between the positive and negative feedback loops will switch the bistable system from a state of healthy low activated ATM concentration into a state of chronically high activated ATM concentration.

As a good sensor of DNA DSBs, active ATM should be able to change back into its inactivated state as soon as possible, as protracted high level of ATM activation may trigger cell death by apoptosis (chapter 2). Levels of active ATM can be lowered by dephosphorylation, or by degradation of active ATM, or by the sequestration of inactive ATM in dimers.

In last decades, many research studies have been carried out to explore the p53 signalling network, but only recently the p53 upstream activator ATM received more attention after Bakkenist and Kastan [6] proposed an ATM activation mechanism. Here, we summarize some recent research works on p53 signalling pathway modelling that include ATM as part of the model. In 2005, Ma et al. [102] proposed a 3-module model of the p53 signalling network. The model contains a DNA damage initiation and repair module, an ATM-mediated DSB signal transduction module, and a p53-Mdm2 oscillator module. In ATM-mediated DSB signal transduction module, the authors considered three components: activated ATM monomer, ATM dimer, and inactive ATM monomer. They showed that p53-Mdm2 negative feedback loop is the basis of the p53 oscillation. The model however omits some known important components in ATM activation such as MRN and Wip1, a positive and negative regulator of ATM (see section 2.5.1).

In 2009, Mouri et al. [114] introduced a 2-module model which contains a DSB-repair mechanism and an ATM-phosphorylation mechanism. [114] also considered the same component as in [102] in ATM-phosphorylation module, except Mouri et al. incorporated the negative feedback between p53 and ATM via Wip1 in the model. The authors showed that the negative feedback affects ATM's dynamical behaviour.

In 2011, Zhang et al. [169] suggested a 4-module model: a DNA repair module, an ATM sensor module, a p53-centered feedback control module, and a cell fate decision module. In ATM sensor module, the authors incorporated Wip1 phosphatase, Mdm2 protein, and p53-dependent damage-inducible nuclear protein 1 (p53DINP1), a p53 activation promoter in the model. The authors showed that Wip1 phosphatase, Mdm2 protein, and p53DINP1 are important in regulating ATM and p53 activity. All these models showed that ATM exhibits a switch-like behavior in which all of ATM is activated rapidly in response to DNA damage signal. Simulation results obtained by these three research works are consistent with the experimental work obtained by [6]. However, none of these models explored in detail the process of ATM activation. In particular, the monomerization and the dimerization processes. [102, 169] only assumed that the monomerization and the dimerization rates of ATM are constant, while [114] does not take into account ATM monomerization and dimerization dynamics in the activation of ATM in their model. Therefore it is important to further investigate the importance of these processes in the activation of ATM during the ionising radiation response.

In this chapter, we construct a better mathematical framework to model the dynamics of various ATM species upon the DNA DSBs induction including ATM monomerization and dimerization processes. We assume that the monomerization rate of ATM is dependent on the concentration of MRN complex (see section 2.5.1 for details about MRN). [10] reported that MRN complex concentration is proportional to the number of DNA DSBs. The model provides a fully satisfactory formalism to link biologically processing of the monomerization and the dimerization to ATM activation.

We only deal with ATM, and this model is a minimal one, which ensures ATM functionality. Initially, our intention was to develop a mechanistic model of radiation-induced bystander response, but due to the complexity of the process involved in the bystander response system, several assumptions have been made (please see section 5.2 for the list of assumptions).

To study the dynamics of ATM protein in DNA damage response pathways in normal cells, we extend the approach of [59] who modeled an open system of autophosphorylating kinase (e.g. ATM) by taking into account sequestration dynamics under several assumptions to simplify the model. By using the ODE framework in [59] and introducing the sequestration dynamics equations, we solve the system of differential equations using MATLAB. We analyse time-courses curves of the active ATM concentration K^* and the bifurcation diagram of equilibrium K^* with respect to the dimer monomerization rate B.

5.2 Model assumptions

To construct a simple model of the dynamics of ATM using the ODE framework in [59], we make the following assumptions:

(1) We lump the activity of ATM, ATR, and DNA-PK into one variable, which describes the activity of ATM;

(2) The only mechanism of activation of ATM is by DNA DSBs induction;

(3) An activated ATM exhibits only one type of post-translation modification (PTM), which is a phosphorylation, and the phosphorylation of ATM is a proxy of ATM activation;

(4) We do not specify the phosphatase that dephosphorylates ATM.

5.3 Justification of assumptions

Here we provide some explanation of the assumptions that we have made in section 5.2:

(1) It is known that ATM, ATR, and DNA-PK are very important components in the DNA damage response pathways (chapter 2). These components share

the same activity, for example to phosphorylate H2AX (see section 2.5.1). For the sake of simplicity, we make the assumption (1) in section 5.2.

(2) Recently in [170], it was demonstrated that there are two pathways involved in the activation of ATM. In one of them, ATM is activated by DNA damage following IR. This pathway is MRN-dependent. In contrast, the second pathway does not involve DNA damage and the MRN complex. [170] found that ATM can also be activated directly by oxidative stress (chapter 2). Since the model that we are developing in this chapter is a minimal one, we only deal with the activation of ATM due to the DNA damage. This means the model that we propose here is more suitable for normal cells under irradiation than for example for bystander cells.

(3) As discussed in chapter 2, the moment there is DNA damage, ATM is activated. It is known that parts of the activation process are acetylation and phosphorylation of inactive ATM [10]. There is also evidence that the autophosphorylation of ATM is a very important process in ATM activation especially in wild-type human cells [144]. In this model we only deal with the ATM phosphorylation process and also assume that this process is a sign of ATM activation.

(4) For truly realistic models, one should model the dynamics of ATM with some specific phosphatases such as Wip1 (section 2.5.1). In our minimal model, we do not specify the phosphatase that dephosphorylates ATM.

5.4 Modelling

According to [6], once DNA damage occurs, an inactive ATM dimer is depolymerised into two inactive monomers and then there is fast activation of the monomers by autophosphorylation. Based on [10], we believe that there is also another important way for inactivate ATM dimer to be activated. The moment there is

DNA damage, an inactive ATM dimer falls apart giving rise to two active ATM monomers.

Thus we are saying that to model the dynamics of ATM on the reception of a DNA damage signal, we need two processes of creating active ATM concentration K^*, autophosphorylation and monomerization of the ATM dimer.

As suggested by [6, 59], the reaction scheme of autophosphorylation is given by:

$$K + K^* \underset{b_1}{\overset{f_1}{\rightleftharpoons}} 2K^*, \tag{5.1}$$

while for the dissociation of inactive ATM dimer, K into active ATM monomers, K^* if there is DNA damage, we suggest the following monomerization scheme:

$$D \xrightarrow{B} 2K^*. \tag{5.2}$$

Here, we suggest the reaction scheme of the dimerization process is given by:

$$K + K \xrightarrow{A} D, \tag{5.3}$$

where A and B are the inactive ATM dimerization rate and the ATM monomerization rate, respectively, while f_1 and b_1 are the rate constants of autophosphorylation of the ATM (see [59]). As suggested by [59], the reaction scheme of the dephosphorylation process is as follows:

$$P + K^* \underset{b_3}{\overset{f_3}{\rightleftharpoons}} C_P \xrightarrow{f_4} P + K, \tag{5.4}$$

where P is a molecule of phosphatase, f_3, b_3, and f_4 are the rate constants of dephosphorylation of the ATM.

To model the dynamics of various ATM species, we employ the ODEs framework in [59]. The chemical reactions as well as the ODEs involved in autophosphorylating kinase model can be found in detail in [59]. The rates of change of concentration of the kinases and complexes are as follows:

$$\frac{dK}{dt} = \alpha - dK - f_1 K K^* + b_1 C_K + f_4 C_P - 2AK^2, \tag{5.5}$$

$$\frac{dK^*}{dt} = -d^* K^* - f_1 K K^* + b_1 C_K + 2 f_2 C_K - f_3 K^* (P_{tot} - C_P) + b_3 C_P + 2BD, \tag{5.6}$$

$$\frac{dC_P}{dt} = f_3 K^* (P_{tot} - C_P) - (b_3 + f_4) C_P, \tag{5.7}$$

$$\frac{dC_K}{dt} = f_1 K K^* - (b_1 + f_2) C_K, \tag{5.8}$$

$$\frac{dD}{dt} = AK^2 - BD. \tag{5.9}$$

We assume the total amount of phosphatase is conserved. Thus, $P + C_P = P_{tot}$ is constant. The other species in the system are: inactive ATM concentration (K), the activated one (K^*), the dimer (D), $K^* - P$ complex (C_P) and $K - K^*$ complex (C_K). According to [59], d and d^* are the rate of degradation of K and K^*, respectively, while α is the rate of synthesis of K. Note that we incorporate monomerization and dimerization dynamics into the ODEs in [59].

Since there is no data concerning the dimerization process, we assume that the dimerization rate A is constant (the same assumption as [102, 114]).

As discussed in chapter 2, the moment there are DNA DSBs, ATM is recruited by the MRN complex to the damage site. Then inactive ATM dimer is transformed into two active monomers by autophosphorylation and monomerization. We assume that the number of active MRN complexes is proportional to the number of DNA DSBs G that is

$$MRN = a_3 G, \tag{5.10}$$

and that the rate of monomerization B is dependent on the concentration of the MRN complex, $B = f(MRN)$, so that $B = f(a_3 G)$.

There is experimental evidence that DNA DSBs decrease exponentially in time [142]. Therefore we assume

$$G(t) = a_4 e^{-a_5 t}, \tag{5.11}$$

where a_3 is the constant of proportionality, a_5 is the rate of the DNA damage repair and a_4 is the initial damage. In the present work, without any guidance from the literature, we assume that a_5 is a constant. According to Y. Shiloh (personal communication), there are very small amounts of K^* in unperturbed cells. Thus we suggest that rate of inactive ATM dimer monomerization is given by

$$B = a_6 + a_3(a_4 e^{-a_5 t}), \tag{5.12}$$

where the very small non-zero constant a_6 is an initial rate of monomerization without DNA damage.

5.5 Simulation results

If we assume that QSSA (Quasi Steady-State Assumption) holds, that is that C_P and C_K are always at a steady state,

$$C_P = \frac{f_3 K^* P_{tot}}{f_3 K^* + (b_3 + f_4)}, \tag{5.13}$$

and

$$C_K = \frac{f_1 K K^*}{b_1 + f_2}, \tag{5.14}$$

then substituting (5.13)-(5.14) into (5.5)-(5.9), those equations can be re-written as

$$\frac{dK}{dt} = \alpha - dK - \beta KK^* + \frac{V_{max}K^*}{K^* + K_M} - 2AK^2,$$
$$\frac{dK^*}{dt} = -d^*K^* + \beta KK^* - \frac{V_{max}K^*}{K^* + K_M} + 2BD, \tag{5.15}$$
$$\frac{dD}{dt} = AK^2 - BD,$$

where $\beta = \dfrac{f_1 f_2}{b_1 + f_2}$, $V_{max} = f_4 P_{tot}$ and $K_M = \dfrac{b_3 + f_4}{f_3}$. According to [59], these parameters can be interpreted as follows: β determines the autophosphorylation strength; V_{max} represents the maximum rate of dephosphorylation by the phosphatase; and K_M, the Michaelis-Menten constant, is the concentration of K^* for which the phosphatase is working half of its maximum rate.

Realistically, since protein turnover acts on a different time-scale from the damage repair response, it makes sense to take $\alpha = d = d^* = 0$. We will consider two idealised regimes.

5.5.1 The "no damage" regime ($a_4 = 0$)

From (5.12), we have $B = a_6$, and without turnover parameters, the equations in (5.15) are

$$\frac{dK}{dt} = -\beta KK^* + \frac{V_{max}K^*}{K^* + K_M} - 2AK^2,$$
$$\frac{dK^*}{dt} = \beta KK^* - \frac{V_{max}K^*}{K^* + K_M} + 2BD, \tag{5.16}$$
$$\frac{dD}{dt} = AK^2 - BD.$$

Since $\dfrac{d}{dt}(K + K^* + 2D) = 0$, let us call the total concentration of ATM, K_{tot}, and so without protein turnover for all time $K_{tot}(t)$ is constant, in which case

$$K_{eq} + K^*_{eq} + 2D_{eq} = K_{tot} = K(0) + K^*(0) + 2D(0). \tag{5.17}$$

Considering equilibria of (5.16), we argue as follows. If $B = a_6 = 0$, the only equilibrium is $K_{eq} = K^*_{eq} = 0$, and $D_{eq} = \frac{1}{2}K_{tot}$. For sufficiently small B, which is a regular perturbation expansion in $\sqrt{B}$ around the equilibrium $(0, 0, \frac{1}{2}K_{tot})$ given that

$$\begin{aligned} K &= 0 + \sqrt{B}K_1 + BK_2 + (\text{ Higher Order Terms in } B), \\ K^* &= 0 + \sqrt{B}K^*_1 + BK^*_2 + (\text{ Higher Order Terms in } B), \\ D &= \tfrac{1}{2}K_{tot} + \sqrt{B}D_1 + BD_2 + (\text{ Higher Order Terms in } B), \end{aligned} \tag{5.18}$$

for some positive constants K_1, K_2, K^*_1, K^*_2, D_1, and D_2 are expansion parameters. By substituting (5.18) into right-hand side of (5.16) and collect terms of same power of B in every equation, the equilibrium continues uniquely as

$$\begin{aligned} K_0 &= 0 + B^{\frac{1}{2}}(\tfrac{1}{2}K_{tot}/A)^{\frac{1}{2}} + O(B), \\ K^*_0 &= 0 + BK_{tot}K_M/V_{max} + O(B^{3/2}), \\ D_0 &= \tfrac{1}{2}K_{tot} + O(B). \end{aligned} \tag{5.19}$$

In our simulation of the damage response we first set $K(0) = 0$, $K^*(0) = 0$, $D(0) = 1/2K_{tot}$ and allow (5.16) with $a_4 = 0$ to converge to the above equilibrium (K_0, K^*_0, D_0) (see (5.19)). Then at time $t = 0$ we switch on damage (i.e. $a_3, a_4 \neq 0$) and integrate (5.16) with B given by (5.12) with the initial conditions (the equilibrium in (5.19)). This situation will be discussed in section 5.5.2. For numerical simulation, we use the parameter values listed in figure 5.1. All the parameter values and the initial conditions we use in this analysis are not obtained from experiments, but are chosen to get a feeling for the dynamics of the ATM system.

5.5.2 The "with damage" regime ($a_4 \neq 0$)

Using MATLAB, the simulations of the reduced system (5.15) are shown in figure 5.1.

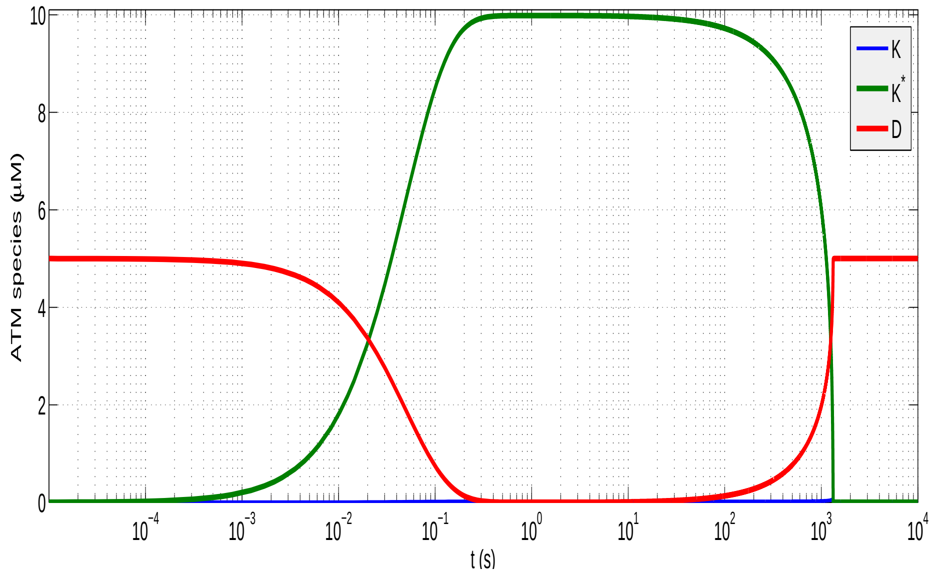

Figure 5.1: The time-courses of K^*, K, and D with $A = 5s^{-1}$, $\alpha = d = d^* = 0$, $f_1 = 3s^{-1}$, $f_2 = 10s^{-1}$,$f_3 = 4s^{-1}$, $f_4 = 0.5s^{-1}$, $b_1 = 10s^{-1}$, $b_3 = 0.1s^{-1}$, $P_{tot} = 0.5\mu M$, $a_3 = 2s^{-1}$, $a_4 = 10\mu M$, $a_5 = 1s^{-1}$, and $a_6 = 0.000000001\mu M$ in logarithmic scale. We set the initial condition as in (5.19).

Figure 5.1 shows that the moment there are DNA DSBs, inactive ATM dimers dissociate into active ATM monomers causing a quick build-up of the amount of active ATM concentration K^*. The ratio of K^*_{max} to the corresponding K and D are $\dfrac{K^*_{max}}{K} = \dfrac{9.983}{0.0164} \approx 609$ and $\dfrac{K^*_{max}}{D} = \dfrac{9.983}{0.0006} \approx 16638$, respectively. These ratios tell us that at maximum response of active ATM concentration K^* is 609 and 16638 times as large as K and D, respectively, which indicates that most of the inactive ATM dimers are transformed into the active ATM. K^* reaches K^*_{max} at $t = 0.621s$, which shows that when damage is high, the dissociation of dimers into active ATM monomers is a rapid process.

We also can investigate the contribution to the dynamics of the ATM sequestration parameter A. First of all, we want to explore the contribution of the rate of dimerization to the active ATM activity over the time which follows for the DNA damage repair process.

As shown in figure 5.2, we found that by increasing A, the maximum concentration of K^* (K^*_{max}) does not change, but the total activity of K^* (the area under the graph) and the half-life $t_{\frac{1}{2}}$ of K^* decrease. These mean if more inactive ATM monomers are sequestered into dimers, then the amount of K^* goes down.

Next, we investigate the contribution of the rate of monomerization B to the activity of active ATM. As discussed in section 5.4, there are five parameters involve in the ATM monomerization process: B, a_3, a_4, a_5 and a_6. But the most important parameters which can describe the ATM monomerization dynamics are the amount of initial DNA damage produced a_4 and the rate of the DNA damage repair a_5. As shown in figure 5.3, K^*_{max} increases with the increasing a_4, until at some stages the total activity of K^* and the level of K^*_{max} do not change as the amount of a_4 increases. This is because K^* is using up all the amount of K there is and increasing the initial damage does not affect the total concentration of the ATM K_{tot} in the cell. The figure also shows that the half-life $t_{\frac{1}{2}}$ of the active ATM increases with the increasing a_4.

Now we want to investigate the contribution of the rate of damage repair a_5 (which we assume is a constant) to the dynamics of the active ATM. The results presented in figure 5.4 show if a_5 is increased to a high value (it means that the damage is corrected very fast), then the half-life and the total activity of the active ATM go down.

Another important result we found here (see blue line in figure 5.4) is if the damage are constantly created without damage repair process (the case where $a_5 = 0$), then the total activity of K^* never goes down and it keeps at the highest level of concentration. See section 5.5.3 for further analysis of parameter B when $a_5 = 0$. As discussed in section 2.7 (chapter 2), our main goal was to model the bystander effects, and clearly we have not done that in this present thesis. But,

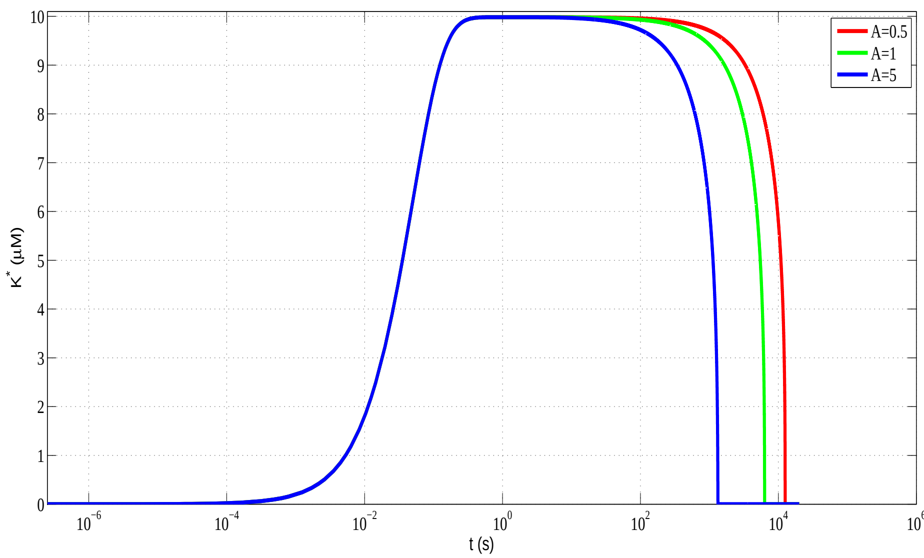

Figure 5.2: The time-courses of K^* for different values of dimerization rate A in logarithmic scale. The rest of the parameters are as in figure 5.1.

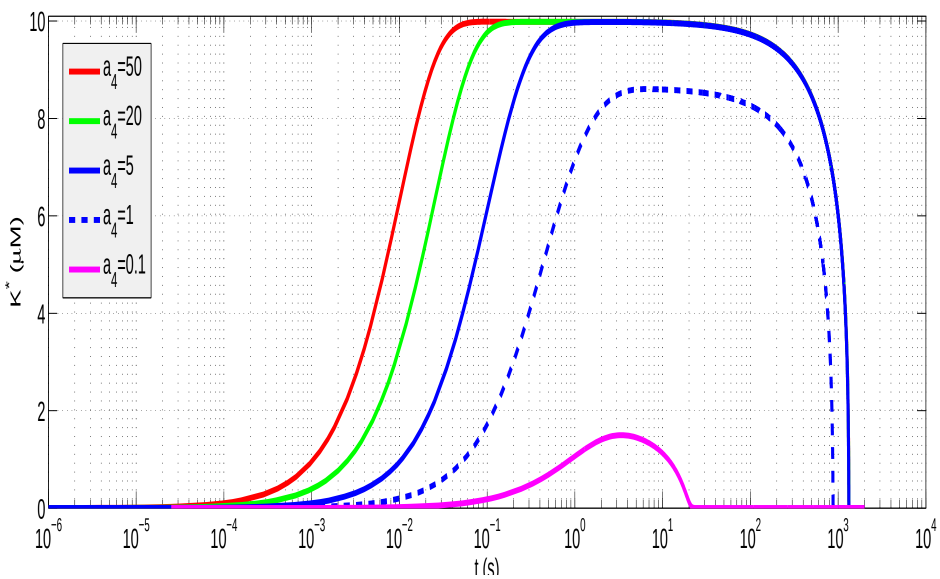

Figure 5.3: The time-courses of K^* for different values of initial damage a_4 in logarithmic scale. The rest of the parameters are as in figure 5.1.

here the bystander situation is found and this situation is equivalent in this part with $a_5 = 0$. It is known that, in bystander cells, the activation of a damage repair response gives result to DNA double strand breaks, thus leading to mutations, chromosomal aberrations, and cell death [129].

As discussed in section 5.4, autophosphorylation of the ATM dimer is one of the important processes for creating active ATM. From the model that we develop, it is shown in figure 5.5 that there is a strong contribution of the autophosphorylation of ATM monomers in maintenance of high level of activated ATM.

Figure 5.5 shows that there is a significant difference in the production of K^* between the system with and without the autophosphorylation process. We found that by autophosphorylating inactive ATM monomers, the total amount of K^*_{max} is larger than the system without the autophosphorylation. The results indicate that if autophosphorylation of ATM monomers is neglected (i. e. we only consider the monomerisation of ATM dimers without autophosphorylation) then K^* cannot efficiently be maintained. Therefore the autophosphorylation of ATM monomers also works in the activation of ATM mechanism. These results are in line with the experimental evidence that autophosphorylation of ATM is important in ATM activation in human cells [144].

The model also can determine how much each parameter that we assume in the autophosphorylation of ATM contributes to the dynamics of active ATM. As shown in figure 5.6 and figure 5.7, there are significant increases of the total activity and the half-life of K^* when the autophosphorylation parameters f_1 and f_2 are increased.

Without using MATLAB, the K^* equation in (5.15) contains β which describes the strength of ATM autophosphorylation. If f_1 and f_2 go up, these values should increase the value of β, thus increase the amount of K^*. All these results suggest that, in order to maintain the activity of K^* at high level as long as there is damage, f_1 and f_2 should be large.

Next, we want to investigate the contribution of the dephosphorylation param-

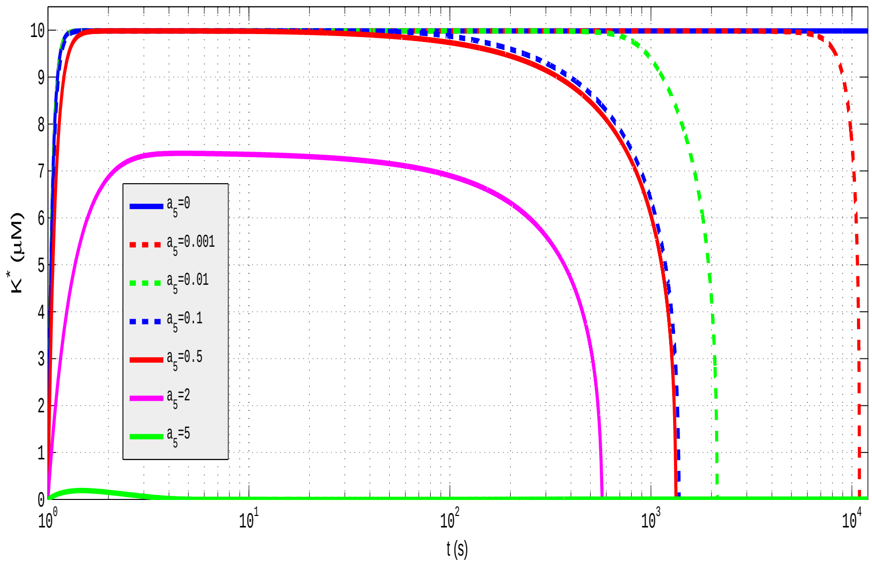

Figure 5.4: The time-courses of K^* for different values of damage repair rate a_5 in logarithmic scale. The rest of the parameters are as in figure 5.1.

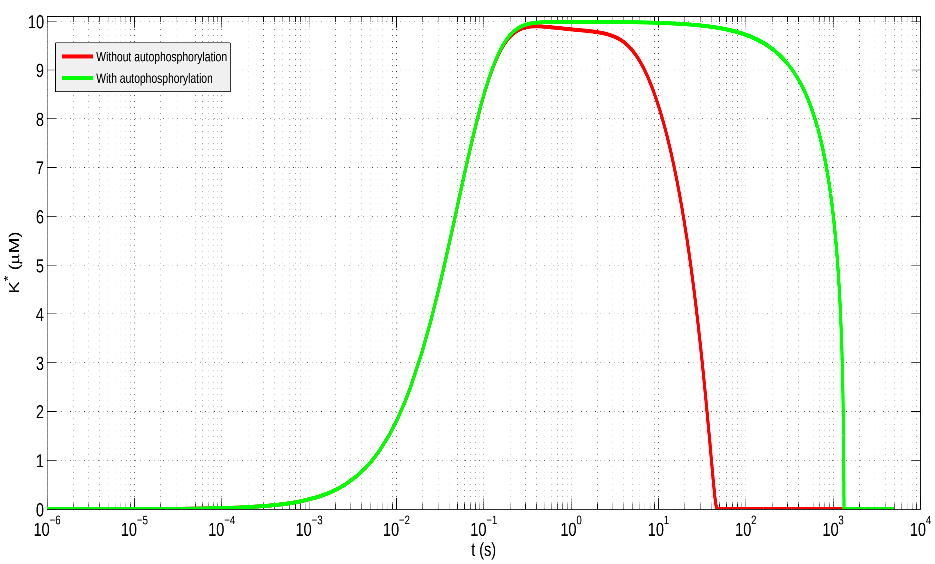

Figure 5.5: The comparison between the ATM dynamics with autophosphorylation and without autophosphorylation process in logarithmic scale. The rest of the parameters are as in figure 5.1.

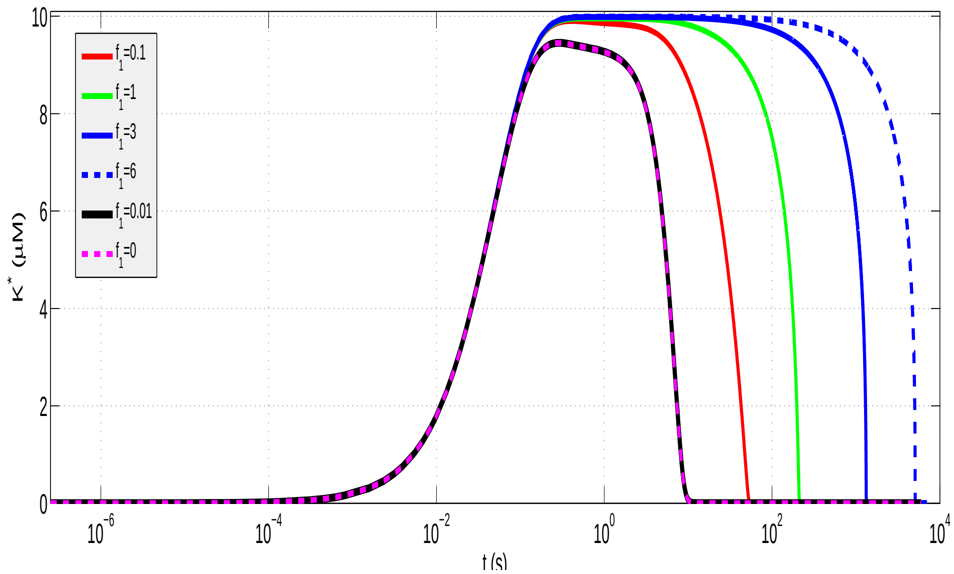

Figure 5.6: The time-courses of K^* for different values of f_1 in logarithmic scale. The rest of the parameters are as in figure 5.1.

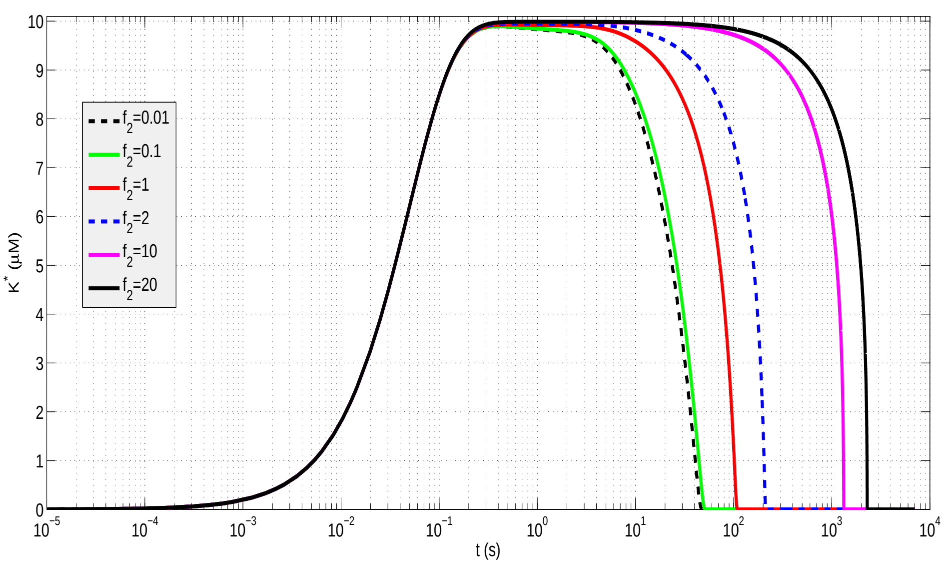

Figure 5.7: The time-courses of K^* for different values of f_2 in logarithmic scale. The rest of the parameters are as in figure 5.1.

eters, P_{tot}, f_3, and f_4 to the dynamics of K^*. In (5.15), the K^* equation contains V_{max} and K_M. From the equation, if V_{max} goes down and K_M goes up, these values should increase the amount of K^*.

Using MATLAB we found that if P_{tot}, f_4, and f_3 are decreased, then the total activity of K^* and its half-life are increased (see figure 5.8, figure 5.9 and figure 5.10). This is because P_{tot} and f_4 are dependent on V_{max}, while f_3 is dependent on K_M. If P_{tot}, f_4, and f_3 are decreased, then V_{max} decreases and K_M increases. Moreover, if these values become smaller and smaller, then the amount of dephosphorylated K^* is reduced, thus keeps the amount of K^* at high level.

In figure 5.10, it is shown that if we fix all the model parameters and f_4 increases, there is a reduction in the maximum of K^* (K^*_{max}), because the C_P will be broken faster into two molecules of K to form a dimer. In contrast, if f_3 is increased, there is no reduction in the maximum of K^* because quite a lot of K^* is sequestered in C_P (see figure 5.9).

The results indicate that, in order to ensure the ATM functionality as a good damage sensor, the level of P_{tot}, f_3, and f_4 must be very low, so that by using these small values, the system can keep K^* at high level until all the DNA DSBs are repaired.

5.5.3 The no repair case ($a_5 = 0$) for $a_4 \neq 0$

In section 5.5.1, we argued that the DNA damage repair a_5 is non-zero and ATM monomerization rate, B is close enough to zero. We found that there is only one equilibrium. The argument was by regular perturbation in B. Now we want to investigate the properties of the system if a_5 is zero. Then (5.12) becomes

$$B = a_6 + a_3(a_4), \tag{5.20}$$

where the dimer monomerisation rate, B is a constant. Here we want to explore the physically relevant concentrations of active ATM concentration K^* for different

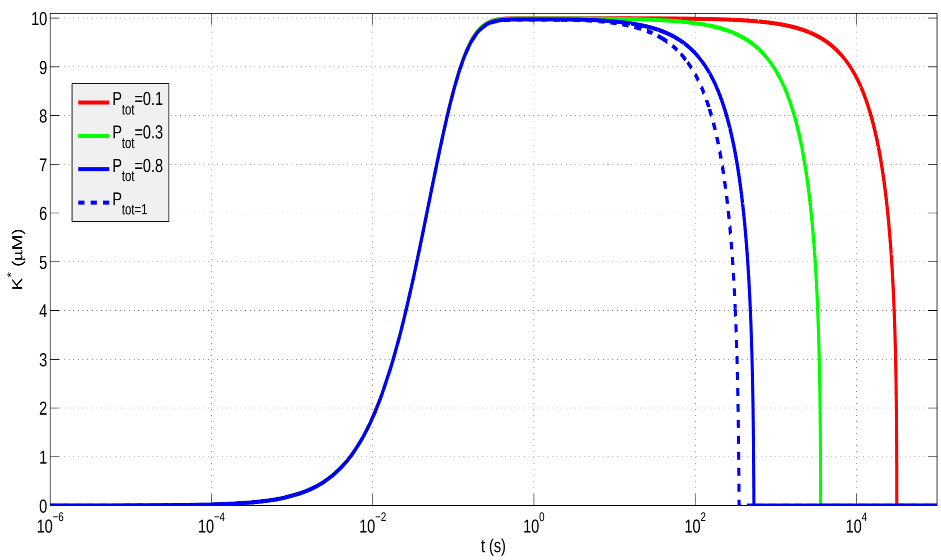

Figure 5.8: The time-courses of K^* for different values of P_{tot} in logarithmic scale. The rest of the parameters are as in figure 5.1.

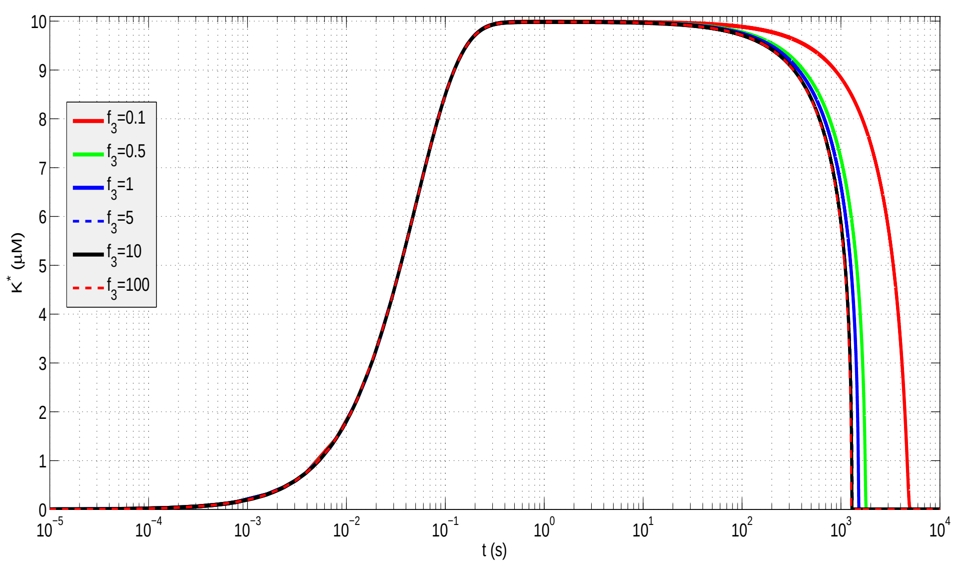

Figure 5.9: The time-courses of K^* for different values of f_3 in logarithmic scale. The rest of the parameters are as in figure 5.1.

values of inactive ATM dimer monomerization rate, B.

Using (5.17) for $V_{max} = 0.25s^{-1}$, $K_{tot} = 10\mu M$, $\beta = \frac{3}{2}\mu M s^{-1}$, and $A = 5s^{-1}$ (the parameter values are the same as in simulation in figure 5.1), the ODEs in (5.16) can be re-written as follows:

$$\begin{aligned} \frac{dK}{dt} &= -\tfrac{3}{2}KK^* + \frac{0.25K^*}{K^* + 0.15} - 10K^2, \\ \frac{dK^*}{dt} &= \tfrac{3}{2}KK^* - \frac{0.25K^*}{K^* + 0.15} + B(10 - K - K^*), \\ \frac{dD}{dt} &= 5K^2 - BD. \end{aligned} \tag{5.21}$$

To explore numerically the dynamics of the model in (5.21), we perform a bifurcation analysis of active ATM concentration (K^*) with respect to the dimer monomerisation rate (B) by the aid of MATCONT. This MATLAB package provides a bifurcation toolbox for the numerical study of dynamical system (see http://www.matcont.ugent.be/ for further details). We vary the parameter B and track the equilibrium points of the model. Figure 5.11 presents a bifurcation diagram of the model in (5.21). The horizontal and vertical axes show the parameter B and active ATM concentration K^*, respectively.

Figure 5.11 shows that if there is no damage, which is when B is sufficiently small then the active ATM concentration K^* very small. In contrast, if the system is overwhelmed by damage (for an example being created via ROS), then the amount of B is high, which results in the value of K^* to be constantly at a high concentration. This result agrees with the result shown in figure 5.4 when $a_5 = 0$ (see blue line in the figure).

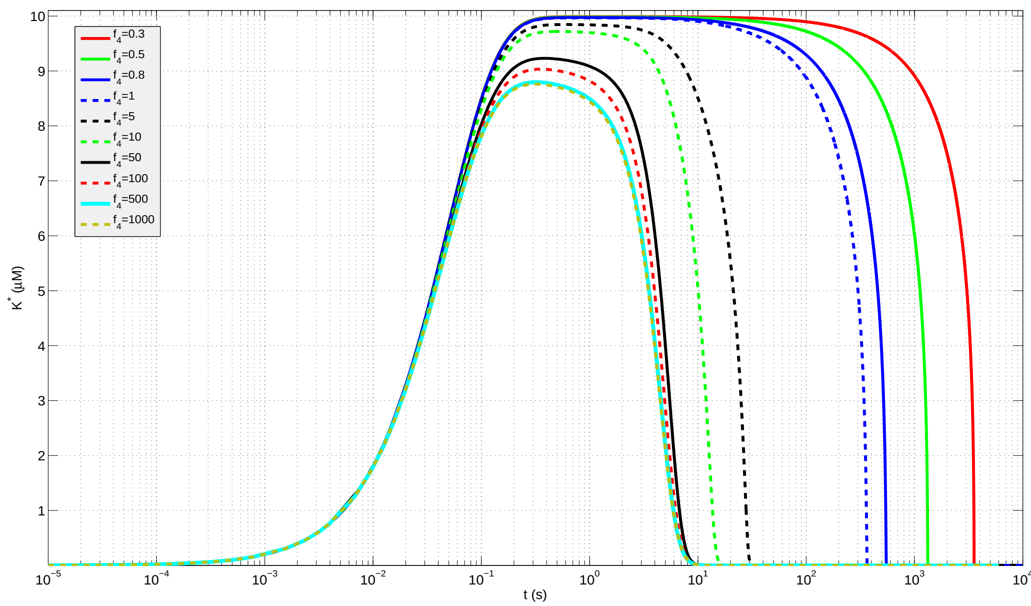

Figure 5.10: The time-courses of K^* for different values of f_4 in logarithmic scale. The rest of the parameters are as in figure 5.1.

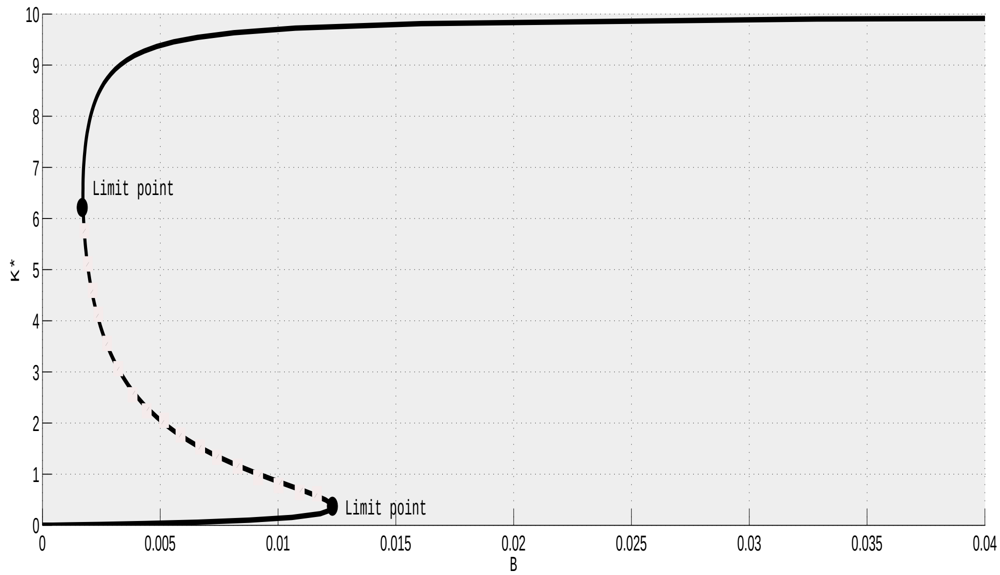

Figure 5.11: Bifurcation diagram of active ATM concentration K^* versus the dimer monomerisation rate B. The two solid lines denote stable steady states: the UP state (upper) and the DOWN state (lower). We can see two saddle-node bifurcations (bold circles) at $B = 0.00171996$ (at equilibrium point (K, K^*, D)=(0.025,6.496,1.740)) and $B = 0.012365083$ (at equilibrium point (K, K^*, D)=(0.109,0.354,4.769)). When $B < 0.00171996$, only the DOWN state is stable; when $B > 0.012365083$, only the UP state is stable. Thus the system exhibits monostable behavior. When $0.00171996 \leq B \leq 0.012365083$, the system is bistable at the two stable steady states, the UP and DOWN states, which are separated by an unstable steady state (dashed line).

5.6 Discussion and conclusions

In this chapter we have discussed a minimal model of the operation of the ATM protein which ensures functionality as a good DNA damage sensor.

The work extends the approach of [59] on the autophosphorylating kinase (e.g. ATM) by taking into consideration of sequestration dynamics, an important aspect of ATM dynamics when there is no DNA damage. By using the ODEs in [59] and the equations of the sequestration process, we simulate the system of ODEs using MATLAB.

The model that we propose here is a minimal one. We made the simplest assumptions on the sequestration parameters A and B. Without any clear guidance from experimental data, we assume that the rate of dimerization A is constant, while the rate of monomerization B is a function of time t which depends on the number of active MRN complexes after the creation of the DNA DSBs.

From all the results shown, it seems likely that the model that we propose is a good model of ATM functionality as we will argue below. The assumption that the damage is being repaired at some fixed rate (which is given by a_5) which is proportional to the DNA damage, and this rate is a constant, is reasonable. As shown in figure 5.4, we can see that when a_5 is very high, that is, the damage is repaired very fast (which indicates that the amount of DNA damage exists is very low), the total activity (or the value) of K^* must also be very low. As what we expect from a good model of ATM is that the half-life and the total activity of K^* should decrease with the increasing a_5. A good ATM model should have the following property: the level of K^* must be always very high while there is still a lot of damage (which is B is high) or always at very low level if there is no more damage (which is B is very low) available after being repaired (see figure 5.11).

Figure 5.12 presents the kind of picture that illustrates the dynamics of K^* activity that one really wants to see and which is found in the simple mathematical framework that we are using. Clearly the assumption that DNA damage decays exponentially over time, which follows from the damage repair and a_5 being a constant, is reasonable. What this means is that there is feedback between the remaining damage and ATM activity, so that we do get an optimal response of the DNA damage. An optimal response is a response that keeps K^* high till everything is done (when all the damage is repaired).

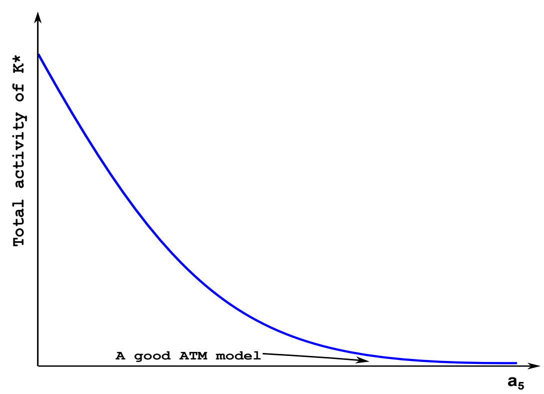

Figure 5.12: The graph of the total activity of K^* (μM) versus the rate of damage repair a_5 ($\mu M s^{-1}$). See text for details.

The mathematical framework suggested in chapter 5, which models the dynamics of various ATM species after DNA damage, might be used to indicate how cancer cell division can be interfered with. It is known that inhibiting ATM signalling is an important target for cancer therapy. For example, it can be done by the ATM inhibitor, KU-55933 [96], or such interference can also be demonstrated by viruses such as adenovirus which can prevent ATM autophosphorylation and signalling [51].

All the results which are presented as time-course curves of active ATM species and also the bifurcation diagram of active ATM concentration K^* with respect to the parameter B might suggest new ways of looking at data that had not been used in the formulation of the model and hence in new experiments. For example, there is no experimental evidence on the mechanism of ATM dimerization and monomerization. Since we made the assumptions that the dimerization rate A and repair rate a_5 are constant, we would like these assumptions checked in vitro. It is known that for phosphorylation we must have an abundant supply of ATP [91]. Hence, it is makes sense to perform in vitro assays of ATM dimerization/monomerization in different ATP regimes and environments (e.g. with or without single-stranded DNA (ssDNA)).

Chapter 6

An example of a structurally unstable bistable system

6.1 Introduction

In section 2.7, we suggested a conceptual scheme for the mechanistic processes leading to the bystander response of ionising radiation as presented in figure 2.13. The figure shows that the scheme contains many network motifs that can give rise to bistability. The bistability curve is shown in figure 2.14. Therefore understanding the mathematics of bistability is important and there is a gap in the literature because it mainly studies closed systems.

It is often claimed in systems biology (see [3]) that biological networks are modular and are best understood in terms of functionalities of modules comprising the network. There are many possible functions a module can have (see [3, 127, 155]). An important type of module is the bistable (or more generally multistable) switch; see the discussion in section 3.5. Bistable switches have been implicated in many aspects in pathology [165].

It is frequently stated that feed-forward loops, i.e. loops of mutual activation, lead to bistability [46, 47, 149]. Such loops are ubiquitous in disease, where they are often called *vicious circles* [112, 123]. Our scheme of figure 2.13 abounds in feed-forward loops, e.g. one involving ROS, MAPK and Cox2, and a longer one involving ROS, DNA damage, ATM, NF-κ B, Cox2 and ROS. Conventional wisdom then would claim that our scheme has bistable elements.

However, in [59] it was suggested, using a very simple and plausible biochemical system, that the connection between feed-forward loops and bistability is not as simple as would appear from the literature. Much of the work on formulating criteria of bistability, such as [4, 98], is restricted to *closed* systems, i.e. systems that do not allow transport into or out of the system, de novo synthesis, or degradation of components. This is clearly biologically unrealistic. The main result of [59] is that under arbitrarily small perturbations of dynamics that destroy closure, the property of bistability can be lost. In other words, topology of a module is not sufficient to determine its functionality in this case.

This result poses two major theoretical questions. The first one is, which closed bistable systems are structurally unstable. The second one is the more important one: what are the criteria for bistability in *open* biochemical systems. Clearly, this question has to be answered in a rigorous manner if we want to establish whether a particular module has the functionality of a bistable switch.

We leave the general discussion of these two question to future work. In this chapter, we show that methods of commutative algebra, such as resultants, combined with regular perturbation methods, can be used effectively to resolve questions of bistability in reasonably complex situations which generally lead to problems involving multivariate polynomials. These tools were unnecessary in [59], as the analysis could there be done "by hand".

We illustrate our methods by considering a modification of the model of [4], described in section 3.5. Surprisingly, as in [59], we find that this model is not structurally stable with respect to bistability under arbitrarily small in- and outfluxes.

Though the work in this chapter does not advance the project of quantitative modelling of the bystander effect, we hope that the flaw in methodology, which considers it sufficient to exhibit a mechanism that only leads to a bistable switch in a closed system, is of considerable general interest, and that the tools we use are versatile enough to be employed in other bistability contexts.

6.2 The modification of the model of Angeli et al. in the case of non-zero kinase turnover

6.2.1 The governing ODEs

The Angeli et al. [4] model (the case of zero kinase turnover) is described in chapter 3. In this chapter we assume that active and inactive Cdc2 are destroyed (or degraded) in a protein turnover process, while only inactive Cdc2 is synthesised. For simplicity we assume that Wee1 is conserved. There is evidence that protein degradation exhibits first-order kinetics, while protein synthesis, which is zero-order [55, 56, 154].

When new terms representing protein turnover are incorporated into the equations proposed by [4] with $\nu = 1$, we obtain the following system of ODEs:

$$\dot{x}_2 = -\alpha_1 x_2 + \frac{\beta_1 x_1 y_1^{\gamma_1}}{K_1 + y_1^{\gamma_1}} + a - d x_2, \tag{6.1}$$

$$\dot{x}_1 = \alpha_1 x_2 - \frac{\beta_1 x_1 y_1^{\gamma_1}}{K_1 + y_1^{\gamma_1}} - d^* x_1, \tag{6.2}$$

$$\dot{y}_2 = -\alpha_2 y_2 + \frac{\beta_2 y_1 {x_1}^{\gamma_2}}{K_2 + x_1^{\gamma_2}}, \tag{6.3}$$

$$\dot{y}_1 = \alpha_2 y_2 - \frac{\beta_2 y_1 {x_1}^{\gamma_2}}{K_2 + x_1^{\gamma_2}}. \tag{6.4}$$

The notation here is the same as in Chapter 3, with the addition of the turnover coefficients d and d^* and the inactive Cdc2 rate a.

To study the structural stability of the Cdc2-cyclinB/Wee1 system, we use from now on the parameters shown in table 6.1 which are taken from [4]. Note that $\gamma_1 = 4$ and $\gamma_2 = 4$; these values result in high degree polynomials that arise in the stability analysis.

Parameter	**Value**
α_1	$1s^{-1}$
α_2	$1s^{-1}$
β_1	$200\mu M s^{-1}$
β_2	$10\mu M s^{-1}$
γ_1	4
γ_2	4
K_1	$30(\mu M)^{-1}$
K_2	$1(\mu M)^{-1}$

Table 6.1: The parameter values for the Cdc2-cyclinB/Wee1 system used by [4].

6.2.2 Mathematical analysis

The main result of this chapter is the following theorem:

Theorem 6.2.1. *For parameter values used by [4], the system (6.1)–(6.4) is structurally unstable with respect to bistability.*

We remind the reader that this means that if when $a = d = d^* = 0$ it exhibits bistability, there are arbitrarily small positive values of a, d, d^* for which the system is monostable.

Proof: Note that if a, d, d^* are non-zero,

$$\frac{d}{dt}(x_2 + x_1) = a - dx_2 - d^* x_1. \tag{6.5}$$

At equilibrium

$$x_2 = \frac{a}{d} - \frac{d^*}{d}x_1. \tag{6.6}$$

Using (6.6), we can substitute the equilibrium value of x_2 in terms of x_1 into (6.1) to obtain

$$-\alpha_1(\frac{a}{d} - \frac{d^*}{d}x_1) + \frac{\beta_1 x_1 y_1^4}{K_2 + y_1^4} + a - d(\frac{a}{d} - \frac{d^*}{d}x_1) = 0, \tag{6.7}$$

or

$$\alpha_1(\frac{a}{d} - \frac{d^*}{d}x_1) - \frac{\beta_1 x_1 y_1^4}{K_2 + y_1^4} - d^* x_1 = 0. \tag{6.8}$$

Since Wee1 is conserved, we use the equation (3.10) in section 3.5.1. Thus, at equilibrium, the algebraic equations to be solved are

$$\begin{aligned} &\alpha_1(\frac{a}{d} - \frac{d^*}{d}x_1) - \frac{\beta_1 x_1 y_1^4}{K_1 + y_1^4} - d^* x_1 = 0 \\ &\alpha_2(1 - y_1) - \frac{\beta_2 y_1 x_1^4}{K_2 + x_1^4} = 0. \end{aligned} \tag{6.9}$$

Our strategy now is to explore the case in which the turnover parameters (a, d and d^*) are very small. The set of equilibrium points of (6.1)–(6.4), that is, of real positive solutions of (6.9) can be found by calculating the resultant of two equations in (6.9) with respect to y_1 using MAPLE. This gives us a 17- degree polynomial $P(x_1)$ the roots are the x_1-coordinates of the equilibria (x_1, y_1).

$$\begin{aligned} &P(x_1) = (-200\,d - 439231\,d^*\,d - 439231\,d^*)\,{x_1}^{17} + \\ &439231\,{x_1}^{16}a + (-159724\,d^* - 800\,d - 159724\,d^*\,d)\,{x_1}^{13} \\ &+159724\,{x_1}^{12}a + (-21786\,d^* - 21786\,d^*\,d - 1200\,d)\,{x_1}^{9} \\ &+21786\,{x_1}^{8}a + (-1324\,d^*\,d - 1324\,d^* - 800\,d)\,{x_1}^{5} \\ &+1324\,{x_1}^{4}a + (-31\,d^*\,d - 31\,d^* - 200\,d)\,x_1 + 31\,a = 0 \end{aligned} \tag{6.10}$$

with three parameters a, d and d^*. Note that we are using the [4] values of parameters throughout. This we have to determine the number of real positive roots of P_1. We will do this by computing the discriminant Δ of the polynomial and using Sturm's theorem. The interested reader is referred to chapter 3 for details of these tools.

From (3.15) in chapter 3, the discriminant of the odd-degree polynomial in (6.10) is given by

$$\Delta = f(d,a) = (-1)^{\frac{1}{2}(17)(16)} \frac{1}{-439231d^* - 200d - 439231d^*d} R(P,P'), \qquad (6.11)$$

where $R(P,P')$ is the resultant of P and $\dfrac{dP}{dx_1}$ with respect to x_1. Using MAPLE, we find that the discriminant of $P(x_1)$ is a polynomial of degree 32 in d, d^*, and a.

According to [161], the rate of Cdc2 degradation is higher in S-phase than in G_1-phase in which an activation of Cdc2 occurs at or before the G_1/S transition in cell cycle (see section 2.2.7 in chapter 2). This indicates that $d > d^*$. However, due to the complexity of the expressions involved, we assume that $d = d^*$. Therefore, $f(d,a)$ is now a polynomial of degree 66 in d and 32 in a.

Next, we need to work out for what (d,a), $P(x_1)$ has three positive roots (so the system is bistable), or one (so the system is monostable). The set $f(d,a) = 0$ is the union of the curves shown in figure 6.1. As we cross these curves, the number of roots of $P_1(x)$ changes. We will show that in the shaded region, the system is bistable and outside it, it is monostable. Note that the region of bistability is bounded.

We are interested in the regime where the protein turnover parameters are very small ($0 < a \ll 1$ and $0 < d \ll 1$). For this, we rescale a and d. Thus, we introduce a small parameter ε and set $a = \varepsilon A$ and $d = \varepsilon\delta$. Therefore, $f(d,a) = 0$ now becomes

$$f(\varepsilon\delta, \varepsilon A) = 0, \qquad (6.12)$$

or expanding in ε,

$$\varepsilon f_1(\delta, A) + \varepsilon^2 f_2(\delta, A) + (\text{ Higher Order Terms in } \varepsilon) = 0. \qquad (6.13)$$

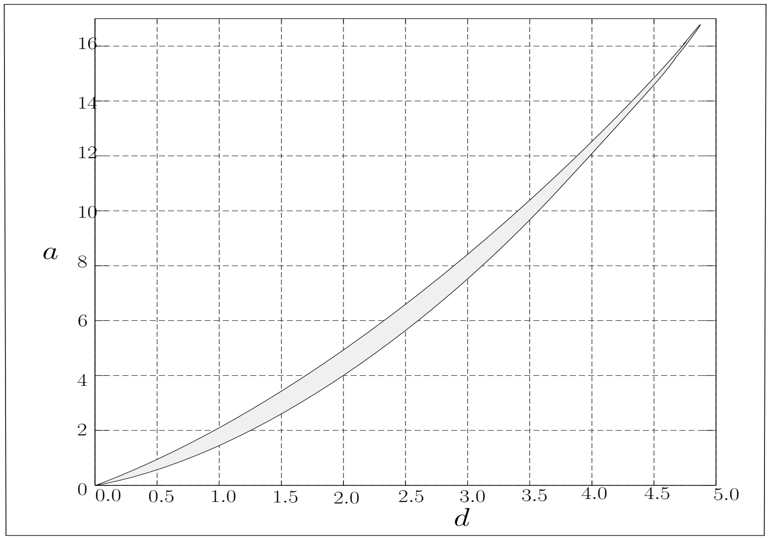

Figure 6.1: The set $f(d, a) = 0$.

As $\varepsilon \ll 1$, we only consider the first term in the left side of the equation in (6.13) and hence we obtain $f_1(\delta, A) = 0$. With the aid of MAPLE, $f_1(\delta, A) = 0$ is illustrated in figure 6.3.

As we can see in figure 6.3, Region II in (d, a)-plane is bounded by two straight lines which pass through the origin. Our next task is to find out the equation of the lines. Suppose the lines are given by

$$A = m\delta, \tag{6.14}$$

where m is the line slope. Then, by substituting (6.14) into $f_1(\delta, A) = 0$, we obtain

$$\begin{aligned} f_1(m\delta, \delta) \approx{} & -2.634193844 \times 10^{147}\, m^4\delta^{33} + 2.787004386 \times 10^{148}\, m^{12}\delta^{33} - \\ & 9.343386656 \times 10^{131}\, m^{28}\delta^{33} + 5.898600220 \times 10^{148}\, m^{16}\delta^{33} - \\ & 2.098048254 \times 10^{123}\, m^{32}\delta^{33} - 6.874031960 \times 10^{147}\, m^{20}\delta^{33} - \\ & 1.045562823 \times 10^{147}\, \delta^{33} - 1.387446145 \times 10^{140}\, m^{24}\delta^{33} + \\ & 2.501077087 \times 10^{147}\, m^8\delta^{33} = 0. \end{aligned} \tag{6.15}$$

By solving (6.15) using MAPLE, we find that the values of the slopes m_1 and m_2 are

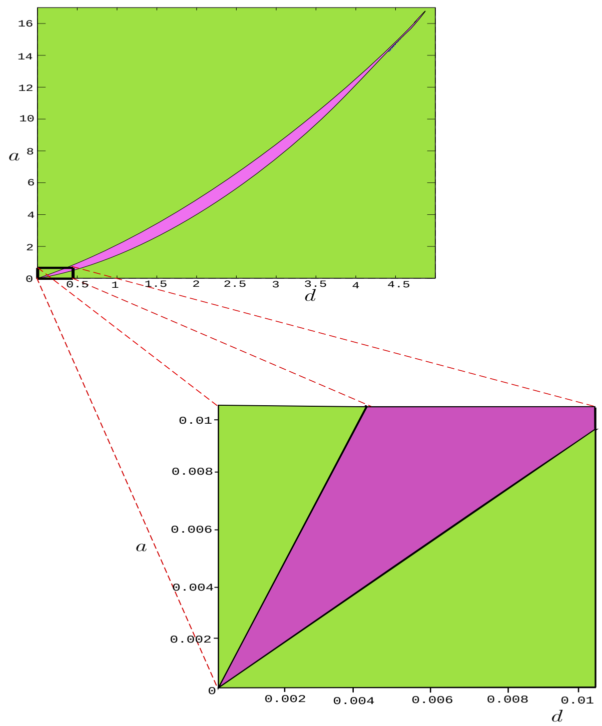

Figure 6.2: We now enlarge the region in figure 6.1 as we want to work with small turnover parameters.

$$m_1 \approx 0.7567928014 \text{ and } m_2 \approx 1.733670494, \tag{6.16}$$

or, equivalently,

$$\frac{A}{\delta} \approx 0.7567928014 \text{ and } \frac{A}{\delta} \approx 1.733670494. \tag{6.17}$$

$$\frac{A}{\delta} = \frac{a}{\varepsilon} \times \frac{\varepsilon}{d} = \frac{a}{d}. \tag{6.18}$$

Therefore, (6.17) implies that

$$\frac{a}{d} \approx 0.7567928014 \text{ and } \frac{a}{d} \approx 1.733670494. \tag{6.19}$$

Next, we aim to show that in Region I $P_1(x_1)$ has only one positive root, while

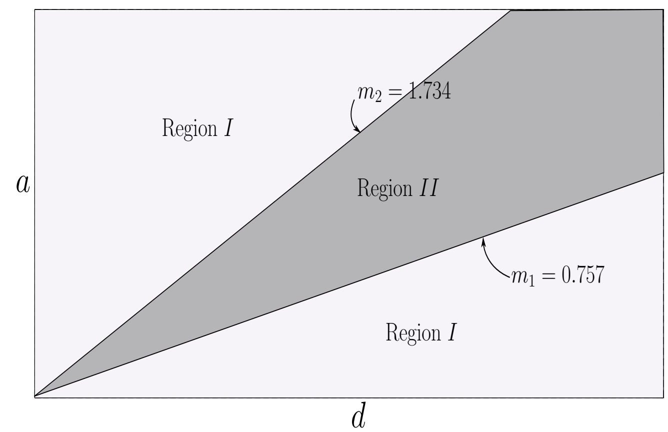

Figure 6.3: The structure of the set $f(A, \delta) = 0$ with d, a being $O(10^{-3})$

in Region II it has exactly three positive roots. This is proved in the following lemma using Sturm's theorem and the Cauchy Criterion (see chapter 3).

Lemma 6.2.2. *Let $f(d, a)$ be given by (6.11) with parameters $0 < a \ll 1$ and $0 < d \ll 1$.*

1. *For any point in the (d, a) plane such that $f(d, a) < 0$ (in Region I, figure 6.3), there is a globally asymptotically stable equilibrium point (x_1^*, y_1^*, x_2^*) in (6.10). Thus the system is monostable.*

2. *For any point in the (d, a) plane such that $f(d, a) > 0$ (in Region II, figure 6.3), there are three equilibrium points: $(x_{11}^*, y_{11}^*, x_{21}^*)$, $(x_{12}^*, y_{12}^*, x_{22}^*)$, and $(x_{13}^*, y_{13}^*, x_{23}^*)$ in (6.10). Two equilibrium points are locally asymptotically stable points, and one point is a saddle, making the system bistable.*

Proof of the Lemma:

Region I

Note that, for $0 < a \ll 1$ and $0 < d \ll 1$, Region I lies outside $f(d, a) = 0$ (see figure 6.1) and within the line with slopes $0 < m \leq 0.757$ and $m \geq 1.734$ (see figure 6.3). Suppose there is an arbitrary point (p, q) that lies in Region I, say on a line $a = \frac{1}{2}d$ with slope $m = 0.5$ for d small enough. Thus with $(p, q) = (d, \frac{1}{2}d)$, and substituting into (6.11), $f(d, \frac{1}{2}d) < 0$, (6.10) becomes

$$P(x_1, d) \approx \tfrac{31}{2} + (-439231\,d - 439431)\,{x_1}^{17} + \tfrac{439231}{2}\,{x_1}^{16} + (-160524 - 159724\,d)\,{x_1}^{13} + 79862\,{x_1}^{12} + (-22986 - 21786\,d)\,{x_1}^{9} + 10893\,{x_1}^{8} + (-1324\,d - 2124)\,{x_1}^{5} + 662\,{x_1}^{4} + (-31\,d - 231)\,x_1. \tag{6.20}$$

We want to show that for sufficiently small $d > 0$ this equation has only one positive solution. So first set $d = 0$, thus (6.20) becomes

$$P(x_1) \approx \tfrac{31}{2} - 439431\,{x_1}^{17} + \tfrac{439231}{2}\,{x_1}^{16} - 160524\,{x_1}^{13} + 79862\,{x_1}^{12} - 22986\,{x_1}^{9} + 10893\,{x_1}^{8} - 2124\,{x_1}^{5} + 662\,{x_1}^{4} - 231\,x_1. \tag{6.21}$$

Using MAPLE to solve (6.20), we see that it has only one positive solution. We can verify this using Sturm's theorem (see chapter 3 for details of this tool).

To find the number of real polynomial roots in (6.21), we first compute the Sturm function (see chapter 3) using MAPLE. This calculation yields a Sturm chain (see chapter 3) of polynomials: $P_0(x_1), P_1(x_1), P_2(x_1), \cdots, P_{16}(x_1), P_{17}(x_1)$, with $P_{17}(x_1)$ is of degree 17, $P_n(x_1)$ is of degree $17 - n$, and $P_0(x_1) = -1$.

After the Sturm sequence (or chain) is computed, we can investigate how many real roots the polynomial has. Using MAPLE, we found that in the interval $x_1 \in [0, \infty]$ there is only one real root. Note that the number of real roots lying in the interval (a, b) can be calculated from the value of $N(b) - N(a)$, where $N(b)$ and $N(a)$ is the number of changes of sign in the Sturm chain given by $P_0(b), \cdots, P_{16}(b), P_{17}(b)$ and $P_0(a), \cdots, P_{16}(a), P_{17}(a)$, respectively.

In our study, we are only interested in positive real roots. Here, we apply the Cauchy Criterion to find where the root of the polynomial $P(x_1)$ is located. Cauchy says the real root of (6.21) is in the interval $[-M, M]$ where:

$$M = 1 + \frac{max_{0 \le i \le 16} |a_i|}{|a_{17}|}, \tag{6.22}$$

or

$$M \approx 1 + \frac{2.196155}{4.39431} \approx 1.4998. \tag{6.23}$$

Here, we found that the root only exists in $[-1.4998, 1.4998]$.

Applying Sturm's theorem, we can reduce the interval for the solution of $P(x_1) = 0$ in (6.21). Table 6.2 shows the number of real roots R lie in interval (a, b) obtained for points separated by $\triangle x_1 = 1.4998$:

a	**b**	**R**
-1.4998	0	0
0	1.4998	1

Table 6.2: The interval of x_1 and the number of real roots

Table 6.2 tells that $P(x_1)$ has a positive real root (for which $0 < x_1 < 1.4998$). By reducing the spacing of x_1 to $\triangle x_1 = 0.001$, we found that the root lies in $x_1 = [0.067, 0.068]$. One can reduce the interval if desired. Here we choose $x_1 = 0.067$. To obtain y_1 at $x_1 = 0.067$, we use the second equation in (6.9). This equation can be rewritten as

$$y_1 = f(x_1) = \frac{1 + {x_1}^4}{1 + 11\, {x_1}^4}. \tag{6.24}$$

Substituting $x_1 = 0.067$ into (6.24) and (6.6), thus $y_1 = 0.37$ and $x_2 = 0.433$. Therefore, the equlibrium point found in Region I for $d = 0$ is $(x_1^*, y_1^*, x_2^*) = (0.067, 0.37, 0.433)$.

Next we need to examine the stability of the equilibrium points of the system. Using the stability analysis of three-dimensional system of ODEs, the Jacobian matrix of the three-variable: x_1, x_2 and y_1 system is given as

$$\begin{bmatrix} -1-d & 200\,\frac{{y_1}^4}{30+{y_1}^4} & 800\,\frac{x_1{y_1}^3}{30+{y_1}^4}-800\,\frac{x_1{y_1}^7}{\left(30+{y_1}^4\right)^2} \\ 1 & -200\,\frac{{y_1}^4}{30+{y_1}^4}-d & -800\,\frac{x_1{y_1}^3}{30+{y_1}^4}+800\,\frac{x_1{y_1}^7}{\left(30+{y_1}^4\right)^2} \\ 0 & -40\,\frac{y_1{x_1}^3}{1+{x_1}^4}+40\,\frac{y_1{x_1}^7}{\left(1+{x_1}^4\right)^2} & -1-10\,\frac{{x_1}^4}{1+{x_1}^4} \end{bmatrix} \tag{6.25}$$

which is evaluated using MAPLE. Substituting the value of $d = 0, x_1 = 0.067$, $y_1 = 0.37$, and $x_2 = 0.433$ into the Jacobian matrix in (6.25), MAPLE gives three real eigenvalues ($\lambda_{10}, \lambda_{20}$, and λ_{30}) which are negative numbers. These values conclude that the equilibrium point $(x_1^*, y_1^*, x_2^*) = (0.067, 0.37, 0.433)$ is globally asymptotically stable . Thus the system in (6.9) for $d = 0$ exhibits monostable behavior.

Since by inspection, the dependence of (6.20) on d is regular, the implicit function theorem (see [88] for details) tells us that there is a unique positive solution $(x = x(d))$ which is defined by $P(x_1(d), d) = 0$ and $x_1(0) = x_0$, where x_0 is the root of $P(x_1, 0) = 0$ in (6.21), i.e., $x_0 = 0.067$. But for sufficiently small d the line $a = \frac{1}{2}d$ is in Region I, hence since the number of positive solutions is the same everywhere in Region I, in Region I we have monostability.

If $x_1 = 0.067$ (or $x_0 = 0.067$) solves $P(x_1) = 0$ in (6.21), then for sufficiently small d, the unique solution of $P(x_1, d) = 0$ in (6.20) will be $x_1 + O(d) = 0.067 + O(d)$. There is no need to find $0(d)$ term. In this case if there are $0(1)$ terms, $0(d)$ terms are much smaller if d is small. It means that every expansion has the form of $a_0 + a_1 d + a_2 d^2$ and so on so for d small enough, no matter what a_1 is, a_0 term dominates as it is not zero and independent of d. So the result is that for small $d > 0$ the unique equilibrium of the system is $(x_1^* + O(d), y_1^* + O(d), x_2^* + O(d)) = (0.067 + O(d), 0.37 + O(d), 0.433 + O(d))$.

The eigenvalues of the Jacobian in (6.25) for small $d > 0$ will be $\lambda_1 = \lambda_{10} + O(d), \lambda_2 = \lambda_{20} + O(d)$, and $\lambda_3 = \lambda_{30} + O(d)$, where $\lambda_{10}, \lambda_{20}$, and λ_{30} are the eigenvalues found by plugging $d = 0, x_1 = 0.067$, $y_1 = 0.37$, and $x_2 = 0.433$ into the Jacobian matrix in (6.25). And since $\lambda_{10}, \lambda_{20}$, and λ_{30} have negative real parts, a small perturbation in d will not do any damage.

Everywhere in Region I except the line $d = 0$, $P(x_1, d)$ has a globally asymptotically stable real root no matter how small a and d are individually. This monostable character is unchanged except if the point (d, a) moves to other region through the transition curve which are the line with slopes $m_1 = 0.757$, $m_2 = 1.734$, and curve $f(d, a) = 0$.

Region II

Note that, for $0 < a \ll 1$ and $0 < d \ll 1$, Region II lies inside $f(d, a) = 0$ and within the slope $0.757 < m < 1.734$ (see figure 6.3). Suppose there is an arbitrary point (p, q) that lies within Region II. Let $m = 1$ be a slope in the region, so that $a = d$ for d small enough. Therefore, we have $(p, q) = (d, d)$. At this point $f(d, d) > 0$ and (6.10) becomes

$$\begin{aligned} P(x_1, d) &\approx 31 + (-439231\, d - 439431)\, {x_1}^{17} + 439231\, {x_1}^{16} + (-160524 - 159724\, d)\, {x_1}^{13} \\ &+159724\, {x_1}^{12} + (-22986 - 21786\, d)\, {x_1}^{9} + 21786\, {x_1}^{8} + (-1324\, d - 2124)\, {x_1}^{5} \\ &+1324\, {x_1}^{4} + (-31\, d - 231)\, x_1. \end{aligned} \tag{6.26}$$

We want to show that for sufficiently small d this equation has three positive solution. So first set $d = 0$, thus (6.26) becomes

$$\begin{aligned} P(x_1) &\approx 31 - 439431\, {x_1}^{17} + 439231\, {x_1}^{16} - 160524\, {x_1}^{13} + 159724\, {x_1}^{12} - 22986\, {x_1}^{9} \\ &+21786\, {x_1}^{8} - 2124\, {x_1}^{5} + 1324\, {x_1}^{4} - 231\, x_1 \end{aligned} \tag{6.27}$$

Performing on (6.27) an analysis similar to that in Region I, thus the Sturm chain of (6.26) is given by polynomials $P_0(x_1), P_1(x_1), P_2(x_1), \cdots, P_{16}(x_1), P_{17}(x_1)$, with $P_{17}(x_1)$ is of degree 17, $P_n(x_1)$ is of degree $17 - n$, and $P_0(x_1) = 1$.

We apply the Cauchy Criterion to find where the root in polynomial $P(x_1)$ is located. Using Cauchy's criterion

$$M = 1 + \frac{4.39231}{4.398702310} = 1.99855. \tag{6.28}$$

Thus all the positive roots of $P(x_1)$ in (6.27) lie in $[0, 1.99855]$. Using Sturm's theorem, we found that each of the root lies in $[0.1, 0.2]$, $[0.5, 0.6]$ and $[0.9, 1]$. By reducing the interval of x_1 to 0.01, the roots are $x_{11} = 0.14$, $x_{12} = 0.51$ and $x_{13} = 0.99$. Then substituting those three values of x_{11}, x_{12}, and x_{13} into (6.24) and (6.6), we obtain $(x^*_{11}, y^*_{11}, x^*_{21}) = (0.99, 0.17, 0.82)$, $(x^*_{12}, y^*_{12}, x^*_{22}) = (0.51, 0.61, 0.49)$ and $(x^*_{13}, y^*_{13}, x^*_{23}) = (0.14, 0.99, 0.86)$. Next we need to examine the stability of these equilibrium points of the system. Using the stability analysis of three-dimensional system of ODEs similar to that in Region I for $d = 0$, we found that equilibrium points: $(x^*_{11}, y^*_{11}, x^*_{21}) = (0.99, 0.17, 0.82)$ and $(x^*_{13}, y^*_{13}, x^*_{23}) = (0.14, 0.99, 0.86)$ are locally asymptotically stable points (the three eigenvalues for both of equilibrium points are negative real numbers), while $(x^*_{12}, y^*_{12}, x^*_{22}) = (0.51, 0.61, 0.49)$ is a saddle point (with two negative real eigenvalues and one positive real eigenvalue).

Since by inspection the dependence of (6.26) on d is regular, the implicit function theorem (see [88] for details) tells you that for sufficiently small $d > 0$ there is a unique positive solution ($x = x(d)$) which is defined by $P(x_1(d), d) = 0$ and $x(0) = x_0$, where x_0 is one of the roots of $P(x_1, 0) = 0$, i.e., $x_0 = 0.99, 0.51$, and 0.14. But for sufficiently small $d > 0$, the line $a = d$ is in Region II, where the number of positive solutions is the same everywhere in Region II.

For sufficiently small $d > 0$, the eigenvalues of the system will be $\lambda_1 = \lambda_{10} + O(d), \lambda_2 = \lambda_{20} + O(d)$, and $\lambda_3 = \lambda_{30} + O(d)$ for each equilibrium point (see the clarification of eigenvalues for $d > 0$ in Region I). The sign of the eigenvalues cannot change for small enough d. In this case if there are $0(1)$ terms, $0(d)$ terms are much smaller if d is small. It means that every expansion has the form of $a_0 + a_1 d + a_2 d^2$ and so on so for d small enough, no matter what a_1 is, a_0 term dominates as it is not zero and independent of d. Therefore everywhere in Region II, the bistability character of the equilibrium points in Region II are unchanged, unless if the point (d, a) moves to other region through the transition curve which are the lines with slopes $m_1 = 0.757$, $m_2 = 1.734$, and a curve $f(d, a) = 0$.

These results show that the system is not structurally stable with respect to bistability (which means that arbitrarily small value of a and d can make bistability disappear). In other words, there is no bistability if there is kinase turnover and $\frac{a}{d} \notin (0.7567928014, 1.733670494)$ and $f(d, a) < 0$ no matter how small d and a are individually.

6.3 Conclusions

In this chapter, we discussed a structurally unstable bistable Cdc2-CyclinB/Wee1 system suggested by [4], in which bistability can vanish when arbitrarily small rates of protein turnover are taken into consideration.

There are other bistability studies that neglect protein turnover such as [27, 98]. In [59] the same phenomenon of structural instability with respect to bistability is shown to occur in an autophosphorylating kinase system proposed by [98]. Compared to our work, [59] deals with a much simpler polynomial (quadratic) while the polynomial in the model that we discuss in this chapter is of degree seventeen. In addition the bistability wedge in the turnover parameters plane in [59] is an open one and infact the region does close for large enough parameters. In contrast, the region of bistability in our case, bounded by (d, a) such that $f(d, a) = 0$ is closed and bounded. Due to the complexity of expression, we work under the assumption that the rate of degradation of both active and inactive form of the Cdc2 kinase is the same, $d = d^*$). We also neglect turnover of Wee1.

In our work, since the degree of polynomial $P(x_1)$ is more than five, we use discriminants, Sturm's theorem, the Cauchy Criterion, and the theorem implicit function to analyse the structural stability of the Cdc2-CyclinB/Wee1 system.

Since bistability is an important property of signal transduction pathways, there is a need to work out how to make bistable behavior in biological systems robust with respect to protein turnover.

Besides, as suggested by [161], the rate of degradation of Cdc2 in active form is smaller than in the inactive form, so that $\frac{d^*}{d} < 1$. It would be interesting to redo the structural stability analysis of the Cdc2-CyclinB/Wee1 system taking this relation and also Wee1 turnover into consideration.

Furthermore, it has been assumed that kinase synthesis has zero order kinetics while kinase degradation has first order kinetics. It is a good idea to verify the validity of these assumptions experimentally.

Chapter 7

Conclusions and further work

To understand ionising radiation damage to mammalian cells, we have analysed three important processes involved in radiation response.

In chapter 4, we suggested a framework to model evolution of cell populations following high dose irradiation. The model proposed in the present work is close in spirit to that of [2]. In addition to differences in assumptions, we extend Albright's work both by analysing the effect of dose fractionation effect on cell death and by developing a method of parameter estimation: neither of these important issues was considered in that work.

We considered a population of cells structured by the number of DSBs and misrepairs incurred after a dose of low LET radiation. The ODE model describes the evolution of the irradiated population of cells in time. The work is in three parts. First, we considered the effect of a single dose D of radiation treatment. We observed that the fraction of surviving cells can be well approximated by the linear quadratic relation (see figure 4.3). Second, in section 4.8, we estimated the six parameters (δ, α_1, α_2, p, V_{max}, and K_m) of the model using real survival data. We estimated the six model parameters using two different types of optimisation methods; i.e a local and a global optimisation techniques namely: Nelder-Mead (NM) simplex algorithm (see section 3.3.2) and Simulated Annealing (SA) algorithm (see section 3.3.3), respectively. Performance of both optimisation methods are evaluated based on the value of the objective function (SSE), computational time and number of interation. We found that the NM simplex algorithm is more superior than the SA algorithm for both low and high LET survival data. In particular, the value of the objective function (SSE) is much smaller than provided by SA method. In addition the value of the correlation between estimated survival data and experimental data r^2 are close to 1 which correspond to an excellent fit. Furthermore, the good fit between estimated survival data and experimental data can also be seen from the value of the LQ parameters for estimated survival data α_{model} and β_{model} which are close to α_{exp} and β_{exp}. The algorithm also performed the shortest computational time of the optimisation runs till convergence and obtained a fewer number of iteration to converge to the minimum value of the objective function.

To determine reliability of the parameter estimation algorithms introduced in section 4.8, in section 4.8.2 two set of model data are generated using chosen sets of parameters (δ, α_1, α_2, p, V_{max}, and K_M) value for low and high LET cell survival model data. Using the generated model data with some of the true parameter values are known, we compared the performance of the NM simplex method and the SA algorithm in terms of the percentage difference between the true values and the estimated values and also the value of the objective function. We observed that for both low and high LET model survival data, the SA algorithm and the NM simplex algorithms returned the true parameter values. It is worth to note that the parameter estimation algorithms which using the model in section 4.5 are applicable and reliable methods of parameter estimation of the model and also there is no restriction for low or high LET IR survival data.

Next, we can relate the LQ bulk parameters α and β to the mechanistic parameters δ, α_1, α_2, p, V_{max}, and K_M using the proposed parameter estimation algorithm discussed in section 4.8. It is of interest to understand the elasticity of α and β with respect to δ and p as these (radiosensitivity and replication fidelity rates, respectively) can be manipulated. We measured the sensitivity of α_{model} and

β_{model} to parameters δ, α_1, α_2, p, V_{max}, and K_m. We found that for low LET survival data, both α_{model} and β_{model} are sensitive to mechanistic parameters δ and p, radiosensitivity and repair fidelity, respectively, which can be experimentally manipulated. In this case, we immediately have a treatment recommendation: to try to increase tumour tissue aeration (which correlates with radiosensitivity) and decrease tumour DNA repair fidelity during pre-radiation treatment. Whereas, for high LET survival data only LQ parameter β is sensitive to δ. Here, we also have a treatment recommendation which is to try to increase tumour tissue aeration prior to irradiation.

In the last section, we dealt with cell killing effects of fractionated doses of radiation. Using the algorithm that we proposed, we observed that the main effect of fractionation is the increment of cell surviving fraction (which is the reflection of repair of sublethal DNA damage between fractions), with very little influence on the $\alpha-$component. It is worth to note that alpha-beta ratio (which is a tissue property) for low and high LET remain unchanged due to fractionation.

For further developments, it is clear that the ODE model can be replaced by a continuum (linear) PDE limit, but the two most promising extensions are by making the model more biologically plausible. One direction would be to allow less restrictive repair mechanisms, in which DSBs are repaired in parallel and not sequentially as in the present version, while the other is to allow a structuring also in respect of the position the cell occupies in the cell cycle, a discrete variable c with values in the set of cell cycle phase: G_1-phase, S-phase, G_2-phase, and M-phase, and allow for both interphase and mitotic death. Due to non-uniqueness of the estimated parameters, Monte Carlo methods and Bayesian calibration are required for further parameter estimation analysis and will become a part of the author's future work.

Apart from direct effects of exposure to ionising radiation that include cell killing and mutation in target cells, ionising radiation can also enhance the frequency of secondary effects in non-targeted cells (bystander cells) which has been referred to the radiation-induced bystander effect (chapter 2). We made a conjecture that bystander response of ionising radiation system can exhibit bistable behaviour (chapter 2). In section 2.7, we suggested a conceptual scheme for the mechanistic processes leading to the bystander response of ionising radiation as presented in figure 2.13. Initially, our intention was to develop a mechanistic model of radiation-induced bystander response in chapter 5, but due to the complexity of the processes involved in the bystander response system, here we limit ourselves by assuming that active ataxia telangiectaxia mutated, ATM (a DNA damage sensor) can be activated only by the DNA damage (see chapter 5 for further details). We will model the full bystander response system in future.

Figure 2.13 shows that the scheme contains many network motifs that can give rise to bistability, an important property of signal transduction pathways. The bistability curve is shown in figure 2.14 for the concentration of active ATM as a function of the strength of feedback loops between double strand breaks (DSBs) and ATM. ATM is one of the important kinases which are involved in the DNA damage bystander response pathways as well as in the targeted radiation effects (see section 2.6). The disbalance between the positive and negative feedback loops will switch the bistable system from a state of healthy low activated ATM concentration into a state of chronically high activated ATM concentration. As a good sensor of DNA DSBs, active ATM should be able to change back into its inactivated state as soon as possible, as protracted high level of ATM activation may trigger cell death by apoptosis (chapter 2). Levels of active ATM can be lowered by dephosphorylation, or by degradation of active ATM, or by the sequestration of inactive ATM in dimers.

Therefore, in chapter 5, a mathematical framework is constructed to model the dynamics of various ATM species following ionising radiation. The work extended the approach of [59] on the autophosphorylating kinase (ATM) by taking into consideration sequestration dynamics, an important aspect of ATM dynamics. By using the ODEs in [59] and the equations of the sequestration process, we solved the system of ODEs using MATLAB. Due to the complexity of the DNA damage response system, the model that we proposed here is a minimal one. We made the simplest assumptions on the sequestration parameters A and B. We assume that the rate of dimerization A is constant, while the rate of monomerization B is a function of time which depends on the number of active MRN complexes after the creation of the DNA DSBs.

From all the results shown, it seems likely that the model that we proposed is a good model of ATM functionality as we will argue below. The assumption that the damage is being repaired at some fixed rate (which is given by a_5) which is proportional to the DNA damage, and this rate is a constant, is reasonable. As shown in figure 5.4, we can see that when a_5 is very high, that is, the damage is repaired very fast (which indicates that the amount of DNA damage exists is very low), the total activity (or the value) of K^* must also be very low. As what we expected from a good model of ATM is that the half-life and the total activity of K^* should decrease with the increasing a_5. A good ATM model should have the following property: the level of K^* must be always very high while there is still a lot of damage (which is B is high) or always at very low level if there is no more damage (which is B is very low) available after being repaired (see figure 5.11).

Figure 5.12 presented the kind of picture that illustrates the dynamics of K^* activity that one really wants to see and which is found in the simple mathematical framework that we are using. It should be noted that figure 5.12 is actually representing the bistable curve shown in figure 2.14 where m in the figure represented B (i.e monomerisation rate) in our model. Clearly the assumption that DNA damage decays exponentially over time, which follows from the damage repair and a_5 being a constant, is reasonable. What this means is that there is feedback between the remaining damage and ATM activity, so that we do get an optimal response of the DNA damage. An optimal response is a response that keeps K^* high till everything is done (when all the damage is repaired).

The mathematical framework suggested in chapter 5 which models the dynamics of various ATM species after DNA damage might be used to indicate how cancer cell division can be interfered with. It is known that inhibiting ATM signalling is an important target for cancer therapy. For example, it can be done by the ATM inhibitor, KU-55933 [96], or such interference can also be demonstrated by viruses such as adenovirus which can prevent ATM autophosphorylation and signalling [51].

All the results which are presented as time-course curves of active ATM species and also the bifurcation diagram of active ATM concentration K^* with respect to the parameter B might suggest new ways of looking at data that had not been used in the formulation of the model and hence in new experiments. For example, there is no experimental evidence on the mechanism of ATM dimerization and monomerization. Since we made the assumptions that the dimerization rate A and repair rate a_5 are constant, we would like these assumptions checked in vitro. It is known that for phosphorylation we must have an abundant supply of ATP [91]. Hence, it is makes sense to perform in vitro assays of ATM dimerization/monomerization in different ATP regimes and environments (e.g. with or without single-stranded DNA (ssDNA)).

In chapter 4 we never considered how ATM activation can be linked to apoptosis or other cell fate outcomes, i.e the model is on completely different level. In chapter 4 we are only saying that the more DSBs the more chance to die. Whereas the model in chapter 5 is just a small step towards a full mechanistic model of cell fate decisions. To develop a mechanistic model of cell death we need a whole giant module involving p53, caspases, mdm2, cytochrome, etc. For an example, see the work of Ma et al. [102].

Since bistability is an important property of signal transduction pathways (as mentioned in section 2.7) and there is a gap in the literature because it mainly studies closed systems, in chapter 6 we analysed the bistable system of [4], who neglected protein turnover (i.e a closed system). To be more realistic, we extended the model of [4] by taking into account protein turnover and focused on structural stability of the model with respect to protein turnover. The results showed that the bistable behaviour of the extended model is not robust with respect to protein turnover. This result is in agreement with [16, 59].

In [59] the same phenomenon of structural instability with respect to bistability is shown to occur in an autophosphorylating kinase system proposed by [98]. Compared to our work, [59] deals with a much simpler polynomial (quadratic) while the polynomial in the model that we discuss in chapter 6 is of degree seventeen. In addition the bistability wedge in the turnover parameters plane in [59] is an open one. In contrast, the region of bistability in our case, bounded by (d, a) such that $f(d, a) = 0$ is compact. In our work, since the degree of polynomial $P(x_1)$ is more than five, we use discriminants, Sturm's theorem, and the Cauchy Criterion to analyse the structural stability of the system.

There is a need to work out how to make bistable behaviour in biological systems robust with respect to protein turnover. Besides, as suggested by [161], the rate of degradation of Cdc2 in active form is smaller than in the inactive form, so that $\dfrac{d^*}{d} < 1$. It would be interesting to redo the structural stability analysis of the Cdc2-CyclinB/Wee1 system taking this relation and also Wee1 turnover into consideration. Furthermore, it has been assumed that kinase synthesis has zero order kinetics while kinase degradation has first order kinetics. It is a good idea to verify the validity of these assumptions experimentally.

Much remains to be done in this area. Experimentally, the most important question is whether the bystander effect is significant in vivo. Clearly, a first step in understanding this is a construction of a mechanistic model of the bystander effect as observed in vitro. This, we propose, will include bistable modules, which necessitate the development of structurally stable models of bistability. The present work is a contribution to that effort. Also, the time-tested LQ formalism can benefit from incorporating data from molecular biology studies which have accumulated in the decades following the introduction of that formalism. We suggest that the bridge between LQ and these data is via structured population models, a simple example of which was considered in the thesis.

Appendix A

Numerical solution of the model in chapter 4 using MATLAB

A.1 LQ curve fitting using *fminsearch* (see figure 4.3)

```
function [estimates, model] = fitcurve(xdata, ydata)
% Call fminsearch with a random starting point.
start_point = rand(1, 2);
model = @LQfun;
estimates = fminsearch(model, start_point);
% LQfun accepts curve parameters as inputs, and outputs sseAverage,
% the sum of squares error for log10(exp(-A.*xdata - B.*(xdata.^2))*100)-ydata,
% and the FittedCurveAverage. FMINSEARCH only needs sseAverage as the objective
%function value, but we want to plot the FittedCurveAverage at the end.
    function [sseAverage, FittedCurveAverage] = LQfun(params)
        A = params(1);
        B = params(2);
        FittedCurveAverage = log10(exp(-A.*xdata - B.*(xdata.^2))*100);
        ErrorVector = FittedCurveAverage - ydata;
        sseAverage = sum(ErrorVector .^ 2);
    end
```

```
end
```

A.2 The algorithm of single-dose treatment (see section 4.7)

The "single-fractionation-new" function is used in the two-dose fractionation code in appendix A.3.

```
function [SingleFraction,S]=single_fractionation_new
%%%%%%%%%%%%%%%%%%%%%%%%%%%%%%%%%%%%%%%%%%%%%
Declaration of the variables in the algorithm
%%%%%%%%%%%%%%%%%%%%%%%%%%%%%%%%%%%%%%%%%%%%%
npoints=30;
iteration=20;
S_rate_total=zeros(1,npoints+1);
num=10000;
%%%%%%%%%%%%%%%%
Parameter values
%%%%%%%%%%%%%%%%
delta=2;
alpha1=1.5;%parameter of the cell death rate
alpha2=0.001;%parameter of the cell death rate
p=0.95;
Vmax=1;%(numerator);%parameter of the damage repair rate
Km=3;%(denominator);%parameter of the damage repair rate
T=24;
for j=1:iteration %to get an average solution
%%%%%%%%%%%%%%%%%%%%%%%
  Initial conditions
%%%%%%%%%%%%%%%%%%%%%%%
for i=1:npoints+1
%**********************************************************************
%To generate random number of DSBs which follows the Poisson distribution
```

```
%*****************************************************************
X(:,i,j)=poissrnd((delta*(i-1)/4),1,num);
nmax(:,i,j)=max(X(:,i,j));
NMAX=max(nmax);
NNMAX=max(NMAX);N=zeros(NNMAX+1,i,j);
end
end
%*******************************************************
%To compute how many cells in each group of the cell population
%*******************************************************
for j=1:1:iteration
for i=1:1:npoints+1
for k=1:1:num
N(X(k,i,j)+1,i,j)=N(X(k,i,j)+1,i,j)+1;
end
end
end
N;
kmax=nmax;
%%%%%%%%%%%%%%%%%%%%%%%%%%%%%%%%%%%%%%%%%%%%%
Matrix A construction (Please refer to chapter 4)
%%%%%%%%%%%%%%%%%%%%%%%%%%%%%%%%%%%%%%%%%%%%%
for j=1:1:iteration
j=j;
for i=1:1:npoints+1
i=i;
Kmax=kmax(:,i,j);
for m=1:1:Kmax+1
for k=1:1:Kmax+1
V(k,:)=(k-1)*(1-p)*Vmax/(Km+(k-1));
if (m-1)+(k-1)<=Kmax
K=k-1;M=m-1;
d6(k,m)=(-alpha1*(m-1)-alpha2*((k-1)^2))-((Vmax*(k-1))/(Km+k-1));
G(k,m)=(k-1)*p*Vmax/(Km+k-1);
else
```

```
continue
end
end
end
s=Kmax+1;
V=V(1:Kmax+1,1);
for l=1:1:Kmax
l;
s=s+(Kmax+1-l);
end
s;
t=0;
A=zeros(s);
for r=1:1:Kmax
n=s-(Kmax-(r-1));
if r-1==0
v1=[V;zeros(n-length(V),1)];
A=A+diag(v1,-(Kmax-(r-1)));
continue
else
r-1;
t;
t=t+(Kmax+1-(r-2));
v2=zeros(t,1);
v4=V(1:Kmax+1-(r-1),1);
v3=[v2;v4];
v1=[v3;zeros(n-length(v3),1)];
A=A+diag(v1,-(Kmax-(r-1)));
end
end
size(A);
x=[d6(1:Kmax+1,1)];
for m=1:1:Kmax
x=[x;d6(1:Kmax+1-m,m+1)];
end
```

```
x;
A1=diag(x);
size(A1);
matrix=A+A1;
G;
GG=[G(2:Kmax+1,1)];
for m=1:1:Kmax
GG=[GG;G(1:Kmax+1-m,m+1)];
end
A3=diag(GG,1);
NN=N(:,i,j);NNN=NN(1:Kmax+1,1);
Nnew=[NNN;zeros(s-length(NNN),1)];
%***************************
system=A+A1+A3;% Matrix A
%**************************************************
solution1=expm(system*T)*Nnew; %Solution of the linear ODEs
%**************************************************
Sol=cumsum(solution1); %Total population after irradiation
S(:,i)=Sol(s,1);
%******if j >1********
end
S_rate=S/num; %the cell surviving fraction in each iteration
S_rate_total=S_rate_total+S_rate;
S_rate_average=S_rate_total/iteration;
end
S_rate_average; %the cell surviving fraction for 20 iterations
percent=S_rate_average*100;
loga=log10(percent); The rate in logarithmic scale
%************************
          Plotting
%************************
STEP=1;
lambda_0=0;for i=1:STEP:npoints+1
X_axis(i)=((i-1)/4)+lambda_0;
end
```

```
xdata = X_axis% X-axis in survival curve
ydata = loga  % Y-axis in survival curve
plot(xdata,ydata,'*'),xlabel('Gray'),ylabel('Surviving Fraction')
hold on
%%%%%%%%%%%%%%%%%%%%%%%%%%%%%%%%%%%%%%%%%%%%%%%%%%%%%%%%%%%%%%%%
%The simulation data is fitted to the LQ-equation using FMINSEARCH
%%%%%%%%%%%%%%%%%%%%%%%%%%%%%%%%%%%%%%%%%%%%%%%%%%%%%%%%%%%%%%%%
[estimates, model] = fitcurve(xdata,ydata)
%For fitcurve function please refer to the appendix A.1.
[sseAverage, FittedCurveAverage] = model(estimates);
%FittedCurveAverage is the Y-axis data for LQ-equation
plot(X_axis,FittedCurveAverage,'b'),xlabel('Gray'),
ylabel('Surviving Fraction')
```

A.3 The algorithm of two-dose fractionation treatment (see section 4.10)

```
function [TwoFraction,S2]=two_fractionation_new
%****************************************
%*********Single Fraction data************
%*****************************************
single_fractionation_new % To generate data for the total dose D given to a population

%*********Two Fractions data***********
%*****************************************
npoints=60;iteration=20;S_rate_total=zeros(1,npoints+1);S_rate_total2=zeros(1,npoints+1);
num=10000;
Vmax=1;%(repair rate parameter)
Km=3;%(repair rate parameter);
alpha1=1.5;%parameter of cell death(linear misrepair)
alpha2=0.001;%parameter of cell death(binary misrepair)
T=48;T2=24;
STEP=1;
p=0.9;delta=2;
```

```
%****************X_axis data************
lambda_0=0;
for i=1:STEP:npoints+1
X_axis(i)=((i-1)/(4))+lambda_0;
end
%**************************************
          The first half dose (d=D/2)
%**************************************
for j=1:iteration
for i=1:npoints+1
X(:,i,j)=poissrnd(delta*(i-1)/8,1,num);
nmax(:,i,j)=max(X(:,i,j));
NMAX=max(nmax);
NNMAX=max(NMAX);N=zeros(NNMAX+1,i,j);
end
end
for j=1:1:iteration
for i=1:1:npoints+1
for k=1:1:num
N(X(k,i,j)+1,i,j)=N(X(k,i,j)+1,i,j)+1;
end
end
end
nmax;
kmax=nmax;
for j=1:1:iteration
j=j;
for i=1:1:npoints+1
i=i;
Kmax=kmax(:,i,j);
for m=1:1:Kmax+1
for k=1:1:Kmax+1
V(k,:)=(k-1)*(1-p)*Vmax/(Km+(k-1));
if (m-1)+(k-1)<=Kmax
K=k-1;M=m-1;
```

```
d6(k,m)=(-alpha1*(m-1)-alpha2*((k-1)^2))-((Vmax*(k-1))/(Km+k-1));
G(k,m)=(k-1)*p*Vmax/(Km+k-1);
else
continue
end
end
end
s=Kmax+1;
V=V(1:Kmax+1,1);
for l=1:1:Kmax
l;
s=s+(Kmax+1-l);
end
s;
t=0;
A=zeros(s);
for r=1:1:Kmax
n=s-(Kmax-(r-1));
if r-1==0
v1=[V;zeros(n-length(V),1)];
A=A+diag(v1,-(Kmax-(r-1)));
continue
else
r-1;
t;
t=t+(Kmax+1-(r-2));
v2=zeros(t,1);
v4=V(1:Kmax+1-(r-1),1);
v3=[v2;v4];
v1=[v3;zeros(n-length(v3),1)];
A=A+diag(v1,-(Kmax-(r-1)));
end
end
size(A);
x=[d6(1:Kmax+1,1)];
```

```
for m=1:1:Kmax
x=[x;d6(1:Kmax+1-m,m+1)];
end
x;
A1=diag(x);
size(A1);
matrix=A+A1;
G;
GG=[G(2:Kmax+1,1)];
for m=1:1:Kmax
GG=[GG;G(1:Kmax+1-m,m+1)];
end
A3=diag(GG,1);
system=A+A1+A3;%Matrix A
[Vec,Val]=eig(system);
VecInv=inv(Vec);
%***************************************
NN=N(:,i,j);NNN=NN(1:Kmax+1,1);
Nnew=[NNN;zeros(s-length(NNN),1)];
%Nnew defines the initial conditions
solution=expm(system*T)*Nnew;
Sol=cumsum(solution);
S(:,i,j)=Sol(s,1);

%***************************************
          The second half dose (d=D/2)
%***************************************

NNMAX;
for m=1:NNMAX+1
for k=1:NNMAX+1
if (m-1)+(k-1)<=NNMAX
w(k,m)=k-1;
else
continue
```

```
end
end
end
ww=w(1:Kmax+1,(NNMAX+1-Kmax):NNMAX+1);
www=ww(hankel(1:size(ww))>0);
Nnewlatest=zeros(1,s+12);for k=1:1:s
k=k;
if ceil(solution(k))==0
Nnew=0;
else
solution(k);
Xnew=poissrnd(delta*(i-1)/8,1,ceil(solution(k)));
Xnewnew=www(k)+Xnew;
XnewnewMMax(k)=max(Xnewnew);XnewnewMax=max(XnewnewMMax);
Nnew=zeros(1,s+12);Nnew_decimalform=zeros(1,s+12);
for m=1:ceil(solution(k))
Nnew(1,Xnewnew(1,m)+1)=Nnew(1,Xnewnew(1,m)+1)+1;
end
Nnew;
Nnew_decimalform=Nnew.*(solution(k)./ceil(solution(k)));
Nnewlatest=Nnewlatest+Nnew_decimalform;
end
end
solutionnew=Nnewlatest';
Kmax2=XnewnewMax;
for m=1:1:Kmax2+1
for k=1:1:Kmax2+1
V2(k,:)=(k-1)*(1-p)*Vmax/(Km+(k-1));
if (m-1)+(k-1)<=Kmax2
K=k-1;M=m-1;
d62(k,m)=(-alpha1*(m-1)-alpha2*((k-1)^2))-((Vmax*(k-1))/(Km+k-1));
G2(k,m)=(k-1)*p*Vmax/(Km+k-1);
else
continue
end
```

```
end
end
s2=Kmax2+1;
V2=V2(1:Kmax2+1,1);
for l=1:1:Kmax2
l;
s2=s2+(Kmax2+1-l);
end
s2;
t=0;
A2=zeros(s2);
for r=1:1:Kmax2
n2=s2-(Kmax2-(r-1));
if r-1==0
v12=[V2;zeros(n2-length(V2),1)];
A2=A2+diag(v12,-(Kmax2-(r-1)));
continue
else
r-1;
t;
t=t+(Kmax2+1-(r-2));
v22=zeros(t,1);
v42=V2(1:Kmax2+1-(r-1),1);
v32=[v22;v42];
v12=[v32;zeros(n2-length(v32),1)];
A2=A2+diag(v12,-(Kmax2-(r-1)));
end
end
size(A2);
x2=[d62(1:Kmax2+1,1)];
for m=1:1:Kmax2
x2=[x2;d62(1:Kmax2+1-m,m+1)];
end
x2;
A12=diag(x2);
```

```
size(A2);
matrix2=A2+A12;
G2;
GG2=[G2(2:Kmax2+1,1)];
for m=1:1:Kmax2
GG2=[GG2;G2(1:Kmax2+1-m,m+1)];
end
A32=diag(GG2,1);
system2=A2+A12+A32;%Matrix A
[Vec2,Val2]=eig(system2);
VecInv2=inv(Vec2);
if length(solutionnew)< s2
solutionnewnew=[solutionnew;zeros(s2-length(solutionnew),1)];
%solutionnewnew defines the initial conditions
else solutionnewnew=solutionnew(1:s2);
end
solution2=expm(system2*T)*solutionnewnew;
%solutionnewnew contains initial conditions
Sol2=cumsum(solution2);
S2(:,i)=Sol2(s2,1);
end
S2_rate=S2/num;size(S2_rate);
size(S_rate_total2);
S_rate_total2=S_rate_total2+S2_rate;
S_rate_average2=S_rate_total2/iteration;
end
S_rate_average2;
%************Plotting***********

xdata = X_axis% X-axis in survival curve
ydata = log10(S_rate_average2*100);%Y-axis in survival curve
plot(xdata,ydata,'*'),xlabel('Gray'),ylabel('Surviving Fraction')
%plot(X_axis,LogbasetenAverage(1,:),'o'),xlabel('LAMBDA'),ylabel('RATE OF SURVIVAL')
hold on
%********************************
```

```
%LQ curve fitting of two-dose fractionation
%**********************************
[estimates, model] = fitcurve(xdata,ydata)
[sseAverage, FittedCurveAverage] = model(estimates);
plot(X_axis,FittedCurveAverage,'r'),xlabel('Gray'),ylabel('Surviving Fraction')
```

A.4 Parameter estimation using Nelder-Mead simplex algorithm (see section 4.8)

A.4.1 Nelder-Mead simplex algorithm using *fminsearch*

```
function[estimates,model,fval,output]=parameterfitting_fminsearch(xdata, ydata,i)

%Random starting values
start_point=[7.6732   11.9704    0.0022    0.1564    0.7285    1.8870;
    11.7853    1.2689    0.0075    0.8555    2.7523    1.0801;
    33.9473    4.9023    0.0020    0.6448    0.8072    3.9520;
    11.6627    7.3601    0.0069    0.3763    2.2965    4.7465;
    32.9428   17.0776    0.0054    0.1909    0.5660    1.6378;
    11.2539    0.3475    0.0080    0.4283    0.8625    3.3563;
    37.3120    0.9210    0.0074    0.4820    0.2733    2.1932;
    15.2994    3.5363    0.0091    0.1206    1.7286    4.1675;
    9.4706   13.5048    0.0090    0.5895    2.0501    3.8443;
    11.5412   15.2199    0.0040    0.2262    1.6398    0.8363;
    25.4097   13.4764    0.0073    0.3846    1.2772    4.3099;
    19.9850    9.3899    0.0028    0.5830    1.9333    4.9494;
    15.3631   11.3849    0.0013    0.2518    1.9429    2.5721;
    33.5715    6.1800    0.0077    0.2904    2.0371    4.4214;
    24.2400   15.4892    0.0055    0.6171    1.9074    2.9401;
    22.8895    3.9508    0.0053    0.2653    2.8355    0.7738;
    36.8534   14.2867    0.0091    0.8244    0.6268    0.9993;
    12.8619    3.8378    0.0065    0.9827    2.1278    2.0348;
    30.7736    7.6783    0.0066    0.7302    0.7087    3.7435;
    30.6417   13.0170    0.0087    0.3439    0.3582    4.1279;
```

16.4569	16.2270	0.0082	0.5841	1.8219	3.9498;
23.5772	1.7121	0.0062	0.1078	1.3504	1.5926;
4.8825	19.3239	0.0026	0.9063	1.3762	2.6703;
4.0501	16.1333	0.0032	0.8797	1.9858	0.4498;
22.1703	10.1346	0.0090	0.8178	2.3109	0.5585;
31.6084	9.0771	0.0013	0.2607	1.0507	0.6815;
37.4924	9.3040	0.0054	0.5944	1.9860	3.3933;
6.9364	6.3882	0.0025	0.0225	1.2485	2.4759;
23.6153	10.5855	0.0098	0.4253	2.5258	0.9486;
19.8368	10.6325	0.0074	0.3127	2.4988	2.4750;
2.4523	17.0035	0.0055	0.1615	0.7693	0.7380;
14.8107	16.5302	0.0052	0.1788	1.8404	0.2749;
15.6941	11.5831	0.0058	0.7475	0.4454	0.8435;
9.1740	11.0184	0.0097	0.7485	1.8594	3.7585;
2.0455	17.2600	0.0020	0.5433	0.7819	1.8418;
14.0239	17.8575	0.0015	0.3381	1.3370	4.7091;
28.5854	16.4098	0.0037	0.8323	2.5320	0.0859;
25.7597	6.6266	0.0062	0.5526	0.5886	4.1453;
22.6364	9.4166	0.0058	0.9575	0.9116	3.1330;
18.6834	15.6457	0.0091	0.8928	1.4499	2.6937;
12.9222	2.3087	0.0059	0.3565	1.0134	3.2525;
21.0630	2.3062	0.0049	0.5464	2.3955	3.6331;
30.9388	5.6311	0.0059	0.3467	2.9625	0.4724;
30.9715	10.9204	0.0074	0.6228	0.4771	4.3879;
23.8901	20.2222	0.0012	0.7966	0.7106	0.0718;
30.4112	14.7774	0.0082	0.7459	2.1067	1.4715;
26.5303	6.5026	0.0023	0.1255	1.1264	0.8996;
6.6823	6.0790	0.0053	0.8224	2.9211	4.6315;
21.1671	17.6831	0.0033	0.0252	2.9169	0.3409;
15.1959	18.9556	0.0043	0.4144	1.9311	2.9055;
5.5016	13.3005	0.0070	0.7314	2.5803	3.1858;
7.6183	5.3298	0.0025	0.7814	1.2057	3.2563;
9.5304	1.8686	0.0035	0.3673	1.8958	4.3231;
27.5463	17.4318	0.0028	0.7449	2.9557	0.2798;
18.3974	12.1678	0.0028	0.8923	1.6784	4.0843;

28.3873	19.7126	0.0039	0.2426	2.8008	2.6446;
11.7578	1.2948	0.0089	0.1296	2.1610	3.4718;
2.3708	12.1662	0.0052	0.2251	1.4521	1.0620;
22.2268	5.9472	0.0046	0.3500	1.9171	2.7164;
12.6169	17.2133	0.0026	0.2871	2.6629	3.5126;
37.9567	3.9930	0.0097	0.9275	0.5962	4.7822;
36.4448	9.2156	0.0047	0.0513	1.1861	2.2227;
16.9220	8.1958	0.0086	0.5927	2.9765	0.4270;
2.9445	17.1893	0.0065	0.1629	1.2071	0.2867;
27.5146	14.0811	0.0044	0.8384	1.9766	3.1473;
33.8125	4.3380	0.0089	0.1676	2.7040	3.9809;
38.9170	6.6323	0.0081	0.5022	2.9861	3.4560;
4.1634	2.8059	0.0052	0.9993	1.9595	1.7265;
19.1123	13.9688	0.0083	0.3554	0.3253	4.7341;
24.1339	11.8828	0.0091	0.0471	0.1083	2.6010;
28.0922	3.5525	0.0049	0.2137	1.8543	4.7691;
29.3384	3.0934	0.0040	0.3978	1.7014	0.3680;
26.7015	9.9122	0.0064	0.3337	2.8859	1.0352;
29.6228	18.8820	0.0091	0.2296	2.2383	3.8751;
16.2062	11.4921	0.0073	0.9361	1.9875	4.5709;
24.1001	0.7116	0.0044	0.6832	1.5699	3.9128;
6.4125	1.1460	0.0076	0.9621	0.7797	1.4777;
4.1909	16.7427	0.0096	0.4380	2.8860	0.7592;
39.2311	9.3993	0.0059	0.9403	1.6206	4.2396;
12.8233	7.9723	0.0059	0.0058	0.0908	3.9243;
24.6090	16.4225	0.0038	0.6103	2.0889	1.3542;
38.5621	7.5911	0.0016	0.8011	1.5591	1.1391;
9.0596	11.0805	0.0026	0.2330	0.1771	1.6051;
9.3355	14.8033	0.0018	0.9325	2.6701	4.1478;
14.9825	18.1216	0.0052	0.7633	0.9906	4.1109;
37.4501	6.8521	0.0011	0.8264	0.6891	2.8534;
16.8454	13.5256	0.0092	0.5735	0.3418	2.8591;
12.3822	20.2675	0.0068	0.7926	0.9328	1.4301;
7.7740	1.6050	0.0010	0.3290	0.6853	3.4957;
17.0901	12.2156	0.0013	0.2235	1.9560	3.9813;

16.2395	8.6209	0.0029	0.3124	0.1985	2.2079;
6.9824	6.4461	0.0051	0.5845	0.8263	2.2311;
18.5315	5.5055	0.0021	0.8299	0.8455	2.3283;
5.4775	15.7814	0.0011	0.2905	2.6402	1.3952;
25.3558	20.6907	0.0075	0.4026	1.3330	3.3769;
2.4172	3.9014	0.0042	0.8621	2.2677	4.5183;
23.7839	16.2461	0.0080	0.6147	1.8099	4.5426;
32.0097	4.0929	0.0049	0.9912	2.3498	3.7360;
10.9439	20.6314	0.0049	0.2037	0.3418	1.3026;
19.0247	16.6845	0.0014	0.8272	2.9357	3.4482;
23.6356	8.8356	0.0014	0.6759	2.5458	0.6592;
4.3333	15.1606	0.0018	0.2489	0.1519	0.6175;
20.8590	10.3747	0.0063	0.4758	1.3986	0.9545;
26.4080	16.8242	0.0032	0.3991	0.9770	0.7287;
10.4081	7.4296	0.0086	0.5994	1.8906	2.9252;
33.8081	1.5484	0.0087	0.8005	0.6909	0.3668;
38.9009	12.2980	0.0097	0.1051	1.7397	4.1116;
34.1622	18.9253	0.0054	0.8214	1.8095	3.6145;
21.2280	4.0507	0.0030	0.8411	1.7996	4.6293;
12.5973	9.0046	0.0030	0.3545	1.3453	2.4632;
30.3715	15.5820	0.0058	0.4301	0.1063	3.2744;
11.0034	0.8413	0.0079	0.5722	1.5414	4.4506;
38.3791	19.6756	0.0041	0.7008	1.2232	2.6926;
25.5699	15.8833	0.0052	0.7425	0.3241	1.4110;
24.8100	11.6301	0.0068	0.7579	1.3796	4.8798;
8.5590	3.8447	0.0093	0.3891	1.3526	0.1821;
5.4332	10.3663	0.0025	0.4293	1.6534	1.6312;
11.7000	10.7794	0.0074	0.9563	2.4162	4.8651;
34.6257	20.6705	0.0062	0.5730	2.1026	1.8252;
36.6205	17.7764	0.0049	0.8497	2.6167	1.5457;
28.5861	20.0094	0.0090	0.2763	0.1566	0.6046;
29.5569	14.1241	0.0045	0.6223	0.6590	4.5788;
10.7357	8.4053	0.0026	0.5884	1.3789	0.6774;
23.8900	19.4400	0.0067	0.9635	2.8756	1.6606;
32.8039	9.9829	0.0066	0.0859	2.3701	4.4874;

```
 17.3460    4.8402    0.0040    0.5005    1.3556    2.4982;
 39.5607    8.2556    0.0082    0.5216    1.0003    3.0764;
  5.4200   14.6667    0.0100    0.0902    0.1773    2.9157;
 14.1958   11.6247    0.0098    0.9047    2.2227    3.4913;
 21.4335   15.7371    0.0021    0.8844    1.5204    0.1467;
  4.3030   20.6962    0.0031    0.4390    0.5998    2.6394;
 29.5761   20.0100    0.0012    0.7817    1.2816    0.1604;
  32.9595    3.3950    0.0068    0.4229    1.7467    4.2536;
 36.4201   16.5189    0.0044    0.0942    1.6222    2.8028;
  6.8255    6.4892    0.0083    0.5985    2.6098    4.6480;
 36.7083   11.0013    0.0058    0.4709    0.7943    3.4833;
 26.0297    3.4669    0.0042    0.6959    0.9542    2.9140;
  5.7065   12.5262    0.0095    0.6999    0.3576    4.0770;
 12.5829    5.4876    0.0089    0.6385    2.8195    4.3951
 22.7815   13.6079    0.0060    0.0336    1.9367    4.9446;
 38.3853   14.3374    0.0066    0.0688    1.4384    0.0026;
 38.6658   15.5610    0.0063    0.3196    1.9180    4.3272;
  7.9893    9.3820    0.0029    0.5309    1.6341    3.0628;
 38.8825    1.7680    0.0037    0.6544    1.9419    4.9498;
 38.3723    4.7818    0.0052    0.4076    1.6317    2.6384;
 20.4443   18.9907    0.0031    0.8200    2.1631    2.3976;
 32.4107    3.1914    0.0086    0.7184    1.5675    4.0067;
  7.3917   17.1736    0.0028    0.9686    2.9811    1.1392;
 18.0269   11.2049    0.0030    0.5313    0.6560    2.4905;
 36.7979   20.7097    0.0025    0.3251    0.3174    4.5043;
 32.1039    1.6508    0.0030    0.1056    0.3291    2.8733;
 38.4607    9.2187    0.0049    0.6110    0.1908    4.2259;
 26.9181    2.2421    0.0038    0.7788    1.2137    3.6932;
  3.3570   19.9989    0.0093    0.4235    1.3451    2.9299;
 34.2669    0.1239    0.0049    0.0908    1.0974    1.2337;
 37.4917   16.1166    0.0027    0.2665    2.2905    3.3321;
 27.7919   16.9968    0.0091    0.1537    1.8837    0.4174;
 30.7941   18.0638    0.0098    0.2810    2.3159    3.1298;
 30.2390    1.7808    0.0049    0.4401    2.7986    3.3047;
 16.9046    8.3281    0.0020    0.5271    2.9182    3.6488;
```

26.9082	5.4232	0.0033	0.4574	0.5761	4.4538;
8.5051	16.6390	0.0047	0.8754	0.4166	4.9115;
28.8298	8.9848	0.0064	0.5181	2.0888	3.8451;
3.2096	18.9348	0.0034	0.9436	0.2815	2.9072;
12.5231	3.8033	0.0064	0.6377	1.5762	4.6416;
3.7545	5.5049	0.0074	0.9577	1.5910	2.9005;
5.6910	3.0494	0.0030	0.2407	2.5834	0.0849;
33.2914	2.8528	0.0021	0.6761	1.4546	0.6043;
28.4035	18.0762	0.0037	0.2891	1.1804	4.3136;
14.0498	12.0637	0.0039	0.6718	2.0143	2.4215;
38.1084	11.4441	0.0048	0.6951	2.2238	4.2243;
3.3090	3.0373	0.0056	0.0680	1.5602	1.0470;
18.6723	17.7386	0.0018	0.2548	1.0431	2.7615;
16.4992	12.9430	0.0034	0.2240	0.4500	3.1494;
31.0896	7.3143	0.0082	0.6678	1.7583	0.1600;
32.2176	10.6839	0.0013	0.8444	0.7864	3.0736;
9.1012	8.3702	0.0094	0.3445	0.1334	1.8121;
20.6110	1.6049	0.0076	0.7805	2.2648	0.2477;
18.9323	5.0089	0.0054	0.6753	0.7284	2.4478;
26.5599	2.5881	0.0062	0.0067	1.3272	0.9626;
28.9559	3.8460	0.0031	0.6022	2.0634	0.6154;
30.6781	5.0097	0.0051	0.3868	1.0777	1.0275;
12.4890	8.6911	0.0097	0.9160	2.2090	0.7326;
27.8287	1.0586	0.0059	0.0012	1.1841	0.9454;
26.8937	18.7702	0.0057	0.4624	2.0502	0.2133;
8.1792	19.6437	0.0031	0.4243	2.1121	3.1760;
6.5219	10.2192	0.0054	0.4609	1.3269	1.4093;
20.9378	10.1857	0.0066	0.7702	0.0587	2.6930;
38.4703	7.0395	0.0071	0.3225	0.9926	3.4758;
14.9347	18.7149	0.0046	0.7847	1.2729	2.4956;
24.2402	7.6941	0.0043	0.4714	0.8108	2.6790;
10.5049	2.3365	0.0099	0.0358	0.5912	2.2259;
30.5481	16.2275	0.0013	0.1759	2.4652	0.6197;
11.6936	8.1196	0.0090	0.7218	1.2898	2.4518;
21.2264	5.0458	0.0092	0.4735	2.6633	4.2650;

28.5649	8.4138	0.0082	0.1527	1.1735	4.3696;
35.8543	2.0303	0.0019	0.3411	2.3073	1.3515;
38.4531	2.7678	0.0034	0.6074	1.1904	1.0423;
22.7942	19.5868	0.0040	0.1917	2.4255	2.8249;
7.2677	19.8793	0.0071	0.7384	2.2652	3.2016;
7.6732	11.9704	0.0022	0.2428	1.1322	2.0851;
11.7853	1.2689	0.0075	0.9174	0.6481	1.0299;
33.9473	4.9023	0.0020	0.2691	2.3712	4.7397;
11.6627	7.3601	0.0069	0.7655	2.8479	0.4104;
32.9428	17.0776	0.0054	0.1887	0.9827	0.5285;
11.2539	0.3475	0.0080	0.2875	2.0138	0.7102;
37.3120	0.9210	0.0074	0.0911	1.3159	0.8323;
15.2994	3.5363	0.0091	0.5762	2.5005	3.1048;
9.4706	13.5048	0.0090	0.6834	2.3066	2.8685;
11.5412	15.2199	0.0040	0.5466	0.5018	0.2604;
25.4097	13.4764	0.0073	0.4257	2.5859	4.6560;
19.9850	9.3899	0.0028	0.6444	2.9696	3.6433;
15.3631	11.3849	0.0013	0.6476	1.5433	3.6892;
33.5715	6.1800	0.0077	0.6790	2.6528	0.3170;
24.2400	15.4892	0.0055	0.6358	1.7641	4.3022;
22.8895	3.9508	0.0053	0.9452	0.4643	4.6720;
36.8534	14.2867	0.0091	0.2089	0.5996	4.9220;
12.8619	3.8378	0.0065	0.7093	1.2209	4.2947;
30.7736	7.6783	0.0066	0.2362	2.2461	3.9278;
30.6417	13.0170	0.0087	0.1194	2.4768	2.5669;
16.4569	16.2270	0.0082	0.6073	2.3699	0.8880;
23.5772	1.7121	0.0062	0.4501	0.9556	1.9929;
4.8825	19.3239	0.0026	0.4587	1.6022	0.6697;
4.0501	16.1333	0.0032	0.6619	0.2699	0.1544;
22.1703	10.1346	0.0090	0.7703	0.3351	4.6957;
31.6084	9.0771	0.0013	0.3502	0.4089	1.5065;
37.4924	9.3040	0.0054	0.6620	2.0360	1.4777;
6.9364	6.3882	0.0025	0.4162	1.4855	1.6647;
23.6153	10.5855	0.0098	0.8419	0.5691	2.3353;
19.8368	10.6325	0.0074	0.8329	1.4850	3.2410;

```
    2.4523   17.0035    0.0055    0.2564    0.4428    0.1261;
   14.8107   16.5302    0.0052    0.6135    0.1649    4.2110];
%**********************************************************************
%************************************************
%using fminsearch built-in package in MATLAB
%************************************************

model = @LQfun; %the model is described in LQfun function
SP=start_point(i,:)
lb=[2 0.0277 0.001 0 0 0];
ub=[40 20.79 0.01 1 3 5];%Parameters range
options=optimset('TolFun',0.000001,'Display','iter');%

%************************************
%Syntax for fminsearch function
%************************************
fun=model;x0=SP;
[estimates, fval, output] = fminsearchbnd(fun,x0,LB,UB,options);
%*********************************************************************
                    The model
%*********************************************************************

    function [fval, FittedCurve] = LQfun(params)
        gamma= params(1);
        alpha1 = params(2);
        alpha2 = params(3);
        p = params(4);
        Vmax = params(5);
        Km=params(6);iteration=1;

%%%%%%%%%%%%%%%%%%%%%%%%%%%%%%%%%%%%
%Generating for the data simulation
%%%%%%%%%%%%%%%%%%%%%%%%%%%%%%%%%%%%
npoints=6; %depends on the total number of experimental data available
num=10000;
```

```
for j=1:1:7
for k=1:1:21
%**************************************************
%initial condition of model
%**************************************************
%We limit the PE procedure for kmax=20
%The initial conditions in PE procedure are not random
%This is because the algorithm that we use here cannot deal with random situation,
%due to out of memory problem
ic(k,j)=((((gamma*xdata(j,1))^(k-1))*exp(-gamma*xdata(j,1)))/factorial(k-1))*num;
end
end
%***************************************************

for i=1:1:npoints+1
Kmax=20;T=24;
for m=1:1:Kmax+1
for k=1:1:Kmax+1
V(k,:)=(k-1)*(1-p)*Vmax/(Km+(k-1));
if (m-1)+(k-1)<=Kmax
K=k-1;M=m-1;
d6(k,m)=(-alpha1*(m-1)-alpha2*((k-1)^2))-((Vmax*(k-1))/(Km+k-1));
G(k,m)=(k-1)*p*Vmax/(Km+k-1);
else
continue
end
end
end
s=Kmax+1;
V=V(1:Kmax+1,1);
for l=1:1:Kmax
l;
s=s+(Kmax+1-l);
end
s;
```

```
t=0;
A=zeros(s);
for r=1:1:Kmax
n=s-(Kmax-(r-1));
if r-1==0
v1=[V;zeros(n-length(V),1)];
A=A+diag(v1,-(Kmax-(r-1)));
continue
else
r-1;
t;
t=t+(Kmax+1-(r-2));
v2=zeros(t,1);
v4=V(1:Kmax+1-(r-1),1);
v3=[v2;v4];
v1=[v3;zeros(n-length(v3),1)];
A=A+diag(v1,-(Kmax-(r-1)));
end
end
size(A);
x=[d6(1:Kmax+1,1)];
for m=1:1:Kmax
x=[x;d6(1:Kmax+1-m,m+1)];
end
x;
A1=diag(x);
size(A1);
matrix=A+A1;
G;
GG=[G(2:Kmax+1,1)];
for m=1:1:Kmax
GG=[GG;G(1:Kmax+1-m,m+1)];
end
A3=diag(GG,1);
system=A+A1+A3;%SYSTEM OF ODE
```

```
NN=ic(:,i);NNN=NN(1:Kmax+1,1);
Nnew=[NNN;zeros(s-length(NNN),1)];

%********************
%Simulation results
%********************
solution=expm(system*T)*Nnew;
Sol=sum(solution);
S(:,i)=Sol/num;
%*********************
end
%************************
%Objective function value (SSE)
%************************

    FittedCurve=log10(S*100);   %The data simulation are generated by
                       %using the estimated parameters value
    ErrorVector =FittedCurve  - ydata';
    fval= sum(ErrorVector.*ErrorVector); %This is the cost function
    end
    end
%****************************************************************

%%%%%%%%%%%%%%%%%%%%%%%%%%%%%%%%%%%%%%%%%%%%%%%%%%%%%%%%%%%%%%%%%%
  We need this command to run the above code in the command window
%%%%%%%%%%%%%%%%%%%%%%%%%%%%%%%%%%%%%%%%%%%%%%%%%%%%%%%%%%%%%%%%%%

%B = [0 2;1.5 1.94;2 1.97;3 1.86;3.5 1.91;4.5 1.75;5 1.73;6 1.59;7.5 1.37
;8.5 1.18;9 1.16;10.5 1.0885]
%experimental data
%xdata=B(:,1);
%ydata= B(:,2);
%for i=1:152
%[estimates, model,fval,output] = parameterfitting_fminsearch(xdata, ydata,i)
```

```
%[fval, FittedCurve ] = model(estimates)
%end
```

A.4.2 Results of parameter estimation using low LET IR survival data for $\xi = 151$

	Column 1						Column 2								Column 3	Column 4	Column 5		Column 6	
	Initial guesses						Estimated parameter values								$\alpha_{exp} = 0.0598$	$\beta_{exp} = 0.0158$	α_{elas}		β_{elas}	
Run	δ	α_1	α_2	p	V_{max}	K_M	δ	α_1	α_2	p	V_{max}	K_M	SSE	r^2	α_{model}	β_{model}	δ	p	δ	p
1	7.6732	11.9704	0.0022	0.1564	0.7285	1.8870	2.0000	16.3061	0.0021	0.8771	0.3432	0.0919	0.0018	0.9997	0.2770	0.0359	1.7000	−6.2000	2.3000	2.9000
2	11.7853	1.2689	0.0075	0.8555	2.7523	1.0800	2.0001	0.9741	0.0029	0.8910	0.6930	3.4512	0.0016	0.9998	0.2769	0.0359	1.5000	−5.7000	1.8000	1.9000
3	33.9473	4.9023	0.0020	0.6448	0.8072	3.9520	2.0006	14.6934	0.0031	0.8940	0.7883	3.9050	0.0016	0.9998	0.2771	0.0359	1.0000	−5.3000	1.4000	1.5000
4	11.6627	7.3601	0.0069	0.3763	2.2965	4.7460	2.0000	12.3068	0.0062	0.9010	1.7243	5.0000	0.0015	0.9998	0.2773	0.0359	1.6000	−6.2000	1.7000	1.7000
5	32.9428	17.0776	0.0054	0.1909	0.5660	1.6370	2.0000	7.0374	0.0057	0.9009	1.5818	4.9999	0.0015	0.9998	0.2774	0.0359	1.7000	−6.2000	1.8000	1.8000
6	11.2539	0.3475	0.0080	0.4283	0.8625	3.3560	2.0000	0.4992	0.0031	0.8934	0.7836	4.1734	0.0016	0.9998	0.2771	0.0359	1.3000	−5.5000	1.7000	1.7000
7	37.3120	0.9210	0.0074	0.4820	0.2733	2.1930	2.0011	1.1461	0.0030	0.8929	0.7498	3.8803	0.0016	0.9998	0.2771	0.0359	1.3000	−5.5000	1.6000	1.6000
8	15.2994	3.5363	0.0091	0.1206	1.7286	4.1670	2.0000	20.6814	0.0022	0.8877	0.5214	4.9991	0.0015	0.9998	0.2771	0.0359	1.4000	−4.8000	1.7000	1.6000
9	9.4706	13.5048	0.0090	0.5895	2.0501	3.8440	2.0000	2.0962	0.0100	0.9011	2.8010	5.0000	0.0015	0.9998	0.2773	0.0359	1.4000	−5.9000	1.6000	1.6000
10	11.5412	15.2199	0.0040	0.2262	1.6398	0.8360	2.0089	20.6587	0.0015	0.8388	0.2258	4.9672	0.0015	0.9998	0.2768	0.0359	2.4000	−3.6000	2.4000	1.8000
11	25.4097	13.4764	0.0073	0.3846	1.2772	4.3090	2.0000	19.7922	0.0036	0.8991	0.9697	4.9836	0.0015	0.9998	0.2773	0.0359	1.8000	−6.2000	1.9000	2.0000
12	19.9850	9.3899	0.0028	0.5830	1.9333	4.9490	2.0000	11.4775	0.0082	0.9011	2.3076	5.0000	0.0015	0.9998	0.2774	0.0359	1.1000	−5.7000	1.4000	1.4000
13	15.3631	11.3849	0.0013	0.2518	1.9429	2.5720	2.0024	9.4693	0.0021	0.8766	0.3580	0.1391	0.0018	0.9997	0.2776	0.0359	1.3000	−5.9000	1.6000	2.1000
14	33.5715	6.1800	0.0077	0.2904	2.0371	4.4210	2.0002	10.0005	0.0039	0.8997	1.0851	4.9993	0.0015	0.9998	0.2775	0.0359	1.0000	−5.4000	1.3000	1.3000
15	24.2400	15.4892	0.0055	0.6171	1.9074	2.9400	2.0000	15.1815	0.0059	0.9010	1.6452	5.0000	0.0015	0.9998	0.2773	0.0359	1.5000	−6.0000	1.6000	1.7000
16	22.8895	3.9508	0.0053	0.2653	2.8355	0.7730	2.0001	0.0282	0.0090	0.7251	1.7771	0.1001	0.0022	0.9997	0.2764	0.0360	1.4000	−2.4000	1.7000	0.8000
17	36.8534	14.2867	0.0091	0.8244	0.6268	0.9990	2.0000	0.2830	0.0058	0.8934	1.4822	3.6014	0.0016	0.9998	0.2771	0.0359	1.6000	−6.1000	1.9000	1.9000
18	12.8619	3.8378	0.0065	0.9827	2.1278	2.0340	2.0000	4.8679	0.0072	0.9011	2.0285	5.0000	0.0015	0.9998	0.2773	0.0359	1.1000	−5.6000	1.4000	1.4000
19	30.7736	7.6783	0.0066	0.7302	0.7087	3.7430	2.0000	0.5374	0.0052	0.8980	1.4015	4.4046	0.0015	0.9998	0.2771	0.0359	1.4000	−5.8000	1.6000	1.7000
20	30.6417	13.0170	0.0087	0.3439	0.3582	4.1270	2.0000	9.6209	0.0030	0.8968	0.7933	4.9489	0.0015	0.9998	0.2773	0.0359	1.4000	−5.5000	1.6000	1.6000
21	16.4569	16.2270	0.0082	0.5841	1.8219	3.9490	2.0000	1.3294	0.0042	0.8998	1.1510	4.9652	0.0015	0.9998	0.2773	0.0359	1.7000	−6.1000	1.7000	1.8000
22	23.5772	1.7121	0.0062	0.1078	1.3504	1.5920	2.0004	0.7815	0.0021	0.8801	0.4219	3.4246	0.0017	0.9997	0.2769	0.0359	2.2000	−5.5000	2.4000	2.5000
23	4.8825	19.3239	0.0026	0.9063	1.3762	2.6700	2.0088	12.4378	0.0012	0.5493	0.0550	4.9684	0.0013	0.9998	0.2773	0.0359	2.9000	−2.1000	2.6000	1.2000
24	4.0501	16.1333	0.0032	0.8797	1.9858	0.4490	2.0073	9.3191	0.0050	0.8938	1.2786	3.2463	0.0017	0.9997	0.2745	0.0362	1.1000	−5.8000	1.4000	1.4000
25	22.1703	10.1346	0.0090	0.8178	2.3109	0.5580	2.0007	2.3372	0.0052	0.9009	1.4124	4.7399	0.0015	0.9998	0.2758	0.0361	1.6000	−6.2000	1.7000	1.7000
26	31.6084	9.0771	0.0013	0.2607	1.0507	0.6810	2.0000	19.7167	0.0021	0.8813	0.3909	1.2082	0.0018	0.9997	0.2767	0.0360	0.5000	−4.7000	0.7000	1.0000
27	37.4924	9.3040	0.0054	0.5944	1.9860	3.3933	2.0003	20.7035	0.0099	0.8973	2.6506	4.2325	0.0015	0.9998	0.2772	0.0359	1.5000	−6.1000	1.7000	1.7000
28	6.9364	6.3882	0.0025	0.0225	1.2485	2.4759	2.0000	9.8619	0.0021	0.8781	0.3716	0.3620	0.0018	0.9997	0.2769	0.0359	0.7000	−5.2000	0.9000	1.4000
29	23.6153	10.5855	0.0098	0.4253	2.5258	0.9486	2.0263	0.0853	0.0100	0.8795	2.9449	4.8637	0.0016	0.9998	0.2780	0.0358	1.4000	−5.0000	1.7000	1.4000
30	19.8368	10.6325	0.0074	0.3127	2.4988	2.475;	2.0003	19.9168	0.0022	0.8867	0.5056	4.7196	0.0015	0.9998	0.2772	0.0359	1.9000	−5.3000	2.0000	2.0000
31	2.4523	17.0035	0.0055	0.1615	0.7693	0.738;	2.0056	0.5179	0.0029	0.8938	0.7601	4.7289	0.0015	0.9998	0.2770	0.0359	1.3000	−5.3000	1.6000	1.6000
32	14.8107	16.5302	0.0052	0.1788	1.8404	0.2749	2.0044	0.2462	0.0036	0.8958	0.9816	4.8937	0.0015	0.9998	0.2764	0.0360	0.8000	−4.9000	1.3000	1.3000
33	15.6941	11.5831	0.0058	0.7475	0.4454	0.8435	2.0000	9.8066	0.0026	0.8938	0.6602	4.9972	0.0015	0.9998	0.2772	0.0359	1.5000	−5.4000	1.8000	1.8000
34	9.1740	11.0184	0.0097	0.7485	1.8594	3.7585	2.0000	8.9205	0.0090	0.9011	2.5133	5.0000	0.0015	0.9998	0.2773	0.0359	1.5000	−6.0000	1.7000	1.6000
35	2.0455	17.2600	0.0020	0.5433	0.7819	1.8418	2.0000	11.1540	0.0026	0.8891	0.5801	3.1643	0.0015	0.9997	0.2767	0.0360	2.2000	−6.3000	2.1000	2.2000
36	14.0239	17.8575	0.0015	0.3381	1.3370	4.7091	2.0001	19.2444	0.0025	0.8910	0.5944	4.3195	0.0016	0.9998	0.2771	0.0359	2.0000	−5.8000	2.1000	2.1000
37	28.5854	16.4098	0.0037	0.8323	2.5320	0.0859	2.0000	18.4167	0.0079	0.9011	2.2074	5.0000	0.0015	0.9998	0.2773	0.0359	1.5000	−6.0000	1.6000	1.6000
38	25.7597	6.6266	0.0062	0.5526	0.5886	4.1453	2.0000	1.3444	0.0050	0.9007	1.3788	4.9998	0.0015	0.9998	0.2773	0.0359	1.8000	−6.2000	1.9000	1.9000
39	22.6364	9.4166	0.0058	0.9575	0.9116	3.133;	2.0000	13.6839	0.0063	0.8941	1.6217	3.6077	0.0015	0.9998	0.2770	0.0359	1.6000	−6.1000	1.8000	1.8000
40	18.6834	15.6457	0.0091	0.8928	1.4499	2.6937	2.0000	0.3235	0.0074	0.8957	1.9546	3.9423	0.0016	0.9998	0.2771	0.0359	1.3000	−5.8000	1.6000	1.6000
41	12.9222	2.3087	0.0059	0.3565	1.0134	3.2525	2.0001	5.7028	0.0038	0.8996	1.0463	5.0000	0.0016	0.9998	0.2773	0.0359	1.3000	−5.7000	1.5000	1.5000
42	21.0630	2.3062	0.0049	0.5464	2.3955	3.6331	2.0004	0.0581	0.0090	0.8602	2.4873	4.9120	0.0015	0.9998	0.2771	0.0359	1.2000	−3.8000	1.5000	1.0000
43	30.9388	5.6311	0.0059	0.3467	2.9625	0.4724	2.0005	10.8985	0.0035	0.8989	0.9446	4.9211	0.0015	0.9998	0.2770	0.0359	1.5000	−5.9000	1.8000	1.8000
44	30.9715	10.9204	0.0074	0.6228	0.4771	4.3879	2.0000	16.4993	0.0069	0.9011	1.9395	5.0000	0.0015	0.9998	0.2772	0.0359	1.2000	−5.7000	1.5000	1.5000

45	23.8901	20.2222	0.0012	0.7966	0.7106	0.0718	2.0001	20.3784	0.0024	0.8819	0.4769	1.2870	0.0015	0.9997	0.2768	0.0359	1.2000	−5.7000	1.7000	2.0000
46	30.4112	14.7774	0.0082	0.7459	2.1067	1.4715	2.0000	17.3331	0.0032	0.8979	0.8621	4.9838	0.0018	0.9998	0.2774	0.0359	1.2000	−5.4000	1.5000	1.5000
47	26.5303	6.5026	0.0023	0.1255	1.1264	0.8996	2.0000	11.4565	0.0031	0.8868	0.7129	2.2938	0.0015	0.9997	0.2767	0.0360	1.3000	−5.8000	1.4000	1.5000
48	6.6823	6.0790	0.0053	0.8224	2.9211	4.6315	2.0000	0.3475	0.0087	0.9008	2.4396	4.9621	0.0017	0.9998	0.2773	0.0359	1.2000	−5.7000	1.5000	1.5000
49	21.1671	17.6831	0.0033	0.0252	2.9169	0.3409	2.0000	0.6628	0.0097	0.9011	2.7085	5.0000	0.0015	0.9998	0.2773	0.0359	1.5000	−6.0000	1.7000	1.7000
50	15.1959	18.9556	0.0043	0.4144	1.9311	2.9055	2.0003	12.9242	0.0028	0.8955	0.7234	4.9999	0.0015	0.9998	0.2772	0.0359	1.8000	−5.8000	1.9000	1.9000
51	5.5016	13.3005	0.0070	0.7314	2.5803	3.1858	2.0000	9.4317	0.0047	0.9006	1.3117	4.9996	0.0015	0.9998	0.2774	0.0359	1.2000	−5.7000	1.5000	1.5000
52	7.6183	5.3298	0.0025	0.7814	1.2057	3.2563	2.0070	18.5738	0.0018	0.8721	0.3614	4.9337	0.0015	0.9998	0.2769	0.0359	2.1000	−4.6000	2.3000	2.0000
53	9.5304	1.8686	0.0035	0.3673	1.8958	4.3231	2.0000	1.4898	0.0034	0.8979	0.9051	4.8774	0.0015	0.9998	0.2772	0.0359	1.8000	−6.0000	1.9000	1.9000
54	27.5463	17.4318	0.0028	0.7449	2.9557	0.2798	2.0048	17.4510	0.0031	0.8880	0.7371	2.6246	0.0015	0.9997	0.2773	0.0359	1.3000	−5.8000	1.6000	1.7000
55	18.3974	12.1678	0.0028	0.8923	1.6784	4.0843	2.0000	10.9807	0.0050	0.9008	1.4052	5.0000	0.0017	0.9998	0.2773	0.0359	1.0000	−5.5000	1.3000	1.3000
56	28.3873	19.7126	0.0039	0.2426	2.8008	2.6446	2.0000	13.7863	0.0085	0.9011	2.3719	5.0000	0.0015	0.9998	0.2772	0.0359	1.6000	−6.1000	1.7000	1.7000
57	11.7578	1.2948	0.0089	0.1296	2.1610	3.4718	2.0000	1.4163	0.0039	0.8986	1.0358	4.6271	0.0015	0.9998	0.2766	0.0360	1.8000	−6.2000	1.8000	1.8000
58	2.3708	12.1662	0.0052	0.2251	1.4521	1.062;	2.0000	5.8831	0.0076	0.9011	2.1420	5.0000	0.0015	0.9998	0.2773	0.0359	1.1000	−5.6000	1.4000	1.4000
59	22.2268	5.9472	0.0046	0.3500	1.9171	2.7164	2.0354	0.1314	0.0052	0.8783	1.3444	2.5489	0.0015	0.9997	0.2771	0.0359	1.4000	−5.6000	1.8000	1.8000
60	12.6169	17.2133	0.0026	0.2871	2.6629	3.5126	2.0001	1.5988	0.0030	0.8962	0.7954	4.8218	0.0018	0.9998	0.2773	0.0359	1.0000	−5.1000	1.3000	1.4000
61	37.9567	3.9930	0.0097	0.9275	0.5962	4.7822	2.0021	0.2773	0.0095	0.9001	2.6549	4.8619	0.0015	0.9998	0.2772	0.0359	1.3000	−5.8000	1.6000	1.6000
62	16.9220	8.1958	0.0086	0.5927	2.9765	0.427;	2.0586	5.5765	0.0022	0.8758	0.5035	0.8175	0.0016	0.9997	0.2814	0.0354	1.4000	−6.2000	1.9000	2.2000
63	2.9445	17.1893	0.0065	0.1629	1.2071	0.2867	2.0191	17.8476	0.0099	0.8991	2.9006	4.9148	0.0020	0.9998	0.2780	0.0358	1.4000	−6.0000	1.6000	1.7000
64	27.5146	14.0811	0.0044	0.8384	1.9766	3.1473	2.0001	2.6458	0.0060	0.8693	1.2232	0.0174	0.0015	0.9997	0.2762	0.0360	1.3000	−6.0000	1.8000	1.9000
65	33.8125	4.3380	0.0089	0.1676	2.7040	3.9809	2.0000	4.9363	0.0077	0.9011	2.1691	5.0000	0.0021	0.9998	0.2773	0.0359	1.1000	−5.6000	1.4000	1.4000
66	38.9170	6.6323	0.0081	0.5022	2.9861	3.456;	2.0233	20.7703	0.0100	0.8989	2.9584	4.9024	0.0015	0.9998	0.2779	0.0358	1.4000	−6.0000	1.7000	1.7000
67	4.1634	2.8059	0.0052	0.9993	1.9595	1.7265	2.0000	1.0403	0.0046	0.9004	1.2648	4.9998	0.0015	0.9998	0.2772	0.0359	1.8000	−6.2000	1.8000	1.9000
68	28.0922	3.5525	0.0049	0.2137	1.8543	4.7691	2.0000	8.7942	0.0089	0.9011	2.4887	5.0000	0.0139	0.9998	0.2773	0.0359	1.4000	−6.0000	1.6000	1.6000
69	29.3384	3.0934	0.0040	0.3978	1.7014	0.368;	2.0010	0.3324	0.0041	0.8817	0.9096	1.5560	0.0015	0.9997	0.2763	0.0360	1.7000	−6.2000	2.0000	2.0000
70	26.7015	9.9122	0.0064	0.3337	2.8859	1.0352	2.0000	8.9522	0.0100	0.8797	2.2381	1.3103	0.0018	0.9997	0.2764	0.0360	1.3000	−6.0000	1.6000	1.6000
71	29.6228	18.8820	0.0091	0.2296	2.2383	3.8751	2.0000	17.0606	0.0092	0.9011	2.5701	5.0000	0.0019	0.9998	0.2773	0.0359	1.5000	−6.0000	1.6000	1.7000
72	16.2062	11.4921	0.0073	0.9361	1.9875	4.5709	2.0000	0.1716	0.0099	0.8973	2.7609	4.8371	0.0015	0.9998	0.2777	0.0358	1.1000	−5.5000	1.6000	1.5000
73	24.1001	0.7116	0.0044	0.6832	1.5699	3.9128	2.0000	0.2758	0.0062	0.8994	1.7066	4.8181	0.0015	0.9998	0.2772	0.0359	1.5000	−6.0000	1.7000	1.6000
74	6.4125	1.1460	0.0076	0.9621	0.7797	1.4777	2.0000	0.2228	0.0084	0.8869	2.0377	2.5112	0.0015	0.9997	0.2766	0.0360	1.2000	−5.7000	1.4000	1.4000
75	4.1909	16.7427	0.0096	0.4380	2.8860	0.7592	2.0001	0.0293	0.0098	0.7872	2.6601	4.7744	0.0017	0.9998	0.2770	0.0359	1.5000	−2.5000	1.8000	0.8000
76	39.2311	9.3993	0.0059	0.9403	1.6206	4.2396	2.0000	13.6783	0.0068	0.9002	1.8899	4.8156	0.0015	0.9998	0.2773	0.0359	1.2000	−5.8000	1.5000	1.5000
77	12.8233	7.9723	0.0059	0.0058	0.0908	3.9243	2.0004	7.3868	0.0012	0.6155	0.0660	4.9687	0.0015	0.9998	0.2770	0.0359	1.1000	−0.4000	1.4000	0.1000
78	24.6090	16.4225	0.0038	0.6103	2.0889	1.3542	2.0156	16.2124	0.0099	0.8991	2.8614	4.8177	0.0013	0.9998	0.2776	0.0358	1.3000	−6.0000	1.7000	1.7000
79	38.5621	7.5911	0.0016	0.8011	1.5591	1.1391	2.0002	6.5884	0.0088	0.9011	2.4527	4.9931	0.0015	0.9998	0.2773	0.0359	1.6000	−6.1000	1.7000	1.7000
80	9.3355	14.8033	0.0018	0.9325	2.6701	4.1478	2.0000	12.5717	0.0041	0.9000	1.1228	4.9941	0.0016	0.9998	0.2773	0.0359	1.7000	−6.1000	1.8000	1.8000
81	14.9825	18.1216	0.0052	0.7633	0.9906	4.1109	2.0000	17.6012	0.0049	0.9008	1.3762	4.9998	0.0015	0.9998	0.2773	0.0359	1.0000	−5.5000	1.4000	1.3000
82	37.4501	6.8521	0.0011	0.8264	0.6891	2.8534	2.0077	0.8603	0.0012	0.6104	0.0635	4.3725	0.0015	0.9998	0.2766	0.0360	1.6000	−0.8000	1.6000	0.3000
83	16.8454	13.5256	0.0092	0.5735	0.3418	2.8591	2.0002	0.0496	0.0100	0.8493	2.7632	4.9996	0.0014	0.9998	0.2773	0.0359	1.5000	−3.7000	1.6000	1.1000
84	12.3822	20.2675	0.0068	0.7926	0.9328	1.4301	2.0001	10.5557	0.0100	0.9005	2.7935	4.9355	0.0015	0.9998	0.2776	0.0358	1.4000	−5.9000	1.8000	1.8000
85	7.7740	1.6050	0.0010	0.3290	0.6853	3.4957	2.0000	10.0935	0.0013	0.7129	0.0883	4.3822	0.0015	0.9998	0.2766	0.0360	3.7000	−3.4000	3.0000	1.9000
86	17.0901	12.2156	0.0013	0.2235	1.9560	3.9813	2.0071	10.8103	0.0014	0.8198	0.1858	4.9992	0.0014	0.9998	0.2762	0.0360	1.3000	−2.1000	1.5000	0.8000
87	16.2395	8.6209	0.0029	0.3124	0.1985	2.2079	2.0000	8.9589	0.0034	0.8987	0.9192	5.0000	0.0014	0.9998	0.2773	0.0359	1.5000	−5.7000	1.7000	1.7000
88	6.9824	6.4461	0.0051	0.5845	0.8263	2.2311	2.0000	0.7096	0.0036	0.8986	0.9872	4.9750	0.0015	0.9998	0.2773	0.0359	1.0000	−5.3000	1.3000	1.3000
89	18.5315	5.5055	0.0021	0.8299	0.8455	2.3283	2.0000	19.5197	0.0028	0.8958	0.7333	4.9882	0.0015	0.9998	0.2773	0.0359	1.2000	−5.2000	1.5000	1.5000
90	25.3558	20.6907	0.0075	0.4026	1.3330	3.3769	2.0000	0.8644	0.0044	0.9000	1.2185	4.9790	0.0014	0.9998	0.2774	0.0359	1.3000	−5.8000	1.5000	1.5000
91	2.4172	3.9014	0.0042	0.8621	2.2677	4.5183	2.0000	19.5749	0.0046	0.9006	1.2859	4.9990	0.0015	0.9998	0.2773	0.0359	1.1000	−5.6000	1.4000	1.4000
92	23.7839	16.2461	0.0080	0.6147	1.8099	4.5426	2.0000	19.7642	0.0079	0.9011	2.2228	5.0000	0.0015	0.9998	0.2773	0.0359	1.1000	−5.7000	1.5000	1.4000
93	32.0097	4.0929	0.0049	0.9912	2.3498	3.736;	2.0000	19.5629	0.0067	0.9011	1.8652	5.0000	0.0015	0.9998	0.2773	0.0359	1.6000	−6.1000	1.7000	1.7000
94	10.9439	20.6314	0.0049	0.2037	0.3418	1.3026	2.0000	20.5842	0.0066	0.9011	1.8430	5.0000	0.0015	0.9998	0.2773	0.0359	1.4000	−6.0000	1.6000	1.7000
95	19.0247	16.6845	0.0014	0.8272	2.9357	3.4482	2.0000	20.6300	0.0074	0.9011	2.0862	5.0000	0.0015	0.9998	0.2773	0.0359	1.1000	−5.6000	1.4000	1.4000
96	23.6356	8.8356	0.0014	0.6759	2.5458	0.6592	2.0004	13.4662	0.0043	0.8998	1.1448	4.5732	0.0015	0.9998	0.2758	0.0361	1.7000	−6.2000	1.8000	1.8000
97	20.8590	10.3747	0.0063	0.4758	1.3986	0.9545	2.0000	19.6469	0.0017	0.8682	0.3322	4.8902	0.0013	0.9998	0.2769	0.0359	0.4000	−2.7000	1.0000	0.8000
98	26.4080	16.8242	0.0032	0.3991	0.9770	0.7287	2.0000	0.5027	0.0035	0.8944	0.9089	3.9950	0.0015	0.9998	0.2770	0.0359	0.8000	−5.2000	1.2000	1.3000
99	10.4081	7.4296	0.0086	0.5994	1.8906	2.9252	2.0000	3.7789	0.0052	0.9008	1.4596	5.0000	0.0016	0.9998	0.2773	0.0359	1.1000	−5.6000	1.4000	1.4000
100	33.8081	1.5484	0.0087	0.8005	0.6909	0.3668	2.0002	0.1445	0.0093	0.8955	2.5685	4.8807	0.0015	0.9998	0.2773	0.0359	1.5000	−5.7000	1.7000	1.6000
101	38.9009	12.2980	0.0097	0.1051	1.7397	4.1116	2.0000	17.2952	0.0051	0.9008	1.4269	4.9998	0.0015	0.9998	0.2773	0.0359	1.2000	−5.7000	1.5000	1.5000
102	32.9595	3.3950	0.0068	0.4229	1.7467	4.2536	2.0000	8.7894	0.0065	0.9011	1.8301	5.0000	0.0015	0.9998	0.2772	0.0359	1.1000	−5.7000	1.4000	1.4000
103	36.4201	16.5189	0.0044	0.0942	1.6222	2.8028	2.0001	10.9494	0.0093	0.8995	2.5938	4.7711	0.0015	0.9998	0.2778	0.0358	1.2000	−5.7000	1.5000	1.5000

104	6.8255	6.4892	0.0083	0.5985	2.6098	4.648;	2.0000	0.7601	0.0099	0.9010	2.7775	4.9614	0.0015	0.9998	0.2772	0.0359	1.2000	−5.7000	1.5000	1.5000
105	36.7083	11.0013	0.0058	0.4709	0.7943	3.4833	2.0000	0.4873	0.0053	0.8969	1.4192	4.1719	0.0015	0.9998	0.2771	0.0359	1.1000	−5.6000	1.5000	1.5000
106	26.0297	3.4669	0.0042	0.6959	0.9542	2.914;	2.0000	1.6465	0.0055	0.9009	1.5243	5.0000	0.0015	0.9998	0.2773	0.0359	1.7000	−6.2000	1.8000	1.8000
107	5.7065	12.5262	0.0095	0.6999	0.3576	4.077;	2.0000	0.3399	0.0052	0.8999	1.4423	4.9255	0.0015	0.9998	0.2773	0.0359	1.2000	−5.7000	1.5000	1.5000
108	12.5829	5.4876	0.0089	0.6385	2.8195	4.3951	2.0166	0.2593	0.0100	0.8990	2.9270	4.9930	0.0015	0.9998	0.2781	0.0358	1.4000	−5.9000	1.6000	1.5000
109	22.7815	13.6079	0.0060	0.0336	1.9367	4.9446	2.0000	1.1742	0.0059	0.9009	1.6448	4.9996	0.0015	0.9998	0.2774	0.0359	1.5000	−6.0000	1.6000	1.6000
110	38.3853	14.3374	0.0066	0.0688	1.4384	0.0026	2.0300	0.4392	0.0099	0.8844	2.5369	2.2111	0.0015	0.9997	0.2775	0.0359	1.5000	−6.2000	1.7000	1.7000
111	38.6658	15.5610	0.0063	0.3196	1.9180	4.3272	2.0000	12.8729	0.0090	0.9011	2.5274	5.0000	0.0018	0.9998	0.2773	0.0359	1.3000	−5.8000	1.5000	1.5000
112	7.9893	9.3820	0.0029	0.5309	1.6341	3.0628	2.1459	0.0278	0.0058	0.7599	2.1859	4.6746	0.0015	0.9997	0.2779	0.0358	1.1000	−2.3000	1.5000	0.5000
113	38.8825	1.7680	0.0037	0.6544	1.9419	4.9498	2.0001	3.9113	0.0047	0.9005	1.3151	4.9714	0.0019	0.9998	0.2773	0.0359	1.1000	−5.5000	1.4000	1.4000
114	38.3723	4.7818	0.0052	0.4076	1.6317	2.6384	2.0000	8.8084	0.0027	0.8919	0.6561	3.7894	0.0015	0.9998	0.2770	0.0359	1.1000	−5.2000	1.5000	1.6000
115	20.4443	18.9907	0.0031	0.8200	2.1631	2.3976	2.0000	20.6240	0.0063	0.9010	1.7503	5.0000	0.0016	0.9998	0.2773	0.0359	1.7000	−6.2000	1.8000	1.8000
116	32.4107	3.1914	0.0086	0.7184	1.5675	4.0067	2.0000	6.4188	0.0053	0.9009	1.4756	4.9995	0.0015	0.9998	0.2773	0.0359	1.4000	−5.9000	1.7000	1.7000
117	7.3917	17.1736	0.0028	0.9686	2.9811	1.1392	2.0160	20.7865	0.0017	0.8713	0.3127	3.4683	0.0015	0.9997	0.2759	0.0360	0.9000	−3.6000	1.4000	1.3000
118	18.0269	11.2049	0.0030	0.5313	0.6560	2.4905	2.0000	4.3582	0.0021	0.8838	0.4668	4.9909	0.0017	0.9998	0.2767	0.0360	2.4000	−5.5000	2.2000	2.1000
119	36.7979	20.7097	0.0025	0.3251	0.3174	4.5043	2.0004	5.6441	0.0016	0.8543	0.2716	4.9992	0.0015	0.9998	0.2765	0.0360	1.7000	−3.4000	1.7000	1.3000
120	38.4607	9.2187	0.0049	0.6110	0.1908	4.2259	2.0001	2.4085	0.0035	0.8988	0.9534	4.9940	0.0013	0.9998	0.2773	0.0359	1.3000	−5.6000	1.5000	1.5000
121	26.9181	2.2421	0.0038	0.7788	1.2137	3.6932	2.0000	12.7630	0.0055	0.9009	1.5482	5.0000	0.0015	0.9998	0.2773	0.0359	1.1000	−5.6000	1.3000	1.3000
122	3.3570	19.9989	0.0093	0.4235	1.3451	2.9299	2.0182	0.1080	0.0100	0.8884	2.9167	4.9622	0.0015	0.9998	0.2780	0.0358	1.4000	−5.3000	1.6000	1.5000
123	34.2669	0.1239	0.0049	0.0908	1.0974	1.2337	2.0060	0.1737	0.0038	0.8829	0.9068	2.6576	0.0015	0.9997	0.2767	0.0359	1.1000	−5.4000	1.7000	1.7000
124	37.4917	16.1166	0.0027	0.2665	2.2905	3.3321	2.0016	0.0731	0.0065	0.8678	1.7208	4.2894	0.0017	0.9998	0.2767	0.0359	1.3000	−4.4000	1.8000	1.4000
125	27.7919	16.9968	0.0091	0.1537	1.8837	0.4174	2.0216	20.7096	0.0031	0.8873	0.7654	2.3202	0.0016	0.9997	0.2757	0.0361	0.8000	−5.5000	1.1000	1.2000
126	30.7941	18.0638	0.0098	0.2810	2.3159	3.1298	2.0001	19.1410	0.0081	0.9013	2.2608	4.9980	0.0018	0.9998	0.2771	0.0359	1.4000	−6.0000	1.7000	1.7000
127	30.2390	1.7808	0.0049	0.4401	2.7986	3.3047	2.0001	5.5543	0.0060	0.9010	1.6917	4.9968	0.0015	0.9998	0.2773	0.0359	1.0000	−5.6000	1.3000	1.3000
128	16.9046	8.3281	0.0020	0.5271	2.9182	3.6488	2.0361	0.0356	0.0098	0.8118	2.9758	4.9709	0.0016	0.9998	0.2779	0.0358	1.1000	−2.7000	1.5000	0.7000
129	26.9082	5.4232	0.0033	0.4574	0.5761	4.4538	2.0000	13.7381	0.0020	0.8821	0.4469	4.9957	0.0015	0.9998	0.2770	0.0359	1.3000	−4.3000	1.6000	1.5000
130	8.5051	16.6390	0.0047	0.8754	0.4166	4.9115	2.0000	13.1132	0.0082	0.9011	2.2924	5.0000	0.0015	0.9998	0.2773	0.0359	1.4000	−6.0000	1.6000	1.6000
131	28.8298	8.9848	0.0064	0.5181	2.0888	3.8451	2.0000	14.7803	0.0034	0.8985	0.9083	4.9845	0.0015	0.9998	0.2773	0.0359	1.9000	−6.2000	2.0000	2.0000
132	3.2096	18.9348	0.0034	0.9436	0.2815	2.9072	2.0000	8.9925	0.0079	0.9010	2.2142	4.9981	0.0015	0.9998	0.2774	0.0359	1.4000	−5.9000	1.5000	1.5000
133	12.5231	3.8033	0.0064	0.6377	1.5762	4.6416	2.0000	4.3603	0.0065	0.9011	1.8207	5.0000	0.0015	0.9998	0.2773	0.0359	1.3000	−5.8000	1.6000	1.6000
134	3.7545	5.5049	0.0074	0.9577	1.5910	2.9005	2.0000	20.7399	0.0027	0.8912	0.6474	3.5312	0.0016	0.9998	0.2769	0.0359	1.0000	−5.2000	1.5000	1.6000
135	5.6910	3.0494	0.0030	0.2407	2.5834	0.0849	2.0000	10.4835	0.0022	0.8785	0.3804	0.4641	0.0018	0.9997	0.2769	0.0359	1.8000	−6.3000	2.4000	2.9000
136	33.2914	2.8528	0.0021	0.6761	1.4546	0.6043	2.0000	0.1431	0.0098	0.8955	2.7199	4.8515	0.0015	0.9998	0.2772	0.0359	1.2000	−5.4000	1.5000	1.4000
137	28.4035	18.0762	0.0037	0.2891	1.1804	4.3136	2.0000	14.2069	0.0037	0.8994	1.0064	4.9926	0.0015	0.9998	0.2773	0.0359	1.6000	−6.0000	1.8000	1.8000
138	14.0498	12.0637	0.0039	0.6718	2.0143	2.4215	2.0007	19.1651	0.0022	0.8800	0.4140	0.8317	0.0018	0.9997	0.2769	0.0359	0.7000	−5.2000	1.1000	1.5000
139	38.1084	11.4441	0.0048	0.6951	2.2238	4.2243	2.0000	20.6784	0.0068	0.9010	1.9166	4.9927	0.0015	0.9998	0.2773	0.0359	1.1000	−5.6000	1.3000	1.4000
140	3.3090	3.0373	0.0056	0.0680	1.5602	1.047;	2.0003	0.0411	0.0049	0.7939	1.0651	1.6837	0.0020	0.9997	0.2762	0.0360	1.2000	−2.9000	1.5000	0.8000
141	18.6723	17.7386	0.0018	0.2548	1.0431	2.7615	2.0000	0.3357	0.0095	0.9007	2.6439	4.9381	0.0015	0.9998	0.2773	0.0359	1.5000	−6.0000	1.6000	1.6000
142	16.4992	12.9430	0.0034	0.2240	0.4500	3.1494	2.0022	0.3362	0.0048	0.8921	1.2140	3.3332	0.0016	0.9997	0.2769	0.0359	1.4000	−5.9000	1.8000	1.8000
143	31.0896	7.3143	0.0082	0.6678	1.7583	0.16;	2.0000	10.4466	0.0100	0.8708	2.0643	0.1762	0.0021	0.9997	0.2759	0.0361	1.3000	−6.0000	1.5000	1.5000
144	9.1012	8.3702	0.0094	0.3445	0.1334	1.8121	2.0003	0.2638	0.0078	0.8839	1.8205	1.9505	0.0018	0.9997	0.2763	0.0360	1.3000	−5.9000	1.6000	1.6000
145	20.6110	1.6049	0.0076	0.7805	2.2648	0.2477	2.0000	10.6576	0.0100	0.9011	2.7940	5.0000	0.0015	0.9998	0.2773	0.0359	1.5000	−6.0000	1.6000	1.6000
146	18.9323	5.0089	0.0054	0.6753	0.7284	2.4478	2.0000	0.9825	0.0048	0.9006	1.3296	4.9997	0.0015	0.9998	0.2773	0.0359	1.5000	−6.0000	1.7000	1.7000
147	26.5599	2.5881	0.0062	0.0067	1.3272	0.9626	2.0000	14.7080	0.0035	0.8991	0.9662	4.9987	0.0015	0.9998	0.2772	0.0359	0.8000	−5.2000	1.2000	1.2000
148	28.9559	3.8460	0.0031	0.6022	2.0634	0.6154	2.0004	0.1181	0.0098	0.8617	2.0155	0.2271	0.0021	0.9997	0.2763	0.0360	1.3000	−5.5000	1.7000	1.6000
149	30.6781	5.0097	0.0051	0.3868	1.0777	1.0275	2.0000	0.5335	0.0054	0.8995	1.4806	4.7302	0.0015	0.9998	0.2772	0.0359	1.5000	−6.0000	1.6000	1.7000
150	12.4890	8.6911	0.0097	0.9160	2.2090	0.7326	2.0005	0.1087	0.0097	0.8766	2.3315	2.4787	0.0017	0.9997	0.2765	0.0360	1.1000	−5.1000	1.5000	1.3000
151	26.8937	18.7702	0.0057	0.4624	2.0502	0.2133	2.0000	19.4703	0.0028	0.8917	0.6682	3.5362	0.0016	0.9998	0.2768	0.0359	1.5000	−5.7000	1.9000	2.0000

Table A.1: The results of optimisations for 151 rounds of Nelder-Mead simplex using low LET IR. Columns 3 and 4 are the value of LQ parameters α_{model} and β_{model} for each run with the value of LQ parameters for the experimental data $\alpha_{exp} = 0.2790$ Gy^{-1} and $\beta_{exp} = 0.0357$ Gy^{-2}. Columns 5 contains the elasticity of LQ parameter α with respect to δ and p, while columns 6 contains the elasticity of LQ parameter β with respect to δ and p.

A.4.3 Results of parameter estimation using high LET IR survival data for $\xi = 147$

	Column 1						Column 2								Column 3	Column 4	Column 5		Column 6	
	Initial guesses						Estimated parameter values								$\alpha_{exp} = 0.0598$	$\beta_{exp} = 0.0158$	α_{elas}		β_{elas}	
Run	δ	α_1	α_2	p	V_{max}	K_M	δ	α_1	α_2	p	V_{max}	K_M	SSE	r^2	α_{model}	β_{model}	δ	p	δ	p
1	7.6732	11.9704	0.0022	0.1564	0.7285	1.887	3.7826	0.1799	0.001	0.7962	2.8144	2.8056	0.0797	0.9564	0.7446	0.0224	0.9612	−4.1585	2.6065	2.9725
2	11.7853	1.2689	0.0075	0.8555	2.7523	1.08	2.3561	13.9755	0.0043	0.6707	2.4681	0.0909	0.0804	0.9561	0.7694	0.0154	0.9737	−2.0741	2.5164	2.491
3	33.9473	4.9023	0.002	0.6448	0.8072	3.952	3.3324	18.7049	0.0011	0.771	1.9408	0.8671	0.0799	0.9563	0.7503	0.0209	0.9564	−3.4839	2.6515	2.5319
4	11.6627	7.3601	0.0069	0.3763	2.2965	4.746	3.6703	18.9734	0.001	0.7942	2.9387	3.756	0.0801	0.9562	0.7459	0.0222	0.9678	−4.0342	2.4898	2.4657
5	32.9428	17.0776	0.0054	0.1909	0.566	1.637	4.1908	14.6395	0.001	0.8207	2.9999	0.0047	0.0789	0.9569	0.7252	0.0285	0.9081	−5.3761	3.0104	3.0837
6	11.2539	0.3475	0.008	0.4283	0.8625	3.356	4.2872	3.1621	0.001	0.8258	2.9999	0.0001	0.0788	0.9569	0.7177	0.0308	0.8869	−5.7486	3.123	3.0619
7	37.312	0.921	0.0074	0.482	0.2733	2.193	3.7241	0.0389	0.001	0.6167	1.1536	3.187	0.077	0.9579	0.7455	0.0226	0.9074	−1.7461	3.2919	3.6805
8	15.2994	3.5363	0.0091	0.1206	1.7286	4.167	4.2858	19.2821	0.001	0.8257	2.9999	0.0001	0.0788	0.9569	0.7179	0.0308	0.8787	−5.7346	3.1628	3.1302
9	9.4706	13.5048	0.009	0.5895	2.0501	3.844	2.9799	0.3822	0.0012	0.7431	1.3378	0.1791	0.08	0.9563	0.7533	0.0198	0.9639	−2.9823	2.5379	2.5127
10	11.5412	15.2199	0.004	0.2262	1.6398	0.836	4.3012	3.8156	0.001	0.8264	2.9987	0.0002	0.0788	0.9569	0.7171	0.0312	0.8761	−5.7941	3.1738	3.2045
11	25.4097	13.4764	0.0073	0.3846	1.2772	4.309	4.2233	0.109	0.001	0.8088	2.2982	0.5852	0.079	0.9568	0.7126	0.0322	0.8938	−5.0405	3.0022	3.5312
12	19.985	9.3899	0.0028	0.583	1.9333	4.949	4.5898	0.0653	0.001	0.7921	2.902	0.3216	0.0769	0.9579	0.7055	0.0345	0.8046	−5.7872	3.6622	3.5729
13	15.3631	11.3849	0.0013	0.2518	1.9429	2.572	4.2877	9.753	0.001	0.8258	2.9999	0.0001	0.0788	0.9569	0.7176	0.0309	0.8875	−5.7446	3.0904	3.1219
14	33.5715	6.18	0.0077	0.2904	2.0371	4.421	3.1571	0.2636	0.0011	0.7487	0.6882	3.887	0.0794	0.9566	0.7330	0.0256	0.964	−3.0127	2.4965	6.0564
15	24.24	15.4892	0.0055	0.6171	1.9074	2.94	4.0271	13.2973	0.001	0.8106	2.96	0.1171	0.0791	0.9567	0.7411	0.0246	0.914	−4.7966	3.0562	2.979
16	22.8895	3.9508	0.0053	0.2653	2.8355	0.773	4.2877	0.8732	0.001	0.8258	2.9999	0.0001	0.0788	0.9569	0.7176	0.0309	0.8845	−5.7473	3.124	3.0383
17	36.8534	14.2867	0.0091	0.8244	0.6268	0.999	2.1079	17.8318	0.0077	0.6309	2.9997	0.0035	0.0806	0.9559	0.7738	0.0139	0.9889	−1.7383	2.2949	2.3745
18	12.8619	3.8378	0.0065	0.9827	2.1278	2.034	4.2877	19.8113	0.001	0.8258	2.9999	0.0001	0.0788	0.9569	0.7176	0.0309	0.8887	−5.7476	3.1162	3.0846
19	30.7736	7.6783	0.0066	0.7302	0.7087	3.743	4.0611	14.5448	0.001	0.8156	2.877	1.1643	0.0794	0.9566	0.7280	0.0277	0.9074	−4.9675	2.9791	2.9179
20	30.6417	13.017	0.0087	0.3439	0.3582	4.127	4.1784	0.0731	0.001	0.7771	2.9016	4.1453	0.079	0.9568	0.7256	0.0283	0.9034	−4.1633	3.0552	3.2867
21	16.4569	16.227	0.0082	0.5841	1.8219	3.949	3.1433	0.3975	0.0011	0.7345	0.423	2.684	0.0766	0.9582	0.7404	0.0234	0.9033	−2.7847	3.2913	8.5299
22	23.5772	1.7121	0.0062	0.1078	1.3504	1.592	4.4164	0.0277	0.001	0.6337	2.2907	0.7371	0.0762	0.9583	0.7245	0.0289	0.8258	−2.8704	3.7682	2.3049
23	4.8825	19.3239	0.0026	0.9063	1.3762	2.67	3.9326	7.1178	0.001	0.8062	2.8509	0.0702	0.0792	0.9567	0.7418	0.0238	0.9257	−4.5642	2.948	2.9074
24	4.0501	16.1333	0.0032	0.8797	1.9858	0.449	4.2877	4.7191	0.001	0.8258	2.9999	0.0001	0.0788	0.9569	0.7177	0.0308	0.8771	−5.7384	3.1688	3.1514
25	22.1703	10.1346	0.009	0.8178	2.3109	0.558	3.3552	0.852	0.0011	0.7729	1.8697	0.6477	0.0799	0.9563	0.7480	0.0216	0.9761	−3.534	2.4287	2.478
26	31.6084	9.0771	0.0013	0.2607	1.0507	0.681	4.2876	20.7876	0.001	0.8258	2.9999	0.0001	0.0788	0.9569	0.7176	0.0309	0.8946	−5.7461	3.0531	3.0631
27	37.4924	9.304	0.0054	0.5944	1.986	3.3933	4.1488	14.4925	0.001	0.8195	2.9037	0.5139	0.0792	0.9567	0.7247	0.0287	0.91	−5.245	2.9376	3.0001
28	6.9364	6.3882	0.0025	0.0225	1.2485	2.4759	2.4867	0.0567	0.0059	0.5802	2.9475	0.0543	0.0799	0.9563	0.7595	0.0179	0.9777	−1.433	2.4379	1.8655
29	23.6153	10.5855	0.0098	0.4253	2.5258	0.9486	2.7502	0.2181	0.003	0.7169	2.999	0.0586	0.0801	0.9562	0.7639	0.0166	0.9697	−2.6012	2.5786	2.6468
30	19.8368	10.6325	0.0074	0.3127	2.4988	2.475	3.2219	2.6807	0.001	0.7624	1.4911	0.0352	0.0798	0.9564	0.7510	0.0206	0.9695	−3.3345	2.5196	2.496
31	2.4523	17.0035	0.0055	0.1615	0.7693	0.738	4.3357	8.3258	0.001	0.8289	2.998	0.0524	0.0789	0.9569	0.7112	0.0324	0.8693	−5.9638	3.1858	3.1607
32	14.8107	16.5302	0.0052	0.1788	1.8404	0.2749	4.2877	18.4335	0.001	0.8258	2.9999	0.0001	0.0788	0.9569	0.7177	0.0308	0.8761	−5.7411	3.1974	3.092
33	15.6941	11.5831	0.0058	0.7475	0.4454	0.8435	3.8375	2.5547	0.001	0.8032	2.6257	1.1521	0.0796	0.9565	0.7381	0.0246	0.9489	−4.3997	2.6549	2.7036
34	9.174	11.0184	0.0097	0.7485	1.8594	3.7585	4.6838	0.0638	0.001	0.7955	2.9857	0.3094	0.0768	0.958	0.6969	0.0371	0.7842	−6.3356	3.7225	3.6091
35	2.0455	17.26	0.002	0.5433	0.7819	1.8418	2.6922	15.6674	0.0019	0.7151	1.5979	0.237	0.0802	0.9562	0.7575	0.0187	0.9661	−2.5767	2.557	2.5065
36	14.0239	17.8575	0.0015	0.3381	1.337	4.7091	4.2864	16.2172	0.001	0.8258	2.9999	0.0028	0.0788	0.9569	0.7177	0.0308	0.8891	−5.7437	3.1026	3.0582
37	28.5854	16.4098	0.0037	0.8323	2.532	0.0859	3.1505	5.1076	0.001	0.7571	1.4011	0.0026	0.0799	0.9563	0.7510	0.0206	0.9693	−3.2333	2.4836	2.5313
38	25.7597	6.6266	0.0062	0.5526	0.5886	4.1453	4.2877	16.1416	0.001	0.8258	2.9999	0.0001	0.0788	0.9569	0.7177	0.0308	0.8888	−5.7422	3.1076	3.1268
39	22.6364	9.4166	0.0058	0.9575	0.9116	3.133	3.5814	0.0277	0.001	0.5167	1.2942	0.0174	0.0771	0.9579	0.7899	0.0090	0.9181	−1.1887	5.0314	5.4229
40	18.6834	15.6457	0.0091	0.8928	1.4499	2.6937	2.2398	0.0688	0.0065	0.5713	2.0972	0.0488	0.0802	0.9562	0.7615	0.0175	0.9788	−1.3647	2.4056	2.0135
41	12.9222	2.3087	0.0059	0.3565	1.0134	3.2525	2.0018	0.0298	0.0062	0.1996	2.3047	4.4907	0.0809	0.9558	0.7729	0.0140	0.9872	−0.2474	2.256	0.4867
42	21.063	2.3062	0.0049	0.5464	2.3955	3.6331	3.1675	0.1627	0.0022	0.7531	2.9674	0.1064	0.0798	0.9564	0.7507	0.0206	0.9732	−3.1725	2.4659	2.6528
43	30.9388	5.6311	0.0059	0.3467	2.9625	0.4724	2.7325	0.0799	0.0013	0.4679	0.4075	4.4716	0.0749	0.9591	0.7752	0.0133	0.9148	−0.8615	4.1826	4.6483
44	30.9715	10.9204	0.0074	0.6228	0.4771	4.3879	4.0603	0.0452	0.0011	0.71	2.2507	0.0134	0.0775	0.9576	0.7386	0.0238	0.8948	−2.9406	3.3772	3.3459
45	23.8901	20.2222	0.0012	0.7966	0.7106	0.0718	3.9005	0.0823	0.001	0.7684	2.3894	3.4741	0.0792	0.9567	0.7387	0.0246	0.9461	−3.6385	2.7387	3.4913
46	30.4112	14.7774	0.0082	0.7459	2.1067	1.4715	2.3809	12.161	0.0058	0.6772	2.9698	0.011	0.0804	0.9561	0.7609	0.0176	0.9759	−2.1462	2.4363	2.5031
47	26.5303	6.5026	0.0023	0.1255	1.1264	0.8996	4.4086	0.0291	0.001	0.642	2.9998	4.9525	0.0778	0.9574	0.7173	0.0310	0.8655	−2.926	3.3385	2.0039
48	6.6823	6.079	0.0053	0.8224	2.9211	4.6315	4.2876	19.0158	0.001	0.8258	2.9999	0.0001	0.0788	0.9569	0.7177	0.0309	0.8855	−5.7426	3.1173	3.088
49	21.1671	17.6831	0.0033	0.0252	2.9169	0.3409	3.5205	17.8096	0.001	0.7832	2.1058	0.6643	0.0798	0.9564	0.7485	0.0214	0.9689	−3.7775	2.5165	2.5704
50	15.1959	18.9556	0.0043	0.4144	1.9311	2.9055	4.2877	20.1813	0.001	0.8258	2.9999	0.0001	0.0788	0.9569	0.7176	0.0309	0.8881	−5.7546	3.0879	3.108
51	5.5016	13.3005	0.007	0.7314	2.5803	3.1858	4.3611	0.0339	0.001	0.6737	2.9603	4.9427	0.078	0.9573	0.7199	0.0302	0.8671	−3.0825	3.3219	2.2833

52	7.6183	5.3298	0.0025	0.7814	1.2057	3.2563	4.2877	4.9593	0.001	0.8258	2.9999	0.0001	0.0788	0.9569	0.7177	0.0308	0.8843	−5.7462	3.1114	3.1217
53	9.5304	1.8686	0.0035	0.3673	1.8958	4.3231	4.0873	3.088	0.001	0.8175	2.9858	1.7486	0.0796	0.9565	0.7256	0.0284	0.9243	−5.0512	2.8607	2.8826
54	27.5463	17.4318	0.0028	0.7449	2.9557	0.2798	4.2878	12.7762	0.001	0.8258	2.9999	0.0001	0.0788	0.9569	0.7177	0.0309	0.8852	−5.7501	3.0952	3.0653
55	18.3974	12.1678	0.0028	0.8923	1.6784	4.0843	2.2273	0.0277	0.0046	0.2432	2.586	3.9371	0.0805	0.956	0.7759	0.0131	0.9758	−0.3157	2.5332	0.6006
56	28.3873	19.7126	0.0039	0.2426	2.8008	2.6446	4.2876	12.971	0.001	0.8258	2.9999	0.0001	0.0788	0.9569	0.7177	0.0309	0.8903	−5.746	3.075	3.0812
57	11.7578	1.2948	0.0089	0.1296	2.161	3.4718	2.9171	8.0092	0.002	0.7333	2.7087	0.0039	0.08	0.9563	0.7675	0.0157	0.9685	−2.8251	2.6028	2.5232
58	2.3708	12.1662	0.0052	0.2251	1.4521	1.062	4.2804	0.1539	0.0011	0.8209	2.9431	0.1984	0.0788	0.9569	0.7165	0.0309	0.8825	−5.5518	3.129	3.3673
59	22.2268	5.9472	0.0046	0.35	1.9171	2.7164	2.7319	0.0959	0.0013	0.5228	0.3854	4.1762	0.0754	0.9588	0.7555	0.0185	0.8998	−1.0601	3.6956	4.208
60	12.6169	17.2133	0.0026	0.2871	2.6629	3.5126	4.2876	3.8048	0.001	0.8258	2.9999	0.0001	0.0788	0.9569	0.7177	0.0308	0.8825	−5.7392	3.1382	3.1757
61	37.9567	3.993	0.0097	0.9275	0.5962	4.7822	4.1723	12.2445	0.001	0.8207	2.9769	0.6602	0.0792	0.9567	0.7239	0.0289	0.8996	−5.3068	3.027	3.0223
62	16.922	8.1958	0.0086	0.5927	2.9765	0.427	4.2876	20.5784	0.001	0.8258	2.9999	0.0001	0.0788	0.9569	0.7176	0.0309	0.8847	−5.7504	3.119	3.1078
63	2.9445	17.1893	0.0065	0.1629	1.2071	0.2867	2.6852	13.2767	0.0011	0.7107	1.0243	0.0028	0.0801	0.9562	0.7676	0.0157	0.9761	−2.5203	2.4819	2.5264
64	27.5146	14.0811	0.0044	0.8384	1.9766	3.1473	3.5757	2.1378	0.001	0.7885	2.9997	4.9341	0.0803	0.9561	0.7496	0.0211	0.9709	−3.853	2.4644	2.5723
65	33.8125	4.338	0.0089	0.1676	2.704	3.9809	3.4328	1.4931	0.001	0.7776	1.8126	0.028	0.0797	0.9564	0.7473	0.0218	0.9693	−3.6536	2.5035	2.5674
66	38.917	6.6323	0.0081	0.5022	2.9861	3.456	3.214	0.0277	0.0023	0.4894	2.7452	2.3419	0.0793	0.9566	0.7542	0.0203	0.9617	−0.99	2.6139	1.2997
67	4.1634	2.8059	0.0052	0.9993	1.9595	1.7265	3.7873	0.1249	0.001	0.7868	2.1022	0.4583	0.0791	0.9568	0.7429	0.0229	0.9411	−3.9846	2.7975	3.5245
68	28.0922	3.5525	0.0049	0.2137	1.8543	4.7691	4.4498	0.0606	0.001	0.7767	2.774	2.4137	0.078	0.9574	0.7092	0.0334	0.8406	−4.8361	3.3996	3.3278
69	29.3384	3.0934	0.004	0.3978	1.7014	0.368	4.2877	9.1711	0.001	0.8258	2.9999	0.0001	0.0788	0.9569	0.7176	0.0309	0.8973	−5.753	3.0414	3.1051
70	26.7015	9.9122	0.0064	0.3337	2.8859	1.0352	4.4111	0.0286	0.001	0.6392	2.5681	2.4884	0.077	0.9579	0.7210	0.0301	0.8413	−2.8957	3.5712	2.204
71	29.6228	18.882	0.0091	0.2296	2.2383	3.8751	4.5202	0.0547	0.001	0.77	2.4524	0.0468	0.0769	0.958	0.7080	0.0338	0.808	−4.9523	3.6482	3.5222
72	16.2062	11.4921	0.0073	0.9361	1.9875	4.5709	3.5807	20.0415	0.0011	0.7858	2.8148	1.0594	0.0797	0.9564	0.7534	0.0201	0.9731	−3.8443	2.5049	2.5529
73	24.1001	0.7116	0.0044	0.6832	1.5699	3.9128	4.2877	7.4677	0.001	0.8258	2.9999	0.0001	0.0788	0.9569	0.7176	0.0309	0.8928	−5.745	3.0718	3.0716
74	6.4125	1.146	0.0076	0.9621	0.7797	1.4777	2.9556	0.2112	0.0014	0.7325	0.4138	1.197	0.0776	0.9576	0.7361	0.0239	0.9117	−2.8042	3.1198	8.3938
75	4.1909	16.7427	0.0096	0.438	2.886	0.7592	2.8647	3.498	0.001	0.7282	1.2763	0.0177	0.0801	0.9562	0.7684	0.0156	0.9776	−2.7557	2.5153	2.563
76	39.2311	9.3993	0.0059	0.9403	1.6206	4.2396	4.0874	0.2289	0.001	0.8159	2.8257	0.6051	0.0793	0.9567	0.7261	0.0273	0.9162	−5.047	2.9519	2.9834
77	12.8233	7.9723	0.0059	0.0058	0.0908	3.9243	4.4112	0.1224	0.001	0.8222	2.9746	1.5019	0.0788	0.9569	0.7071	0.0338	0.8597	−5.93	3.2143	3.5289
78	24.609	16.4225	0.0038	0.6103	2.0889	1.3542	4.2877	3.9854	0.001	0.8258	2.9999	0.0001	0.0788	0.9569	0.7177	0.0308	0.8852	−5.7448	3.1244	3.0959
79	38.5621	7.5911	0.0016	0.8011	1.5591	1.1391	3.8544	0.1868	0.001	0.8014	2.796	2.5668	0.0797	0.9564	0.7397	0.0241	0.9417	−4.3426	2.7356	2.9579
80	9.3355	14.8033	0.0018	0.9325	2.6701	4.1478	4.2431	11.874	0.001	0.8239	2.8303	0.065	0.0791	0.9568	0.7188	0.0311	0.8924	−5.5556	3.075	3.0471
81	14.9825	18.1216	0.0052	0.7633	0.9906	4.1109	4.2241	6.8305	0.001	0.8227	2.9999	0.2933	0.079	0.9568	0.7226	0.0296	0.901	−5.5006	3.0209	2.9808
82	37.4501	6.8521	0.0011	0.8264	0.6891	2.8534	2.9183	0.1068	0.0024	0.7146	2.008	0.006	0.0797	0.9564	0.7497	0.0207	0.9639	−2.5975	2.5274	2.7841
83	16.8454	13.5256	0.0092	0.5735	0.3418	2.8591	4.7558	0.0363	0.001	0.7246	2.9616	0.0008	0.0754	0.9588	0.6991	0.0366	0.7443	−5.3884	4.0316	2.8017
84	12.3822	20.2675	0.0068	0.7926	0.9328	1.4301	4.2283	0.2628	0.001	0.8226	2.9939	0.0254	0.0789	0.9569	0.7214	0.0293	0.8904	−5.5152	3.1173	3.1201
85	7.774	1.605	0.001	0.329	0.6853	3.4957	4.2576	15.301	0.001	0.8245	2.9622	0.024	0.0789	0.9569	0.7189	0.0304	0.8989	−5.6312	3.0345	3.0142
86	17.0901	12.2156	0.0013	0.2235	1.956	3.9813	4.2877	20.665	0.001	0.8258	2.9999	0.0001	0.0788	0.9569	0.7176	0.0309	0.8938	−5.7541	3.0674	3.0809
87	16.2395	8.6209	0.0029	0.3124	0.1985	2.2079	2.7112	0.0277	0.0031	0.3917	1.8855	0.3349	0.079	0.9568	0.7681	0.0155	0.9586	−0.6671	2.838	1.1445
88	6.9824	6.4461	0.0051	0.5845	0.8263	2.2311	3.78	0.3277	0.0011	0.801	2.9801	2.5627	0.0799	0.9563	0.7385	0.0241	0.9448	−4.2789	2.7143	2.6429
89	18.5315	5.5055	0.0021	0.8299	0.8455	2.3283	3.8152	3.9776	0.001	0.8019	2.611	1.2335	0.0797	0.9565	0.7390	0.0243	0.9491	−4.3383	2.6724	2.6842
90	25.3558	20.6907	0.0075	0.4026	1.333	3.3769	2.0787	6.9852	0.0096	0.6313	2.78	0.0106	0.0807	0.9559	0.7626	0.0171	0.9785	−1.7384	2.3923	2.3876
91	2.4172	3.9014	0.0042	0.8621	2.2677	4.5183	4.2877	20.4726	0.001	0.8258	2.9999	0.0001	0.0788	0.9569	0.7176	0.0309	0.8962	−5.7601	3.0442	3.1173
92	23.7839	16.2461	0.008	0.6147	1.8099	4.5426	4.2877	13.738	0.001	0.8258	2.9999	0.0001	0.0788	0.9569	0.7177	0.0308	0.8823	−5.7413	3.1709	3.1407
93	32.0097	4.0929	0.0049	0.9912	2.3498	3.736	4.2877	18.6303	0.001	0.8258	2.9999	0.0001	0.0788	0.9569	0.7177	0.0308	0.8822	−5.7461	3.1391	3.1154
94	10.9439	20.6314	0.0049	0.2037	0.3418	1.3026	3.9204	16.3836	0.001	0.8084	2.994	2.425	0.0797	0.9564	0.7358	0.0253	0.94	−4.5902	2.7396	2.6899
95	19.0247	16.6845	0.0014	0.8272	2.9357	3.4482	4.1749	5.0863	0.001	0.821	2.9893	0.4811	0.0792	0.9567	0.7223	0.0294	0.9062	−5.3431	2.9958	2.9338
96	23.6356	8.8356	0.0014	0.6759	2.5458	0.6592	2.3255	0.1872	0.005	0.6607	2.9705	0.0297	0.0804	0.9561	0.7730	0.0139	0.9818	−1.9934	2.4059	2.5563
97	20.859	10.3747	0.0063	0.4758	1.3986	0.9545	4.2851	15.3402	0.001	0.8264	2.9145	0.1986	0.0791	0.9568	0.7150	0.0318	0.8965	−5.741	2.9992	3.0599
98	26.408	16.8242	0.0032	0.3991	0.977	0.7287	4.3309	0.0558	0.001	0.7591	2.6378	1.715	0.0777	0.9575	0.7206	0.0292	0.8657	−4.1751	3.3575	3.3714
99	10.4081	7.4296	0.0086	0.5994	1.8906	2.9252	3.0508	0.0306	0.0025	0.4966	2.9874	1.9407	0.0794	0.9566	0.7643	0.0169	0.9544	−1.0148	2.8453	1.4938
100	33.8081	1.5484	0.0087	0.8005	0.6909	0.3668	3.2161	3.3963	0.0011	0.761	2.706	4.6091	0.0804	0.956	0.7650	0.0169	0.9774	−3.2314	2.4085	2.4182
101	38.9009	12.298	0.0097	0.1051	1.7397	4.1116	2.2169	8.8385	0.0071	0.6551	2.7203	0.2001	0.0806	0.956	0.7598	0.0178	0.9898	−1.9356	2.2321	2.2523
102	32.9595	3.395	0.0068	0.4229	1.7467	4.2536	4.2842	12.8669	0.001	0.8256	2.9999	0.0008	0.0788	0.9569	0.7183	0.0308	0.8895	−5.7329	3.0986	3.0955
103	36.4201	16.5189	0.0044	0.0942	1.6222	2.8028	3.8686	0.0278	0.001	0.559	2.9097	4.458	0.0786	0.9571	0.7677	0.0163	0.9453	−1.5187	3.1674	2.2075
104	6.8255	6.4892	0.0083	0.5985	2.6098	4.648	4.2177	20.5891	0.001	0.8229	2.9636	0.3948	0.0791	0.9568	0.7207	0.0299	0.8978	−5.4864	3.0309	2.9671
105	36.7083	11.0013	0.0058	0.4709	0.7943	3.4833	3.6646	6.2901	0.001	0.7929	2.5572	1.7222	0.0798	0.9564	0.7455	0.0224	0.952	−4.0209	2.6433	2.662
106	26.0297	3.4669	0.0042	0.6959	0.9542	2.914	4.1565	0.0277	0.001	0.6031	2.2046	0.0236	0.0764	0.9582	0.7544	0.0199	0.8769	−2.1253	3.9164	2.7144
107	5.7065	12.5262	0.0095	0.6999	0.3576	4.077	4.3365	0.029	0.001	0.632	2.9929	4.7141	0.0778	0.9575	0.7265	0.0283	0.8672	−2.6653	3.4307	2.0189
108	12.5829	5.4876	0.0089	0.6385	2.8195	4.3951	2.4902	0.0277	0.006	0.3547	2.7876	0.2907	0.0797	0.9564	0.7591	0.0182	0.9795	−0.568	2.4047	0.8643
109	22.7815	13.6079	0.006	0.0336	1.9367	4.9446	3.7616	6.447	0.001	0.7996	2.9897	3.4847	0.08	0.9563	0.7426	0.0232	0.9528	−4.217	2.6085	2.581
110	38.3853	14.3374	0.0066	0.0688	1.4384	0.0026	4.2737	0.0977	0.001	0.8038	2.7438	1.1535	0.0784	0.9572	0.7226	0.0293	0.8941	−5.0452	3.1326	3.5197

111	38.6658	15.561	0.0063	0.3196	1.918	4.3272	3.9822	10.9701	0.001	0.8102	2.6456	0.0278	0.0792	0.9567	0.7336	0.0259	0.9297	−4.7315	2.8755	2.8681
112	7.9893	9.382	0.0029	0.5309	1.6341	3.0628	2.4748	0.0505	0.0017	0.2442	0.265	2.2869	0.0724	0.9604	0.7808	0.0112	0.8648	−0.3099	5.9832	2.4698
113	38.8825	1.768	0.0037	0.6544	1.9419	4.9498	4.2877	19.5145	0.001	0.8258	2.9999	0.0001	0.0788	0.9569	0.7177	0.0308	0.8793	−5.7415	3.1714	3.1906
114	38.3723	4.7818	0.0052	0.4076	1.6317	2.6384	4.2883	0.0958	0.001	0.8032	2.6968	0.1455	0.078	0.9573	0.7236	0.0289	0.872	−5.0697	3.306	3.7742
115	20.4443	18.9907	0.0031	0.82	2.1631	2.3976	4.157	0.0502	0.001	0.7291	2.4999	3.9498	0.0785	0.9571	0.7283	0.0276	0.9033	−3.2935	3.1002	3.1309
116	32.4107	3.1914	0.0086	0.7184	1.5675	4.0067	3.4714	14.5233	0.001	0.7815	1.6748	0.0055	0.0798	0.9564	0.7405	0.0243	0.9529	−3.7483	2.5998	2.5025
117	7.3917	17.1736	0.0028	0.9686	2.9811	1.1392	3.7487	12.6061	0.001	0.7973	2.3897	0.2696	0.0795	0.9565	0.7416	0.0235	0.9367	−4.1943	2.806	2.8007
118	18.0269	11.2049	0.003	0.5313	0.656	2.4905	4.6333	0.0541	0.001	0.7781	2.4168	1.121	0.0782	0.9573	0.6853	0.0410	0.7778	−5.4841	3.5312	3.289
119	36.7979	20.7097	0.0025	0.3251	0.3174	4.5043	2.9244	12.4863	0.0011	0.7387	1.2971	0.9271	0.0802	0.9562	0.7548	0.0195	0.9662	−2.9001	2.5343	2.4871
120	38.4607	9.2187	0.0049	0.611	0.1908	4.2259	4.4593	0.1593	0.001	0.8302	2.9702	0.1368	0.0785	0.9571	0.7040	0.0348	0.8471	−6.3878	3.2772	3.4805
121	26.9181	2.2421	0.0038	0.7788	1.2137	3.6932	4.2876	17.99	0.001	0.8258	2.9999	0.0001	0.0788	0.9569	0.7176	0.0309	0.8898	−5.7527	3.0861	3.1277
122	3.357	19.9989	0.0093	0.4235	1.3451	2.9299	3.5836	16.4461	0.001	0.7891	2.9998	4.9315	0.0803	0.9561	0.7490	0.0212	0.9738	−3.8685	2.4423	2.3669
123	34.2669	0.1239	0.0049	0.0908	1.0974	1.2337	4.3025	0.0583	0.001	0.7614	2.9309	4.5531	0.0787	0.957	0.7179	0.0305	0.8849	−4.0996	3.1384	3.1767
124	37.4917	16.1166	0.0027	0.2665	2.2905	3.3321	3.8572	6.7236	0.001	0.8052	2.9709	2.9104	0.0799	0.9563	0.7379	0.0247	0.9472	−4.4324	2.6588	2.7189
125	27.7919	16.9968	0.0091	0.1537	1.8837	0.4174	2.164	0.0801	0.0032	0.5414	0.4499	1.1154	0.0787	0.957	0.7601	0.0172	0.9576	−1.1672	2.8091	4.048
126	30.7941	18.0638	0.0098	0.281	2.3159	3.1298	2.6191	10.1898	0.0011	0.703	0.974	0.0639	0.0802	0.9562	0.7694	0.0151	0.9699	−2.4217	2.6464	2.6874
127	30.239	1.7808	0.0049	0.4401	2.7986	3.3047	4.3258	0.0735	0.0011	0.7898	2.5246	1.6708	0.0787	0.957	0.7083	0.0337	0.8731	−4.7319	3.1146	3.4463
128	16.9046	8.3281	0.002	0.5271	2.9182	3.6488	3.5673	0.2062	0.0013	0.7853	2.7803	1.1031	0.0798	0.9564	0.7447	0.0224	0.9538	−3.8313	2.6216	2.7617
129	26.9082	5.4232	0.0033	0.4574	0.5761	4.4538	4.2936	6.9756	0.001	0.8264	2.982	0.0648	0.0789	0.9569	0.7160	0.0313	0.8833	−5.7748	3.1145	3.1642
130	8.5051	16.639	0.0047	0.8754	0.4166	4.9115	3.1554	3.1749	0.001	0.7569	1.4256	0.0558	0.0799	0.9563	0.7534	0.0199	0.9701	−3.2275	2.5287	2.5752
131	28.8298	8.9848	0.0064	0.5181	2.0888	3.8451	4.2876	20.4349	0.001	0.8258	2.9999	0.0001	0.0788	0.9569	0.7177	0.0308	0.8857	−5.7419	3.1394	3.1643
132	3.2096	18.9348	0.0034	0.9436	0.2815	2.9072	2.0877	0.9194	0.0094	0.6317	2.9322	0.0231	0.0806	0.9559	0.7649	0.0164	0.9836	−1.7464	2.3714	2.3293
133	12.5231	3.8033	0.0064	0.6377	1.5762	4.6416	4.264	14.0603	0.001	0.8248	2.9772	0.017	0.0789	0.9569	0.7186	0.0304	0.8883	−5.6608	3.074	3.105
134	3.7545	5.5049	0.0074	0.9577	1.591	2.9005	4.2877	10.0992	0.001	0.8258	2.9999	0.0001	0.0788	0.9569	0.7176	0.0309	0.8898	−5.7562	3.0774	3.1092
135	5.691	3.0494	0.003	0.2407	2.5834	0.0849	3.5749	12.6619	0.001	0.7885	2.998	4.969	0.0803	0.9561	0.7495	0.0211	0.9581	−3.8437	2.593	2.6499
136	33.2914	2.8528	0.0021	0.6761	1.4546	0.6043	4.5169	0.1113	0.001	0.8224	2.996	0.0053	0.078	0.9574	0.7056	0.0349	0.8424	−6.3421	3.3582	3.6879
137	28.4035	18.0762	0.0037	0.2891	1.1804	4.3136	3.9145	0.2182	0.001	0.8073	2.9163	3.0466	0.0798	0.9564	0.7340	0.0256	0.9377	−4.5393	2.7543	2.9448
138	14.0498	12.0637	0.0039	0.6718	2.0143	2.4215	2.251	0.3109	0.007	0.6591	2.7673	0.0051	0.0805	0.956	0.7606	0.0179	0.9822	−1.9707	2.3663	2.4017
139	38.1084	11.4441	0.0048	0.6951	2.2238	4.2243	4.2973	7.2006	0.001	0.8263	2.987	0.0072	0.0789	0.9569	0.7172	0.0312	0.8867	−5.7787	3.1073	3.0309
140	3.309	3.0373	0.0056	0.068	1.5602	1.047	2.418	0.0982	0.0013	0.1362	0.2209	4.9973	0.0746	0.9592	0.7980	0.0064	0.9022	−0.1458	7.184	1.32
141	18.6723	17.7386	0.0018	0.2548	1.0431	2.7615	4.0364	0.1311	0.001	0.8039	2.8495	2.8718	0.0794	0.9566	0.7324	0.0263	0.9304	−4.5848	2.8079	3.2407
142	16.4992	12.943	0.0034	0.224	0.45	3.1494	2.6023	0.0451	0.0057	0.551	2.9713	0.0034	0.0798	0.9564	0.7530	0.0200	0.979	−1.2742	2.4365	1.5869
143	31.0896	7.3143	0.0082	0.6678	1.7583	0.16	4.6039	0.0349	0.001	0.7046	2.8744	1.7054	0.0765	0.9582	0.7071	0.0341	0.8014	−4.3001	3.7456	2.5713
144	9.1012	8.3702	0.0094	0.3445	0.1334	1.8121	2.5142	0.0499	0.0058	0.5565	2.9917	0.0161	0.0798	0.9564	0.7606	0.0177	0.9821	−1.3033	2.4253	1.7655
145	20.611	1.6049	0.0076	0.7805	2.2648	0.2477	2.2476	0.1442	0.0068	0.6463	2.6134	0.0001	0.0804	0.9561	0.7618	0.0173	0.9814	−1.8724	2.3413	2.3573
146	18.9323	5.0089	0.0054	0.6753	0.7284	2.4478	2.975	0.0949	0.0033	0.7126	2.9809	0.085	0.0797	0.9564	0.7489	0.0213	0.9626	−2.569	2.6	2.5929
147	26.5599	2.5881	0.0062	0.0067	1.3272	0.9626	3.8688	19.6093	0.0011	0.8041	2.8072	0.0157	0.0794	0.9566	0.7374	0.0245	0.9404	−4.4711	2.7639	2.6801

Table A.2: The results of optimisations for 147 rounds of Nelder-Mead simplex algorithm for high LET IR. Columns 3 and 4 are the value of LQ parameters α_{model} and β_{model} for each run with the value of LQ parameters for the experimental data $\alpha_{exp} = 0.8$ Gy^{-1} and $\beta_{exp} = 0.01$ Gy^{-2}. Columns 5 contains the elasticity of LQ parameter α with respect to δ and p, while columns 6 contains the elasticity of LQ parameter β with respect to δ and p.

A.4.4 Estimated parameters using 1000 bootstrap survival data sets for low LET

Run	δ	α_1	α_2	p	V_{max}	K_M

1	2.000000000000097	4.881984859736194	0.001000000000476	0.911131075319700	2.999999999963492	0.000000002683233
2	3.202430663728046	3.767602742838697	0.001000000000004	0.991490326414063	2.999999999942736	0.000000000036500
3	2.000027984020099	0.027700249020744	0.001000010971177	0.488460133543588	2.939962907324357	0.058590360294186
4	2.000000000010589	4.067557628770040	0.001000000000085	0.918312459575821	2.999999999141900	0.000000000171601
5	3.045735284681504	8.881892616347475	0.001000000000003	0.890878147588777	2.999999999985956	0.000000000042231
6	2.366325488428549	18.559522207077183	0.001000000000655	0.929509479571391	2.999999999497507	0.000000000085780
7	2.000000000050447	10.670042318362542	0.001000000000121	0.945674006015738	2.999999999707775	0.000000001648892
8	2.000000000069742	1.413576073190071	0.001000000000009	0.772605378523416	2.999999999681174	0.000000000542980
9	2.000001423454121	0.027714122167783	0.001000217505602	0.844848905703739	2.999164863642831	0.106481592451970
10	2.000000000018015	9.122482703632093	0.001000000000061	0.847309981891276	2.999999999221457	0.000000000000248
11	2.000000000033571	9.165789705352474	0.001000000000001	0.964600000239884	2.999999998605476	0.000000001747478
12	2.000075560174747	0.028296036827426	0.001000828319954	0.163250798486192	0.877631134464042	3.121646570204606
13	2.000000000133902	8.374511480894205	0.001000000000003	0.958195249796683	2.999999999885896	0.000000002561415
14	2.000000000024488	8.670798947614490	0.001000000000412	0.999999999983919	2.999999999999612	0.000000000206785
15	2.000000000000730	9.240894871057773	0.001000000000127	0.886506958259417	2.999999999785863	0.000000000015266
16	2.000000000071506	4.726063579441607	0.001000000000072	0.893107932536318	2.999999999563030	0.000000000036051
17	2.676847818991433	6.512963196848577	0.001000000000037	0.921392503976073	2.999999999991776	0.000000000002018
18	2.000017206508580	0.027712626102726	0.001000524906195	0.823311960688969	2.997911068424928	0.284643316061369
19	2.000000000000192	12.959618442624155	0.001000000000236	0.802865075041855	2.999999999996524	0.000000000087924
20	2.000000000000245	1.268281356398583	0.001000000000063	0.912501222427599	2.999999999787646	0.000000000883361
21	2.000000000001861	5.936348486317896	0.001000000000017	0.881717806212269	2.999999999594976	0.000000000145290
22	2.402441466557435	6.676646923215810	0.002771721507066	0.999999999999999	0.845967129048342	0.000000000001860
23	2.000000000051419	6.117189507581812	0.001000000000004	0.867437910369327	2.999999999971567	0.000000000250310
24	2.000000000002363	15.380759963130751	0.001000000000054	0.853119077275219	2.999999999777764	0.000000000730032
25	2.000000000025223	16.279048310161052	0.001000000000102	0.845906471287120	2.999999999945745	0.000000001335258
26	2.000000000069288	4.839691941053734	0.001000000000283	0.920722483554472	2.999999998625685	0.000000011218808
27	2.000045377673660	0.027701555414115	0.001000210452576	0.211943342144396	2.893724380454259	0.054758985521767
28	2.000000000091116	8.815500083682379	0.001000000000003	0.995715874070972	2.999999999409941	0.000000000286164
29	2.000000000062800	9.247967040241839	0.001000000000160	0.809532548297195	2.999999999702042	0.000000000065327
30	2.000000000030308	5.088350750167704	0.001000000000007	0.907655050910268	2.999999999995069	0.000000000025007
31	2.000000000001268	2.415575168120930	0.001000000000121	0.815659211799896	2.999999999760929	0.000000000699905
32	3.136814364450113	0.027701465641693	0.001000300440771	0.864240676167989	2.999961941126817	0.097897209851885
33	2.000000000016184	8.275665555949674	0.001000000000020	0.972279277503988	2.999999999994718	0.000000000355730
34	2.000000000046983	20.789996459144646	0.001000000000006	0.776061208942220	2.999999998931873	0.000000000192347
35	2.000000000025393	13.003852884279514	0.001000000000017	0.874161194592666	2.999999999856187	0.000000000034174
36	2.000000000017782	7.672258449574736	0.001000000000085	0.841996043524280	2.999999999902172	0.000000000698154
37	2.000000000005896	4.508744683427340	0.001000000000158	0.861490479000873	2.999999999886752	0.000000000012197
38	2.000000000000287	3.811231260082664	0.001000000000090	0.909757275397543	2.999999999994494	0.000000000479951
39	2.790437622719732	13.342394085913849	0.001000000000002	0.922013792448272	2.999999999980450	0.000000001891956
40	2.000000000002987	2.347195672845776	0.001000000000017	0.902889068975140	2.999999999992688	0.000000001264357
41	2.209511172336413	0.027700016380258	0.001000000001435	0.573625758708209	2.999996573685777	0.000027525110765
42	2.000000000828810	2.996716697877960	0.001000000000003	0.926788941001508	2.999999999341437	0.000000000056398
43	2.000000000028452	11.061223734894767	0.002334300074118	0.999999999952724	0.293055318060166	0.000000001880502
44	2.000000000011155	7.926715615254821	0.001000000000160	0.953170878757228	2.999999999289446	0.000000000826323
45	2.000000000049839	5.421539368407112	0.001000000000087	0.963485568726754	2.999999999829007	0.000000003523331
46	2.000000000012427	7.999161276066127	0.001000000000088	0.982029199168499	2.999999999964496	0.000000002169701
47	2.000000000003740	7.551753317515957	0.001000000000423	0.929489118826691	2.999999999971522	0.000000000082135
48	2.000000000018297	7.547963479649064	0.001000000000167	0.837821371462249	2.999999999499369	0.000000000208273
49	2.650030787094623	13.198714924484705	0.001000000000113	0.900765869007292	2.999999999993930	0.000000000261179
50	2.000000000201695	7.522176861831982	0.001000000000354	0.891401040277098	2.999999999834054	0.000000000158207
51	2.000000000074545	18.471671090710284	0.001000000001071	0.883461822101022	2.999999999916476	0.000000001867166
52	2.000000000025870	6.216271364481714	0.001000000000005	0.917440604452798	2.999999999910580	0.000000000136127
53	2.000003669678318	0.027725511374719	0.001000003706174	0.748513074130766	2.990663101459295	0.708299363552511
54	2.000000000109669	6.005292868037250	0.001000000000014	0.992792544235729	2.999999999814500	0.000000000022161
55	2.000000000009035	2.241716505964421	0.001000000000197	0.865511736190807	2.999999999867243	0.000000000024555
56	2.000000000051768	7.065595543262016	0.001000000000071	0.921977264275696	2.999999999993968	0.000000000272067
57	2.000000000050717	8.917671017108807	0.001000000000004	0.870506019946231	2.999999999578169	0.000000001025672
58	2.000000000040891	15.010677489494546	0.001000000000070	0.750697319542495	2.999999999988253	0.000000000692878
59	2.481556985019386	5.877535043590273	0.001000000000006	0.850630906695364	2.999999999748994	0.000000001996237

60	2.000000000162689	10.250905408078506	0.001000000000006	0.869361945071589	2.999999998987646	0.000000000415769
61	2.000003031743442	0.027700051220890	0.001000680008230	0.180805313814657	2.929195383497405	4.086790216197586
62	2.000000000010433	2.653957012268377	0.001000000000002	0.705853079614156	2.999999999982071	0.000000001065061
63	2.828634118295906	20.669281220245153	0.001000000000000	0.929845809015708	2.999999999996337	0.000000000010226
64	2.000000000068487	8.216874395270704	0.001000000000022	0.946577990914402	2.999999999669401	0.000000000014642
65	2.902090219701100	0.110509684412430	0.001000000000278	0.999999999989769	2.999999999475418	0.000000000344634
66	2.000000000000095	3.836857603935878	0.001000000000123	0.792934684380019	2.999999999710211	0.000000000073020
67	2.000000000076969	4.302486023420753	0.001000000000057	0.953205232447713	2.999999999700020	0.000000000518478
68	2.000000000010946	12.157407529594964	0.001000000000108	0.861201206432145	2.999999999563668	0.000000000834181
69	3.230613964670987	5.536601823528168	0.001000000000085	0.999999999999751	2.999999999286983	0.000000000610642
70	3.199255111794994	12.172937672945300	0.001000000000003	0.999999999698344	2.999999999255453	0.000000000209844
71	2.000000000000084	9.889217425821474	0.001000000000048	0.861834508916600	2.999999999839689	0.000000000060012
72	2.857915925488177	14.542799793740686	0.001000000000061	0.890159494040697	2.999999999092788	0.000000008514218
73	2.000000000001371	1.674479256942205	0.001000000000196	0.853951313224819	2.999999999998998	0.000000005623876
74	2.000000000000044	8.057253899324630	0.001000000000420	0.960275640103757	2.999999999976905	0.000000001332967
75	2.000000000038978	9.833182704002395	0.001000000000073	0.804575633335032	2.999999999998802	0.000000000019705
76	2.000000000065588	6.691794975754054	0.001000000000039	0.959116797574516	2.999999999702912	0.000000001768317
77	2.000008911641490	0.028934586492991	0.001000391590385	0.626687208328209	2.997697538668510	0.000110452434464
78	2.000000000030593	5.913786020031556	0.001000000000150	0.889512007797587	2.999999999422825	0.000000000389117
79	2.443735893029715	0.027725672271759	0.001000066302494	0.847413762183664	2.996963762193316	0.142224669102769
80	2.000000000000821	15.992735421407557	0.001000000000135	0.776882314912562	2.999999999703670	0.000000005324737
81	2.000000000272913	9.443029180296371	0.001000000000045	0.853270535847858	2.999999997668442	0.000000000850386
82	2.675710132969484	7.946469512166357	0.001000000000059	0.945917065699517	2.999999999999799	0.000000003495109
83	2.000000000004318	7.518576009636849	0.001000000000003	0.835345714526223	2.999999999702941	0.000000000934460
84	2.000000000096464	0.027700000021864	0.001000000000048	0.631773975690253	2.999999999808768	0.000000000924825
85	2.000000000030616	1.315407923532462	0.001000000000045	0.758904018601156	2.999999999992659	0.000000000000808
86	2.000000000041919	9.694738462843667	0.001000000000000	0.817754663239647	2.999999999422365	0.000000000728493
87	2.000000000354166	6.636383954392657	0.001000000000000	0.841692315435258	2.999999999981197	0.000000000619344
88	2.000000000005191	3.706871042304380	0.001000000000273	0.951099439578063	2.999999999995815	0.000000000158313
89	2.000007015499376	0.027700047620277	0.001000541308722	0.278778991953512	2.999098437623654	4.773478002683310
90	2.000000000304761	10.794102310294120	0.001000000000001	0.939611233368032	2.999999999954043	0.000000000673682
91	2.772953616468278	3.599517446078853	0.001000000000037	0.983312464135865	2.999999999969559	0.000000000410967
92	2.000000000004428	8.252312177181191	0.001000000000070	0.882776123025863	2.999999999950272	0.000000002327155
93	2.000000000003639	2.332134130475294	0.001000000000004	0.870999203045545	2.999999999885784	0.000000004441280
94	2.000000000013102	3.657712149869544	0.001000000000071	0.934768435107215	2.999999999995745	0.000000000261726
95	2.000000000058703	7.639112440051216	0.001000000000179	0.806357687539041	2.999999999995748	0.000000000073029
96	2.000047344935757	0.027700006787423	0.001000177679025	0.418721210566967	2.442348258299832	3.233186456056687
97	2.000000000000475	10.922654688267341	0.001000000000377	0.809805164294083	2.999999999875143	0.000000000002030
98	2.701024479733777	10.405303553067997	0.001000000000003	0.845084251555013	2.999999999520452	0.000000000316640
99	2.000193452374492	0.027708098251869	0.001001719319648	0.736036850058660	2.989725326747873	0.573448975444485
100	2.000000000070012	7.537762208465373	0.001000000000091	0.992415198789799	2.999999999974072	0.000000001276322
101	2.000000000097894	3.791543608022019	0.001000000000113	0.935377601245417	2.999999998905896	0.000000003751564
102	2.000000000000869	10.198473116844475	0.001000000000032	0.867914785018086	2.999999999430504	0.000000002090985
103	2.000000000004784	3.446337257944690	0.001000000000009	0.798365937917195	2.999999999893057	0.000000007027188
104	2.000000000019457	3.083852556778161	0.001000000000048	0.925958890428144	2.999999999056823	0.000000002179916
105	2.000000000028064	2.657020773288890	0.001000000000109	0.805213984687562	2.999999999759426	0.000000000000352
106	2.000000000160755	7.523736242359541	0.001000000000003	0.821726991621418	2.999999999938887	0.000000000659822
107	2.000000000031021	7.474079789650080	0.001000000000005	0.939608701022194	2.999999998629490	0.000000001262878
108	2.000000000000002	8.245590032577532	0.001000000000016	0.785519561866910	2.999999999884560	0.000000001221978
109	2.000000000028602	8.080467168948543	0.001000000000073	0.867298877105206	2.999999999687772	0.000000000315968
110	2.000000000025646	11.832191106541041	0.001000000000352	0.855119585590478	2.999999999591331	0.000000000751877
111	2.000000000005873	1.620454357584758	0.001000000000175	0.811200441796444	2.999999999847002	0.000000000602712
112	2.000000000003637	7.324581707095185	0.001000000000006	0.984091065830250	2.999999999448368	0.000000002605693
113	2.000006604005675	0.027849059476912	0.001003252242043	0.576342083164206	2.971309375739042	1.314095784813935
114	2.000000000013905	5.497500369370160	0.001000000000078	0.828494235224035	2.999999999959487	0.000000000465838
115	2.000000000214423	3.616978750450438	0.001000000000097	0.864676227262701	2.999999999992743	0.000000000096089
116	2.000000000013770	3.734842058758576	0.001000000000236	0.920825368184874	2.999999999987153	0.000000000012512
117	2.000000000189219	1.250989017841732	0.001000000000035	0.928531250544251	2.999999999962419	0.000000001556245
118	2.000000000009039	13.067262414770822	0.001000000000214	0.960089437231979	2.999999999914659	0.000000000001837

119	2.000000748515689	0.027731267778590	0.001000001533799	0.808125930478187	2.997707697640413	0.000691008315450
120	2.527297807661609	18.751769788166012	0.001000000000224	0.809291501666924	2.999999999332890	0.000000000090882
121	2.000000000052649	8.546837236445551	0.001000000000041	0.908080621727608	2.999999999999846	0.000000000394665
122	2.000000000020982	2.703212314010314	0.001000000000090	0.837284164907781	2.999999998019507	0.000000000016224
123	2.000000000086035	9.498914192882230	0.001000000000073	0.734727902491360	2.999999999817537	0.000000000100150
124	2.001315910398557	0.111797857998970	0.001000639961230	0.454692334909627	0.196699706420071	0.382176070721370
125	2.000000000088587	12.874681504093751	0.001000000000084	0.973473600504037	2.999999999975960	0.000000002055668
126	2.620685289713280	0.027725270162201	0.001000004709946	0.756396235552492	2.981276338056205	0.018578838569131
127	2.000000000001025	2.107639607917602	0.001000000000064	0.995333814809553	2.999999999906416	0.000000000000623
128	2.000000000000977	4.744465213828554	0.001000000000022	0.839973458246782	2.999999999134831	0.000000000013169
129	2.000000000052345	12.795540366192458	0.001000000000012	0.861345542982484	2.999999998655837	0.000000000265877
130	2.000232871925470	0.027700921849042	0.001000770987526	0.377575356196680	2.907759975301983	4.310019783694955
131	2.000000000017559	11.522542497332125	0.001000000000031	0.940007995505151	2.999999999918225	0.000000000007224
132	3.151279021021606	15.610461093859097	0.001000000000091	0.999999999999664	2.999999999987371	0.000000000594171
133	2.000000000002799	2.065691823760293	0.001000000000024	0.894676887426583	2.999999999996024	0.000000000560275
134	2.669712777864248	3.499357048771532	0.001000000000000	0.870182219892219	2.999999999994646	0.000000004082950
135	2.000000000010043	5.421208842345743	0.001000000000225	0.867180824163366	2.999999999825052	0.000000000401336
136	2.000000000042851	0.878367739831189	0.001000000000095	0.944900379448893	2.999999998759770	0.000000000027350
137	2.000000000000795	9.060977746290625	0.001000000000033	0.883091502358860	2.999999999974151	0.000000002154205
138	2.000000000079456	7.403902878665853	0.001000000000032	0.797965851907019	2.999999999941196	0.000000000183948
139	2.555221446341659	16.054367025662714	0.001000000000043	0.999999999998388	2.999999999993107	0.000000000111368
140	2.000000000000247	9.165142880362009	0.001000000000002	0.885906635165090	2.999999999991788	0.000000000286014
141	2.000000689037877	0.027700307376936	0.001000081449818	0.774492679420835	2.999995175682916	0.152711782567870
142	2.000029288582613	0.028340117838812	0.001000341195225	0.825484262317135	2.962332201617265	0.342769169436066
143	2.000000000018934	8.253595667817356	0.001000000000294	0.819748601182620	2.999999999977795	0.000000002650234
144	2.000000000020691	9.445099448409298	0.001000000000000	0.988434158617740	2.999999999897500	0.000000001116034
145	2.000000000043456	5.330633951389092	0.001000000000123	0.964267072458909	2.999999999948800	0.000000000051383
146	2.000000000025699	20.786775345924553	0.001000000000005	0.767201189617255	2.999999999743249	0.000000000131987
147	2.000000000000532	7.742892028813832	0.001000000000014	0.806485165610753	2.999999999996514	0.000000000463521
148	2.000000000089319	2.837870890303147	0.001000000000174	0.842854815523938	2.999999999999377	0.000000000836352
149	2.000000006259443	0.027700008224706	0.001000000014848	0.832061519156339	2.999999981978044	0.000000891257208
150	2.000474953452470	0.027748152658213	0.001000043089435	0.526853137346833	2.899541680897172	1.213928755537662
151	2.000000000020390	13.436821177379503	0.001000000000029	0.958831273981178	2.999999999999962	0.000000003114546
152	2.000000000002129	6.647487792751504	0.001000000000161	0.852026009556134	2.999999998561459	0.000000001277604
153	2.000000000011868	1.503517476606589	0.001000000000020	0.919779696748324	2.999999998624374	0.000000001069760
154	2.000000000041130	10.099987198360546	0.001000000000018	0.854313749568490	2.999999999996412	0.000000000650360
155	2.000000000004567	3.759874558997467	0.001000000000096	0.860719017872759	2.999999999772190	0.000000000052593
156	3.179871178471764	12.505554185670279	0.001000000000000	0.998162245636489	2.999999996996394	0.000000004357114
157	3.179871178471764	12.505554185670279	0.001000000000000	0.998162245636489	2.999999996996394	0.000000004357114
158	2.000010597228831	0.027702667250886	0.001000013118611	0.442025533586618	2.873547888198440	0.378640468677650
159	2.000000000025151	4.490557336207933	0.001000000000000	0.837896079035029	2.999999998196452	0.000000000000588
160	2.000000000022463	9.272958994367953	0.001000000000461	0.807222807284124	2.999999999867624	0.000000000147159
161	2.000000000000819	10.149932759556071	0.001000000000115	0.918539204007946	2.999999999933776	0.000000000982813
162	2.000000000135261	7.299599968025407	0.001000000000134	0.831781050755671	2.999999998127496	0.000000000600032
163	3.017962418266800	5.639363022579323	0.001000000000060	0.960963054055620	2.999999999999994	0.000000001144102
164	2.000000000002936	10.201312721762623	0.001000000000010	0.910178783171319	2.999999999967476	0.000000002422796
165	2.000000000024370	4.441005165326167	0.001000000000406	0.909962221722487	2.999999999961990	0.000000001674527
166	2.000000001294591	15.978709182355257	0.001571963987528	0.999999999999771	0.665547272982219	0.000000000008849
167	2.000000012891043	0.027700452318521	0.001000004312745	0.721883575598394	2.999973763960709	0.000069209924795
168	2.000000000006385	13.992347048892098	0.001000000013690	0.988867355042706	0.773046274725932	4.999999446761605
169	2.000000000061007	12.264313695949012	0.001000000000014	0.872840808056514	2.999999999999607	0.000000002115840
170	2.000000000051594	7.296929746056459	0.001000000000250	0.999999999993425	2.999999999961939	0.000000000033705
171	2.000000000073522	10.113550079250567	0.001000000000044	0.798458082933615	2.999999999764122	0.000000000167268
172	2.000000000112858	8.258445018249962	0.001000000000013	0.810080315559345	2.999999999877523	0.000000000000181
173	2.000017835526125	0.028383558225122	0.001000007445480	0.632726448248830	2.981102279053291	0.028791469729170
174	2.000000000087988	8.743401004073258	0.001000000000235	0.999999999999997	2.999999999898856	0.000000000461883
175	2.000000000007915	3.148071938663809	0.001000000000212	0.835194400787473	2.999999999108918	0.000000000052079
176	2.000000543549394	0.027700289661597	0.001000004344974	0.479522835287421	2.968037348698094	0.001444000811965
177	2.000000000007693	7.893522228059494	0.001000000000271	0.980862032322713	2.999999999569432	0.000000000225169

178	2.000000000003472	8.331685182612818	0.001000000000649	0.999999999991722	2.999999999925214	0.000000000006310
179	2.000000000000006	8.032029929264454	0.001000000000036	0.832320699773492	2.999999997385978	0.000000000014078
180	2.000000000014945	3.630395475715561	0.001000000000066	0.898791180376088	2.999999999932369	0.000000001600079
181	2.000000000045171	8.994977060618819	0.001000000000018	0.999999999968672	2.999999999622915	0.000000000291608
182	2.036084474495404	7.632325526063671	0.001000000000028	0.931883400324283	2.999999999764459	0.000000000011317
183	2.548265420514787	0.037768850670950	0.001002575735660	0.816574771565792	2.925749762425001	0.099341257409249
184	2.071990878037261	17.090837293700510	0.001000000000038	0.839029030135087	0.419879365530573	0.000000090060000
185	2.000000000045530	8.645712260456858	0.001000000000002	0.843179506433033	2.999999999502731	0.000000001472408
186	2.000000000063135	10.914920708336982	0.001608686291184	0.880224689868341	2.093623998999662	0.000000000532861
187	2.000000000001810	8.511686213567241	0.001000000000010	0.818636781072606	2.999999999893325	0.000000001485745
188	2.680460563010242	19.634998951350529	0.001000000000006	0.952319472212218	2.999999999969282	0.000000000725020
189	2.000000000092908	7.791984600165745	0.001000000000120	0.999999999993889	2.999999996352800	0.000000000000630
190	2.000000000059975	7.368771302800265	0.001000000000019	0.858243177679114	2.999999999967333	0.000000002666041
191	2.000000000039364	14.451761147264259	0.001000000000168	0.811653925852335	2.999999998847038	0.000000000572735
192	2.000000000001481	7.127050756508685	0.001000000000023	0.804942773278677	2.999999999103169	0.000000000236461
193	2.763941135511376	9.148332880157559	0.001000000000136	0.890322167517727	2.999999999999606	0.000000000049532
194	2.000000000000230	20.505914198575141	0.001000000000030	0.680184925374032	0.159635914200821	0.000000047374202
195	2.000000000005963	9.595968351056190	0.001000000000177	0.822248429015700	2.999999999999799	0.000000000534310
196	2.000002398937956	0.027703792416947	0.001000061485124	0.836956435500976	2.999648853597778	0.050950796886563
197	2.000000000002538	9.740066951496164	0.001000000000001	0.974476362816870	2.999999999649035	0.000000000039657
198	2.000000000085681	7.652985651624710	0.001000000000036	0.999999999999878	2.999999999446006	0.000000000205315
199	2.000000000016055	4.161340823353601	0.001000000000038	0.896373347160440	2.999999999990050	0.000000000123048
200	2.443735893029715	0.027725672271759	0.001000066302494	0.847413762183664	2.996963762193316	0.142224669102769
201	2.000000000033624	12.338867773625536	0.001000000000226	0.901947361511115	2.999999999953268	0.000000000352599
202	3.152017350729908	0.445962465216080	0.001000000000048	0.999999999997069	2.999999999998197	0.000000000620148
203	2.000000000037710	14.518952899196650	0.001000000000102	0.872029819099651	2.999999999877957	0.000000000560881
204	2.000015543345742	0.067119414448809	0.001001233203390	0.341656077662973	0.196452201986259	0.036760882451506
205	2.898596128752612	7.618684657306866	0.001000000000029	0.999999999994567	2.999999999258236	0.000000000026323
206	2.000000000000120	7.916762897214863	0.001000000000001	0.980503349865132	2.999999999999961	0.000000003280367
207	2.000000000000196	10.913252026092515	0.001000000000002	0.841107933689641	2.999999999352710	0.000000000093102
208	2.000000000029184	2.578483380727449	0.001000000000037	0.838473694072622	2.999999998011524	0.000000001142045
209	2.000106654163110	0.031862566700863	0.001000442668625	0.616597424603421	2.975468234831744	3.479085142397773
210	2.000000000006109	9.440507445840343	0.001000000000071	0.956800981603031	2.999999999835697	0.000000003018422
211	2.000000000000616	7.069406879192483	0.001000000000113	0.813288654485866	2.999999998859400	0.000000000087733
212	2.000000000001603	2.476600587875064	0.001000000000007	0.813439175779269	2.999999998915384	0.000000000248165
213	2.000000000000034	19.023290416408539	0.001000000000003	0.915743316514438	2.999999999998868	0.000000000315852
214	2.000000000070060	2.638947787082222	0.001000000000040	0.795397490485122	2.999999999747464	0.000000001036670
215	2.000000072923230	0.027702780328434	0.001000007513972	0.905077072970541	2.999916500647664	0.003158137681996
216	2.000000000030612	8.195713798496268	0.001000000000801	0.881721589700214	2.999999999999309	0.000000000078186
217	2.000000000015878	14.983647097292202	0.001000000000074	0.942316112555886	2.999999999597723	0.000000000237423
218	2.000000000012193	11.868209165723144	0.001000000000103	0.872765931273993	2.999999999242331	0.000000000724453
219	2.000000000071680	2.514266644425777	0.001000000000003	0.921081073286154	2.999999999737987	0.000000001219033
220	2.000000000056442	1.684936850693366	0.001000000000039	0.776017670529475	2.999999999999760	0.000000000042016
221	2.000000000012007	7.536180694390785	0.001000000000001	0.964786225519135	2.999999999934024	0.000000000229424
222	2.000000000007946	15.557985629451407	0.001000000000024	0.871854623891867	2.999999999865006	0.000000000101373
223	2.002981033951802	0.027700146743683	0.001000186776420	0.434559401825857	2.982165583858567	0.703216379746141
224	2.000000000004717	8.111954002057216	0.001000000000040	0.926626483741865	2.999999999848647	0.000000000154212
225	2.378049840161784	16.611848501451579	0.001000000000000	0.812422619483977	2.999999999992822	0.000000000071108
226	2.000002955142678	0.027782679322798	0.001000000170588	0.657670180839497	2.978646920979966	0.170274169825298
227	3.214585364012005	20.505178553188696	0.001000000000007	0.999999999999291	2.999999999402866	0.000000000294895
228	2.000000000044346	2.180568227920128	0.001000000000000	0.908994171855161	2.999999999777934	0.000000000117014
229	2.000000000015120	18.292850139198080	0.001000000000028	0.763068650117365	2.999999999933620	0.000000000095675
230	2.000000000193599	1.493695941349627	0.001000000000958	0.696614715526299	2.999999999451875	0.000000000117709
231	2.000000000005818	2.477088334708323	0.001000000000004	0.917495746332297	2.999999999899472	0.000000000131893
232	2.000000000043935	4.774374036843981	0.001000000000149	0.943238917440200	2.999999999570941	0.000000000001129
233	2.000000000017365	5.853908845554432	0.001000000000117	0.876330582641799	2.999999999983344	0.000000000016493
234	2.000000000004888	15.926896195518468	0.001000000000054	0.930664051357480	2.999999999586610	0.000000000005657
235	2.000000000086906	8.253394582389882	0.001000000000081	0.930145198723611	2.999999999899287	0.000000000025967
236	2.280821155870536	0.991543055340290	0.001000000000123	0.806923424894904	2.999999999561832	0.000000000011749

237	2.000000000046346	2.331829582090113	0.001000000000001	0.943767490430247	2.999999999999386	0.000000002117725
238	2.000000000000445	19.240931051019651	0.001000000000002	0.916906041103218	2.999999999909760	0.000000000058630
239	2.000000001197585	0.027700004570288	0.001000000000668	0.720208064211016	2.999999970804824	0.000000318474707
240	2.000000000000093	6.871598488278184	0.001000000000008	0.844502550512579	2.999999999947565	0.000000000393926
241	2.000000000097284	13.846330220469317	0.001000000000037	0.828440638402214	2.999999999962242	0.000000000421587
242	2.000000000001848	4.147254153148742	0.001000000000017	0.835257830838055	2.999999999781696	0.000000004801844
243	2.000000875263488	0.027715319145092	0.001000545511800	0.753481254764979	2.992043688041257	0.082569452851634
244	2.000000012269828	0.027722518417898	0.001000019796601	0.934049596178244	2.999817372762487	0.018933771327485
245	2.000000000007976	1.475578106635135	0.001000000000012	0.907852295278860	2.999999999492002	0.000000000234719
246	2.753912924324322	17.933101412514137	0.001000000000069	0.895286259619525	2.999999999955801	0.000000000589492
247	2.000000000007313	11.136731140335534	0.001000000000206	0.839547722029244	2.999999999682076	0.000000000647922
248	3.082210560066276	4.550459248638123	0.001000000000094	0.952050717160349	2.999999999363623	0.000000000262012
249	3.209759388587379	8.583978177998430	0.001000000000001	0.999999999870578	2.999999999926247	0.000000000485746
250	2.839953732126288	1.389398709979975	0.001000000000011	0.999999999976521	2.999999999521277	0.000000001056138
251	2.000000000066310	1.435203378251756	0.001000000000041	0.942548152026765	2.999999999366178	0.000000000678759
252	2.398281851176041	12.544923208232124	0.001000000000335	0.965392218022557	2.999999998657311	0.000000000160846
253	2.000000000033375	8.726512023958996	0.001000000000158	0.999999999984231	2.999999999955477	0.000000000189311
254	2.000000000014222	1.174446010502382	0.001000000000093	0.887792597333493	2.999999999995248	0.000000000744934
255	2.000000000000447	6.034695706453269	0.001000000000146	0.894119843064044	2.999999999801807	0.000000000009974
256	2.006467814519240	0.038212489815792	0.001000962330991	0.239481728435064	0.285154197513128	0.011980256507358
257	2.000000007573118	0.027724116985075	0.001000051560246	0.914418918200203	2.996922294168376	0.004057955666627
258	2.000000000008297	3.035376351367785	0.001000000000134	0.944248908999862	2.999999997831250	0.000000000458734
259	2.000000000002295	9.035404910836286	0.001000000000071	0.836099290363369	2.999999999879807	0.000000000269128
260	2.772953616468278	3.599517446078853	0.001000000000037	0.983312464135865	2.999999999969559	0.000000000410967
261	2.000000000035932	2.802736014359758	0.001000000000322	0.838234172973337	2.999999999971771	0.000000000003852
262	2.019975477151374	0.116483532045749	0.001000167647433	0.544983377120195	0.369570593677081	0.003338495000128
263	3.072533582595052	13.736779752245980	0.001000000000202	0.952336295641202	2.999999999994371	0.000000000001284
264	2.000000000000169	6.697043169408555	0.001000000000012	0.985857205585788	2.999999999740276	0.000000001427924
265	3.206439568309612	0.325691839097990	0.001000000000002	0.999999999999129	2.999999999472450	0.000000001667639
266	2.000051670135789	0.028521590626764	0.001000175222758	0.586832830134164	2.999297166100074	0.002940573655366
267	2.000000000036772	4.323168639701740	0.001000000000025	0.935496249507035	2.999999998948554	0.000000000762045
268	3.060040759796541	2.983330670518756	0.001000000000206	0.957060243458932	2.999999995743491	0.000000009557795
269	3.183694500461031	5.782137724530517	0.001000000000256	0.999999999999995	2.999999999221181	0.000000000572523
270	2.000000000014203	7.304356116921033	0.001000000000009	0.999999999994118	2.999999999922496	0.000000000016116
271	2.593750731738681	0.029412385083257	0.001003505088317	0.697647618527767	2.967631205106792	1.417642428157548
272	2.000000000000549	9.294820841283038	0.001000000000016	0.999373507623920	2.999999998842967	0.000000000441233
273	2.000000000000006	1.689890293205769	0.001000000000147	0.933663908129499	2.999999999913399	0.000000003794029
274	2.218443942467125	6.878006784468410	0.002105139090745	0.870643741612865	2.012365611864316	0.000000000920816
275	2.000007866920191	0.027702425527048	0.001001102631526	0.725014993936191	2.971802612672124	0.011479663585968
276	2.000000000024630	13.448212059759223	0.001000000000004	0.877599237977752	2.999999999945592	0.000000000000051
277	2.000000000046834	2.655502472816534	0.001000000000129	0.739192599722104	2.999999999991924	0.000000000263885
278	2.000000000010916	3.581042714076709	0.001000000000099	0.911534873351581	2.999999999994674	0.000000000392974
279	2.000000000000029	7.369047255142767	0.001000000000044	0.820909347720091	2.999999999398731	0.000000000006363
280	2.000000000011969	2.561836955522597	0.001000000000018	0.913557752130044	2.999999999998282	0.000000000966008
281	2.000006713546759	0.027939967120744	0.001002395277571	0.717621197777842	2.976917733349370	0.742717046283418
282	2.000000000939961	2.182738819322616	0.001000000000120	0.786396023939115	2.999999999891547	0.000000000876502
283	2.000000000057311	7.779853289682697	0.001000000000017	0.798261852449472	2.999999999859116	0.000000000009074
284	2.000000000043123	6.084093277180500	0.001000000000000	0.986486179883017	2.999999999918150	0.000000000310327
285	2.000000000003569	8.018119020679714	0.001000000000118	0.977431786707768	2.999999999952294	0.000000000060772
286	2.000000000000439	11.789952857453443	0.001000000000003	0.746100218818984	2.999999999556793	0.000000002319970
287	2.000000000000012	3.476769337377554	0.001000000000001	0.959244571011386	2.999999998950827	0.000000000392790
288	2.000000000020535	12.772321984059307	0.001000000000016	0.854805505423121	2.999999999874244	0.000000000270325
289	2.000000000003021	6.347661865040727	0.001000000000358	0.925291625079987	2.999999999992746	0.000000000017922
290	2.000000000007984	13.742219350386925	0.001000000000190	0.818622852638358	2.999999999177694	0.000000000042879
291	2.000264432114564	0.027715361488184	0.001000613580184	0.382201863279347	2.940292934915417	4.022949374693742
292	2.405960170625866	8.278777052845758	0.001000000000025	0.908595103428220	2.999999999484102	0.000000000174609
293	2.000000000004636	4.945114358561581	0.001000000000000	0.677385726749746	2.999999999954533	0.000000000042232
294	2.000000000220755	6.561398164559672	0.001000000000001	0.915779254207041	2.999999999838454	0.000000001329300
295	2.000000000081559	2.298790525741214	0.001000000000060	0.927343122318276	2.999999999913531	0.000000001313047

296	2.000000000094553	2.922706653288552	0.001000000000261	0.851402792589266	2.999999998990314	0.000000007726788
297	2.000000000000124	4.914392008478097	0.001000000000198	0.904132724030852	2.999999998795081	0.000000000669008
298	2.000000000007645	9.365736009176947	0.001000000000267	0.877924002224588	2.999999998776421	0.000000000477040
299	2.000000000003033	8.600939197906406	0.001000000000084	0.950137988916714	2.999999999943686	0.000000000205650
300	2.000000000074961	8.048827101761836	0.001000000000186	0.961719632111829	2.999999999996762	0.000000000802554
301	2.000000000002841	9.092859159069743	0.001000000000009	0.932560990895270	2.999999999913486	0.000000000598288
302	3.226829784213418	11.048830699360309	0.001000000000112	0.999999999986111	2.999999999867807	0.000000000483760
303	3.233302502744712	0.720067646179020	0.001000000000048	0.999999999907318	2.999999999996590	0.000000000152769
304	2.002104363736391	0.080198352662537	0.001002697622664	0.613492315753945	2.997499438798374	1.933626476258933
305	2.000001187990166	0.027705722547364	0.001000008259820	0.860585768259656	2.999997222968106	0.000021506975688
306	2.000000000011228	6.526007122452424	0.001000000000059	0.975395620714527	2.999999999953926	0.000000006479228
307	2.000000000205285	3.306271218669032	0.001000000000000	0.788277632975636	2.999999999190816	0.000000000267471
308	2.000000000002852	15.140394756496358	0.001000000000209	0.917313595233460	2.999999999595312	0.000000000921621
309	2.395597761502384	4.974333071492838	0.001000000000001	0.926588538433043	2.999999998126133	0.000000009399738
310	2.000083537249468	0.027762007353273	0.001000375220123	0.788466799441681	2.927775045512939	0.427828351272822
311	2.000000000015892	2.618596924147673	0.001000000000042	0.957312646081437	2.999999999969504	0.000000000004318
312	2.000000000002487	20.634468839856918	0.001000000000015	0.769514604004526	2.999999999999815	0.000000000068990
313	2.000000000003515	3.255157910685340	0.001000000000150	0.800796961092368	2.999999999903630	0.000000000002982
314	2.000000000000034	12.058428858703449	0.001000000000092	0.872081717502057	2.999999999922656	0.000000002070238
315	3.119947906811647	8.518907896209781	0.001000000000111	0.922241546316027	2.999999999419329	0.000000000005153
316	2.000000000014000	3.507834411782622	0.001000000000002	0.924348530966310	2.999999999846134	0.000000000010171
317	2.000000000000798	1.156093811348558	0.001000000001163	0.855824727165220	2.999999999998866	0.000000000188046
318	2.000000000001863	4.480722272066942	0.001000000000093	0.703282120962882	2.999999999947790	0.000000001465573
319	2.000000000002527	2.648001493970057	0.001000000000260	0.913516563189115	2.999999999788130	0.000000001373046
320	2.000000000045237	3.691084036811545	0.001000000000007	0.914768009605017	2.999999999678256	0.000000000063994
321	2.000000000081918	15.160112919744613	0.001000000000065	0.786927274670731	2.999999999427081	0.000000000468520
322	2.000000000014538	6.962917947826061	0.001000000000037	0.754020052419815	2.999999998343078	0.000000001838720
323	2.000000000003462	2.838440981667564	0.001000000000019	0.908049451403748	2.999999999541613	0.000000000002217
324	2.000000000002232	15.121501453973977	0.001000000000083	0.863022958238666	2.999999999835730	0.000000000037780
325	2.000000000054027	4.843781302807237	0.001000000000168	0.812606641770921	2.999999999330984	0.000000000106010
326	2.000000000017285	11.004935738788310	0.001000000000126	0.845380895890373	2.999999999964432	0.000000000238745
327	2.527550582702559	11.774200253315502	0.001000000000039	0.999999999986144	2.999999999783083	0.000000000110389
328	2.000000000000224	7.520053310919357	0.001000000000002	0.804334457212603	2.999999999972742	0.000000000116160
329	2.000000000014701	2.886255039601198	0.001000000000135	0.843741123281393	2.999999999944142	0.000000000263047
330	2.000032493159582	0.027701729643404	0.001000171346739	0.608158169947735	2.996143159193458	0.280282962313964
331	2.000000000000023	5.784098652586721	0.001000000000000	0.899862329295866	2.999999999968383	0.000000001283697
332	2.000000000012769	19.160216909402816	0.001000000000163	0.891286636034633	2.999999999330288	0.000000000462931
333	2.113988249749977	10.552798522536657	0.001000000000165	0.999999999994990	2.999999999959642	0.000000000007506
334	2.004346354329841	0.027703386729230	0.001000916625087	0.440229811539359	2.846156055441899	1.690858898156767
335	2.000000000004736	0.027700000014863	0.001000000008442	0.410161119005851	2.995867057015128	0.000001148531948
336	2.000000000007124	3.510655564366111	0.001000000000334	0.937734319604285	2.999999999942133	0.000000000056751
337	2.000000000052637	3.362443570169534	0.001000000000064	0.785430687724930	2.999999999306628	0.000000000320546
338	2.000000000024199	8.222360622936517	0.001000000000045	0.875272936435730	2.999999999943865	0.000000000067612
339	2.785462867631414	9.352596298654335	0.001000000000046	0.905340835344620	2.999999999918912	0.000000000939529
340	2.000000000159344	9.851105946657651	0.001000000001009	0.819973020219618	2.999999999913460	0.000000005843481
341	2.000000007001078	0.027700056580042	0.001000000564826	0.524713299827537	2.999997380957171	0.000000036271709
342	2.000000000214039	12.010042697466291	0.001000000000250	0.818013882722308	2.999999999941767	0.000000003825152
343	2.000000000001713	1.588962519700264	0.001000000000149	0.843549992838988	2.999999999534881	0.000000000025753
344	2.000000000003027	13.182705004142766	0.001000000000068	0.845826709052701	2.999999999868346	0.000000000435761
345	2.000000000096533	3.721035534810335	0.001000000000056	0.905125586643640	2.999999999834330	0.000000001396497
346	3.441488379131348	1.253726562214529	0.001000000000052	0.999999999999808	2.999999999950362	0.000000001622149
347	2.000000000064553	7.398688652370217	0.001000000000098	0.888801122456054	2.999999999568013	0.000000000000826
348	2.309145564860459	10.526579129787562	0.001000000000014	0.863193293256894	2.999999999984084	0.000000002592274
349	2.000000000004698	0.799805109783903	0.001000000000203	0.789095288543548	2.999999995489207	0.000000211430191
350	2.000000000000059	18.686416700191216	0.001000000000111	0.773295141489634	2.999999999908573	0.000000001685791
351	2.000000000008722	14.465372224642584	0.001000000000007	0.882469624898132	2.999999999255870	0.000000000057300
352	2.000000000052664	5.401323461267801	0.001000000000042	0.801894429291308	2.999999999912381	0.000000000008783
353	2.000000130921805	0.027702943610321	0.001000241613265	0.588447555725227	2.999801455336001	0.217773788067512
354	2.000000000031365	6.798076714068332	0.001000000000112	0.850165713280753	2.999999999765378	0.000000000031470

355	2.000041745218125	0.027704826900011	0.001000381264600	0.834041466358913	2.999583395521836	0.218130228056488
356	2.000000000018038	6.879848798547506	0.001000000000338	0.851056561667859	2.999999999505434	0.000000000001248
357	2.000000000010237	11.194764116265073	0.001000000000022	0.924577999846556	2.999999999993053	0.000000002017271
358	3.228919991753541	8.827090595977436	0.001000000000015	0.999999999999995	2.999999999955573	0.000000000008121
359	2.000000000075678	2.058056391332767	0.001000000000237	0.847089922297367	2.999999999998117	0.000000000106677
360	2.000000000335586	8.326237972584469	0.001000000000129	0.820050199201729	2.999999999996597	0.000000000690818
361	2.000000000017835	5.645469221119379	0.001000000000009	0.801906026926002	2.999999999904721	0.000000000249636
362	2.000000000241786	3.271315506407759	0.001000000000105	0.859985611707032	2.999999999862745	0.000000000002425
363	2.000000000003966	13.499236630401832	0.001000000000014	0.770221366518133	2.999999999999623	0.000000000943211
364	2.000000000001620	5.836861777996531	0.001000000000031	0.992136783391150	2.999999999820067	0.000000002349715
365	2.000000000024362	7.227075557392342	0.001000000000083	0.871770603294209	2.999999999190683	0.000000000732761
366	2.166682216529335	6.798586107870737	0.001000000000478	0.995102584014037	2.999999999923253	0.000000002031125
367	2.000000000003137	10.456625243218125	0.001000000000064	0.861137997481933	2.999999999980066	0.000000000088850
368	2.000000000041661	4.927708273694371	0.001000000000213	0.964337193567284	2.999999999913696	0.000000000004228
369	2.000000004560614	0.027700089624496	0.001000004151809	0.717802397251579	2.999997957601330	0.002529043256854
370	2.000000000224168	3.473712195156055	0.001000000000011	0.859047451300302	2.999999999991776	0.000000001337299
371	2.000000000013846	7.634413265858691	0.001000000000000	0.999999999994665	2.999999999847234	0.000000000935752
372	2.000000000021733	3.985119441149247	0.001000000000005	0.934941398575979	2.999999999773839	0.000000000071114
373	2.000000000155846	4.757134479638834	0.001000000000261	0.709003801561539	2.999999999994385	0.000000000503668
374	2.000000000080240	18.810370520421149	0.001000000000028	0.885913995571118	2.999999999798421	0.000000000195111
375	2.000465433508643	0.027797937092044	0.001000517040472	0.396423477364910	2.869608698131216	0.007522738468154
376	2.000000000027524	19.914350690259173	0.001000000000155	0.759536394737223	2.999999999901709	0.000000004946887
377	2.000000000050740	2.573144250060545	0.001000000000019	0.800147323564122	2.999999999869458	0.000000000011473
378	2.000000000007467	18.768075401133817	0.001000000000012	0.759763782173017	2.999999999819517	0.000000000466499
379	2.000000000000019	5.901414293833285	0.001000000000082	0.836148908145315	2.999999999760183	0.000000001287411
380	2.000000000118780	2.027953529519166	0.001000000000000	0.921163280505106	2.999999999678826	0.000000000015349
381	2.000000000041866	3.019623199815614	0.001000000000101	0.933171537351429	2.999999999870016	0.000000000000010
382	2.000000000049293	5.957963517352790	0.001000000000028	0.652161629944559	2.999999998552749	0.000000002891718
383	2.623484747921095	12.710120262938771	0.001000000000268	0.924807523123119	2.999999999877224	0.000000000043616
384	2.000405314488290	0.027706116529228	0.001000298880810	0.342707702559315	2.988316079465976	0.367537012135558
385	2.000000000008809	12.945406418995294	0.001000000000034	0.782894675143468	2.999999999993239	0.000000000523731
386	2.000000000235834	11.354710327423069	0.001000000000163	0.818818293816453	2.999999999603794	0.000000014728377
387	2.070428257276244	15.548010213109782	0.001151175692714	0.732306830362518	0.655225763132754	0.427040231613668
388	2.000000000006731	7.277655219471880	0.001000000000062	0.854498558221205	2.999999999999884	0.000000000776298
389	2.000000000091728	3.392335109919889	0.001000000000005	0.885054377912519	2.999999999818809	0.000000000000205
390	2.000000000014937	6.792250567227083	0.001000000000014	0.992678573992630	2.999999999146712	0.000000000000336
391	2.000000101649260	0.027700563533232	0.001000034068016	0.781112543053434	2.999330427445074	0.005391812894385
392	2.000000000004415	3.324149753088201	0.001000000000185	0.850440377653020	2.999999999189891	0.000000000098506
393	2.000000000088988	5.905938277154190	0.001000000000564	0.838524247969668	2.999999999405604	0.000000001092804
394	2.000000000005056	14.024717779305051	0.001000000000053	0.727417506435570	2.999999999142072	0.000000002408670
395	2.000000000033525	16.013975653205154	0.001000000000139	0.738940098100685	2.999999999902499	0.000000001057585
396	2.000000000002348	1.735728643630921	0.001000000000018	0.969507304922564	2.999999999982141	0.000000002257592
397	2.000000000010418	14.269590500836916	0.001000000000089	0.786646398631464	2.999999999986430	0.000000000094457
398	2.000000000005166	2.511028911007213	0.001000000000201	0.708457104168304	2.999999999940097	0.000000001626064
399	2.000000000005105	2.008371682064118	0.001000000000000	0.981181328801612	2.999999999879734	0.000000000058984
400	2.542056486588994	7.357790907326837	0.001000000000151	0.999999999996095	2.999999999678845	0.000000000060947
401	2.000000000006592	17.157290501473167	0.001000000045550	0.920653626713002	0.409982152821171	4.999999182417775
402	2.000000000005710	3.407140771667662	0.001000000000033	0.942294651753074	2.999999999837232	0.000000000724703
403	2.000000000001055	19.408425835503536	0.001000000000012	0.907283974543571	2.999999999746168	0.000000000797858
404	2.000000000000234	7.833566284118434	0.001000000000768	0.899736340927762	2.999999999704924	0.000000000144461
405	2.000061196209197	0.027701484237753	0.001000547053129	0.570420914268738	2.987182057654405	0.000017023269197
406	2.000000000000646	1.857152786871769	0.001000000000064	0.902261534109045	2.999999999718613	0.000000001033480
407	2.000397341483006	0.050388389126438	0.001000047029807	0.759802268854949	2.956111221085475	0.535760108285073
408	2.000000000001108	16.543220598471230	0.001000000000062	0.775715867461218	2.999999999989804	0.000000000483167
409	2.000000000000690	20.782052169589576	0.001000000000066	0.728143486082288	2.999999999970020	0.000000001574878
410	2.000000000027024	4.350942356519185	0.001000000000140	0.936855549350674	2.999999999822432	0.000000000718649
411	3.203836724323690	0.139832649121551	0.001000000000014	0.999999999999667	2.999999999998836	0.000000000663981
412	3.246411194645379	9.864410535016615	0.001000000000035	0.987044196618865	2.999999999999528	0.000000002394344
413	2.000000000004889	20.536477905426789	0.001000000000004	0.818277898664942	2.999999999792898	0.000000000070173

414	2.000000000052668	9.032402485479892	0.001000000000001	0.902813746963732	2.999999999466048	0.000000000155964
415	2.000000000061212	12.837394877403138	0.001000000000187	0.821370373509541	2.999999999669619	0.000000004086694
416	2.000000000029675	12.816139593601966	0.001000000000122	0.856655497329406	2.999999999820610	0.000000000040396
417	2.000000000007265	5.921408440932922	0.001000000000000	0.980954501061368	2.999999999908228	0.000000000398024
418	2.571184284740609	7.718528178124392	0.001000000000006	0.864673627062957	2.999999999980779	0.000000001548786
419	2.000000000001051	5.733754236268296	0.001000000000085	0.892406458237319	2.999999999390633	0.000000000334361
420	2.000000000018654	3.585819944392202	0.001000000000111	0.955237450459114	2.999999999844459	0.000000003065942
421	2.000000001034852	0.027700000000607	0.001000000000409	0.918662199043699	2.999999999969663	0.000000001904759
422	2.599420274691603	2.077990097893399	0.001000000000004	0.877745005342221	2.999999999755935	0.000000000047344
423	2.000000000150159	11.467715388445017	0.001000000000265	0.880807691410818	2.999999999472319	0.000000027592077
424	2.000000000054662	8.365464418971623	0.001000000000218	0.923761014832685	2.999999998932529	0.000000001128595
425	2.000000000000974	3.362218254587100	0.001000000000025	0.945743003717175	2.999999999939552	0.000000000041802
426	2.000000000010969	6.621847875113085	0.001000000000024	0.799376552659448	2.999999999991105	0.000000003466017
427	2.134574585535819	11.059732190395176	0.001000000000484	0.886356065722649	2.999999999811403	0.000000000008593
428	2.000000000012037	0.027700000428524	0.001000000000075	0.677708814952111	2.999999997816810	0.000000003761116
429	2.915195324606937	20.012363101556680	0.001000000000124	0.849444650728435	2.999999999495637	0.000000000784875
430	2.000000000021172	17.756263551245127	0.001000000000011	0.951466287083174	2.999999997760554	0.000000001094893
431	2.000000000070803	20.498408496637701	0.001000000000078	0.942048022427066	2.999999999253972	0.000000000040437
432	2.000000018134849	5.348109717024117	0.001000000463338	0.858844247974835	2.999998065251184	0.000073623908134
433	2.000000000020677	5.171047210048119	0.001000000000000	0.979311575432256	2.999999999989050	0.000000000310785
434	2.000022904450582	0.027733226120232	0.001000073239392	0.433788137485385	2.918917710369947	0.000947386946477
435	2.000000000065185	2.264661070997749	0.001000000000010	0.886683243742200	2.999999999749129	0.000000000037312
436	2.879590713315969	0.143654856702584	0.001000000000004	0.999999999999278	2.999999999937145	0.000000000015912
437	3.246745971685696	0.027700805142066	0.001000001060459	0.917948542211817	2.999987512538068	0.000125536215758
438	3.197156138316332	15.343029533370526	0.001000000000172	0.985502958626753	2.999999997419520	0.000000003116260
439	2.306947833620995	8.744881698067994	0.003258684208683	0.841394919871849	1.319141591109487	0.000000059237830
440	2.677670278736822	13.387672007778061	0.001000000000133	0.855999430895723	2.999999999991747	0.000000000528812
441	2.118688653967289	10.190322330240571	0.003277972867834	0.839223457580010	2.636684796123324	0.000000000115686
442	2.001020539666103	0.027776787248057	0.001000584968577	0.512354361244037	2.991105956759740	0.003944681011001
443	2.000000000025014	5.757526335485676	0.001000000000112	0.845018602876068	2.999999999947215	0.000000000978710
444	2.000000000000502	8.360553695199572	0.001000000000002	0.813297593934993	2.999999998689296	0.000000000636315
445	2.000000000180755	1.316428263652821	0.001000000000062	0.811142494977024	2.999999999949371	0.000000001148849
446	2.000000000024670	9.861222917525527	0.001000000000004	0.889345801949110	2.999999999813740	0.000000000623120
447	2.000000000039548	8.237416692910456	0.001000000000691	0.902296522293014	2.999999999761114	0.000000000249903
448	2.243075072352712	8.950628375290179	0.001000000000000	0.856889881207218	2.999999999617129	0.000000000418987
449	2.000000000026013	5.255849260283995	0.001000000000461	0.928790362921703	2.999999999985504	0.000000000110264
450	2.000000000034687	3.574678776783778	0.001000000000038	0.824986830608165	2.999999999997793	0.000000000168754
451	2.000000000000106	6.069189511467803	0.001000000000161	0.945197918611715	2.999999999457047	0.000000000146033
452	3.104033890295842	8.628651518122132	0.001000000000821	0.964575995909526	2.999999999979872	0.000000003064146
453	2.000000000029819	5.565944661190832	0.001000000000054	0.789594200795181	2.999999999659679	0.000000000653141
454	2.000000000023429	5.583425590451076	0.001000000000010	0.981570910625470	2.999999999513875	0.000000000083594
455	2.000000000026427	1.981861676234635	0.001000000000179	0.852544939193263	2.999999999951802	0.000000000415296
456	2.000000000014542	7.692528907042878	0.001000000000139	0.787789359735597	2.999999999976338	0.000000000064905
457	2.000000000005204	9.786108259548350	0.001000000000001	0.738653179344284	2.999999999072140	0.000000001769085
458	2.000000000043328	5.153130853749879	0.001000000000057	0.838708390876034	2.999999999444853	0.000000001768912
459	2.000313938798723	0.027854968545153	0.001000156456404	0.506318192990368	2.868143308587945	1.739348983818272
460	2.000000000471648	5.926789148356602	0.001000000000236	0.775244959987741	2.999999999923654	0.000000000030152
461	2.000000000172137	14.134510211805011	0.001000000000000	0.929833913231057	2.999999999834055	0.000000000001442
462	2.000000000057033	8.611301942950563	0.001000000000036	0.869269312830036	2.999999999969513	0.000000000025491
463	2.000000000000028	20.220864417252063	0.001000000000000	0.864885797299368	2.999999999973428	0.000000000002086
464	2.000000000038079	2.325196343941789	0.001000000000138	0.850780088590406	2.999999999796839	0.000000000047932
465	2.000000000000190	7.488457648396878	0.001000000000007	0.960706793632535	2.999999999554039	0.000000000880112
466	2.774375183863590	15.265950726760364	0.001000000000209	0.977454372218700	2.999999999421862	0.000000015302476
467	2.000000000002439	20.513037411384310	0.001000000000006	0.856196410791856	2.999999999987543	0.000000000623221
468	2.000000618733266	0.027709308935041	0.001000013644453	0.621243461269500	2.988008402215338	0.311982642011669
469	2.000000000003997	8.635252000951320	0.001000000000025	0.825247027658837	2.999999999825857	0.000000000851624
470	2.000000000000943	3.816302895343680	0.001000000000029	0.799707174394717	2.999999999777946	0.000000001003629
471	2.000000000001557	5.832062674925086	0.001000000000349	0.902318202945022	2.999999999802820	0.000000001785360
472	2.000020454034843	0.027700710014357	0.001000016444194	0.427883041780828	2.999937232798752	0.000945535930417

473	2.000000000015241	9.251584394563103	0.001000000000018	0.808996289779354	2.999999999941720	0.000000001264212
474	2.000000000006271	12.850774329193911	0.001000000000000	0.896295253792852	2.999999999995110	0.000000001188204
475	2.000000000000059	11.270915562039821	0.001000000000003	0.964347893679194	2.999999999924794	0.000000000012298
476	2.000000000226581	17.820123578833318	0.001000000016818	0.999999975521759	0.136547685886385	0.000020997370316
477	2.000000000030863	6.409978171973528	0.001000000000384	0.864422861472763	2.999999999469995	0.000000001733316
478	2.000000000019506	8.739974106543444	0.001000000000021	0.967956542696454	2.999999998969498	0.000000001187972
479	2.000000000001557	13.799840934845667	0.001000000000003	0.960647105419761	2.999999999971129	0.000000000113704
480	2.743171734050642	15.284794844543836	0.001000000000203	0.972803010601229	2.999999999947129	0.000000000320726
481	2.000000000000015	7.369853990629737	0.001000000000257	0.855608265974225	2.999999999992609	0.000000001027377
482	2.000000000126614	16.326384179723092	0.001000000000190	0.777407995068367	2.999999999996738	0.000000000711768
483	2.000000000030125	2.032176827927144	0.001000000000008	0.905478583256117	2.999999999597478	0.000000000721808
484	2.000000000016038	15.213217842089804	0.001000000000118	0.846676915774989	2.999999999999602	0.000000000229837
485	2.000000000224502	5.953437615584643	0.001000000000131	0.981649248393929	2.999999999044316	0.000000004130675
486	2.000000000028463	7.840925789325385	0.001000000000007	0.881965507719634	2.999999998399562	0.000000003413666
487	2.000000000129713	7.847371254594606	0.001000000000324	0.882303407702586	2.999999999966770	0.000000000445655
488	2.000034708747070	0.027700329656383	0.001000012839940	0.322329458737851	2.990271372084341	2.505484118861052
489	2.000000000000985	5.045116604011659	0.001000000000058	0.923391108238242	2.999999997738107	0.000000000574666
490	2.000000000010828	12.861864577345560	0.001000000000037	0.863149541296312	2.999999999228219	0.000000002096250
491	2.000000000091057	7.966164875465500	0.001000000000009	0.838919291363061	2.999999999999895	0.000000001316784
492	3.378471412975435	5.803690216762253	0.001000000000412	0.999999999979751	2.999999999486268	0.000000003339667
493	2.000000000039573	20.230292679788636	0.001000000000011	0.739230854459338	2.999999999999983	0.000000000344393
494	2.000000000032270	7.238033470310108	0.001000000000476	0.987685252219019	2.999999998782573	0.000000003512588
495	2.000000000022771	11.823656988516335	0.001000000000003	0.882166678060950	2.999999999944289	0.000000002184269
496	2.000765096641640	0.027713345992101	0.001003495729679	0.593909583119024	2.999067587000137	3.218138688735668
497	2.000000000020189	14.150834167558912	0.001000000000029	0.882150946595235	2.999999998882548	0.000000001902064
498	2.000000000567410	4.772161373927560	0.001000000000178	0.823892981969083	2.999999999931339	0.000000000001485
499	2.836989064551966	10.202517964734531	0.001000000000147	0.948292518647730	2.999999999143967	0.000000000080745
500	2.000000000013827	4.568229803030558	0.001000000000000	0.863607525300337	2.999999999866125	0.000000000170637
501	2.000016930826377	0.027709583890340	0.001000004440274	0.854723882021601	2.999990086339926	0.000161037011853
502	2.800715851056557	5.164918943655377	0.001000000000006	0.964973263465735	2.999999997467008	0.000000000140770
503	2.000000000154659	1.436333550986904	0.001000000000069	0.850438319042786	2.999999999720036	0.000000001119395
504	2.000000000004691	8.341895363372807	0.001000000000130	0.635607278973513	2.999999998911127	0.000000001125669
505	2.000000000460386	4.181281405575970	0.001000000000027	0.665430773997543	2.999999999893837	0.000000000208558
506	2.000000000046245	9.644349063876961	0.001000000000002	0.848895205977900	2.999999999969855	0.000000003219120
507	2.623358138613364	0.028122057307993	0.001001619637758	0.671519691584770	2.673687328910077	0.146762899268713
508	3.425523650001881	0.027847335711926	0.001000024642346	0.995849806487674	2.999902281054024	0.014276191719895
509	2.000000489028342	0.027700009168249	0.001000008221757	0.523666158747970	2.997787653718906	0.002479243554525
510	2.000000000086683	4.919127946069553	0.001000000000146	0.795835294592621	2.999999999844846	0.000000001498228
511	2.000000000093557	10.474059015084990	0.001000000000144	0.741382722151891	2.999999999633200	0.000000015682971
512	2.000000000008562	3.365854491422291	0.001000000000648	0.947308021809579	2.999999999974247	0.000000000371424
513	2.021474115303346	13.354771267133215	0.002270449396220	0.929715997760991	0.675336946390462	0.000000059442787
514	2.000000232675742	0.027700298495396	0.001000000000048	0.891829570833693	2.999782014925308	0.004242147540006
515	2.000000216405558	0.027700277376753	0.001000000477754	0.360937001528093	2.260950741976367	0.000647150757709
516	2.000000000022489	18.979256655464798	0.001000000000375	0.794088591518264	2.999999999999528	0.000000000359388
517	2.000000000013175	4.733715002475420	0.001000000000045	0.920789552720756	2.999999999752736	0.000000004564499
518	2.000000000472918	19.024776695908429	0.001000000001012	0.827682865757656	2.999999999579738	0.000000004746724
519	2.000000000000620	2.396870766411220	0.001000000000183	0.989139227498606	2.999999999971678	0.000000002054847
520	2.000000000054360	13.230072850695038	0.001000000000316	0.730652406996569	2.999999999926479	0.000000000239685
521	2.000000000003704	9.321456315807604	0.001000000000093	0.852848936457261	2.999999999994792	0.000000001674225
522	2.000000000063363	4.328736826283408	0.001000000000205	0.920351585377523	2.999999996523407	0.000000000018733
523	2.000000000017099	5.643764202559957	0.001000000000009	0.866831095588337	2.999999998826200	0.000000002066327
524	2.000000000351103	2.477676964339007	0.001000000000621	0.836025668955104	2.999999999676556	0.000000001398877
525	2.000000000004086	5.704366959047241	0.001000000000075	0.980657019451218	2.999999999898421	0.000000000033033
526	2.000000000057969	3.349861843552497	0.001000000000178	0.929788817133628	2.999999999973144	0.000000000511885
527	2.000000000048964	4.601650572886348	0.001000000000044	0.811233826005472	2.999999999881573	0.000000000004046
528	2.000145298096395	0.027888491822778	0.001000176183952	0.480887100307410	2.924078644431522	4.619171640273492
529	2.000000000106347	2.204971063822672	0.001000000000070	0.834493769038965	2.999999999965455	0.000000000552699
530	2.000000000019624	2.698342755682770	0.001000000000001	0.956452722354965	2.999999999737601	0.000000000990308
531	2.000000000006457	14.289234649751261	0.001000000000110	0.680696871708153	2.999999999906003	0.000000003502233

532	2.816375467840987	0.028954223571164	0.001000026792067	0.681260964589351	2.999166159731471	0.255315330620400
533	2.000003062703376	0.027700059664864	0.001000000016345	0.430252684632241	2.957906912020914	0.003175597197718
534	2.000000000003626	6.999470222260249	0.001000000000260	0.906490836932689	2.999999999518727	0.000000000187560
535	2.000000000002000	5.755638844500163	0.001000000001486	0.846240773194602	2.999999999891526	0.000000000751742
536	2.000000000017972	10.026720519600387	0.001000000000087	0.868653585362020	2.999999999999764	0.000000000003761
537	2.000000000140840	19.134953434468247	0.001000000000224	0.771410046944782	2.999999999863422	0.000000000378544
538	2.000000000011568	3.018356707565085	0.001000000000675	0.825304411365074	2.999999999989925	0.000000001727135
539	2.000000000003194	7.527668805742536	0.001000000000079	0.759134763103790	2.999999999769033	0.000000000001135
540	2.000000000039028	0.918218383113001	0.001000000000111	0.952855084343879	2.999999999977859	0.000000000263135
541	2.000000000038326	0.027700000255649	0.001000000000153	0.653040132584967	2.999999990017824	0.000000017964678
542	2.000000000087191	2.832120638112175	0.001000000000083	0.932883451933069	2.999999999646278	0.000000000092718
543	2.933143731441160	9.907124948773978	0.001000000000188	0.962408463099560	2.999999999843291	0.000000001187070
544	2.000000000007077	6.254443161496228	0.001000000000148	0.876134535871286	2.999999999954376	0.000000000648286
545	2.000093387115672	0.055254707787329	0.001000353649202	0.455154415016246	0.480463793106072	0.054333440765276
546	2.000000000268213	11.332305376757725	0.001000000000278	0.700278794091266	2.999999999687184	0.000000005541111
547	2.000000000126486	7.965713224135803	0.001000000001426	0.923111688169611	2.999999999689154	0.000000003960457
548	2.000000000058486	5.310002079136744	0.001000000000006	0.919999780201355	2.999999999742690	0.000000000072039
549	2.848990663847663	3.575171691175398	0.001000000000046	0.835081654130402	2.999999999300505	0.000000000041346
550	2.902497878379377	11.656112547059525	0.001000000000017	0.999999999999880	2.999999999999423	0.000000000098672
551	2.000000000016517	2.487303961718101	0.001000000000085	0.846348004171795	2.999999999533060	0.000000000608389
552	2.000000000000002	12.323602248979370	0.001000000000246	0.963060905100947	2.999999999939512	0.000000000520710
553	3.055359711719642	6.444480537720506	0.001000000000000	0.960725558816170	2.999999999399185	0.000000000040370
554	2.000000000193322	20.285341139145579	0.001000000000002	0.999999999998482	0.122473947382240	0.000000000080078
555	3.154251350795621	8.634471660030545	0.001000000000000	0.987929344240939	2.999999999997788	0.000000001853017
556	2.000000000000002	19.438407396228826	0.001000000000020	0.882863143270785	2.999999999963280	0.000000000045738
557	2.000000000073189	7.474610926057939	0.001000000000004	0.855698710879646	2.999999999490624	0.000000001096500
558	2.509536218305101	18.837540283268250	0.001000000000067	0.999999999999993	2.999999999492590	0.000000000042923
559	2.976445064697136	0.944093577948713	0.001000000000016	0.937103447699637	2.999999999898773	0.000000001879572
560	2.000000000023064	8.671155220184014	0.001000000000114	0.925653444164750	2.999999999993441	0.000000000044283
561	2.000000000039889	12.730872244774877	0.001000000000180	0.923139694671266	2.999999999280685	0.000000004723214
562	2.000000000000093	19.086836640620149	0.001000000008344	0.681918031576024	0.477253004620962	0.000000204395241
563	2.000000000001994	0.027700000110191	0.001000000018797	0.460249312625044	2.999999999409778	0.000000121772560
564	2.000000000076009	16.312394436208670	0.001000000000042	0.877586580938060	2.999999999753068	0.000000000923331
565	2.000000000007794	2.427382445386789	0.001000000000016	0.991464097088919	2.999999999996033	0.000000000000339
566	2.000000000001276	1.836178329653089	0.001000000000355	0.850677420467843	2.999999999594488	0.000000000237305
567	2.000000000164417	2.645290432274743	0.001000000000029	0.882938621985197	2.999999999685756	0.000000000104773
568	2.000000000086290	5.058502551108501	0.001000000000026	0.640955104623718	2.999999996897058	0.000000000019015
569	2.000000000033435	6.193772519006644	0.001000000000019	0.890622350680256	2.999999999844680	0.000000000466662
570	2.000000000033158	11.019269708430869	0.001000000000107	0.780289732719004	2.999999999998110	0.000000000024826
571	2.001711354992211	0.029090436095150	0.001000160330658	0.604277871967987	2.960314051134464	0.683979815730144
572	2.000000000002873	12.610695977082960	0.001000000000023	0.941019656026698	2.999999999509015	0.000000002707081
573	2.000000000000312	3.444360427429158	0.001000000000006	0.996489283190438	2.999999999999151	0.000000000312125
574	2.000000000010288	8.973855609678575	0.001000000000004	0.983532972614953	2.999999999487764	0.000000000642476
575	2.000000000034314	1.346933523655250	0.001000000000155	0.804320901356601	2.999999999826380	0.000000000017439
576	2.000001169147382	0.027732146844518	0.001000003693948	0.833069802654473	2.999990246348580	0.000377980927189
577	2.000000000293959	17.482320002838112	0.001781927937160	0.836496623917542	0.404158296023340	0.000001308319487
578	2.000000000019696	3.800453388413120	0.001000000000005	0.909317842517355	2.999999999978936	0.000000001598322
579	2.000000000005381	8.451924912484447	0.001000000000043	0.999999999999857	2.999999998971016	0.000000001226891
580	2.000000000033557	8.448294677826528	0.001000000000130	0.999999999996564	2.999999999798084	0.000000001229467
581	2.000000000086166	8.639088948564654	0.001000000000042	0.875350033068555	2.999999999984258	0.000000000128672
582	2.000000000014909	3.616374380739302	0.001000000000015	0.849371543089117	2.999999999591320	0.000000001112316
583	2.000000000392095	10.676253753195519	0.001000000000002	0.807229891376451	2.999999999835476	0.000000000999516
584	2.000000000069189	13.145779958684102	0.001000000000031	0.968332798222495	2.999999998911669	0.000000000006378
585	2.000000000098898	2.854746498100782	0.001000000000175	0.826074868344520	2.999999998977768	0.000000000256900
586	2.000000000095656	1.321618694541916	0.001000000000272	0.754604298743653	2.999999999924328	0.000000001592522
587	2.000000000027264	1.760698247218773	0.001000000000006	0.791621984638931	2.999999999757133	0.000000002065886
588	2.205782756936931	14.432856157163323	0.001000000000007	0.799338567062124	2.999999999985507	0.000000000459386
589	2.000000000120952	7.313252438250188	0.001000000000002	0.999999999994388	2.999999999895885	0.000000006459143
590	2.000000000013346	14.810497896070434	0.001000000000045	0.966042390002237	2.999999999997118	0.000000003445128

591	2.000000005655023	19.996274045511406	0.001000000491804	0.999999999806264	0.743306298535027	4.999999123532187
592	2.482915521467587	1.474036293998605	0.001000000000040	0.987360397364783	2.999999999972701	0.000000001830335
593	2.000000000085014	6.480179172249420	0.001000000000192	0.924642445432649	2.999999999886729	0.000000000028801
594	2.000000000024159	16.573011347099708	0.001000000000050	0.776301509562112	2.999999999006028	0.000000003740170
595	2.000000000000278	8.851667497601381	0.001000000000001	0.993255478837236	2.999999999994806	0.000000000001114
596	2.000000000000025	20.642052823146170	0.001000000000058	0.938625349721025	2.999999999999865	0.000000000260949
597	2.000000000031228	3.508914321411441	0.001000000000268	0.914165956335304	2.999999999999806	0.000000000134660
598	2.000000000003350	7.527154226469110	0.001000000000054	0.788635789505788	2.999999999524555	0.000000001359063
599	2.915832932461051	14.380361432559639	0.001000000000027	0.999999999965362	2.999999998424891	0.000000025794239
600	2.041194477231357	0.059943833585324	0.001020408407733	0.328015517443639	0.246337429513696	0.002770564810297
601	2.000000000107916	3.849342373623932	0.001000000000000	0.933700465534985	2.999999999509230	0.000000000303137
602	2.000000000025471	7.948197391150319	0.001000000000158	0.786403346182191	2.999999999998550	0.000000000579167
603	2.000002676327419	0.027710807752797	0.001000458647337	0.816454663099971	2.998891119299718	0.225053451182789
604	2.000000000056039	1.149568399979681	0.001000000000247	0.834023711037209	2.999999999907923	0.000000000181160
605	2.000000313233422	0.027708300515652	0.001000067864555	0.671550661661639	2.988094059797409	0.121080881180171
606	2.000000000022584	11.545791431004531	0.001000000000126	0.814928126980524	2.999999999998384	0.000000000631311
607	2.000000000107266	20.650031423424895	0.001000000000011	0.211653387664815	0.110132454604380	0.000000000101935
608	2.000000845035427	0.027700770856791	0.001000090905797	0.376833867869101	2.752016445726151	4.976957291361358
609	2.000000000003457	8.757086825048459	0.001000000000031	0.998852965773707	2.999999999549804	0.000000001130355
610	2.000000002729352	0.027700237016832	0.001000006940036	0.629937890723533	2.999767822771033	0.003037476362633
611	2.000000000014207	1.269105616858056	0.001000000000127	0.696683206934956	2.999999999305683	0.000000000622997
612	2.000000000004021	19.036664675374510	0.001000000000030	0.862356507171242	2.999999999999798	0.000000000430812
613	2.000000000101263	4.173436654202475	0.001000000000098	0.892479120816452	2.999999999950636	0.000000001530606
614	2.000000000322491	0.027700000185992	0.001000000000288	0.867553191797863	2.999999999735712	0.000000003349098
615	2.000000000097772	7.824257505015947	0.001000000000120	0.976010584024054	2.999999999948739	0.000000000381629
616	2.000000000054362	2.752724794370919	0.001000000000005	0.709367987578493	2.999999999952884	0.000000002340719
617	2.000000000033491	8.515680666039629	0.001000000000027	0.985980325883269	2.999999999894397	0.000000000022458
618	2.000000011436910	0.027700048982432	0.001000009559149	0.371939398331637	2.977777869373597	0.000933933084981
619	2.000000000035441	9.488288018341532	0.001000000000003	0.992827352327867	2.999999999825229	0.000000000609919
620	2.728453500048965	6.981303057795693	0.001000000000247	0.896041745403350	2.999999999863563	0.000000002798940
621	2.000000129763590	0.027700309873101	0.001000005523116	0.635493431084961	2.998395569582898	0.000382997822564
622	2.000000000053942	14.419705986214099	0.001000000000011	0.785192179728025	2.999999999963496	0.000000000007352
623	2.000000000028372	4.026614786788623	0.001000000000030	0.958602002074604	2.999999999993229	0.000000000058202
624	2.000000000011471	10.324013344721019	0.001000000000005	0.832035105888055	2.999999999998716	0.000000000020971
625	2.058929664216015	0.045790837977975	0.001004167871025	0.178177003183517	0.280037211630787	0.293217482813007
626	2.000000000016240	8.829948758958942	0.001000000000012	0.823971270730032	2.999999999758035	0.000000000697674
627	2.000000000049202	16.926424636891788	0.001000000000022	0.757421285342608	2.999999999999903	0.000000001226814
628	2.000000000101303	10.763152608561228	0.001000000000373	0.901971406551864	2.999999999975393	0.000000001250582
629	2.000000000036909	8.035189917789776	0.001000000000170	0.950349286137544	2.999999999981697	0.000000000528849
630	2.000000000055041	4.031968111310389	0.001000000000026	0.905340058108121	2.999999999877590	0.000000000084583
631	2.000000000016694	7.407889455256690	0.001000000000017	0.974507443618731	2.999999998454948	0.000000001002481
632	2.000000000790870	4.389121648996341	0.001000000000005	0.929461804233341	2.999999999473214	0.000000000898225
633	2.000000000126665	12.084497760473740	0.001000000000046	0.695203271512332	2.999999999819462	0.000000000293053
634	2.000000000000941	12.175488384558264	0.001000000000291	0.860401218792817	2.999999999937593	0.000000003963840
635	2.000023982077585	0.027751673604374	0.001000056479066	0.602242786977608	2.999808318169809	0.000925418496067
636	2.000000000338476	18.858497474120163	0.001000000000054	0.759969430327716	2.999999999995209	0.000000002955351
637	2.000000123378031	0.027777809864462	0.001000000078586	0.888037591774405	2.999997234525254	0.000008217399227
638	2.339513222226167	5.850858513548066	0.001000000000002	0.903156167267340	2.999999999947926	0.000000000005318
639	2.000000000000654	5.839553715077678	0.001000000000063	0.947286526296346	2.999999999601714	0.000000000284225
640	2.624072334951456	19.296417038872722	0.004232321534246	0.960136397684340	1.404116493897879	0.000000010032591
641	2.000000000005139	20.497425479928157	0.001000000000055	0.669372917165278	2.999999999880089	0.000000000014069
642	2.000000000001812	1.939027416297269	0.001000000000037	0.916445702676472	2.999999999999805	0.000000000035860
643	2.981715324090747	9.877618057822556	0.001000000000245	0.887545318257685	2.999999999419348	0.000000000244794
644	2.000000000020723	4.311108671203928	0.001000000000004	0.965518649637370	2.999999999731738	0.000000000916283
645	2.000000000023282	4.182255978870681	0.001000000000008	0.908171750535472	2.999999999976082	0.000000004080195
646	2.000000000055208	14.137549654033361	0.001000000000012	0.895215840167643	2.999999999694856	0.000000000055393
647	2.000000000118453	18.092427864716289	0.001000000000164	0.828625470254112	2.999999999893700	0.000000000631797
648	2.000000000001747	3.943556598617291	0.001000000000047	0.754781865691876	2.999999999501580	0.000000000024026
649	2.000000000005303	7.402948490746351	0.001000000000147	0.991246361812741	2.999999999538797	0.000000000097793

650	2.265334729161886	18.383446798340046	0.001000000000135	0.953563831438952	2.999999999399339	0.000000000086396
651	2.000000000030044	7.974520692760602	0.001000000000219	0.999999999998079	2.999999999788588	0.000000001166434
652	2.000000000005124	3.692022446974766	0.001000000000275	0.908176956431341	2.999999999464885	0.000000001037735
653	2.000000000023687	12.553695734058858	0.001000000000053	0.834819391206138	2.999999999996757	0.000000000016135
654	2.000000000008645	13.711888790604007	0.001000000000494	0.841209532849150	2.999999999956653	0.000000000087810
655	2.985274524322867	12.212922771446829	0.001000000000041	0.912834012229599	2.999999999726740	0.000000000212784
656	2.000000000000150	6.396379099564332	0.001000000000319	0.897395449936067	2.999999999968757	0.000000002898262
657	2.000000000090357	3.488904921748798	0.001000000000005	0.791996527686719	2.999999999970195	0.000000000857271
658	2.000000000004544	5.975002432363129	0.001000000000012	0.788650051326846	2.999999999999248	0.000000002630516
659	2.234343140191936	0.694613316266156	0.001002463153282	0.244271850654319	0.130503946884764	0.374705180877828
660	2.000000217440712	0.027704674046289	0.001000043053912	0.871840894416440	2.999182954442567	0.001947148541664
661	2.000000000035757	6.939734670796584	0.001000000000001	0.855203605251996	2.999999999053423	0.000000000089251
662	2.000000000024311	18.449304328396380	0.001025542571691	0.999999999995428	0.159033263379723	0.000000002697910
663	2.000000000001761	14.604905514889014	0.001000000000165	0.871420589619875	2.999999999998797	0.000000000594599
664	2.000000000761911	2.119406768042574	0.001000000000037	0.938347257210549	2.999999998953137	0.000000001743606
665	2.000000000000342	9.123822577764845	0.001000000000156	0.955525879667650	2.999999999998298	0.000000000038149
666	2.000000000026235	7.490707706598343	0.001000000000148	0.994938104315461	2.999999999999051	0.000000004104371
667	2.000000000061646	5.017287748062618	0.001000000000022	0.770422105215612	2.999999999994206	0.000000000969401
668	2.734651827691388	0.027848618370822	0.001000042843098	0.769607555216501	2.962968615002045	0.109118660844547
669	2.000000000123760	8.870896041110269	0.001000000000001	0.965157895546507	2.999999999917450	0.000000000315135
670	2.000000000001553	16.577844589847054	0.001801768607218	0.867724274624517	1.582791970230675	0.000000020973156
671	2.000000000000348	18.655908511651937	0.001000000000000	0.961247989413509	2.999999999981789	0.000000000264362
672	2.000000000002898	2.919286889891394	0.001000000000043	0.830136856456780	2.999999999853574	0.000000001187950
673	2.000000000001361	13.567293743829726	0.001000000000001	0.941617668399987	2.999999999998922	0.000000000344481
674	2.523984302317790	0.027706651681025	0.001000027609064	0.603021949455933	2.844633017643168	0.018131354546504
675	2.000000000109247	20.440157682771289	0.001000000000000	0.726403748113181	2.999999999999457	0.000000000013672
676	2.000000000005716	7.531945349231829	0.001000000000019	0.919720500686466	2.999999999339126	0.000000001217689
677	2.000000000044169	6.670455465233621	0.001000000000102	0.984109052337258	2.999999999976962	0.000000000697460
678	2.000000000045515	16.091236306234709	0.001000000000238	0.872605329420476	2.999999998403088	0.000000002439691
679	2.869702766919210	14.450018053041140	0.001000000000001	0.964973174920951	2.999999999997028	0.000000000636342
680	2.857026606152524	11.910313392248717	0.001000000000078	0.989983531901674	2.999999999681918	0.000000000647178
681	2.000000000011254	8.759951630760391	0.001000000000126	0.999999999970521	2.999999999960417	0.000000000340655
682	2.000000000043054	9.508989222803592	0.001000000000092	0.819611974207667	2.999999999704718	0.000000000324567
683	2.389179979756994	5.470548169977348	0.001000000000006	0.975871609931729	2.999999999676815	0.000000000112797
684	2.000000000024313	6.207404106699493	0.001000000000001	0.831031518461092	2.999999999999052	0.000000000000347
685	2.000000028399898	0.027700861667100	0.001000011054120	0.645720234245474	2.999448997510729	0.055341664151682
686	2.000000000019599	13.888733576252884	0.001000000000019	0.757134487567207	2.999999999993533	0.000000000113898
687	2.000001212566212	0.027701554302881	0.001000016280696	0.823263458483410	2.999842543614943	0.015025897208573
688	2.000000000005145	9.650771911862609	0.001000000000301	0.960999305727747	2.999999999898610	0.000000002426250
689	2.000000000007727	20.436898993461867	0.001000000000061	0.885876233669766	2.999999999972585	0.000000000099635
690	2.000000000091368	8.784658301177613	0.001000000000084	0.999999999991977	2.999999998480756	0.000000000405267
691	2.000000000008638	1.249230101205990	0.001000000000057	0.842077264922184	2.999999999980930	0.000000000672273
692	2.000000000068464	18.864199286066828	0.001000000000034	0.950833883265402	2.999999999191869	0.000000000094780
693	2.000000001583576	3.427734127094282	0.001000000000250	0.930885534011737	2.999999999550646	0.000000001058134
694	2.000000000000538	18.610338892743776	0.001000000000002	0.762315620053592	2.999999999944691	0.000000001262911
695	2.453976467215965	12.069305074666870	0.001000000000008	0.935253828280892	2.999999999696566	0.000000000178398
696	2.000000000003508	7.746572379736668	0.001000000000193	0.974848232498403	2.999999999982029	0.000000000980887
697	2.000000000000884	10.361924511403750	0.001000000000000	0.992201980211766	2.999999999984627	0.000000000103750
698	2.714697886906690	0.090082712978667	0.001003609610583	0.812743270373105	2.950125354652846	0.057085557995848
699	2.000000000002658	15.011051539495028	0.001000000000073	0.966760320949486	2.999999999885455	0.000000000005607
700	2.000000000007828	13.982348296912479	0.001000000000105	0.752204802450933	2.999999999865608	0.000000001181185
701	2.000000000039638	9.736123320038265	0.001000000000354	0.873245822041274	2.999999999733029	0.000000000526263
702	2.000000000046621	12.140624793935599	0.001000000000607	0.914716987297116	2.999999999575020	0.000000002189728
703	2.987046650292411	9.197048785803649	0.001000000000072	0.964300381860092	2.999999999576999	0.000000000174660
704	2.000000000014686	13.532887833241499	0.001000000000068	0.945824716367835	2.999999994558497	0.000000000101051
705	2.000000000004484	11.226431991805006	0.001000000000332	0.871367600538408	2.999999999846575	0.000000000254448
706	2.000000000003831	8.875284892860524	0.001000000000120	0.920833666557102	2.999999999738812	0.000000000045387
707	2.000000000097959	8.608475756833451	0.001000000000017	0.801774132742525	2.999999999979981	0.000000003719067
708	2.000000021429969	0.027709897774137	0.001000000006169	0.842121102483995	2.999999493712034	0.000014365792965

709	2.000000000002076	5.583984293842301	0.001000000000006	0.979600624849201	2.999999999561251	0.000000000138770
710	2.000000000006305	4.828992578551593	0.001000000000434	0.942098609553410	2.999999998440154	0.000000002310523
711	2.000000000021360	3.244493749115861	0.001000000000002	0.919556444895046	2.999999998339967	0.000000004134576
712	2.000000000001131	6.535740458289378	0.001000000000259	0.975742478052484	2.999999999944015	0.000000000641372
713	2.000000952186825	0.027703782081710	0.001000100685869	0.759233984984154	2.998768808331588	0.045477667146053
714	2.000000000000175	6.489961658669252	0.001000000000241	0.878844723646038	2.999999999813200	0.000000000115618
715	2.000000000000021	6.992220577962046	0.001000000000025	0.994105673251033	2.999999999978973	0.000000000910991
716	2.000000310506642	0.028172869540406	0.001000284236611	0.718782900146579	2.998584751232600	0.000105406386152
717	2.000000000047770	5.038195099694552	0.001000000000121	0.866142916808666	2.999999999563329	0.000000000134630
718	2.000000000022134	2.132393333680917	0.001000000000104	0.962975746635835	2.999999999959570	0.000000000368154
719	2.000000000033551	3.392444515080876	0.001000000000030	0.847061440871421	2.999999999904991	0.000000000253201
720	2.000000000050139	1.816904386793844	0.001000000000182	0.777762271558542	2.999999999985594	0.000000000309914
721	2.000000107488351	0.027704197036277	0.001000000266459	0.668020345185296	2.999996234822877	0.000003022557960
722	2.000000000031072	6.300261695780265	0.001000000000092	0.783124004260393	2.999999999911461	0.000000000167848
723	2.000000000029846	10.814167322307579	0.001000000000033	0.839024302453416	2.999999998953242	0.000000000791535
724	2.000000000062532	0.027700000000745	0.001000000000019	0.843879275632397	2.999999999932919	0.000000004365898
725	2.000000000000224	11.181918746909478	0.001000000000006	0.954284391558900	2.999999999972916	0.000000000267570
726	3.143871363737295	9.359268180342561	0.001000000000104	0.915639862600248	2.999999999953920	0.000000001685994
727	2.000000000075579	2.967638329258644	0.001000000000276	0.909536818927361	2.999999999913341	0.000000000734202
728	3.185590406814167	4.522283356028011	0.001000000000468	0.981129664272766	2.999999998055255	0.000000006396756
729	2.000000000000738	14.529899993413798	0.001000000000015	0.889983260186557	2.999999999988473	0.000000000846287
730	2.000000000008075	20.658607852468901	0.001000000000001	0.770992162350760	2.999999999889909	0.000000000003924
731	2.000000000027290	12.918434577187391	0.001000000000012	0.939441224569917	2.999999999812792	0.000000000318591
732	2.000000000051928	0.027700000013972	0.001000000000567	0.493144539113589	2.999999992490515	0.000000000169434
733	2.000000000018881	4.888305801368865	0.001000000000006	0.787340116135511	2.999999999714730	0.000000000898525
734	2.532279128737045	12.981627749269505	0.001000035377079	0.825204980329438	2.999431670926669	4.306698339075644
735	2.000000000000074	6.221642540565773	0.001000000000622	0.713798212254109	2.999999999975271	0.000000000169796
736	2.000000010775892	0.027700232581394	0.001000000059306	0.817812046143241	2.999999476406661	0.000000040314848
737	2.000000000001441	8.492401573901084	0.001000000000004	0.999999999999981	2.999999999984045	0.000000000698437
738	2.000006302834446	0.027700782459434	0.001000018153371	0.493009508728668	2.966750011893570	0.003575646997575
739	2.000000000139357	5.239084132404528	0.001000000000037	0.796843366429922	2.999999999814345	0.000000008840227
740	3.022608463055691	3.210226159542300	0.001000000000284	0.966271172268855	2.999999999991506	0.000000003598993
741	2.499397480718746	16.196885472853726	0.003700150941174	0.999999999999850	1.379832542662839	0.000000006444267
742	2.000000000363349	5.904922698437321	0.001000000000025	0.868141066846150	2.999999998583243	0.000000000078677
743	2.000000000014194	13.631122038383431	0.001000000000532	0.886945393402934	2.999999999998019	0.000000001168456
744	2.000000000001595	3.385717520397448	0.001000000000000	0.878618525122250	2.999999999934863	0.000000000123492
745	2.625247976620538	4.100113876447195	0.001000000000106	0.888269748094304	2.999999999897857	0.000000000035863
746	2.000000000030888	3.290351756559385	0.001000000000034	0.846653776978707	2.999999999999298	0.000000000014304
747	2.000014279139657	0.053064659803263	0.001001426730248	0.351381684530436	0.337354693450305	0.507417668307417
748	2.000000000000123	4.465806667451286	0.001000000000009	0.961926197915314	2.999999999168768	0.000000000012326
749	2.000000000021851	7.730502939590499	0.001000000000179	0.922750598696232	2.999999999829669	0.000000001159570
750	2.000000000008838	9.908521034801602	0.001000000000258	0.976437032037206	2.999999999406046	0.000000000125422
751	2.000000000000378	3.983812711521572	0.001000000000073	0.828417530712078	2.999999999795219	0.000000003402496
752	2.000000000007147	1.020690514163368	0.001000000000084	0.854103484733834	2.999999999950707	0.000000000052235
753	2.000000000017696	16.800778501665043	0.001000000000014	0.971871685591352	2.999999998753926	0.000000000597644
754	2.000000000048124	9.674049739311780	0.001000000000069	0.965841487311534	2.999999999684984	0.000000000009754
755	2.000101832433260	0.027797813206007	0.001000000164589	0.255469096447817	0.296374051701909	0.019500164890038
756	2.000000000142139	5.779170485594736	0.001000000000110	0.832709014921452	2.999999999935104	0.000000004621690
757	2.000000000001053	20.774352050920424	0.001000000000000	0.877614430755225	2.999999999786173	0.000000000275489
758	2.578334309059079	0.027720846413749	0.001000005956977	0.735276909171997	2.994172738894437	0.014091365777689
759	2.000034587141963	0.027956041414344	0.001000023257164	0.609442804988451	2.999920448434957	0.001347284504262
760	2.000000000000812	11.310904158966963	0.001000000000094	0.878627114302639	2.999999999949830	0.000000004708327
761	2.000000000004270	6.453545860520298	0.001000000000000	0.776882663482916	2.999999999993045	0.000000002066834
762	2.000000000049517	4.297878366413874	0.001000000000014	0.814995015539975	2.999999999824496	0.000000000000931
763	2.000000000014154	8.656545004627592	0.001000000000103	0.976962353526757	2.999999998954778	0.000000004750103
764	2.000000000061450	20.519588106087884	0.001000000000217	0.845269276677003	2.999999999708523	0.000000002563509
765	2.316019680605664	7.573015226342240	0.001000000000008	0.902896632993963	2.999999999353802	0.000000002890055
766	2.126320074239096	10.544654577460861	0.001000000000995	0.837798849383116	2.999999999974450	0.000000001297034
767	2.000000000032405	6.098432891728535	0.001000000000153	0.932700353578598	2.999999999994481	0.000000000765872

768	2.545104287416168	19.294932825626905	0.001001441043544	0.919995180307942	2.999578122823640	4.999907272416992
769	2.000000000000726	20.667747636644791	0.001000000000013	0.737248594750064	2.999999999725966	0.000000000000347
770	2.000002054923791	0.028508004425029	0.001000009317962	0.644890774979605	2.994850166409733	0.001297114231686
771	2.000000003848893	0.059162487897362	0.001000007184738	0.849619713222908	2.999719517311300	0.436199718673099
772	2.000000041293012	15.287071885665869	0.001001247775706	0.914845479572856	2.207637521063308	4.999916697556563
773	2.000000000010433	2.653957012268377	0.001000000000002	0.705853079614156	2.999999999982071	0.000000001065061
774	2.000000000002570	1.987345418274966	0.001000000000001	0.902895442233768	2.999999999821656	0.000000000121276
775	2.000000000006613	9.570796458243457	0.001000000000003	0.881865054588127	2.999999999719586	0.000000000191509
776	2.000000000035485	8.738233150390379	0.001000000000223	0.999999999996552	2.999999999999554	0.000000000000002
777	2.000000000002304	1.346842131575131	0.001000000000228	0.854521858876941	2.999999999998083	0.000000007795296
778	2.000000000097264	2.776805623296635	0.001000000000011	0.945633521596915	2.999999999946308	0.000000000462223
779	2.000000000008370	2.186851958045786	0.001000000000031	0.806488673661367	2.999999999004906	0.000000000925659
780	2.000000000004681	4.863198951527688	0.001000000000012	0.790131533444612	2.999999999913139	0.000000001526028
781	2.000000000000057	20.027639494968270	0.001000000000006	0.882716928637697	2.999999999938569	0.000000000898306
782	2.000000000023486	1.231096918961830	0.001000000000010	0.895187661819236	2.999999999971334	0.000000000210206
783	2.000000000038852	9.017108961309305	0.001000000000014	0.966941683685206	2.999999998005350	0.000000000075228
784	2.000000000007364	6.902054978173774	0.001000000000155	0.937389598021164	2.999999999791736	0.000000000485154
785	2.000000000035835	8.196951249986228	0.001000000000133	0.841244157951435	2.999999999760841	0.000000000036166
786	2.000000000356318	6.183350969177465	0.001000000000002	0.766038617321503	2.999999999791084	0.000000005157428
787	2.000000000024765	4.417005897850417	0.001000000000362	0.860391048448718	2.999999999999996	0.000000000743324
788	2.000000000047971	7.750752038597011	0.001000000000024	0.837998179164794	2.999999999981901	0.000000000049132
789	2.000006958769657	0.028828690937661	0.001000356114272	0.823417460933928	2.999764001991527	0.005166415540767
790	2.000000000063462	13.175511891634397	0.001000000000001	0.779756332462127	2.999999999820400	0.000000000320342
791	3.196737317721375	1.440629144589775	0.001000000000005	0.999999999999297	2.999999999928765	0.000000000339274
792	2.000000000022624	11.056162675747554	0.001000000000018	0.846836790556733	2.999999999950883	0.000000000276209
793	2.000000000054351	5.110679105031664	0.001000000000001	0.902011529309241	2.999999998946452	0.000000000292402
794	2.000000000070286	5.474031324429350	0.001000000000007	0.834971757486520	2.999999999804837	0.000000001408440
795	2.000000000003896	1.932377624671989	0.001000000000001	0.906068811387845	2.999999999867494	0.000000000000141
796	2.000000000000295	4.455932822981637	0.001000000000001	0.829126222702532	2.999999999851404	0.000000000092581
797	2.000000000031335	6.051689605322348	0.001000000000005	0.897099732110381	2.999999999699442	0.000000000044544
798	2.000000000024136	17.748372283534025	0.001000000000062	0.755967218328776	2.999999999540145	0.000000000024979
799	2.000000000179143	8.211948144756637	0.001000000000032	0.910312820459433	2.999999999919187	0.000000000140720
800	2.000000000001783	14.082021579757306	0.001000000000003	0.753491660709460	2.999999999673844	0.000000000089785
801	2.000000000057509	20.707990477472578	0.001000000000023	0.780032248388406	2.999999998475877	0.000000000000357
802	2.000000000000410	6.366534117850117	0.001000000000214	0.933617141348245	2.999999999773881	0.000000000577400
803	2.000000000004619	10.891044416651409	0.001000000000046	0.982750360793735	2.999999999548451	0.000000000711078
804	2.000000010913460	0.027700023866674	0.001000000000702	0.848217942612740	2.999999902001001	0.000023084918397
805	2.528009760528656	8.519788400986494	0.001000000000130	0.999999999987574	2.999999999912243	0.000000000058903
806	2.000000016480168	0.027700539104975	0.001000008855325	0.725149198679354	2.998936045998978	0.000427728535122
807	2.000000000005710	7.458737429940846	0.001000000000165	0.698237304404151	2.999999999940062	0.000000000017571
808	3.591036395548694	4.392697586507403	0.001000000000006	0.999999999999885	2.999999999873242	0.000000000100375
809	2.000000000214163	6.852350376783005	0.001000000000079	0.918157094965580	2.999999999665437	0.000000000031480
810	2.000034563540990	0.027702284917394	0.001000000003342	0.691244166213815	2.999790964035167	0.070935802209677
811	2.000000000002287	17.143027544181848	0.001000000000000	0.944769258907158	2.999999999828070	0.000000000871125
812	2.000000001509326	19.912521573481072	0.001000000000314	0.558410021273782	0.190631033639567	0.000000103070852
813	2.000007002899258	0.027700050123280	0.001000035648949	0.439657465067055	2.357492600323125	0.000177134859582
814	2.000000000030595	4.069474758357762	0.001000000000031	0.877412658638939	2.999999999830422	0.000000002413301
815	2.000000000037232	15.713213186112657	0.001000000000170	0.846457747950496	2.999999999431288	0.000000000854712
816	2.000000000008440	10.912675659929404	0.001000000000051	0.879469935469101	2.999999999491899	0.000000000006384
817	2.124145003763354	0.046158359482486	0.001001161028364	0.787788092291153	2.866981500430453	0.483416063830490
818	2.000000000044985	16.743366883896396	0.001000000000006	0.824442141910102	2.999999999957395	0.000000000561201
819	2.000000000005286	5.820542572081427	0.001000000000047	0.950462045339912	2.999999998857472	0.000000000249038
820	2.000000000002318	20.425111851614876	0.001000000000000	0.732113399228296	2.999999999651566	0.000000000308335
821	2.000000000113051	3.122685409373053	0.001000000000220	0.749775602358423	2.999999999723587	0.000000000587226
822	2.000000000000004	5.399470988039180	0.001000000000363	0.811645165782507	2.999999999740609	0.000000000000780
823	2.000622720121181	0.033513068713428	0.001000194563698	0.356047648011684	0.468781268120083	0.225057753083261
824	2.000182690194350	0.058262179645677	0.001001078798205	0.680049374457671	2.106186570731425	2.213009937775770
825	2.000000000003944	10.116756179601522	0.001000000000001	0.840822275826919	2.999999999914811	0.000000000570833
826	2.000000000005149	3.537611149486823	0.001000000000105	0.664552879604338	2.999999999904932	0.000000001423576

827	2.000000000030068	0.688121117143619	0.001000000000140	0.879455838883621	2.999999894755593	0.000000729118770
828	2.000000000010612	8.118633856895627	0.001000000000197	0.988674748036814	2.999999999588986	0.000000000439279
829	2.000000000072415	20.652521046127980	0.001000000000061	0.819752616204765	2.999999999411296	0.000000000313351
830	2.000000000065103	2.892210360425627	0.001000000001540	0.943851775992817	2.999999945254845	0.000004411725097
831	2.894849893745252	20.586981420567540	0.001000000000113	0.999999999994200	2.999999999951021	0.000000000095989
832	2.000000000009305	10.717402326086876	0.001000000000028	0.852834495335475	2.999999999957533	0.000000000671707
833	2.000000000017124	6.954622528437890	0.001000000000005	0.873663252507353	2.999999999902342	0.000000000156920
834	2.000000000046091	2.420202317102924	0.001000000000047	0.904321338763866	2.999999999739237	0.000000000653372
835	2.000000000044290	11.093926360167757	0.001000000000000	0.810911459030175	2.999999999803873	0.000000001366682
836	2.308272824112491	3.308909727305342	0.001000000000204	0.901272925926110	2.999999998606894	0.000000003420966
837	2.000000000594957	0.027700002164390	0.001000000000091	0.931592434274253	2.999999981205452	0.000000061224791
838	2.000000000030663	7.295096639174937	0.001000000000019	0.976508528605069	2.999999999789802	0.000000005026841
839	2.000000000941573	16.082476604735710	0.001000000000145	0.649306681061644	0.332176573113975	0.000000007584654
840	2.000000000067101	8.873996720406733	0.001000000000193	0.859207397312322	2.999999999960925	0.000000000004789
841	2.000000000000648	4.327453236132687	0.001000000000058	0.808484843881551	2.999999999802268	0.000000000533592
842	2.000000000004702	5.819849964817736	0.001000000000021	0.911093257530646	2.999999999959455	0.000000002529701
843	2.000198905180830	0.030702789712925	0.001000003041542	0.525330526986131	2.818363681448636	0.148040669025834
844	2.000000000085305	1.672721174506356	0.001000000000039	0.915378151375736	2.999999999999978	0.000000000018135
845	2.000000000060142	4.931488735161823	0.001000000000002	0.859573509321016	2.999999999478174	0.000000001326140
846	2.000000000004061	5.493078926851665	0.001000000000470	0.877046716593885	2.999999999975188	0.000000004564127
847	2.951839673559395	0.027700046094716	0.001000000052046	0.869584710552273	2.999978343892120	0.000016008562480
848	2.000000000006470	7.108224923862798	0.001000000000050	0.983736626633554	2.999999999870168	0.000000000086406
849	2.000000000049973	16.005738578565389	0.001000000000023	0.862834777793757	2.999999999998568	0.000000000049047
850	2.734235560737523	0.027869121763239	0.001001605991449	0.728909779194314	2.994761992797794	1.215378764730323
851	2.000000000045186	5.054139580758348	0.001000000000033	0.901251782910541	2.999999999730468	0.000000000686627
852	2.000000000047205	6.701672550554296	0.001000000000005	0.861570540293532	2.999999999940293	0.000000005319818
853	2.000000000000074	9.509250951542484	0.001000000000015	0.741873431242915	2.999999999990985	0.000000000342076
854	2.000000000709186	19.078555179469031	0.001000000009967	0.707337045304806	0.409573045476351	0.000009484671151
855	2.000000000044169	6.670455465233621	0.001000000000102	0.984109052337258	2.999999999976962	0.000000000697460
856	3.452884855090726	19.707881746414305	0.001000000000008	0.999999999971700	2.999999999879402	0.000000000017000
857	2.000000000267639	7.596072280922241	0.001000000000064	0.925091944136194	2.999999999878754	0.000000000024435
858	2.000000000028541	12.410215176450764	0.001000000000629	0.833785597090541	2.999999999976152	0.000000005301268
859	2.000000000001620	5.459628222567251	0.001000000000082	0.806206179098556	2.999999999866128	0.000000002168882
860	2.000000000000494	4.313316181700746	0.001000000000265	0.764275449890966	2.999999998805822	0.000000000678587
861	2.830372832375209	8.462392213489505	0.001000000000001	0.921703309900251	2.999999999610519	0.000000000522746
862	2.000000000001622	20.420366964397616	0.001000000000002	0.873136101159180	2.999999999708229	0.000000000449027
863	2.000005144053671	0.027702926336785	0.001000036074933	0.788630593134531	2.999530283259706	0.028398584392214
864	2.000000000049673	2.293207078284687	0.001000000000778	0.816631912005783	2.999999998859270	0.000000000160588
865	2.874954353057093	9.288496248770587	0.001000000000311	0.999999999999178	2.999999999639109	0.000000002064376
866	2.000000000000321	1.001581687062628	0.001000000000200	0.942774221634187	2.999999999757182	0.000000000099254
867	2.000000000000367	3.393084033316650	0.001000000000435	0.793670955213889	2.999999999852373	0.000000000557411
868	2.000000000005031	6.922692926932285	0.001000000000016	0.999999999996211	2.999999998971820	0.000000000691452
869	2.000000000071216	3.518326806733515	0.001000000000006	0.918935731957808	2.999999999516112	0.000000000545024
870	2.000000000030568	8.277915231393285	0.001000000000233	0.861395960784161	2.999999999779340	0.000000001834949
871	2.000000000027224	10.284416174237860	0.001000000000085	0.866433784561708	2.999999999504895	0.000000000016881
872	2.434051428345315	0.027700077804389	0.001000000562452	0.623177080811884	2.999509042491767	0.000217039251924
873	2.000000000032852	6.237666623192183	0.001000000000042	0.866827429241088	2.999999999917519	0.000000000011563
874	3.310760064352622	0.122222690676216	0.001000000000475	0.999999999999061	2.999999999999930	0.000000000891175
875	2.000000000000798	17.637560094750864	0.001000000000092	0.926169650387132	2.999999999918517	0.000000001084551
876	2.000000000025516	9.519868120666700	0.001000000000016	0.997016027501626	2.999999999957702	0.000000000078976
877	2.540345252844707	0.686792974929406	0.001000000000005	0.999999999999522	2.999999999773977	0.000000005043596
878	2.000000000006219	16.662378369100288	0.001000000000018	0.809380653656980	2.999999999986812	0.000000000138485
879	2.000000000017797	1.825560350463616	0.001000000000019	0.866438019571988	2.999999999762999	0.000000001501380
880	2.000000000115065	0.027700000547103	0.001000000000132	0.780841890232598	2.999999998598371	0.000000120028349
881	2.000000000017264	19.234396094075368	0.001000000000001	0.900588508722992	2.999999999990516	0.000000000046771
882	3.274767738717782	11.581409664235371	0.001000000000063	0.990341244715394	2.999999999858819	0.000000001458942
883	2.000000000009937	7.516115010904096	0.001000000000000	0.937068271876574	2.999999999991530	0.000000000614659
884	2.000000000036615	7.804176333099865	0.001000000000044	0.964747477524015	2.999999999998060	0.000000000503594
885	2.000000001303405	5.254026362454675	0.001000000002138	0.785958875976362	2.999999999761152	0.000000007135515

886	2.000000000097894	3.791543608022019	0.001000000000113	0.935377601245417	2.999999998905896	0.000000003751564
887	2.000000000027773	10.237667589264674	0.001000000000244	0.982878265236398	2.999999999907023	0.000000003178218
888	2.000000000002475	7.431471960289490	0.001000000000128	0.882035586621132	2.999999999998392	0.000000004387622
889	2.000000676227716	0.027701042245812	0.001000145865751	0.556563052474352	2.977672085435178	0.004268167308011
890	2.000000000011902	10.206558817379149	0.001000000000409	0.819361126416118	2.999999999863338	0.000000000864173
891	2.000000000121083	2.435915147433633	0.001000000000009	0.863216370829632	2.999999999980760	0.000000001352533
892	2.000000000029169	8.098753580648562	0.001000000000229	0.920847426320977	2.999999999979672	0.000000000957473
893	2.000000000004928	2.634082582696466	0.001000000000139	0.907869377315498	2.999999999997745	0.000000000210039
894	2.000000000619812	13.166688764414992	0.001000000000007	0.815605510413618	2.999999999999951	0.000000005669131
895	2.000010203019930	0.027768905616923	0.001001430229712	0.687620006103658	2.910763285981887	0.014164217489475
896	2.000000000001462	3.478968568928526	0.001000000000049	0.948561155584572	2.999999998645509	0.000000001971002
897	2.000000000002375	6.920805132891387	0.001000000000244	0.883704072479753	2.999999999975209	0.000000000158328
898	2.000008866850087	0.027704162427353	0.001000002705550	0.769257195313336	2.999977964032337	0.000039427462821
899	2.000000000016667	6.638335931269090	0.001000000000160	0.695171234400127	2.999999999908796	0.000000000666330
900	2.000000000098268	17.243171601863907	0.001000000000169	0.759280178465837	2.999999999887580	0.000000009221506
901	2.000000000126276	4.277207801525975	0.001000000000040	0.739636971645027	2.999999999728686	0.000000000058146
902	2.000000000000095	3.064657850736345	0.001000000000011	0.956496618030884	2.999999999924779	0.000000001006135
903	2.000007021479191	0.027720476598353	0.001000340035432	0.887748936283366	2.998562321045792	0.149360437226802
904	3.011055255551598	15.905338755687316	0.001000000000020	0.998802793242142	2.999999998966930	0.000000000373691
905	2.000000000036383	4.024916252412865	0.001000000000181	0.930747347287114	2.999999998685943	0.000000001051787
906	2.000000000037362	20.789872287779708	0.001000000000023	0.886220427338143	2.999999999992014	0.000000000546521
907	2.000000000036868	11.533795938833961	0.001000000000145	0.907225433615489	2.999999999964963	0.000000002813940
908	2.521841183981487	1.386056412958235	0.001000000000330	0.946327122494403	2.999999999114766	0.000000000085933
909	2.000000000002538	9.740066951496164	0.001000000000001	0.974476362816870	2.999999999649035	0.000000000039657
910	2.002165521167342	0.027850483963399	0.001000085939918	0.597672914121342	2.921417269642855	0.000055973694950
911	2.000000000005750	1.835075989411978	0.001000000000238	0.815078696675236	2.999999999217986	0.000000000263609
912	2.000013245801708	0.030132250734163	0.001001313592144	0.662248750684962	2.998637932832199	0.131035488135025
913	3.344079154945566	1.420194578118230	0.001000000000078	0.916175448782055	2.999999999014840	0.000000000202057
914	2.000000000005000	6.534363433395383	0.001000000000017	0.753660634842902	2.999999999567284	0.000000001510948
915	3.220052433690743	0.027940826544197	0.001000109545962	0.990334362695861	2.999901431642997	0.035811888178773
916	2.000000000043054	9.508989222803592	0.001000000000092	0.819611974207667	2.999999999704718	0.000000000324567
917	3.230984059920571	8.011677911041719	0.001000000001186	0.999999999987850	2.999999999588157	0.000000000003565
918	2.000000000002475	12.430615176392626	0.001000000000005	0.910034162776789	2.999999999933098	0.000000000549712
919	2.000000000082936	5.509789926771034	0.001000000000118	0.933173524686877	2.999999999672101	0.000000000512848
920	2.000008630564806	0.027755867193607	0.001000585580119	0.735901839659791	2.920341407257221	0.002515652294988
921	2.000000000041598	11.391504559899280	0.001000000000113	0.872533272188513	2.999999998817978	0.000000000203461
922	2.000000015669300	0.027700003697129	0.001000000008891	0.497630916596669	2.999956213965232	0.000080281881755
923	2.000000000015150	14.706025543321598	0.001000000000173	0.816908037130823	2.999999999987312	0.000000000654914
924	2.618784923616762	19.411452587163851	0.001000000000211	0.868448492065075	2.999999999972061	0.000000000436416
925	2.000002549717783	0.027715016154396	0.001000264169758	0.730025715440382	2.999113088087456	0.210289677588024
926	2.000000000040659	8.955786881572646	0.001000000000157	0.934312088795762	2.999999999997177	0.000000003144477
927	3.197923662531957	6.902439487451662	0.001000000000029	0.999999999986022	2.999999999986148	0.000000002374436
928	2.000000000001915	2.438841121538708	0.001000000000000	0.778280789632899	2.999999999990177	0.000000000096259
929	2.000000001446061	19.619847334407073	0.001000000040543	0.837174481241653	2.999999993931019	4.999999759129117
930	2.000016243303918	0.028390604379467	0.001000176910153	0.876571811686398	2.998979144625634	0.041597850933029
931	2.000000000026098	8.254824304691606	0.001000000000000	0.803531560976080	2.999999999816535	0.000000000527615
932	2.000000000137340	2.224302943379982	0.001000000000072	0.900982893342549	2.999999999578848	0.000000000768251
933	3.053061907908624	6.034857124240603	0.001000000000063	0.964529331540948	2.999999999741563	0.000000000139270
934	2.734117443225243	7.003576953048649	0.001000000000049	0.903542690322153	2.999999999769197	0.000000001617308
935	2.000000000010448	3.052166202858865	0.001000000000106	0.847940391967704	2.999999999617480	0.000000000239715
936	2.000000000001633	8.942464061888776	0.001000000000005	0.959825718360301	2.999999999946072	0.000000000224318
937	2.751280325246635	12.621280505613214	0.001000000000002	0.968176162439294	2.999999999900647	0.000000000141525
938	2.093520136272753	9.497849322228310	0.001000057878468	0.736718193191673	2.999718059230878	0.237096906442299
939	2.000000333456961	0.027700672244524	0.001000001652061	0.725054424385510	2.998969422380392	0.000183675426619
940	2.000013027122887	0.027700048765811	0.001001045569681	0.378463372482678	2.818794796310562	2.269187064155416
941	2.000000000007421	3.340850154707236	0.001000000000013	0.919800917049689	2.999999999951453	0.000000000216541
942	2.000000000006904	5.660550984802939	0.001000000000001	0.900495199156930	2.999999999786406	0.000000003628934
943	2.000008366388438	0.027700006469175	0.001000010530790	0.574015285885804	2.999957267682600	0.000310372826124
944	2.000000000206260	4.332751997354619	0.001000000000004	0.900989431561578	2.999999999997894	0.000000013348143

945	2.000000000057760	8.222060951112951	0.001000000000033	0.791705110037270	2.999999999355558	0.000000000001773
946	2.000000000019223	2.348073435586865	0.001000000000180	0.790186478240037	2.999999999142677	0.000000001462711
947	2.000000000007276	3.743089031498672	0.001000000000146	0.941322815211808	2.999999999766257	0.000000000004308
948	2.697367649858657	13.914890434413206	0.001000000000011	0.926386634647962	2.999999999966446	0.000000000038813
949	2.000000000000707	7.155546700276960	0.001000000000077	0.975339127627670	2.999999999463495	0.000000001021572
950	2.001166720126117	0.029667723555929	0.001010676231991	0.553330144276673	2.926123650825184	0.337961601727470
951	2.000000000018422	14.761022882936132	0.001000000000024	0.858532900268601	2.999999999839528	0.000000000161927
952	2.000000000043528	3.136145210693213	0.001000000000056	0.849662837027640	2.999999999983949	0.000000001998371
953	2.000000000000835	15.217646809865915	0.001000000000000	0.754834835964032	2.999999999897251	0.000000001457814
954	2.000000000000637	9.880028150424156	0.001000000000465	0.940076717321059	2.999999999806055	0.000000000008606
955	2.000000000017061	10.486466892047483	0.001000000000040	0.930769372981286	2.999999999957909	0.000000000195543
956	2.000000000015137	19.984152628132843	0.001000000000002	0.698528067351069	2.999999999909645	0.000000000894586
957	2.000000000033525	16.013975653205154	0.001000000000139	0.738940098100685	2.999999999902499	0.000000001057585
958	2.000000000000028	2.901574467629715	0.001000000000025	0.922848974069012	2.999999999332705	0.000000000077711
959	2.000000000000025	3.049144493253644	0.001000000000152	0.944391791400141	2.999999999067500	0.000000001208639
960	2.000000000009996	6.776485997819758	0.001000000000005	0.979245895914008	2.999999999427810	0.000000000048666
961	2.000000000046983	5.868555836910509	0.001000000000112	0.764072038853804	2.999999999966560	0.000000000207046
962	2.000000000067799	7.109449712735372	0.001000000001190	0.851937901967580	2.999999998963700	0.000000002931889
963	2.000000000024773	8.885331669419537	0.001000000000027	0.994926612983856	2.999999999741787	0.000000002070306
964	2.000000000003768	11.142739568230791	0.001000000000013	0.883714223528585	2.999999999887493	0.000000000656882
965	2.000000000061323	2.997318371056890	0.001000000000015	0.815116255536615	2.999999999801997	0.000000000624525
966	2.000000000040855	0.027700000054477	0.001000000000048	0.650729821660036	2.999999998049157	0.000000000993902
967	2.739496969396552	0.027701565928342	0.001001037395085	0.812706035976720	2.527486043262162	0.492758526887205
968	2.000000000001605	13.099010590212865	0.001000000000003	0.923886593831302	2.999999999992138	0.000000001727483
969	2.000000000003396	17.495243386249790	0.001000000000084	0.920012502610114	2.999999999576130	0.000000001541456
970	2.070855002011800	19.370877985315239	0.001000000000001	0.882857260628199	2.999999999677044	0.000000000002338
971	2.764411325669046	0.028313358657251	0.001000518692464	0.700255371637917	2.996261251912810	0.074980714670314
972	2.000000000000046	7.811567350383785	0.001000000000042	0.949622310966632	2.999999999380855	0.000000001766914
973	2.000000000474650	0.027700000703238	0.001000000002708	0.703664994477938	2.999999982724642	0.000000153302759
974	2.000000000049012	1.975032484258850	0.001000000000014	0.834506123348780	2.999999999898605	0.000000000268593
975	2.000000000047922	5.500557228485836	0.001000000000102	0.897924666442406	2.999999999874393	0.000000000200268
976	2.000000000024984	14.947546821708144	0.001000000000658	0.850258868991724	2.999999999392393	0.000000001147211
977	2.001237305276453	0.040197748048112	0.001005359612274	0.379403483308224	0.694813799042483	3.191735779789943
978	2.000000000009594	9.252874926547888	0.001000000000089	0.999999999988499	2.999999999989818	0.000000000548575
979	2.000000000127487	3.281269839043940	0.001000000000161	0.945902325347352	2.999999999486428	0.000000000257892
980	2.172154295837123	7.366358769940761	0.001000000000260	0.879784440259025	2.999999998577649	0.000000000520756
981	3.159046580208624	20.082307369823312	0.001000000000027	0.893517207531645	2.999999999181717	0.000000000073006
982	2.000000000070343	4.868728461061635	0.001000000000552	0.896031561312046	2.999999999264186	0.000000000339488
983	2.000000000003008	1.473020647934131	0.001000000000117	0.922401723627342	2.999999998649261	0.000000000319240
984	2.000022841075460	0.073437344084026	0.001000000019310	0.800194463035739	2.969274930165557	0.688952317176200
985	2.000000000002320	7.527324493153841	0.001000000000011	0.939145079739417	2.999999999996335	0.000000000006866
986	2.000043580596109	0.027728415723922	0.001000398987762	0.714576331391768	2.945228750398973	0.201896708291528
987	3.037300148703291	3.912826907994053	0.001000000000006	0.913752669459471	2.999999999410793	0.000000000664688
988	2.000000000121832	8.294195468733031	0.001000000000037	0.879478358625578	2.999999999997344	0.000000000744805
989	2.000000000035234	10.412170177342039	0.001000000000009	0.916426200203786	2.999999999999589	0.000000000266002
990	2.000000000044773	6.491326300777807	0.001000000000278	0.804654413625355	2.999999998991348	0.000000000000977
991	2.106573563480180	0.076798125960047	0.001237828797745	0.059587192729011	0.115621013657718	0.384926756717298
992	2.000000000003911	2.273970054505849	0.001000000000223	0.797401843080372	2.999999997856554	0.000000001679344
993	2.691198125477383	6.669800536522661	0.001000000000022	0.896735691466608	2.999999999580513	0.000000000248875
994	2.000000000003462	8.478481848617461	0.001000000000013	0.973739308327716	2.999999999996857	0.000000002091000
995	2.000000000002782	14.733210645394657	0.001000000000054	0.874185503491463	2.999999999018652	0.000000000141237
996	2.000000000006297	4.404573454707332	0.001000000000040	0.924715345358176	2.999999999994151	0.000000003724177
997	2.000000000115890	9.862102596467205	0.001000000000103	0.736688980959709	2.999999999851565	0.000000000164268
998	2.000000000000104	3.801578651648775	0.001000000000000	0.927610698029244	2.999999999983892	0.000000000006846
999	2.000000000053073	2.048933380490236	0.001000000000112	0.816904278852341	2.999999999991373	0.000000000008812
1000	2.000000000045920	10.414003876706982	0.001000000000013	0.902314929199628	2.999999999539643	0.000000004568365

Table A.3: The results of optimisations for 1000 rounds of Nelder-Mead simplex algorithm for low LET IR using 1000 bootstrap data sets.

A.4.5 Estimated parameters using 1000 bootstrap survival data sets for high LET

Run	δ	α_1	α_2	p	V_{max}	K_M
1	2.000000000059444	20.374867983879465	0.001000000000001	0.999999999999762	2.999999999329699	0.000000001669725
2	2.000000000984723	15.625548597360575	0.001000000000074	0.999999999999794	2.999999999622534	0.000000000675759
3	2.000000000124310	2.614552495834114	0.001000000000000	0.999999999999187	2.999999997976015	0.000000000000023
4	2.000000000008478	18.285708562647798	0.001000000000013	0.999999999999985	2.999999999974956	0.000000001824129
5	2.000000000409338	20.199863323024136	0.001000000000004	0.999999999998499	2.999999999882046	0.000000000055728
6	2.000000000037693	14.778858311666092	0.001000000000074	0.999999999999256	2.999999999977909	0.000000000000075
7	2.000000000056490	15.597380991156669	0.001000000000140	0.999999999999476	2.999999999837676	0.000000000100847
8	2.000000000114215	17.573197694217210	0.001000000000271	0.999999999998443	2.999999999965709	0.000000000053627
9	2.000000000056712	4.359935625908421	0.001000000000011	0.999999999999932	2.999999999999881	0.000000000234285
10	2.000000000056712	4.359935625908421	0.001000000000011	0.999999999999932	2.999999999999881	0.000000000234285
11	2.000000000018179	5.193754685752817	0.001000000000021	0.999999999999992	2.999999999754524	0.000000000002343
12	2.000000000101413	12.231813996183911	0.001000000000046	0.999999999998595	2.999999999722242	0.000000000094737
13	2.000000000590529	20.594560209807462	0.001000000000018	0.999999999999537	2.999999999927048	0.000000001388488
14	2.000000000018768	16.114056991655701	0.001000000000959	0.999999999997550	2.999999999966998	0.000000000000061
15	2.000000001083014	17.107039814043482	0.001000000000055	0.999999999999835	2.999999999492968	0.000000000248052
16	2.000000000368305	19.009892232532412	0.001000000000181	0.999999999999613	2.999999999435802	0.000000001677706
17	2.000000000059946	20.231395399989690	0.001000000000000	0.999999999999989	2.999999999797264	0.000000000054756
18	2.000000000007326	11.621985622021601	0.001000000000002	0.999999999999995	2.999999999725284	0.000000000317004
19	2.000000000006851	9.156379903734937	0.001000000000103	0.999999999997520	2.999999999994619	0.000000000296961
20	2.000000000000061	15.710629637833067	0.001000000000013	0.999999999999728	2.999999999645472	0.000000000343611
21	2.000000000002369	19.233603815998066	0.001000000000062	0.999999999999945	2.999999999972345	0.000000000041625
22	2.000000000065708	7.389239283395876	0.001000000000187	0.999999999999776	2.999999999980348	0.000000000000083
23	2.000000000075427	20.337228012400050	0.001000000000098	0.999999999999999	2.999999999521442	0.000000001769089
24	2.000000000036012	13.459574720273976	0.001000000000054	1.000000000000000	2.999999999872550	0.000000000121282
25	2.000000000196438	20.023616159156976	0.001000000000000	0.999999999996981	2.999999999968607	0.000000000438478
26	2.000000000018179	5.193754685752817	0.001000000000021	0.999999999999992	2.999999999754524	0.000000000002343
27	2.000000000009450	0.823814280752754	0.001000000000294	0.999999999999893	2.999999999948431	0.000000000001120
28	2.000000000085537	19.629869370776412	0.001000000000002	0.999999999998723	2.999999999896581	0.000000000002575
29	2.000000000018972	2.609727199072349	0.001000000000002	0.999999999999701	2.999999999946365	0.000000000000005
30	2.000000000035812	20.764686281090011	0.001000000000005	0.999999999999998	2.999999999819912	0.000000000482783
31	2.000000000064755	11.865699768854151	0.001000000000003	0.999999999999904	2.999999999990302	0.000000000001471
32	2.000000000001491	20.540834814816503	0.001000000000060	0.999999999998868	2.999999999722271	0.000000000000093
33	2.000000000036012	13.459574720273976	0.001000000000054	1.000000000000000	2.999999999872550	0.000000000121282
34	2.000000000000981	1.873728810619090	0.001000000000423	0.999999999999747	2.999999999986899	0.000000000087632
35	2.000000000002042	18.278274853865113	0.001000000000044	0.999999999999863	2.999999999963998	0.000000000001157
36	2.000000000033293	4.651964168884549	0.001000000000220	0.999999999999796	2.999999999652761	0.000000000251195
37	2.000000000171114	20.495875012171300	0.001000000000148	0.999999999998998	2.999999999647413	0.000000000382650
38	2.000000000002413	8.725514561328257	0.001000000000017	0.999999999999996	2.999999999801306	0.000000000005021
39	2.000000000200659	19.914892599878552	0.001000000000220	0.999999999999813	2.999999999346287	0.000000000005433
40	2.000000000073847	16.223117401847261	0.001000000000153	0.999999999999838	2.999999999979057	0.000000000427856
41	2.000000000129858	20.546846177245545	0.001000000000096	0.999999999999827	2.999999999941862	0.000000000201909
42	2.000000000028171	18.251770149481807	0.001000000000022	1.000000000000000	2.999999999964680	0.000000002117372
43	2.000000000015553	10.685419950527919	0.001000000000159	0.999999999999916	2.999999999999439	0.000000000181167

44	2.000000000066438	19.914707703864245	0.001000000000676	0.999999999999748	2.999999999949472	0.000000000185916
45	2.000000000129668	20.314763763089683	0.001000000000738	0.999999999999236	2.999999998868620	0.000000000117654
46	2.000000000003305	0.847638479690710	0.001000000000061	0.999999999999725	2.999999999982312	0.000000000255829
47	2.000000000138840	20.056195331704323	0.001000000000025	0.999999999999866	2.999999999999270	0.000000000196489
48	2.000000000007326	11.621985622021601	0.001000000000002	0.999999999999995	2.999999999725284	0.000000000317004
49	2.000000000000032	16.467092861285028	0.001000000000009	0.999999999999825	2.999999999961636	0.000000000001660
50	2.000000000047352	20.773907054990595	0.001000000000197	0.999999999999657	2.999999999998372	0.000000000926397
51	2.000000000201950	18.907436117431651	0.001000000000137	0.999999999996463	2.999999999721814	0.000000000063383
52	2.000000000029405	13.459905524990791	0.001000000000000	1.000000000000000	2.999999999953210	0.000000000413310
53	2.000000000068278	16.551692018483394	0.001000000000038	0.999999999999881	2.999999999976861	0.000000000222339
54	2.000000000001803	17.584282540085930	0.001000000000018	0.999999999999608	2.999999999951305	0.000000000001218
55	2.000000000037427	18.939560995952910	0.001000000000003	0.999999999998166	2.999999999881105	0.000000002643604
56	2.000000000006661	11.826803233744755	0.001000000000031	0.999999999999643	2.999999999999610	0.000000000049717
57	2.000000000004504	16.367948375300802	0.001000000000037	0.999999999999693	2.999999999999845	0.000000000031004
58	2.000000000000374	19.655584253011124	0.001000000000035	0.999999999996056	2.999999999843622	0.000000000043723
59	2.000000000029405	13.459905524990791	0.001000000000000	1.000000000000000	2.999999999953210	0.000000000413310
60	2.000000000037307	19.185564008520529	0.001000000000721	0.999999999998002	2.999999999938102	0.000000000331180
61	2.000000000015376	15.195538372366364	0.001000000001071	0.999999999999163	2.999999999543292	0.000000000114943
62	2.000000000000374	19.655584253011124	0.001000000000035	0.999999999996056	2.999999999843622	0.000000000043723
63	2.000000000003677	19.655218074330268	0.001000000000018	0.999999999999778	2.999999999747017	0.000000001921850
64	2.000000000141199	0.952476230342684	0.001000000000059	0.999999999999987	2.999999999910053	0.000000000035278
65	6.356445247892557	7.545256237393655	0.001000000000032	0.999999999999980	2.999999999982381	0.000000000018576
66	2.000000000026695	19.871864164761472	0.001000000000196	0.999999999999257	2.999999999963632	0.000000000001479
67	2.000000000116122	0.399643685604631	0.001000000000024	0.999999999999916	2.999999999896495	0.000000000006944
68	2.000000000105416	20.325323681756554	0.001000000000184	0.999999999998342	2.999999999542480	0.000000000640510
69	2.000000000006733	18.210452615704192	0.001000000000001	0.999999999998990	2.999999999972370	0.000000000148522
70	2.000000000268441	20.446486536857105	0.001000000000017	0.999999999995906	2.999999999861767	0.000000003069253
71	2.000000000056712	4.359935625908421	0.001000000000011	0.999999999999932	2.999999999999881	0.000000000234285
72	2.000000000096411	4.651997056588666	0.001000000000196	0.999999999999854	2.999999999998066	0.000000000003854
73	2.000000000002365	12.061912890176778	0.001000000000001	0.999999999999947	2.999999999811313	0.000000000114722
74	2.000000000018158	14.986883615790347	0.001000000000034	0.999999999999969	2.999999999982447	0.000000000136799
75	2.000000000000097	13.393769821667522	0.001000000000001	0.999999999999783	2.999999999951200	0.000000000000584
76	2.000000000051033	14.967739908397757	0.001000000000157	0.999999999997471	2.999999999996174	0.000000000024102
77	2.000000000005324	15.625035141564441	0.001000000000032	0.999999999999975	2.999999999866502	0.000000000037760
78	2.000000000129668	20.314763763089683	0.001000000000738	0.999999999999236	2.999999998868620	0.000000000117654
79	2.000000000003677	19.655218074330268	0.001000000000018	0.999999999999778	2.999999999747017	0.000000001921850
80	2.000000000000023	6.460611441143363	0.001000000000006	0.999999999998314	2.999999999768991	0.000000000298454
81	2.000000000077627	20.686074576420189	0.001000000000022	0.999999999999200	2.999999999751130	0.000000000288937
82	2.000000000017915	19.350339206369366	0.001000000000009	0.999999999999755	2.999999999850645	0.000000000724249
83	2.000000000000367	18.818737219456736	0.001000000000003	0.999999999999931	2.999999999986929	0.000000000207283
84	2.000000000180820	18.912220793289986	0.001000000000073	0.999999999998920	2.999999999326213	0.000000000094297
85	2.000000000020537	19.082982269469412	0.001000000000083	0.999999999999039	2.999999999410027	0.000000000024059
86	2.000000000000374	19.655584253011124	0.001000000000035	0.999999999996056	2.999999999843622	0.000000000043723
87	2.000000000215718	19.801323964939616	0.001000000000040	0.999999999999766	2.999999999999229	0.000000000056911
88	2.000000000000496	20.136030100257244	0.001000000000391	0.999999999995324	2.999999998722894	0.000000000728251
89	2.000000000140426	10.541718584772882	0.001000000000013	0.999999999994739	2.999999999999711	0.000000000495474
90	2.000000000121193	20.245495711267086	0.001000000000198	0.999999999997447	2.999999999662197	0.000000000752580
91	2.000000000002228	19.051543128758052	0.001000000000028	0.999999999999997	2.999999999996157	0.000000000114161
92	2.000000000078333	18.912262099326526	0.001000000000394	0.999999999999166	2.999999999910539	0.000000000316794
93	2.417054373563151	20.682557339107962	0.001000000000003	0.999999999999952	2.999999999998885	0.000000000352866
94	2.000000000132094	15.489859591107345	0.001000000000045	0.999999999999988	2.999999999900425	0.000000001602693
95	2.000000000011271	15.465397813864335	0.001000000000000	0.999999999999984	2.999999999995018	0.000000000175297
96	2.000000000139545	7.299565912368973	0.001000000000066	0.999999999999932	2.999999999128995	0.000000000148091
97	2.000000000020537	19.082982269469412	0.001000000000083	0.999999999999039	2.999999999410027	0.000000000024059
98	2.000000000167275	18.335695590398668	0.001000000000552	0.999999999999979	2.999999999901800	0.000000000000004
99	2.000000000155138	4.354690480330338	0.001000000000322	0.999999999999864	2.999999999993615	0.000000005068813
100	2.000000000001831	20.417734992821792	0.001000000000035	0.999999999999984	2.999999999994390	0.000000000067355
101	2.000000000012290	18.884557159491418	0.001000000000096	0.999999999999997	2.999999999409513	0.000000000010080
102	2.000000000121193	20.245495711267086	0.001000000000198	0.999999999997447	2.999999999662197	0.000000000752580

103	2.000000000000032	11.602799670138085	0.001000000000003	0.999999999999996	2.999999999997960	0.000000000000517
104	2.000000000045068	20.242261041906534	0.001000000000064	0.999999999999756	2.999999999971248	0.000000000873709
105	2.000000000295170	20.123621339785032	0.001000000000239	0.999999999999749	2.999999999026489	0.000000000802086
106	2.000000000484068	10.910603753181588	0.001000000000002	0.999999999998762	2.999999999453784	0.000000001791114
107	2.000000000018179	5.193754685752817	0.001000000000021	0.999999999999992	2.999999999754524	0.000000000002343
108	2.000000000029405	13.459905524990791	0.001000000000000	1.000000000000000	2.999999999953210	0.000000000413310
109	5.931817821914540	0.028636709721689	0.001000000000063	0.999999999999760	2.999999999672700	0.000000000030825
110	2.000000000173291	17.107686186124301	0.001000000000023	0.999999999999709	2.999999999536430	0.000000000089159
111	2.000000000119406	20.588573245188563	0.001000000000001	0.999999999999996	2.999999999954536	0.000000000112864
112	2.000000000019605	20.077704075970015	0.001000000000000	0.999999999999917	2.999999999966773	0.000000000243944
113	2.000000000124884	20.137961357147979	0.001000000000214	0.999999999999904	2.999999999854041	0.000000000000047
114	2.000000000942925	20.296583394845218	0.001000000000437	0.999999999993972	2.999999999625428	0.000000000037002
115	2.000000000020436	1.874783365725943	0.001000000000040	0.999999999999152	2.999999999817360	0.000000000134221
116	2.000000000196438	20.023616159156976	0.001000000000000	0.999999999996981	2.999999999968607	0.000000000438478
117	2.000000000000304	20.787319103597710	0.001000000000006	0.999999999999994	2.999999999997500	0.000000000059564
118	2.000000000038107	15.974916616490992	0.001000000000005	0.999999999999838	2.999999999603517	0.000000000071890
119	2.000000000245950	20.450098492275732	0.001000000000299	0.999999999998865	2.999999999858258	0.000000000001339
120	2.000000000037588	7.634671658404160	0.001000000000000	0.999999999999988	2.999999999996963	0.000000000047341
121	2.000000000018179	5.193754685752817	0.001000000000021	0.999999999999992	2.999999999754524	0.000000000002343
122	2.000000000051033	14.967739908397757	0.001000000000157	0.999999999997471	2.999999999996174	0.000000000024102
123	2.000000000020436	1.874783365725943	0.001000000000040	0.999999999999152	2.999999999817360	0.000000000134221
124	2.000000000291978	14.956009839600384	0.001000000000008	0.999999999998685	2.999999999806906	0.000000001225190
125	2.000000000001491	20.540834814816503	0.001000000000060	0.999999999998868	2.999999999722271	0.000000000000093
126	2.000000000091667	20.265894815059045	0.001000000000061	0.999999999999916	2.999999999407388	0.000000001788220
127	2.000000000000118	0.408850433046796	0.001000000000010	0.999999999999795	2.999999998567619	0.000000000089681
128	2.000000000008471	20.448665100666837	0.001000000000460	0.999999999999965	2.999999999896097	0.000000002759160
129	2.000000000375741	18.885197817793383	0.001000000000029	0.999999999999671	2.999999999992050	0.000000001342992
130	2.000000000000500	20.546920748963434	0.001000000000195	0.999999999993406	2.999999999447572	0.000000001499002
131	2.000000000012273	10.697462747781351	0.001000000000002	0.999999999999968	2.999999999991163	0.000000000020755
132	2.000000000020436	1.874783365725943	0.001000000000040	0.999999999999152	2.999999999817360	0.000000000134221
133	4.746237577940350	19.785292210846080	0.001000000000085	0.999999999995226	2.999999999707698	0.000000001555008
134	2.000000000018394	14.958197507656726	0.001000000000141	0.999999999999769	2.999999999516898	0.000000001044971
135	2.000000000043908	1.872364050262448	0.001000000000091	0.999999999999996	2.999999999544694	0.000000000384918
136	2.000000000106458	20.785786204525202	0.001000000000243	0.999999999999571	2.999999999700628	0.000000000072335
137	2.000000000124884	20.137961357147979	0.001000000000214	0.999999999999904	2.999999999854041	0.000000000000047
138	2.000000000000023	6.460611441143363	0.001000000000006	0.999999999998314	2.999999999768991	0.000000000298454
139	2.000000000093667	18.912163069001384	0.001000000000390	0.999999999999003	2.999999999998680	0.000000002839273
140	2.000000000296631	13.278118728151133	0.001000000001370	0.999999999999432	2.999999998494644	0.000000000133600
141	2.000000000002053	12.745509404794934	0.001000000000012	0.999999999999966	2.999999999881033	0.000000000069081
142	2.000000000059876	20.591397347287970	0.001000000000010	1.000000000000000	2.999999999978060	0.000000000023982
143	2.000000000107631	19.930739054112447	0.001000000000103	0.999999999998263	2.999999999758416	0.000000000089855
144	2.000000000015553	10.685419950527919	0.001000000000159	0.999999999999916	2.999999999999439	0.000000000181167
145	2.000000000025147	0.951154307010030	0.001000000000014	0.999999999999997	2.999999999997594	0.000000000720934
146	2.000000000307482	17.103096133219683	0.001000000000143	0.999999999999590	2.999999999996156	0.000000007492419
147	2.000000000139545	7.299565912368973	0.001000000000066	0.999999999999932	2.999999999128995	0.000000000148091
148	2.000000000002641	9.140540510820037	0.001000000000005	0.999999999999980	2.999999999985751	0.000000000021687
149	2.000000000091452	20.764675531299371	0.001000000000046	1.000000000000000	2.999999999828107	0.000000000038948
150	2.000000000029405	13.459905524990791	0.001000000000000	1.000000000000000	2.999999999953210	0.000000000413310
151	2.000000000028635	1.874496394763732	0.001000000000000	0.999999999999406	2.999999999839794	0.000000000687123
152	2.000000000368305	19.009892232532412	0.001000000000181	0.999999999999613	2.999999999435802	0.000000001677706
153	2.000000000323988	16.443197912782963	0.001000000000011	0.999999999997383	2.999999999928235	0.000000000013980
154	2.000000000065382	13.239519239429297	0.001000000000015	0.999999999999773	2.999999999983039	0.000000000208908
155	2.000000000284389	17.048977708880027	0.001000000000004	0.999999999997906	2.999999999533023	0.000000000104689
156	2.000000000069379	18.917437640049670	0.001000000000021	0.999999999999984	2.999999999803686	0.000000001693023
157	2.000000000186391	19.690419732832275	0.001000000000189	0.999999999998810	2.999999999066257	0.000000001690292
158	2.000000000011912	18.701208392277341	0.001000000000004	0.999999999999995	2.999999999979045	0.000000000042602
159	2.000000000297496	16.558168643936732	0.001000000000027	0.999999999997690	2.999999999762020	0.000000000780759
160	2.000000000033293	4.651964168884549	0.001000000000220	0.999999999999796	2.999999999652761	0.000000000251195
161	2.000000000000084	2.492547276646806	0.001000000000006	0.999999999999967	2.999999999874957	0.000000000025350

162	2.000000000028635	1.874496394763732	0.001000000000000	0.999999999999406	2.999999999839794	0.000000000687123
163	2.000000000020537	19.082982269469412	0.001000000000083	0.999999999999039	2.999999999410027	0.000000000024059
164	2.000000000144496	17.049573659419114	0.001000000000091	0.999999999995633	2.999999999988408	0.000000000238854
165	2.000000000176297	20.433829643477200	0.001000000000011	0.999999999999271	2.999999999789953	0.000000002121122
166	2.000000000000374	19.655584253011124	0.001000000000035	0.999999999996056	2.999999999843622	0.000000000043723
167	2.000000000001118	7.273261907661723	0.001000000000014	0.999999999996717	2.999999999999165	0.000000000574470
168	2.000000000090640	20.092438795337532	0.001000000000049	0.999999999999981	2.999999999890854	0.000000000989271
169	2.000000000021240	20.212663143072415	0.001000000000007	1.000000000000000	2.999999999998892	0.000000000851444
170	2.000000000000023	6.460611441143363	0.001000000000006	0.999999999998314	2.999999999768991	0.000000000298454
171	2.000000000296169	5.475782900868603	0.001000000000011	0.999999999999945	2.999999999799636	0.000000000340485
172	2.000000000067704	19.791611366467844	0.001000000000046	0.999999999999997	2.999999999907768	0.000000002289426
173	2.000000000034127	15.268165902736392	0.001000000000066	0.999999999999921	2.999999999855589	0.000000001064229
174	2.000000000001612	0.546214518882735	0.001000000000002	0.999999999996597	2.999999999403937	0.000000000001510
175	2.000000000665239	20.092462553759383	0.001000000000042	0.999999999999581	2.999999999712876	0.000000002017706
176	2.000000000112200	9.101554002695449	0.001000000000015	0.999999999995721	2.999999996057326	0.000000005453143
177	2.000000000000500	20.546920748963434	0.001000000000195	0.999999999993406	2.999999999447572	0.000000001499002
178	2.000000000020436	1.874783365725943	0.001000000000040	0.999999999999152	2.999999999817360	0.000000000134221
179	2.000000000033426	14.545400871125413	0.001000000000014	0.999999999999994	2.999999999338882	0.000000000028574
180	2.000000000083508	19.735187948498883	0.001000000000299	0.999999999999986	2.999999999637273	0.000000000006223
181	2.000000000028399	20.255896823909172	0.001000000000072	0.999999999997673	2.999999999581569	0.000000000209686
182	2.000000000050160	0.866936339640635	0.001000000000028	0.999999999999654	2.999999999969210	0.000000000145084
183	2.000000000501859	20.607497262214419	0.001000000000035	0.999999999999761	2.999999999743579	0.000000000308043
184	2.000000000008471	20.448665100666837	0.001000000000460	0.999999999999965	2.999999999896097	0.000000002759160
185	2.000000000000023	6.460611441143363	0.001000000000006	0.999999999998314	2.999999999768991	0.000000000298454
186	2.000000000100734	20.290745547779050	0.001000000000845	0.999999999999700	2.999999999998060	0.000000001641789
187	2.000000000129858	20.546846177245545	0.001000000000096	0.999999999999827	2.999999999941862	0.000000000201909
188	2.000000000000068	20.029846452343516	0.001000000000017	0.999999999999918	2.999999999972962	0.000000000064656
189	2.000000000006807	17.927488532149038	0.001000000000000	0.999999999999386	2.999999999997969	0.000000000050665
190	2.000000000002639	17.763281322823044	0.001000000000000	0.999999999999731	2.999999999835676	0.000000000770084
191	2.000000001083014	17.107039814043482	0.001000000000055	0.999999999999835	2.999999999492968	0.000000000248052
192	2.000000000514404	19.118274862335017	0.001000000000757	0.999999999993150	2.999999998630500	0.000000003910361
193	2.000000000093667	18.912163069001384	0.001000000000390	0.999999999999003	2.999999999998680	0.000000002839273
194	2.000000000000496	20.136030100257244	0.001000000000391	0.999999999995324	2.999999998722894	0.000000000728251
195	2.000000000219481	17.137358718463453	0.001000000000000	0.999999999996949	2.999999999419268	0.000000000347836
196	2.000000000007839	19.112321725352853	0.001000000000013	0.999999999999531	2.999999999901186	0.000000000215067
197	2.000000000002369	19.233603815998066	0.001000000000062	0.999999999999945	2.999999999972345	0.000000000041625
198	2.000000000003677	20.239174650037306	0.001000000000010	0.999999999997808	2.999999999896909	0.000000000110573
199	2.000000000005077	14.958005371348623	0.001000000000083	0.999999999999996	2.999999999999984	0.000000000018670
200	2.000000000293280	15.566285047439845	0.001000000000302	0.999999999999929	2.999999999885130	0.000000000881783
201	2.000000000073611	19.941294664931455	0.001000000000006	0.999999999999941	2.999999999849495	0.000000000677708
202	2.000000000121193	20.245495711267086	0.001000000000198	0.999999999997447	2.999999999662197	0.000000000752580
203	2.000000000028089	20.418664791893015	0.001000000000325	1.000000000000000	2.999999996712892	0.000000000867254
204	2.000000000080858	18.106127481064888	0.001000000000059	0.999999999999771	2.999999999970403	0.000000001056265
205	2.000000000291978	14.956009839600384	0.001000000000008	0.999999999998685	2.999999999806906	0.000000001225190
206	2.000000000025147	0.951154307010030	0.001000000000014	0.999999999999997	2.999999999997594	0.000000000720934
207	2.000000000001118	7.273261907661723	0.001000000000014	0.999999999996717	2.999999999999165	0.000000000574470
208	2.000000001027346	19.248179280377251	0.001000000000078	0.999999999999997	2.999999999470742	0.000000007695537
209	2.000000000090640	20.092438795337532	0.001000000000049	0.999999999999981	2.999999999890854	0.000000000989271
210	2.000000000000502	17.422517280554406	0.001000000000010	0.999999999998973	2.999999999976178	0.000000000065820
211	2.000000000000951	14.747783363191582	0.001000000000128	0.999999999999942	2.999999999304313	0.000000000044716
212	2.000000000004708	18.176552653922155	0.001000000000023	0.999999999999961	2.999999999992464	0.000000000266532
213	2.000000000215718	19.801323964939616	0.001000000000040	0.999999999999766	2.999999999999229	0.000000000056911
214	2.000000000002641	9.140540510820037	0.001000000000005	0.999999999999980	2.999999999985751	0.000000000021687
215	2.000000000019818	20.316343469065849	0.001000000000125	0.999999999996546	2.999999999910491	0.000000000324517
216	2.000000000013948	19.109772065817729	0.001000000000993	0.999999999999875	2.999999999582878	0.000000000413790
217	2.000000000219481	17.137358718463453	0.001000000000000	0.999999999996949	2.999999999419268	0.000000000347836
218	2.000000000018394	14.958197507656726	0.001000000000141	0.999999999999769	2.999999999516898	0.000000001044971
219	2.000000000019818	20.316343469065849	0.001000000000125	0.999999999996546	2.999999999910491	0.000000000324517
220	2.000000000000656	1.414290351157161	0.001000000000009	0.999999999999480	2.999999999189583	0.000000000117963

221	2.000000000000487	0.070073604920370	0.001000000000000	0.999999999999852	2.999999999976426	0.000000000018979
222	2.000000000022847	3.905566375869756	0.001000000000010	0.999999999999929	2.999999999959014	0.000000000009831
223	2.000000000040195	16.265455904660005	0.001000000000030	0.999999999999998	2.999999999215623	0.000000000045052
224	2.000000000089984	19.551145367788330	0.001000000000006	0.999999999999427	2.999999999148618	0.000000000026205
225	2.000000000012205	19.801734752702565	0.001000000000013	0.999999999998354	2.999999999421613	0.000000000027902
226	2.000000000017403	19.050556481053313	0.001000000000007	0.999999999999947	2.999999999913626	0.000000000052006
227	2.000000000028142	18.215637058002681	0.001000000000000	0.999999999999839	2.999999999924225	0.000000000006705
228	2.000000000004381	18.211498178087723	0.001000000000024	0.999999999999996	2.999999999992582	0.000000000049364
229	2.000000000084953	12.472016447380270	0.001000000000159	0.999999999999998	2.999999999999985	0.000000000147816
230	2.000000000230999	20.049595893140367	0.001000000000059	0.999999999998566	2.999999998595591	0.000000000179153
231	2.000000000165476	20.598239422758919	0.001000000000032	0.999999999999959	2.999999999969352	0.000000000164498
232	2.000000000027437	16.410764852849702	0.001000000000041	0.999999999999909	2.999999999876263	0.000000000240337
233	2.000000000140787	19.794734547739903	0.001000000000089	0.999999999999844	2.999999999829830	0.000000000167770
234	2.000000000004708	18.176552653922155	0.001000000000023	0.999999999999961	2.999999999992464	0.000000000266532
235	2.000000000000181	16.685435632441777	0.001000000000264	0.999999999999969	2.999999999576240	0.000000000003329
236	2.000000000022092	13.249441268474952	0.001000000000020	0.999999999998398	2.999999999807999	0.000000000101948
237	2.000000000375741	18.885197817793383	0.001000000000029	0.999999999999671	2.999999999992050	0.000000001342992
238	2.000000000084191	20.452787792241764	0.001000000000277	0.999999999999782	2.999999999929472	0.000000001690566
239	2.000000000000500	20.546920748963434	0.001000000000195	0.999999999993406	2.999999999447572	0.000000001499002
240	2.000000000025284	9.474983507027096	0.001000000000010	0.999999999999950	2.999999999970586	0.000000000159004
241	2.000000000000038	14.929475495875893	0.001000000000301	0.999999999999119	2.999999999940974	0.000000000411393
242	2.000000000056910	18.633866462257281	0.001000000000050	0.999999999999847	2.999999999616130	0.000000000037814
243	2.000000000005723	19.081659721965021	0.001000000000799	0.999999999995135	2.999999999952479	0.000000000199845
244	2.000000000003329	15.359993649410770	0.001000000000012	0.999999999999657	2.999999999758193	0.000000000084209
245	2.000000000009328	20.068558831834977	0.001000000000291	0.999999999999916	2.999999999238089	0.000000000824715
246	2.000000000077182	20.541045546955630	0.001000000000185	0.999999999998872	2.999999999999978	0.000000000817203
247	2.000000000000945	15.084816449921240	0.001000000000000	1.000000000000000	2.999999999972823	0.000000000558357
248	2.000000000000964	20.316113604686585	0.001000000000009	0.999999999999740	2.999999999990327	0.000000000010306
249	2.000000000056712	4.359935625908421	0.001000000000011	0.999999999999932	2.999999999999881	0.000000000234285
250	2.000000000001118	7.273261907661723	0.001000000000014	0.999999999996717	2.999999999999165	0.000000000574470
251	2.000000000119096	19.545912884335401	0.001000000000002	0.999999999999591	2.999999999912222	0.000000000138398
252	2.000000000139545	7.299565912368973	0.001000000000066	0.999999999999932	2.999999999128995	0.000000000148091
253	2.000000000007951	13.279944970757555	0.001000000000000	0.999999999998480	2.999999999579723	0.000000000299423
254	2.000000000029405	13.459905524990791	0.001000000000000	1.000000000000000	2.999999999953210	0.000000000413310
255	2.000000000009963	2.648760509307296	0.001000000000006	1.000000000000000	2.999999999999546	0.000000000000663
256	2.000000000007056	18.207142358615712	0.001000000000000	0.999999999999890	2.999999999976293	0.000000000016368
257	2.000000000058530	19.554783844269327	0.001000000000049	0.999999999999939	2.999999999999720	0.000000000805341
258	2.000000000124884	20.137961357147979	0.001000000000214	0.999999999999904	2.999999999854041	0.000000000000047
259	2.000000000004449	20.290916401710497	0.001000000000036	0.999999999994087	2.999999999702825	0.000000000439640
260	2.000000000078333	18.912262099326526	0.001000000000394	0.999999999999166	2.999999999910539	0.000000000316794
261	2.000000000042585	20.316486578463387	0.001000000000281	0.999999999999800	2.999999999971059	0.000000000060491
262	2.000000000020537	19.082982269469412	0.001000000000083	0.999999999999039	2.999999999410027	0.000000000024059
263	2.000000000028142	18.215637058002681	0.001000000000000	0.999999999999839	2.999999999924225	0.000000000006705
264	2.000000000033293	4.651964168884549	0.001000000000220	0.999999999999796	2.999999999652761	0.000000000251195
265	2.000000001254019	20.075994273685577	0.001000000003952	0.999999999998184	2.999999999964126	0.000000005296387
266	2.000000000000500	20.546920748963434	0.001000000000195	0.999999999993406	2.999999999447572	0.000000001499002
267	2.000000000000239	20.771894635877945	0.001000000000030	0.999999999999628	2.999999999927539	0.000000000432407
268	2.000000000186927	0.407613707409658	0.001000000000026	0.999999999999999	2.999999999224154	0.000000000305112
269	2.000000000155138	4.354690480330338	0.001000000000322	0.999999999999864	2.999999999993615	0.000000005068813
270	2.000000000176297	20.433829643477200	0.001000000000011	0.999999999999271	2.999999999789953	0.000000002121122
271	2.000000000201950	18.907436117431651	0.001000000000137	0.999999999996463	2.999999999721814	0.000000000063383
272	2.000000000000219	20.350171293899113	0.001000000000183	0.999999999999996	2.999999999812399	0.000000001516437
273	2.000000000019820	19.801196790271277	0.001000000000075	0.999999999999135	2.999999999845574	0.000000000086171
274	2.000000000197385	20.318135237444029	0.001000000000080	0.999999999998780	2.999999999850737	0.000000000147164
275	2.000000000001803	17.584282540085930	0.001000000000018	0.999999999999608	2.999999999951305	0.000000000001218
276	2.000000000020238	11.435305646146372	0.001000000000058	0.999999999999269	2.999999999976297	0.000000000680191
277	2.000000000029405	13.459905524990791	0.001000000000000	1.000000000000000	2.999999999953210	0.000000000413310
278	2.000000000015553	10.685419950527919	0.001000000000159	0.999999999999916	2.999999999999439	0.000000000181167
279	2.000000000003346	16.454091450921190	0.001000000000002	1.000000000000000	2.999999999890498	0.000000000036055

280	2.000000000124884	20.137961357147979	0.001000000000214	0.999999999999904	2.999999999854041	0.000000000000047
281	2.000000000200218	18.102392678474182	0.001000000000028	0.999999999999960	2.999999999934211	0.000000000623475
282	2.000000000004305	18.758487338682102	0.001000000000000	0.999999999991014	2.999999999764739	0.000000002374342
283	2.000000000000270	18.279390010522395	0.001000000000012	0.999999999999974	2.999999999998507	0.000000000183685
284	2.000000000002557	19.865495208815631	0.001000000000019	0.999999999999680	2.999999999999380	0.000000000000018
285	2.000000000044671	0.847581971628956	0.001000000000004	0.999999999999477	2.999999999993300	0.000000000326246
286	5.384689073379001	20.746406098943737	0.001000000000017	0.999999999990243	2.999999999388093	0.000000002807956
287	2.218546719162732	20.063969118504392	0.001000000000000	0.999999999999997	2.999999999963785	0.000000000002964
288	2.000000000086999	20.061318033544964	0.001000000000021	0.999999999998822	2.999999999576226	0.000000000234696
289	2.000000000023575	20.757886009887120	0.001000000000001	0.999999999999874	2.999999999275877	0.000000000121251
290	2.000000000000023	6.460611441143363	0.001000000000006	0.999999999998314	2.999999999768991	0.000000000298454
291	2.000000000129668	20.314763763089683	0.001000000000738	0.999999999999236	2.999999998868620	0.000000000117654
292	2.000000000268441	20.446486536857105	0.001000000000017	0.999999999995906	2.999999999861767	0.000000003069253
293	2.000000000001257	17.986390491962400	0.001000000000051	1.000000000000000	2.999999999834150	0.000000000234622
294	2.000000000053109	4.651887507246677	0.001000000000307	0.999999999999584	2.999999999526662	0.000000000207259
295	2.000000000107631	19.930739054112447	0.001000000000103	0.999999999998263	2.999999999758416	0.000000000089855
296	2.000000000769843	20.140677094176969	0.001000000000000	0.999999999998729	2.999999997658303	0.000000000882749
297	2.000000000000981	1.873728810619090	0.001000000000423	0.999999999999747	2.999999999986899	0.000000000087632
298	2.000000000022847	3.905566375869756	0.001000000000010	0.999999999999929	2.999999999959014	0.000000000009831
299	2.000000000091186	14.781881091576130	0.001000000000042	0.999999999999830	2.999999999506785	0.000000000099153
300	2.000000000013948	19.109772065817729	0.001000000000993	0.999999999999875	2.999999999582878	0.000000000413790
301	2.000000000000964	20.316113604686585	0.001000000000009	0.999999999999740	2.999999999990327	0.000000000010306
302	2.000000000311332	20.441577406682686	0.001000000000007	0.999999999996792	2.999999999886981	0.000000000023814
303	2.000000000000363	0.544486062503442	0.001000000000421	0.999999999999790	2.999999999394015	0.000000000122253
304	2.000000000167058	18.102363710997551	0.001000000000006	0.999999999999569	2.999999999970886	0.000000000336856
305	2.000000000012884	13.459258157589883	0.001000000000062	0.999999999999556	2.999999999618755	0.000000000049055
306	2.000000000018179	5.193754685752817	0.001000000000021	0.999999999999992	2.999999999754524	0.000000000002343
307	2.000000000020478	20.212660528082374	0.001000000000007	0.999999999999998	2.999999999998255	0.000000000871649
308	2.000000000000981	1.873728810619090	0.001000000000423	0.999999999999747	2.999999999986899	0.000000000087632
309	2.000000000000169	8.526952333778237	0.001000000000006	0.999999999999999	2.999999999964370	0.000000000002305
310	2.000000000002335	2.681201443100794	0.001000000000051	0.999999999999879	2.999999999997226	0.000000000321584
311	2.000000000012884	13.459258157589883	0.001000000000062	0.999999999999556	2.999999999618755	0.000000000049055
312	2.000000000006575	20.060263170700868	0.001000000000015	0.999999999999870	2.999999999998547	0.000000000114076
313	2.000000000000262	20.290846885252666	0.001000000000345	0.999999999998617	2.999999999492750	0.000000000308312
314	2.000000000139545	7.299565912368973	0.001000000000066	0.999999999999932	2.999999999128995	0.000000000148091
315	2.000000000001859	20.778499890249687	0.001000000000016	0.999999999999999	2.999999999980230	0.000000000622163
316	2.000000000245950	20.450098492275732	0.001000000000299	0.999999999998865	2.999999999858258	0.000000000001339
317	2.000000000000000	20.083373217384690	0.001000000000001	0.999999999999835	2.999999999547400	0.000000000000027
318	2.000000000056712	4.359935625908421	0.001000000000011	0.999999999999932	2.999999999999881	0.000000000234285
319	2.000000000022073	19.082982830446156	0.001000000000096	0.999999999999147	2.999999999415225	0.000000000019447
320	2.000000000002487	4.652089680768934	0.001000000000296	0.999999999999748	2.999999999980603	0.000000000111973
321	2.000000000002917	0.642045684723102	0.001000000000000	0.999999999999933	2.999999999999655	0.000000000072846
322	2.000000000139545	7.299565912368973	0.001000000000066	0.999999999999932	2.999999999128995	0.000000000148091
323	2.000000000010252	20.267057024688654	0.001000000000044	0.999999999998545	2.999999999799760	0.000000001643684
324	2.000000000007799	18.207037675117377	0.001000000000006	0.999999999999892	2.999999999926201	0.000000000049519
325	2.000000000000002	19.393512869168315	0.001000000000254	0.999999999999638	2.999999999838018	0.000000000020686
326	2.000000000291978	14.956009839600384	0.001000000000008	0.999999999998685	2.999999999806906	0.000000001225190
327	2.000000000000262	20.290846885252666	0.001000000000345	0.999999999998617	2.999999999492750	0.000000000308312
328	2.000000000027765	1.961268326236680	0.001000000000138	0.999999999999933	2.999999999825652	0.000000000282762
329	2.000000000000542	8.526764936558099	0.001000000000003	0.999999999999996	2.999999999954646	0.000000000000697
330	2.000000000000023	6.460611441143363	0.001000000000006	0.999999999998314	2.999999999768991	0.000000000298454
331	2.000000000000654	0.638911809518345	0.001000000000001	0.999999999999840	2.999999999865050	0.000000000195388
332	2.000000000380958	19.718813990268188	0.001000000000331	0.999999999999788	2.999999999629644	0.000000000232824
333	2.000000000116122	0.399643685604631	0.001000000000024	0.999999999999916	2.999999999896495	0.000000000006944
334	2.000000000000774	5.191474108038015	0.001000000000004	0.999999999999798	2.999999999988340	0.000000000359278
335	2.000000000006773	15.982341095677629	0.001000000000023	0.999999999999867	2.999999999872628	0.000000000014078
336	2.000000000018179	5.193754685752817	0.001000000000021	0.999999999999992	2.999999999754524	0.000000000002343
337	2.000000000124884	20.137961357147979	0.001000000000214	0.999999999999904	2.999999999854041	0.000000000000047
338	2.000000000004504	16.367948375300802	0.001000000000037	0.999999999999693	2.999999999999845	0.000000000031004

339	2.000000000022575	15.970153329071868	0.001000000000031	0.999999999999995	2.999999999999073	0.000000000622805
340	2.000000000099978	20.557865991155804	0.001000000000001	0.999999999998974	2.999999998894436	0.000000002533405
341	2.000000000018394	14.958197507656726	0.001000000000141	0.999999999999769	2.999999999516898	0.000000001044971
342	2.000000000201950	18.907436117431651	0.001000000000137	0.999999999996463	2.999999999721814	0.000000000063383
343	2.000000000001911	20.217289955037927	0.001000000000196	0.999999999992195	2.999999999955826	0.000000000077882
344	2.000000000245950	20.450098492275732	0.001000000000299	0.999999999998865	2.999999999858258	0.000000000001339
345	2.000000000037286	17.627548237938559	0.001000000000042	0.999999999999228	2.999999999916042	0.000000000036711
346	5.032929137312148	13.031530358089134	0.001000000000065	0.999999999998468	2.999999999905829	0.000000000039840
347	2.000000000000374	19.655584253011124	0.001000000000035	0.999999999996056	2.999999999843622	0.000000000043723
348	2.000000000014182	19.225359373462162	0.001000000000002	0.999999999999919	2.999999999932488	0.000000000003215
349	2.000000000011912	18.701208392277341	0.001000000000004	0.999999999999995	2.999999999979045	0.000000000042602
350	2.000000000025638	18.217165731348135	0.001000000000000	0.999999999999830	2.999999999831180	0.000000000151320
351	2.000000000022356	16.562226694741021	0.001000000000042	0.999999999999059	2.999999999436119	0.000000000601330
352	2.000000000096411	4.651997056588666	0.001000000000196	0.999999999999854	2.999999999998066	0.000000000003854
353	2.000000000024419	14.611088415732070	0.001000000000010	1.000000000000000	2.999999999860783	0.000000000241429
354	2.000000000001283	18.207218920985866	0.001000000000020	0.999999999999999	2.999999999955479	0.000000000038685
355	2.000000000001491	20.540834814816503	0.001000000000060	0.999999999998868	2.999999999722271	0.000000000000093
356	2.000000000000901	2.676261472868217	0.001000000000009	0.999999999998819	2.999999999943896	0.000000000203360
357	2.000000000017797	2.622512737467474	0.001000000000324	0.999999999999952	2.999999999986763	0.000000000001429
358	2.000000000200218	18.102392678474182	0.001000000000028	0.999999999999960	2.999999999934211	0.000000000623475
359	2.000000000049730	20.137980616223096	0.001000000000229	0.999999999999898	2.999999999657784	0.000000000004515
360	2.000000000000243	14.776445987493636	0.001000000000007	0.999999999999987	2.999999998992805	0.000000000154041
361	2.000000000036012	13.459574720273976	0.001000000000054	1.000000000000000	2.999999999872550	0.000000000121282
362	2.000000000284389	17.048977708880027	0.001000000000004	0.999999999997906	2.999999999533023	0.000000000104689
363	2.000000000034127	15.268165902736392	0.001000000000066	0.999999999999921	2.999999999855589	0.000000001064229
364	2.000000000000262	20.290846885252666	0.001000000000345	0.999999999998617	2.999999999492750	0.000000000308312
365	2.000000000000374	19.655584253011124	0.001000000000035	0.999999999996056	2.999999999843622	0.000000000043723
366	2.000000000097527	17.221951947948526	0.001000000000000	0.999999999999959	2.999999999854683	0.000000000179066
367	2.000000000020436	1.874783365725943	0.001000000000040	0.999999999999152	2.999999999817360	0.000000000134221
368	2.000000000002917	15.548036124664932	0.001000000000015	0.999999999999752	2.999999999984782	0.000000000048664
369	2.000000000139545	7.299565912368973	0.001000000000066	0.999999999999932	2.999999999128995	0.000000000148091
370	2.000000000196438	20.023616159156976	0.001000000000000	0.999999999996981	2.999999999968607	0.000000000438478
371	2.000000000017717	18.276077472033791	0.001000000000005	0.999999999999460	2.999999999679315	0.000000000199293
372	2.000000000000433	0.823639041772745	0.001000000000023	0.999999999998164	2.999999999998403	0.000000000373299
373	2.000000000066438	19.914707703864245	0.001000000000676	0.999999999999748	2.999999999949472	0.000000000185916
374	2.000000000004109	19.071258228388540	0.001000000000000	0.999999999999988	2.999999999998291	0.000000000000865
375	2.000000000245950	20.450098492275732	0.001000000000299	0.999999999998865	2.999999999858258	0.000000000001339
376	2.000000000155138	4.354690480330338	0.001000000000322	0.999999999999864	2.999999999993615	0.000000005068813
377	2.000000000024811	20.653497760986365	0.001000000000006	0.999999999999930	2.999999999981131	0.000000000314861
378	2.000000000000433	0.823639041772745	0.001000000000023	0.999999999998164	2.999999999998403	0.000000000373299
379	2.000000000099978	20.557865991155804	0.001000000000001	0.999999999998974	2.999999998894436	0.000000002533405
380	2.000000000056712	4.359935625908421	0.001000000000011	0.999999999999932	2.999999999999881	0.000000000234285
381	2.000000000003664	13.249857132523797	0.001000000000024	0.999999999999706	2.999999999986313	0.000000000094655
382	2.000000000129858	20.546846177245545	0.001000000000096	0.999999999999827	2.999999999941862	0.000000000201909
383	2.000000000064755	11.865699768854151	0.001000000000003	0.999999999999904	2.999999999990302	0.000000000001471
384	2.000000000005774	0.893398298380466	0.001000000000106	0.999999999999855	2.999999999798456	0.000000000004567
385	2.000000000441880	20.059583351312074	0.001000000000270	0.999999999999686	2.999999999989103	0.000000000286001
386	2.000000000065382	13.239519239429297	0.001000000000015	0.999999999999773	2.999999999983039	0.000000000208908
387	2.000000000043083	12.129521277505020	0.001000000000011	0.999999999999855	2.999999999976043	0.000000000067288
388	2.000000000000500	20.546920748963434	0.001000000000195	0.999999999993406	2.999999999447572	0.000000001499002
389	2.000000000129668	20.314763763089683	0.001000000000738	0.999999999999236	2.999999998868620	0.000000000117654
390	2.000000000019818	20.316343469065849	0.001000000000125	0.999999999996546	2.999999999910491	0.000000000324517
391	2.000000000196438	20.023616159156976	0.001000000000000	0.999999999996981	2.999999999968607	0.000000000438478
392	2.000000000044671	0.847581971628956	0.001000000000004	0.999999999999477	2.999999999993300	0.000000000326246
393	2.000000000013289	0.317994858513494	0.001000000000173	0.999999999999947	2.999999999999985	0.000000000002961
394	2.000000000011811	17.315803381925924	0.001000000000011	0.999999999998506	2.999999999844714	0.000000000030792
395	2.000000000018223	8.501106349366477	0.001000000000042	0.999999999999767	2.999999999987170	0.000000000002948
396	2.000000000015540	14.425332519481218	0.001000000000000	0.999999999999205	2.999999999859826	0.000000000143160
397	2.000000000005715	20.781608582694119	0.001000000000118	0.999999999999507	2.999999999708355	0.000000000559357

398	2.000000000036012	13.459574720273976	0.001000000000054	1.000000000000000	2.999999999872550	0.000000000121282
399	2.000000000001612	0.546214518882735	0.001000000000002	0.999999999996597	2.999999999403937	0.000000000001510
400	2.000000000057165	20.611961876901528	0.001000000000003	0.999999999998702	2.999999999957552	0.000000000004229
401	2.000000000484068	10.910603753181588	0.001000000000002	0.999999999998762	2.999999999453784	0.000000001791114
402	2.000000000124884	20.137961357147979	0.001000000000214	0.999999999999904	2.999999999854041	0.000000000000047
403	2.000000000034107	20.043713756766330	0.001000000000250	0.999999999999900	2.999999991582902	0.000000008499398
404	2.000000000000374	19.655584253011124	0.001000000000035	0.999999999996056	2.999999999843622	0.000000000043723
405	2.000000000195803	19.803714056286978	0.001000000000198	0.999999999998643	2.999999999603038	0.000000000841408
406	2.000000000000500	20.546920748963434	0.001000000000195	0.999999999993406	2.999999999447572	0.000000001499002
407	2.000000000071079	10.626939032346060	0.001000000000034	0.999999999999845	2.999999999690783	0.000000000001083
408	2.000000000139545	7.299565912368973	0.001000000000066	0.999999999999932	2.999999999128995	0.000000000148091
409	2.000000000018179	5.193754685752817	0.001000000000021	0.999999999999992	2.999999999754524	0.000000000002343
410	2.000000000001019	17.091351052637993	0.001000000000050	0.999999999999893	2.999999999956101	0.000000000000566
411	2.000000000284389	17.048977708880027	0.001000000000004	0.999999999997906	2.999999999533023	0.000000000104689
412	2.000000000019818	20.316343469065849	0.001000000000125	0.999999999996546	2.999999999910491	0.000000000324517
413	2.000000000020436	1.874783365725943	0.001000000000040	0.999999999999152	2.999999999817360	0.000000000134221
414	2.000000000066438	19.914707703864245	0.001000000000676	0.999999999999748	2.999999999949472	0.000000000185916
415	2.000000000665239	20.092462553759383	0.001000000000042	0.999999999999581	2.999999999712876	0.000000002017706
416	2.000000000317530	5.261572743825170	0.001000000000127	0.999999999999800	2.999999999992958	0.000000000519871
417	2.000000000000487	0.070073604920370	0.001000000000000	0.999999999999852	2.999999999976426	0.000000000018979
418	2.000000000097156	20.313616349213671	0.001000000000252	0.999999999997149	2.999999999072962	0.000000001982643
419	2.000000000164733	20.543634999259808	0.001000000000019	0.999999999995981	2.999999999999913	0.000000000000678
420	2.000000000030641	1.434748955705915	0.001000000000006	0.999999999999993	2.999999999999786	0.000000000101305
421	2.000000000078333	18.912262099326526	0.001000000000394	0.999999999999166	2.999999999910539	0.000000000316794
422	2.000000000196438	20.023616159156976	0.001000000000000	0.999999999996981	2.999999999968607	0.000000000438478
423	2.000000000115658	20.450824459918028	0.001000000000108	0.999999999987834	2.999999995116987	0.000000000677091
424	2.000000000058384	20.539351588304879	0.001000000000004	0.999999999999960	2.999999999998187	0.000000000023124
425	2.000000000096411	4.651997056588666	0.001000000000196	0.999999999999854	2.999999999998066	0.000000000003854
426	2.000000000160257	13.239070788507636	0.001000000000005	0.999999999999817	2.999999999848610	0.000000000000027
427	2.000000000769843	20.140677094176969	0.001000000000000	0.999999999998729	2.999999997658303	0.000000000882749
428	2.000000000062471	20.555086315974208	0.001000000000010	0.999999999999315	2.999999999494000	0.000000000109957
429	2.000000000010497	19.878760306710241	0.001000000000075	0.999999999999609	2.999999999993622	0.000000000566745
430	2.000000000001029	18.594090358957935	0.001000000000049	0.999999999999963	2.999999999983830	0.000000000146724
431	2.000000000010043	19.796923363555386	0.001000000000006	0.999999999998983	2.999999999902507	0.000000001025933
432	2.000000000375741	18.885197817793383	0.001000000000029	0.999999999999671	2.999999999992050	0.000000001342992
433	2.000000000012834	20.457133909103586	0.001000000000073	0.999999999999908	2.999999999802810	0.000000000456206
434	2.000000000029893	18.795812034149773	0.001000000000012	0.999999999999751	2.999999999989705	0.000000000156209
435	2.000000000037307	19.185564008520529	0.001000000000721	0.999999999998002	2.999999999938102	0.000000000331180
436	2.000000000022092	13.249441268474952	0.001000000000020	0.999999999998398	2.999999999807999	0.000000000101948
437	2.000000000051033	14.967739908397757	0.001000000000157	0.999999999997471	2.999999999996174	0.000000000024102
438	2.000000000118902	17.430424390893741	0.001000000000100	0.999999999999211	2.999999999011326	0.000000000021140
439	2.000000000665239	20.092462553759383	0.001000000000042	0.999999999999581	2.999999999712876	0.000000002017706
440	2.000000000045165	11.223412279578893	0.001000000000070	0.999999999999952	2.999999999980274	0.000000000167731
441	2.000000000006733	18.210452615704192	0.001000000000001	0.999999999998990	2.999999999972370	0.000000000148522
442	2.000000000034561	15.904258409043543	0.001000000000029	1.000000000000000	2.999999999701065	0.000000000310511
443	2.000000000056712	4.359935625908421	0.001000000000011	0.999999999999932	2.999999999999881	0.000000000234285
444	2.000000000028635	1.874496394763732	0.001000000000000	0.999999999999406	2.999999999839794	0.000000000687123
445	2.000000000001283	18.207218920985866	0.001000000000020	0.999999999999999	2.999999999955479	0.000000000038685
446	2.000000000030641	1.434748955705915	0.001000000000006	0.999999999999993	2.999999999999786	0.000000000101305
447	2.000000000018394	14.958197507656726	0.001000000000141	0.999999999999769	2.999999999516898	0.000000001044971
448	2.000000000136956	7.299553507247629	0.001000000000064	0.999999999999940	2.999999999118063	0.000000000163209
449	2.000000000014701	19.869166505502118	0.001000000000005	0.999999999999527	2.999999999516683	0.000000000404348
450	2.000000000000374	19.655584253011124	0.001000000000035	0.999999999996056	2.999999999843622	0.000000000043723
451	2.000000000521641	13.244264065781181	0.001000000000115	0.999999999999428	2.999999999847408	0.000000000521542
452	2.000000000001721	19.655110084448243	0.001000000000010	0.999999999999643	2.999999999857462	0.000000000012538
453	2.000000000665239	20.092462553759383	0.001000000000042	0.999999999999581	2.999999999712876	0.000000002017706
454	2.000000000018673	12.803212689458386	0.001000000000000	0.999999999999864	2.999999999997963	0.000000000016276
455	2.000000000008478	18.285708562647798	0.001000000000013	0.999999999999985	2.999999999974956	0.000000001824129
456	2.000000000171912	19.082725852713601	0.001000000000043	0.999999999996566	2.999999999967562	0.000000000080015

457	2.000000000006733	18.210452615704192	0.001000000000001	0.999999999998990	2.999999999972370	0.000000000148522
458	2.000000000019493	18.358336039679973	0.001000000000012	0.999999999999988	2.999999999717514	0.000000000104152
459	2.000000000020436	1.874783365725943	0.001000000000040	0.999999999999152	2.999999999817360	0.000000000134221
460	2.000000000608824	19.787616351769323	0.001000000000069	0.999999999999987	2.999999999672366	0.000000002044337
461	2.000000000038771	19.927739734225007	0.001000000000038	0.999999999999840	2.999999999456624	0.000000000228482
462	2.000000000000141	1.425342633276796	0.001000000000031	0.999999999997863	2.999999999984127	0.000000000008301
463	2.000000000088134	19.878647428505488	0.001000000000010	0.999999999999889	2.999999999788279	0.000000000000543
464	2.000000000028142	18.215637058002681	0.001000000000000	0.999999999999839	2.999999999924225	0.000000000006705
465	2.000000000001491	20.540834814816503	0.001000000000060	0.999999999998868	2.999999999722271	0.000000000000093
466	2.000000000186391	19.690419732832275	0.001000000000189	0.999999999998810	2.999999999066257	0.000000001690292
467	2.000000000096411	4.651997056588666	0.001000000000196	0.999999999999854	2.999999999998066	0.000000000003854
468	2.000000000003118	10.877403598708121	0.001000000000001	0.999999999998991	2.999999999966342	0.000000000025882
469	2.000000000153931	20.355359294290512	0.001000000000029	0.999999999999782	2.999999999982260	0.000000000656638
470	2.000000000091140	11.808402401923802	0.001000000000209	0.999999999999981	2.999999999952373	0.000000000000010
471	2.000000000009963	10.519232407837649	0.001000000000599	0.999999999997554	2.999999999754730	0.000000000276021
472	2.000000000000608	17.217882120127214	0.001000000000001	1.000000000000000	2.999999999987392	0.000000000033215
473	2.000000000000363	0.544486062503442	0.001000000000421	0.999999999999790	2.999999999394015	0.000000000122253
474	2.000000000000374	19.655584253011124	0.001000000000035	0.999999999996056	2.999999999843622	0.000000000043723
475	2.000000000003508	11.452547647945083	0.001000000000000	0.999999999999204	2.999999999965557	0.000000000043084
476	2.000000000001283	18.207218920985866	0.001000000000020	0.999999999999999	2.999999999955479	0.000000000038685
477	2.000000000007847	16.950269675633123	0.001000000000004	0.999999999999814	2.999999999990410	0.000000000004225
478	2.000000000219481	17.137358718463453	0.001000000000000	0.999999999996949	2.999999999419268	0.000000000347836
479	2.000000000015553	10.685419950527919	0.001000000000159	0.999999999999916	2.999999999999439	0.000000000181167
480	2.000000000029893	18.795812034149773	0.001000000000012	0.999999999999751	2.999999999989705	0.000000000156209
481	2.000000000007326	11.621985622021601	0.001000000000002	0.999999999999995	2.999999999725284	0.000000000317004
482	2.000000000012884	13.459258157589883	0.001000000000062	0.999999999999556	2.999999999618755	0.000000000049055
483	2.000000000091140	11.808402401923802	0.001000000000209	0.999999999999981	2.999999999952373	0.000000000000010
484	2.000000000229067	7.299600554534313	0.001000000000001	0.999999999999045	2.999999999993859	0.000000000487601
485	2.000000000007056	18.207142358615712	0.001000000000000	0.999999999999890	2.999999999976293	0.000000000016368
486	2.000000000000565	1.344526978589959	0.001000000000023	0.999999999999563	2.999999999943916	0.000000000033777
487	2.000000000017915	19.350339206369366	0.001000000000009	0.999999999999755	2.999999999850645	0.000000000724249
488	2.000000000003677	19.655218074330268	0.001000000000018	0.999999999999778	2.999999999747017	0.000000001921850
489	2.000000000000219	20.350171293899113	0.001000000000183	0.999999999999996	2.999999999812399	0.000000001516437
490	2.000000000026695	19.871864164761472	0.001000000000196	0.999999999999257	2.999999999963632	0.000000000001479
491	2.000000000160257	13.239070788507636	0.001000000000005	0.999999999999817	2.999999999848610	0.000000000000027
492	2.000000000058530	19.554783844269327	0.001000000000049	0.999999999999939	2.999999999999720	0.000000000805341
493	2.000000000014386	13.439064246977912	0.001000000000170	0.999999999999906	2.999999999989766	0.000000000186688
494	2.000000000029405	13.459905524990791	0.001000000000000	1.000000000000000	2.999999999953210	0.000000000413310
495	2.000000000396420	19.943016760109973	0.001000000000248	0.999999999999999	2.999999999883304	0.000000000000551
496	2.000000000124884	20.137961357147979	0.001000000000214	0.999999999999904	2.999999999854041	0.000000000000047
497	2.000000000000028	11.783235118397560	0.001000000000024	0.999999999999754	2.999999999496916	0.000000000012602
498	2.000000000296631	13.278118728151133	0.001000000001370	0.999999999999432	2.999999998494644	0.000000000133600
499	2.000000000352198	19.962210612572200	0.001000000000166	0.999999999999693	2.999999999807781	0.000000000391200
500	2.000000000000359	18.458981430886972	0.001000000000018	0.999999999999999	2.999999999999916	0.000000000039698
501	2.000000000153642	20.092388623199945	0.001000000000034	0.999999999999915	2.999999999490263	0.000000000955590
502	2.000000000006733	18.210452615704192	0.001000000000001	0.999999999998990	2.999999999972370	0.000000000148522
503	2.000000000007233	19.876105362732833	0.001000000000033	0.999999999999998	2.999999999982911	0.000000001862328
504	2.000000000003677	19.655218074330268	0.001000000000018	0.999999999999778	2.999999999747017	0.000000001921850
505	2.000000000001080	0.316186275884172	0.001000000000041	0.999999999999975	2.999999999839500	0.000000000737134
506	2.000000000002133	12.231547894962924	0.001000000000004	0.999999999999919	2.999999999974406	0.000000000076797
507	2.000000000018293	16.854749846691046	0.001000000000069	0.999999999999225	2.999999999677017	0.000000000041801
508	2.000000000129668	20.314763763089683	0.001000000000738	0.999999999999236	2.999999998868620	0.000000000117654
509	2.000000000000040	18.214594741083719	0.001000000000026	0.999999999999434	2.999999999990260	0.000000000007815
510	2.000000000002719	19.734492055169230	0.001000000000103	0.999999999998754	2.999999999689534	0.000000001669805
511	2.000000000018394	14.958197507656726	0.001000000000141	0.999999999999769	2.999999999516898	0.000000001044971
512	2.000000000984723	15.625548597360575	0.001000000000074	0.999999999999794	2.999999999622534	0.000000000675759
513	2.000000000000327	10.886425357268829	0.001000000000029	0.999999999999210	2.999999999899646	0.000000000002099
514	2.000000000001491	20.540834814816503	0.001000000000060	0.999999999998868	2.999999999722271	0.000000000000093
515	2.000000000000578	16.391940000231557	0.001000000000000	0.999999999999987	2.999999999998224	0.000000000086471

516	2.000000000000673	20.613391951765678	0.001000000000022	0.999999999999635	2.999999999893601	0.000000000017925
517	2.000000000219481	17.137358718463453	0.001000000000000	0.999999999996949	2.999999999419268	0.000000000347836
518	2.000000000009963	10.519232407837649	0.001000000000599	0.999999999997554	2.999999999754730	0.000000000276021
519	2.000000000003305	0.847638479690710	0.001000000000061	0.999999999999725	2.999999999982312	0.000000000255829
520	2.000000000138840	20.056195331704323	0.001000000000025	0.999999999999866	2.999999999999270	0.000000000196489
521	2.000000000020478	20.212660528082374	0.001000000000007	0.999999999999998	2.999999999998255	0.000000000871649
522	2.000000000096411	4.651997056588666	0.001000000000196	0.999999999999854	2.999999999998066	0.000000000003854
523	2.000000000124310	2.614552495834114	0.001000000000000	0.999999999999187	2.999999997976015	0.000000000000023
524	2.000000000139545	7.299565912368973	0.001000000000066	0.999999999999932	2.999999999128995	0.000000000148091
525	2.000000000007839	19.112321725352853	0.001000000000013	0.999999999999531	2.999999999901186	0.000000000215067
526	2.000000000066438	19.914707703864245	0.001000000000676	0.999999999999748	2.999999999949472	0.000000000185916
527	2.000000000085520	17.329946893117544	0.001000000000039	0.999999999999941	2.999999999906958	0.000000000000443
528	2.000000000001118	7.273261907661723	0.001000000000014	0.999999999996717	2.999999999999165	0.000000000574470
529	4.566147363301654	20.736449650121987	0.001000000000004	0.999999999999994	2.999999999971753	0.000000000007329
530	2.000000000000154	20.036679997649749	0.001000000000091	0.999999999999973	2.999999999841543	0.000000000009958
531	2.000000000116122	0.399643685604631	0.001000000000024	0.999999999999916	2.999999999896495	0.000000000006944
532	2.000000000004449	20.290916401710497	0.001000000000036	0.999999999994087	2.999999999702825	0.000000000439640
533	2.000000000002765	17.820846350468223	0.001000000000067	0.999999999999200	2.999999999565437	0.000000000001985
534	2.000000000005774	0.893398298380466	0.001000000000106	0.999999999999855	2.999999999798456	0.000000000004567
535	2.000000000022073	19.082982830446156	0.001000000000096	0.999999999999147	2.999999999415225	0.000000000019447
536	2.000000000011587	17.400689230733722	0.001000000000040	0.999999999999430	2.999999999988055	0.000000002002658
537	2.000000000000190	20.591309794184202	0.001000000000353	0.999999999999939	2.999999999983224	0.000000000256200
538	2.000000000200378	1.946571080311953	0.001000000000042	0.999999999999942	2.999999999909329	0.000000000466729
539	3.874101472647747	20.266206805975887	0.001000000000162	0.999999999999469	2.999999999884982	0.000000000067423
540	2.000000000000196	5.720819008686378	0.001000000000001	0.999999999999997	2.999999999990529	0.000000000004615
541	2.000000000020742	9.094482928245034	0.001000000000035	0.999999999999891	2.999999999869421	0.000000000040751
542	2.000000000160257	13.239070788507636	0.001000000000005	0.999999999999817	2.999999999848610	0.000000000000027
543	2.000000000034127	15.268165902736392	0.001000000000066	0.999999999999921	2.999999999855589	0.000000001064229
544	2.000000000124884	20.137961357147979	0.001000000000214	0.999999999999904	2.999999999854041	0.000000000000047
545	2.000000000016036	16.227218270881131	0.001000000000000	0.999999999999968	2.999999999865630	0.000000000004343
546	2.000000000066438	19.914707703864245	0.001000000000676	0.999999999999748	2.999999999949472	0.000000000185916
547	2.000000000044671	0.847581971628956	0.001000000000004	0.999999999999477	2.999999999993300	0.000000000326246
548	5.181461041496615	19.930073901576819	0.001000000000000	0.999999999999534	2.999999999897534	0.000000000025520
549	2.000000000018251	2.849771804238354	0.001000000000003	0.999999999999933	2.999999999886556	0.000000000015632
550	2.000000000071480	20.006559674271116	0.001000000000001	0.999999999999157	2.999999999999988	0.000000000058950
551	2.000000000003118	10.877403598708121	0.001000000000001	0.999999999998991	2.999999999966342	0.000000000025882
552	2.000000000000327	10.886425357268829	0.001000000000029	0.999999999999210	2.999999999899646	0.000000000002099
553	2.000000000047829	20.013148450031302	0.001000000000007	0.999999999999029	2.999999999968173	0.000000000096519
554	2.000000000012884	13.459258157589883	0.001000000000062	0.999999999999556	2.999999999618755	0.000000000049055
555	2.000000000001612	0.546214518882735	0.001000000000002	0.999999999996597	2.999999999403937	0.000000000001510
556	2.000000000000374	19.655584253011124	0.001000000000035	0.999999999996056	2.999999999843622	0.000000000043723
557	2.000000000003525	18.348631497412754	0.001000000000145	0.999999999996384	2.999999999845829	0.000000000143903
558	2.000000000028157	20.096266642754063	0.001000000000156	0.999999999999942	2.999999999993502	0.000000000029278
559	2.000000000001612	0.546214518882735	0.001000000000002	0.999999999996597	2.999999999403937	0.000000000001510
560	2.000000000001521	15.068882993958709	0.001000000000005	0.999999999999941	2.999999999998408	0.000000000096217
561	2.000000000021913	19.667523728245875	0.001000000000158	0.999999999999819	2.999999999749834	0.000000001548794
562	2.000000000001019	17.091351052637993	0.001000000000050	0.999999999999893	2.999999999956101	0.000000000000566
563	2.000000000200659	19.914892599878552	0.001000000000220	0.999999999999813	2.999999999346287	0.000000000005433
564	2.000000000375741	18.885197817793383	0.001000000000029	0.999999999999671	2.999999999992050	0.000000001342992
565	2.000000000020735	19.191841865047621	0.001000000000042	0.999999999999838	2.999999999618779	0.000000000020481
566	2.000000000002580	20.242440915639847	0.001000000000003	0.999999999998884	2.999999999809621	0.000000000263447
567	2.000000000245950	20.450098492275732	0.001000000000299	0.999999999998865	2.999999999858258	0.000000000001339
568	3.752012447027545	20.469329122227901	0.001000000000001	1.000000000000000	2.999999999942419	0.000000000012431
569	2.000000000009963	2.648760509307296	0.001000000000006	1.000000000000000	2.999999999999546	0.000000000000663
570	2.000000000056712	4.359935625908421	0.001000000000011	0.999999999999932	2.999999999999881	0.000000000234285
571	2.000000000000374	19.655584253011124	0.001000000000035	0.999999999996056	2.999999999843622	0.000000000043723
572	2.000000000140426	10.541718584772882	0.001000000000013	0.999999999994739	2.999999999999711	0.000000000495474
573	2.000000000036025	9.668148834082890	0.001000000000129	0.999999999999625	2.999999998905749	0.000000000007299
574	2.000000000042431	20.133931166489869	0.001000000000059	0.999999999998888	2.999999999520052	0.000000000003092

575	2.000000000056712	4.359935625908421	0.001000000000011	0.999999999999932	2.999999999999881	0.000000000234285
576	2.000000000005778	19.329033022226987	0.001000000000041	0.999999999997961	2.999999999999566	0.000000000317235
577	2.000000000293725	20.722815524630878	0.001000000000864	0.999999999999682	2.999999999352709	0.000000003686312
578	2.000000000014895	14.856382683246384	0.001000000000008	0.999999999999989	2.999999999992770	0.000000000026372
579	2.000000000095888	19.409831119682146	0.001000000000365	0.999999999998774	2.999999999952614	0.000000000415913
580	2.000000000124884	20.137961357147979	0.001000000000214	0.999999999999904	2.999999999854041	0.000000000000047
581	2.000000000002169	18.964469497315765	0.001000000000006	0.999999999999895	2.999999999995219	0.000000000647215
582	2.000000000011030	19.920811896203329	0.001000000000131	0.999999999999933	2.999999999997015	0.000000002183977
583	2.000000000014701	19.869166505502118	0.001000000000005	0.999999999999527	2.999999999516683	0.000000000404348
584	2.000000000201579	20.017890089161572	0.001000000000102	0.999999999999513	2.999999996175329	0.000000002143519
585	2.000000000000262	20.290846885252666	0.001000000000345	0.999999999998617	2.999999999492750	0.000000000308312
586	2.000000000000262	20.290846885252666	0.001000000000345	0.999999999998617	2.999999999492750	0.000000000308312
587	2.000000000001491	20.540834814816503	0.001000000000060	0.999999999998868	2.999999999722271	0.000000000000093
588	2.000000000033531	17.032460102900039	0.001000000000013	1.000000000000000	2.999999999395417	0.000000000206548
589	2.000000000042431	20.133931166489869	0.001000000000059	0.999999999998888	2.999999999520052	0.000000000003092
590	2.000000000139545	7.299565912368973	0.001000000000066	0.999999999999932	2.999999999128995	0.000000000148091
591	2.000000000665239	20.092462553759383	0.001000000000042	0.999999999999581	2.999999999712876	0.000000002017706
592	2.000000000014382	20.340289110876153	0.001000000000062	0.999999999998716	2.999999999970350	0.000000002193136
593	2.000000000042431	20.133931166489869	0.001000000000059	0.999999999998888	2.999999999520052	0.000000000003092
594	2.000000000035350	1.873967132966709	0.001000000000250	0.999999999999855	2.999999999999748	0.000000000694720
595	2.000000000059210	10.755749837614712	0.001000000000089	0.999999999999641	2.999999998318587	0.000000000384595
596	2.000000000064559	14.599738845134540	0.001000000000017	0.999999999999891	2.999999999939302	0.000000000027004
597	2.000000000029405	13.459905524990791	0.001000000000000	1.000000000000000	2.999999999953210	0.000000000413310
598	2.000000000066438	19.914707703864245	0.001000000000676	0.999999999999748	2.999999999949472	0.000000000185916
599	2.000000000000774	5.191474108038015	0.001000000000004	0.999999999999798	2.999999999988340	0.000000000359278
600	2.000000000038535	15.922350551343600	0.001000000000000	0.999999999999875	2.999999999995792	0.000000000002588
601	2.000000000245950	20.450098492275732	0.001000000000299	0.999999999998865	2.999999999858258	0.000000000001339
602	2.000000000000496	20.136030100257244	0.001000000000391	0.999999999995324	2.999999998722894	0.000000000728251
603	2.000000000123176	16.095259929626003	0.001000000000247	0.999999999998409	2.999999999866188	0.000000000023618
604	2.000000000602462	20.223150567090080	0.001000000001234	0.999999999991654	2.999999994196428	0.000000000244255
605	2.000000000186391	19.690419732832275	0.001000000000189	0.999999999998810	2.999999999066257	0.000000001690292
606	2.000000000251732	19.243826481861753	0.001000000000435	0.999999999999598	2.999999998750990	0.000000000275188
607	2.000000000000774	5.191474108038015	0.001000000000004	0.999999999999798	2.999999999988340	0.000000000359278
608	2.000000000068278	16.551692018483394	0.001000000000038	0.999999999999881	2.999999999976861	0.000000000222339
609	2.000000000124884	20.137961357147979	0.001000000000214	0.999999999999904	2.999999999854041	0.000000000000047
610	2.000000000014701	19.869166505502118	0.001000000000005	0.999999999999527	2.999999999516683	0.000000000404348
611	2.000000000019818	20.316343469065849	0.001000000000125	0.999999999996546	2.999999999910491	0.000000000324517
612	2.000000000015553	10.685419950527919	0.001000000000159	0.999999999999916	2.999999999999439	0.000000000181167
613	2.000000000121193	20.245495711267086	0.001000000000198	0.999999999997447	2.999999999662197	0.000000000752580
614	2.000000000003664	13.249857132523797	0.001000000000024	0.999999999999706	2.999999999986313	0.000000000094655
615	2.000000000017915	19.350339206369366	0.001000000000009	0.999999999999755	2.999999999850645	0.000000000724249
616	2.000000000121193	20.245495711267086	0.001000000000198	0.999999999997447	2.999999999662197	0.000000000752580
617	2.000000000000008	2.469298652044758	0.001000000000000	0.999999999999997	2.999999999989168	0.000000000013894
618	2.000000000051033	14.967739908397757	0.001000000000157	0.999999999997471	2.999999999996174	0.000000000024102
619	2.000000000000063	20.077652030794400	0.001000000000000	0.999999999999997	2.999999999914078	0.000000000000814
620	2.000000000105199	20.549486089070736	0.001000000000419	0.999999999999929	2.999999999759621	0.000000000779003
621	2.000000000078131	20.208162690781275	0.001000000000007	0.999999999994382	2.999999999992721	0.000000000058699
622	2.000000000000118	0.408850433046796	0.001000000000010	0.999999999999795	2.999999998567619	0.000000000089681
623	2.000000000025147	0.951154307010030	0.001000000000014	0.999999999999997	2.999999999997594	0.000000000720934
624	2.000000000001803	17.584282540085930	0.001000000000018	0.999999999999608	2.999999999951305	0.000000000001218
625	2.000000000042431	20.133931166489869	0.001000000000059	0.999999999998888	2.999999999520052	0.000000000003092
626	2.000000000129858	20.546846177245545	0.001000000000096	0.999999999999827	2.999999999941862	0.000000000201909
627	2.000000000009226	20.170341249201329	0.001000000000007	0.999999999998460	2.999999999397661	0.000000002606483
628	2.000000000521641	13.244264065781181	0.001000000000115	0.999999999999428	2.999999999847408	0.000000000521542
629	2.000000000129668	20.314763763089683	0.001000000000738	0.999999999999236	2.999999998868620	0.000000000117654
630	2.000000000196438	20.023616159156976	0.001000000000000	0.999999999996981	2.999999999968607	0.000000000438478
631	2.000000000009963	10.519232407837649	0.001000000000599	0.999999999997554	2.999999999754730	0.000000000276021
632	2.000000000984723	15.625548597360575	0.001000000000074	0.999999999999794	2.999999999622534	0.000000000675759
633	2.000000000018179	5.193754685752817	0.001000000000021	0.999999999999992	2.999999999754524	0.000000000002343

634	2.000000000003645	19.752581898099685	0.001000000000000	0.999999999999998	2.999999999923431	0.000000000179697
635	2.000000000006069	17.090869603923231	0.001000000000052	0.999999999999999	2.999999999732076	0.000000000016017
636	2.000000000003677	19.655218074330268	0.001000000000018	0.999999999999778	2.999999999747017	0.000000001921850
637	2.000000000001118	7.273261907661723	0.001000000000014	0.999999999996717	2.999999999999165	0.000000000574470
638	2.000000000002696	17.434460851049693	0.001000000000034	0.999999999999908	2.999999999451913	0.000000000154223
639	2.000000000004449	20.290916401710497	0.001000000000036	0.999999999994087	2.999999999702825	0.000000000439640
640	2.000000000023676	20.433085372823697	0.001000000000088	0.999999999999950	2.999999999191416	0.000000000091286
641	2.000000000018179	5.193754685752817	0.001000000000021	0.999999999999992	2.999999999754524	0.000000000002343
642	2.000000000000656	1.414290351157161	0.001000000000009	0.999999999999480	2.999999999189583	0.000000000117963
643	2.000000000009463	14.591827450423464	0.001000000000013	0.999999999999998	2.999999999987625	0.000000000183299
644	2.000000000124884	20.137961357147979	0.001000000000214	0.999999999999904	2.999999999854041	0.000000000000047
645	2.000000000121193	20.245495711267086	0.001000000000198	0.999999999997447	2.999999999662197	0.000000000752580
646	2.000000000028635	1.874496394763732	0.001000000000000	0.999999999999406	2.999999999839794	0.000000000687123
647	2.000000000011003	19.081629994695721	0.001000000000243	0.999999999998315	2.999999999350678	0.000000001554123
648	2.000000000028846	11.622665717847809	0.001000000000011	0.999999999999964	2.999999999818628	0.000000000046779
649	2.000000000029405	13.459905524990791	0.001000000000000	1.000000000000000	2.999999999953210	0.000000000413310
650	2.000000000015426	16.393516158293490	0.001000000000002	1.000000000000000	2.999999999841093	0.000000001026816
651	2.000000000206405	20.749726708368538	0.001000000000061	0.999999999999066	2.999999999115961	0.000000001044879
652	2.000000000139545	7.299565912368973	0.001000000000066	0.999999999999932	2.999999999128995	0.000000000148091
653	2.000000000021145	19.618520825043021	0.001000000000047	0.999999999999951	2.999999999800767	0.000000000295288
654	2.000000000307362	12.841209324959628	0.001000000000400	0.999999999999974	2.999999999937436	0.000000000774176
655	2.000000000000063	20.077652030794400	0.001000000000000	0.999999999999997	2.999999999914078	0.000000000000814
656	2.000000000079093	16.986486882962293	0.001000000000003	0.999999999999979	2.999999999917057	0.000000000097468
657	2.000000000004291	19.945404278649669	0.001000000000009	0.999999999999991	2.999999999544558	0.000000000146547
658	2.000000000000171	9.204467327228544	0.001000000000004	0.999999999999988	2.999999999999742	0.000000000031203
659	2.000000000003786	4.176457026176712	0.001000000000075	0.999999999999916	2.999999999936919	0.000000000458399
660	2.000000000007951	13.279944970757555	0.001000000000000	0.999999999998480	2.999999999579723	0.000000000299423
661	2.000000000042431	20.133931166489869	0.001000000000059	0.999999999998888	2.999999999520052	0.000000000003092
662	2.000000000051033	14.967739908397757	0.001000000000157	0.999999999997471	2.999999999996174	0.000000000024102
663	2.000000000105416	20.325323681756554	0.001000000000184	0.999999999998342	2.999999999542480	0.000000000640510
664	2.000000000019059	0.083508762004345	0.001000000000000	0.999999999999981	2.999999999936402	0.000000000002805
665	2.000000000000025	19.752621250794196	0.001000000000000	0.999999999999398	2.999999999869876	0.000000000362095
666	2.000000000108233	19.640115728507268	0.001000000000016	0.999999999999885	2.999999999584076	0.000000000175743
667	2.000000000231283	19.032814021947225	0.001000000000008	0.999999999999908	2.999999999859857	0.000000000251691
668	2.000000000049730	20.137980616223096	0.001000000000229	0.999999999999898	2.999999999657784	0.000000000004515
669	2.000000000016158	19.050106353348880	0.001000000000004	0.999999999999676	2.999999999999780	0.000000000335382
670	2.000000000484068	10.910603753181588	0.001000000000002	0.999999999998762	2.999999999453784	0.000000001791114
671	2.000000000001787	16.448620366249589	0.001000000000033	0.999999999999690	2.999999999704913	0.000000000115846
672	2.000000000020478	20.212660528082374	0.001000000000007	0.999999999999998	2.999999999998255	0.000000000871649
673	2.000000000083508	19.735187948498883	0.001000000000299	0.999999999999986	2.999999999637273	0.000000000006223
674	2.000000000053109	4.651887507246677	0.001000000000307	0.999999999999584	2.999999999526662	0.000000000207259
675	2.000000000056910	18.633866462257281	0.001000000000050	0.999999999999847	2.999999999616130	0.000000000037814
676	2.000000000049730	20.137980616223096	0.001000000000229	0.999999999999898	2.999999999657784	0.000000000004515
677	2.000000000037307	19.185564008520529	0.001000000000721	0.999999999998002	2.999999999938102	0.000000000331180
678	2.000000000196438	20.023616159156976	0.001000000000000	0.999999999996981	2.999999999968607	0.000000000438478
679	2.000000000166379	17.501245987008407	0.001000000000000	0.999999999999504	2.999999999987055	0.000000000124966
680	2.000000000002025	17.131037204044876	0.001000000000038	1.000000000000000	2.999999999703596	0.000000004085941
681	2.000000000001335	13.923506849546252	0.001000000000042	0.999999999999043	2.999999999949623	0.000000000054393
682	2.000000000000156	20.779284886882216	0.001000000000017	0.999999999999986	2.999999999947313	0.000000000002712
683	2.000000000000219	19.744917906392555	0.001000000000075	0.999999999995359	2.999999999283040	0.000000000012636
684	2.000000000022560	18.360966431340035	0.001000000000002	0.999999999999948	2.999999999989617	0.000000000159736
685	2.000000000001856	20.238240679365585	0.001000000000105	0.999999999996428	2.999999999924530	0.000000001267038
686	2.000000000015553	10.685419950527919	0.001000000000159	0.999999999999916	2.999999999999439	0.000000000181167
687	2.000000000012205	19.801734752702565	0.001000000000013	0.999999999998354	2.999999999421613	0.000000000027902
688	2.000000000012789	20.290774738211724	0.001000000000312	0.999999999998315	2.999999999408692	0.000000000029701
689	2.000000000033628	17.032494774530196	0.001000000000015	0.999999999999889	2.999999999410921	0.000000000097990
690	2.000000000005077	14.958005371348623	0.001000000000083	0.999999999999996	2.999999999999984	0.000000000018670
691	2.000000000003118	10.877403598708121	0.001000000000001	0.999999999998991	2.999999999966342	0.000000000025882
692	2.000000000011564	8.392176984447193	0.001000000000045	0.999999999999932	2.999999999738547	0.000000000060509

693	2.000000000004504	16.367948375300802	0.001000000000037	0.999999999999693	2.999999999999845	0.000000000031004
694	2.000000000308166	15.552093624347203	0.001000000000001	0.999999999999971	2.999999999899689	0.000000000867924
695	2.000000000265663	20.246602150473560	0.001000000000000	0.999999999999844	2.999999999870286	0.000000000210535
696	2.000000000042431	20.133931166489869	0.001000000000059	0.999999999998888	2.999999999520052	0.000000000003092
697	2.000000000029405	13.459905524990791	0.001000000000000	1.000000000000000	2.999999999953210	0.000000000413310
698	2.000000000144496	17.049573659419114	0.001000000000091	0.999999999995633	2.999999999988408	0.000000000238854
699	2.000000000001118	7.273261907661723	0.001000000000014	0.999999999996717	2.999999999999165	0.000000000574470
700	2.000000000030496	20.345492668534192	0.001000000000013	0.999999999999870	2.999999999862077	0.000000000106189
701	2.000000000015825	17.726571791356470	0.001000000000007	0.999999999999410	2.999999999842810	0.000000000018054
702	2.000000000003915	19.806543269530636	0.001000000000043	0.999999999999450	2.999999999954730	0.000000000336345
703	2.000000000139545	7.299565912368973	0.001000000000066	0.999999999999932	2.999999999128995	0.000000000148091
704	2.000000000090640	20.092438795337532	0.001000000000049	0.999999999999981	2.999999999890854	0.000000000989271
705	2.000000000000139	18.046213570379059	0.001000000000003	0.999999999999979	2.999999999999441	0.000000000008464
706	2.000000000000565	1.344526978589959	0.001000000000023	0.999999999999563	2.999999999943916	0.000000000033777
707	2.000000000006136	18.523282349138420	0.001000000000002	0.999999999999899	2.999999999982228	0.000000000046310
708	2.000000000011283	9.870445070474030	0.001000000000046	0.999999999999972	2.999999999991465	0.000000000057574
709	2.000000000124884	20.137961357147979	0.001000000000214	0.999999999999904	2.999999999854041	0.000000000000047
710	2.000000000003645	19.752581898099685	0.001000000000000	0.999999999999998	2.999999999923431	0.000000000179697
711	2.000000000000968	18.213732878265937	0.001000000000017	0.999999999999808	2.999999999985898	0.000000000105392
712	2.000000000029405	13.459905524990791	0.001000000000000	1.000000000000000	2.999999999953210	0.000000000413310
713	2.000000000027587	11.451444559287015	0.001000000000125	0.999999999999779	2.999999999988714	0.000000000030883
714	2.000000000139545	7.299565912368973	0.001000000000066	0.999999999999932	2.999999999128995	0.000000000148091
715	2.000000000034898	18.331189693379116	0.001000000000051	1.000000000000000	2.999999999085885	0.000000000120295
716	2.000000000123690	14.960349226679204	0.001000000000000	0.999999999997475	2.999999999582864	0.000000001930592
717	2.000000000769843	20.140677094176969	0.001000000000000	0.999999999998729	2.999999997658303	0.000000000882749
718	2.000000000000374	19.655584253011124	0.001000000000035	0.999999999996056	2.999999999843622	0.000000000043723
719	2.000000000001491	20.540834814816503	0.001000000000060	0.999999999998868	2.999999999722271	0.000000000000093
720	2.000000000000588	17.071326542548601	0.001000000000052	0.999999999999994	2.999999999917189	0.000000000005011
721	2.000000000029405	13.459905524990791	0.001000000000000	1.000000000000000	2.999999999953210	0.000000000413310
722	2.000000000129858	20.546846177245545	0.001000000000096	0.999999999999827	2.999999999941862	0.000000000201909
723	2.000000000003118	10.877403598708121	0.001000000000001	0.999999999998991	2.999999999966342	0.000000000025882
724	2.000000000308166	15.552093624347203	0.001000000000001	0.999999999999971	2.999999999899689	0.000000000867924
725	2.000000000001283	18.207218920985866	0.001000000000020	0.999999999999999	2.999999999955479	0.000000000038685
726	2.000000000013762	11.899990136666654	0.001000000000162	0.999999999999787	2.999999999778879	0.000000000100002
727	2.000000000010497	19.878760306710241	0.001000000000075	0.999999999999609	2.999999999993622	0.000000000566745
728	2.000000000024239	20.400132234255686	0.001000000000082	0.999999999989730	2.999999999933332	0.000000000159543
729	2.000000000000262	20.290846885252666	0.001000000000345	0.999999999998617	2.999999999492750	0.000000000308312
730	2.000000000124310	2.614552495834114	0.001000000000000	0.999999999999187	2.999999997976015	0.000000000000023
731	2.000000000159844	20.024438213228542	0.001000000000297	0.999999999999816	2.999999999863704	0.000000000725601
732	2.000000000025147	0.951154307010030	0.001000000000014	0.999999999999997	2.999999999997594	0.000000000720934
733	2.000000000117921	19.931011584182556	0.001000000000006	0.999999999999998	2.999999999967577	0.000000000007726
734	2.000000000169306	19.048366134660480	0.001000000000019	0.999999999998242	2.999999999940854	0.000000000014745
735	2.000000000000259	18.176575396521656	0.001000000000052	0.999999999999841	2.999999999992346	0.000000000006089
736	2.000000000047829	20.013148450031302	0.001000000000007	0.999999999999029	2.999999999968173	0.000000000096519
737	2.000000000032070	5.245152200900452	0.001000000000011	0.999999999999986	2.999999998100291	0.000000000019659
738	2.000000000002133	12.231547894962924	0.001000000000004	0.999999999999919	2.999999999974406	0.000000000076797
739	2.000000000025092	0.031640438436114	0.001000000000001	0.999999999999355	2.999999999999988	0.000000000193307
740	2.000000000000981	1.873728810619090	0.001000000000423	0.999999999999747	2.999999999986899	0.000000000087632
741	2.000000000001612	0.546214518882735	0.001000000000002	0.999999999996597	2.999999999403937	0.000000000001510
742	2.000000000200659	19.914892599878552	0.001000000000220	0.999999999999813	2.999999999346287	0.000000000005433
743	2.000000000170268	19.930312988650215	0.001000000000001	0.999999999999131	2.999999999368095	0.000000000140220
744	2.000000000010507	19.624227347315358	0.001000000000001	1.000000000000000	2.999999999678365	0.000000001602921
745	2.000000000010497	19.878760306710241	0.001000000000075	0.999999999999609	2.999999999993622	0.000000000566745
746	2.000000000005723	19.081659721965021	0.001000000000799	0.999999999995135	2.999999999952479	0.000000000199845
747	2.000000000124884	20.137961357147979	0.001000000000214	0.999999999999904	2.999999999854041	0.000000000000047
748	2.000000000000901	2.676261472868217	0.001000000000009	0.999999999998819	2.999999999943896	0.000000000203360
749	5.427194466193700	1.267396896856063	0.001000000000010	0.999999999999669	2.999999999968322	0.000000000000738
750	2.000000000139545	7.299565912368973	0.001000000000066	0.999999999999932	2.999999999128995	0.000000000148091
751	2.000000000042431	20.133931166489869	0.001000000000059	0.999999999998888	2.999999999520052	0.000000000003092

752	2.000000000018179	5.193754685752817	0.001000000000021	0.999999999999992	2.999999999754524	0.000000000002343
753	2.000000000033715	18.789820159423243	0.001000000000055	0.999999999999997	2.999999999983155	0.000000000155460
754	2.000000000003238	12.861954670707009	0.001000000000005	0.999999999999996	2.999999999998751	0.000000000117065
755	2.005639202821065	0.028412755351337	0.001011013626040	0.868638853417518	2.998192136340824	0.002519621554927
756	2.000000000003428	17.504629393445430	0.001000000000242	0.999999999997457	2.999999999999592	0.000000001112402
757	2.000000001254019	20.075994273685577	0.001000000003952	0.999999999998184	2.999999999964126	0.000000005296387
758	2.000000000005609	0.670857668754045	0.001000000000000	0.999999999999930	2.999999999993960	0.000000000013972
759	2.000000000360577	19.922308051028487	0.001000000000545	0.999999999992728	2.999999999324785	0.000000000139698
760	2.000000000025075	20.355074414043195	0.001000000000013	0.999999999998012	2.999999999775277	0.000000000687720
761	2.000000000042431	20.133931166489869	0.001000000000059	0.999999999998888	2.999999999520052	0.000000000003092
762	2.000000000000487	0.070073604920370	0.001000000000000	0.999999999999852	2.999999999976426	0.000000000018979
763	5.020223602231199	3.182255013321456	0.001000000000029	0.999999999999995	2.999999999912002	0.000000000223302
764	2.000000000665239	20.092462553759383	0.001000000000042	0.999999999999581	2.999999999712876	0.000000002017706
765	2.000000000042585	20.316486578463387	0.001000000000281	0.999999999999800	2.999999999971059	0.000000000060491
766	2.000000000140787	19.794734547739903	0.001000000000089	0.999999999999844	2.999999999829830	0.000000000167770
767	2.000000000001118	7.273261907661723	0.001000000000014	0.999999999996717	2.999999999999165	0.000000000574470
768	2.000000000009963	10.519232407837649	0.001000000000599	0.999999999997554	2.999999999754730	0.000000000276021
769	2.000000000000040	18.214594741083719	0.001000000000026	0.999999999999434	2.999999999990260	0.000000000007815
770	2.000000000079093	16.986486882962293	0.001000000000003	0.999999999999979	2.999999999917057	0.000000000097468
771	2.000000000029405	13.459905524990791	0.001000000000000	1.000000000000000	2.999999999953210	0.000000000413310
772	2.000000000025284	9.474983507027096	0.001000000000010	0.999999999999950	2.999999999970586	0.000000000159004
773	2.000000000001430	4.976311152613478	0.001000000000073	0.999999999999582	2.999999999970363	0.000000000080805
774	2.000000000000374	19.655584253011124	0.001000000000035	0.999999999996056	2.999999999843622	0.000000000043723
775	2.000000000001491	20.540834814816503	0.001000000000060	0.999999999998868	2.999999999722271	0.000000000000093
776	2.000000000025638	18.217165731348135	0.001000000000000	0.999999999999830	2.999999999831180	0.000000000151320
777	2.000000000000023	14.758391231661127	0.001000000000010	0.999999999999968	2.999999999943109	0.000000000036061
778	2.000000000028089	20.418664791893015	0.001000000000325	1.000000000000000	2.999999996712892	0.000000000867254
779	2.000000000029405	13.459905524990791	0.001000000000000	1.000000000000000	2.999999999953210	0.000000000413310
780	2.000000000015553	10.685419950527919	0.001000000000159	0.999999999999916	2.999999999999439	0.000000000181167
781	2.000000000020436	1.874783365725943	0.001000000000040	0.999999999999152	2.999999999817360	0.000000000134221
782	2.000000000031492	14.045520688366384	0.001000000000014	0.999999999999950	2.999999999987182	0.000000000198828
783	2.000000000025147	0.951154307010030	0.001000000000014	0.999999999999997	2.999999999997594	0.000000000720934
784	2.000000000000500	20.546920748963434	0.001000000000195	0.999999999993406	2.999999999447572	0.000000001499002
785	2.000000000068278	16.551692018483394	0.001000000000038	0.999999999999881	2.999999999976861	0.000000000222339
786	2.000000000000076	20.749758823307239	0.001000000000021	0.999999999999891	2.999999999930917	0.000000001513261
787	2.000000000018025	17.005362402493951	0.001000000000002	0.999999999999946	2.999999999562556	0.000000000063209
788	2.000000000002194	19.926579575909670	0.001000000000005	0.999999999999974	2.999999999996241	0.000000000059773
789	2.000000000012290	18.884557159491418	0.001000000000096	0.999999999999997	2.999999999409513	0.000000000010080
790	2.000000000014701	19.869166505502118	0.001000000000005	0.999999999999527	2.999999999516683	0.000000000404348
791	2.000000000005324	15.625035141564441	0.001000000000032	0.999999999999975	2.999999999866502	0.000000000037760
792	2.000000000027946	20.390942491494005	0.001000000000033	0.999999999999879	2.999999999995872	0.000000000061929
793	2.000000000002133	12.231547894962924	0.001000000000004	0.999999999999919	2.999999999974406	0.000000000076797
794	2.000000000062576	20.746962413564003	0.001000000000025	0.999999999999758	2.999999998323625	0.000000000029194
795	2.000000000590529	20.594560209807462	0.001000000000018	0.999999999999537	2.999999999927048	0.000000001388488
796	2.000000000002487	4.652089680768948	0.001000000000296	0.999999999999748	2.999999999980603	0.000000000111973
797	2.000000000018179	5.193754685752817	0.001000000000021	0.999999999999992	2.999999999754524	0.000000000002343
798	2.000000000116122	0.399643685604631	0.001000000000024	0.999999999999916	2.999999999896495	0.000000000006944
799	2.000000000019831	2.787976637377566	0.001000000000006	0.999999999999977	2.999999999999018	0.000000000128347
800	2.000000000022356	16.562226694741021	0.001000000000042	0.999999999999059	2.999999999436119	0.000000000601330
801	2.000000000056910	18.633866462257281	0.001000000000050	0.999999999999847	2.999999999616130	0.000000000037814
802	2.000000000133478	18.463352225009601	0.001000000000171	0.999999999999272	2.999999999812191	0.000000000572184
803	2.000000000003312	0.193494570917950	0.001000000000001	0.999999999999863	2.999999999999958	0.000000000016225
804	2.000000000002373	2.605086517116613	0.001000000000143	0.999999999999448	2.999999999968974	0.000000000023924
805	2.000000000054826	20.635274253861464	0.001000000000045	0.999999999999893	2.999999999965866	0.000000000020750
806	2.000000000029405	13.459905524990791	0.001000000000000	1.000000000000000	2.999999999953210	0.000000000413310
807	2.000000000001283	18.207218920985866	0.001000000000020	0.999999999999999	2.999999999955479	0.000000000038685
808	2.000000000010043	19.796923363555386	0.001000000000006	0.999999999998983	2.999999999902507	0.000000001025933
809	2.000000000007957	17.950969620307976	0.001000000000045	0.999999999996962	2.999999999612818	0.000000001009952
810	2.000000000199022	20.210070689199746	0.001000000000210	0.999999999996264	2.999999999638432	0.000000000170884

811	2.000000000014515	4.384785664902368	0.001000000000376	0.999999999997094	2.999999999895813	0.000000000013082
812	3.185321007464684	18.989526152873765	0.001000000000000	1.000000000000000	2.999999999142935	0.000000000211340
813	2.000000000000407	0.029596624609635	0.001000000000004	0.999999999999555	2.999999999968158	0.000000000011236
814	2.000000000665239	20.092462553759383	0.001000000000042	0.999999999999581	2.999999999712876	0.000000002017706
815	2.000000000004493	15.687786505937360	0.001000000000000	0.999999999999970	2.999999999942112	0.000000000088647
816	2.000000000204386	20.374518205270196	0.001000000000208	0.999999999999794	2.999999999199008	0.000000000180169
817	2.000000000000374	19.655584253011124	0.001000000000035	0.999999999996056	2.999999999843622	0.000000000043723
818	2.000000000121193	20.245495711267086	0.001000000000198	0.999999999997447	2.999999999662197	0.000000000752580
819	2.000000000150115	19.924904331074345	0.001000000000003	0.999999999999976	2.999999999966112	0.000000000225619
820	2.000000000124884	20.137961357147979	0.001000000000214	0.999999999999904	2.999999999854041	0.000000000000047
821	2.000000000013416	18.211536508673039	0.001000000000001	0.999999999999678	2.999999999999544	0.000000000005120
822	2.000000000031551	19.081481403652138	0.001000000000272	0.999999999999199	2.999999999999362	0.000000001362649
823	2.000000000029405	13.459905524990791	0.001000000000000	1.000000000000000	2.999999999953210	0.000000000413310
824	2.000000000004449	20.290916401710497	0.001000000000036	0.999999999994087	2.999999999702825	0.000000000439640
825	2.000000000000374	19.655584253011124	0.001000000000035	0.999999999996056	2.999999999843622	0.000000000043723
826	2.000000000020537	19.082982269469412	0.001000000000083	0.999999999999039	2.999999999410027	0.000000000024059
827	2.000000000006069	17.090869603923231	0.001000000000052	0.999999999999999	2.999999999732076	0.000000000016017
828	2.000000000002888	18.200091988312060	0.001000000000011	0.999999999999906	2.999999999996937	0.000000000130540
829	2.000000000000635	20.057150700813136	0.001000000000120	0.999999999999848	2.999999999798309	0.000000000201259
830	2.000000000006649	20.451169644062475	0.001000000000004	0.999999999999965	2.999999999877922	0.000000002314429
831	2.000000000056910	18.633866462257281	0.001000000000050	0.999999999999847	2.999999999616130	0.000000000037814
832	2.000000000019270	2.374613548046293	0.001000000000013	0.999999999999830	2.999999999836445	0.000000000024825
833	2.000000000000124	20.760920588956381	0.001000000000050	0.999999999999046	2.999999999480795	0.000000000065249
834	2.000000000001057	7.525008587833630	0.001000000000036	0.999999999999756	2.999999999599019	0.000000000189430
835	2.000000000056712	4.359935625908421	0.001000000000011	0.999999999999932	2.999999999999881	0.000000000234285
836	2.000000000000262	20.290846885252666	0.001000000000345	0.999999999998617	2.999999999492750	0.000000000308312
837	2.000000000140787	19.794734547739903	0.001000000000089	0.999999999999844	2.999999999829830	0.000000000167770
838	2.000000000000074	19.410195874123808	0.001000000000079	0.999999999998614	2.999999998811951	0.000000000137967
839	2.000000000000363	0.544486062503442	0.001000000000421	0.999999999999790	2.999999999394015	0.000000000122253
840	2.000000000000363	0.544486062503442	0.001000000000421	0.999999999999790	2.999999999394015	0.000000000122253
841	2.000000000892002	18.542109703320619	0.001000000000673	0.999999999998520	2.999999997775745	0.000000008472276
842	2.000000000013344	20.446510639370317	0.001000000000566	0.999999999998690	2.999999999872115	0.000000001197349
843	2.000000000028635	1.874496394763732	0.001000000000000	0.999999999999406	2.999999999839794	0.000000000687123
844	2.000000000001491	20.540834814816503	0.001000000000060	0.999999999998868	2.999999999722271	0.000000000000093
845	2.000000000001491	20.540834814816503	0.001000000000060	0.999999999998868	2.999999999722271	0.000000000000093
846	2.000000000000968	18.213732878265937	0.001000000000017	0.999999999999808	2.999999999985898	0.000000000105392
847	2.000000000022092	13.249441268474952	0.001000000000020	0.999999999998398	2.999999999807999	0.000000000101948
848	2.000000000020478	20.212660528082374	0.001000000000007	0.999999999999998	2.999999999998255	0.000000000871649
849	2.000000000047829	20.013148450031302	0.001000000000007	0.999999999999029	2.999999999968173	0.000000000096519
850	2.000000000000374	19.655584253011124	0.001000000000035	0.999999999996056	2.999999999843622	0.000000000043723
851	2.000000000051033	14.967739908397757	0.001000000000157	0.999999999997471	2.999999999996174	0.000000000024102
852	2.000000000046239	20.771709531983998	0.001000000000138	0.999999999998367	2.999999999920488	0.000000001441340
853	2.000000000029405	13.459905524990791	0.001000000000000	1.000000000000000	2.999999999953210	0.000000000413310
854	2.000000000003795	20.537495660652858	0.001000000000000	0.999999999999632	2.999999999903988	0.000000000745391
855	2.000000000023313	20.418686799490697	0.001000000000001	0.999999999999962	2.999999999784849	0.000000000177904
856	2.000000000155749	19.927585800149327	0.001000000000030	0.999999999999937	2.999999999901735	0.000000000179226
857	2.000000000199613	16.669921969603731	0.001000000000079	0.999999999994774	2.999999999996329	0.000000003863834
858	2.000000000007799	18.207037675117377	0.001000000000006	0.999999999999892	2.999999999926201	0.000000000049519
859	2.000000000001491	20.540834814816503	0.001000000000060	0.999999999998868	2.999999999722271	0.000000000000093
860	2.000000000000374	19.655584253011124	0.001000000000035	0.999999999996056	2.999999999843622	0.000000000043723
861	2.000000000042431	20.133931166489869	0.001000000000059	0.999999999998888	2.999999999520052	0.000000000003092
862	2.000000000139545	7.299565912368973	0.001000000000066	0.999999999999932	2.999999999128995	0.000000000148091
863	2.000000000013416	18.211536508673039	0.001000000000001	0.999999999999678	2.999999999999544	0.000000000005120
864	2.000000000007839	19.112321725352853	0.001000000000013	0.999999999999531	2.999999999901186	0.000000000215067
865	2.000000000038482	19.145469018918782	0.001000000000002	0.999999999999896	2.999999999714088	0.000000000443392
866	2.000000000129668	20.314763763089683	0.001000000000738	0.999999999999236	2.999999998868620	0.000000000117654
867	2.000000000014701	19.869166505502118	0.001000000000005	0.999999999999527	2.999999999516683	0.000000000404348
868	2.000000000172638	18.444859769977803	0.001000000000158	0.999999999999895	2.999999999516251	0.000000000396980
869	2.000000000003645	19.752581898099685	0.001000000000000	0.999999999999998	2.999999999923431	0.000000000179697

870	2.000000000000462	0.028251321566992	0.001000000000002	0.999999999999993	2.999999999990862	0.000000000011134
871	2.000000000000040	18.214594741083719	0.001000000000026	0.999999999999434	2.999999999990260	0.000000000007815
872	2.000000000090640	20.092438795337532	0.001000000000049	0.999999999999981	2.999999999890854	0.000000000989271
873	2.000000000014701	19.869166505502118	0.001000000000005	0.999999999999527	2.999999999516683	0.000000000404348
874	2.000000000026695	19.871864164761472	0.001000000000196	0.999999999999257	2.999999999963632	0.000000000001479
875	2.000000000000704	20.250272594024544	0.001000000000108	0.999999999998616	2.999999995101161	0.000000000437056
876	3.944814618695992	3.796225361930251	0.001000000000005	0.999999999999996	2.999999999966864	0.000000000006978
877	2.000000000019270	2.374613548046293	0.001000000000013	0.999999999999830	2.999999999836445	0.000000000024825
878	2.000000000066438	19.914707703864245	0.001000000000676	0.999999999999748	2.999999999949472	0.000000000185916
879	2.000000000000363	0.544486062503442	0.001000000000421	0.999999999999790	2.999999999394015	0.000000000122253
880	2.000000000003616	8.982962140623897	0.001000000000002	0.999999999999975	2.999999999949541	0.000000000012544
881	2.000000000044091	16.844226016038167	0.001000000000290	0.999999999999286	2.999999999968832	0.000000000733607
882	2.000000000051033	14.967739908397757	0.001000000000157	0.999999999997471	2.999999999996174	0.000000000024102
883	2.000000000025147	0.951154307010030	0.001000000000014	0.999999999999997	2.999999999997594	0.000000000720934
884	2.000000000145708	17.017920008915770	0.001000000000144	0.999999999999033	2.999999999441966	0.000000000096138
885	2.000000000005723	19.081659721965021	0.001000000000799	0.999999999995135	2.999999999952479	0.000000000199845
886	2.000000000145658	14.485435133715240	0.001000000000018	0.999999999999880	2.999999999979814	0.000000000009617
887	2.000000000085486	20.087285556929949	0.001000000000007	0.999999999999106	2.999999999858031	0.000000000596561
888	2.000000000075016	14.107492947653597	0.001000000000002	0.999999999999976	2.999999999995949	0.000000000003537
889	2.000000000062905	17.520795809274265	0.001000000000012	1.000000000000000	2.999999999723458	0.000000000015057
890	2.000000000296631	13.278118728151133	0.001000000001370	0.999999999999432	2.999999998494644	0.000000000133600
891	2.000000001434370	19.742200522929519	0.001000000000379	0.999999999999510	2.999999999808131	0.000000000063758
892	2.000000000056712	4.359935625908421	0.001000000000011	0.999999999999932	2.999999999999881	0.000000000234285
893	2.000000000159913	0.399952380447090	0.001000000000615	0.999999999999661	2.999999999983414	0.000000000009848
894	2.000000000254992	17.610357663004955	0.001000000000000	0.999999999998837	2.999999999866663	0.000000000157378
895	2.000000000000363	0.544486062503442	0.001000000000421	0.999999999999790	2.999999999394015	0.000000000122253
896	2.000000000005723	19.081659721965021	0.001000000000799	0.999999999995135	2.999999999952479	0.000000000199845
897	2.000000000020537	19.082982269469412	0.001000000000083	0.999999999999039	2.999999999410027	0.000000000024059
898	2.000000000022092	13.249441268474952	0.001000000000020	0.999999999998398	2.999999999807999	0.000000000101948
899	2.000000000516277	20.275161302934627	0.001000000000220	0.999999999999931	2.999999999839442	0.000000000732303
900	2.000000000159913	0.399952380447090	0.001000000000615	0.999999999999661	2.999999999983414	0.000000000009848
901	2.000000000000981	1.873728810619090	0.001000000000423	0.999999999999747	2.999999999986899	0.000000000087632
902	2.000000000591738	20.336585231580592	0.001000000004625	0.999999999999610	2.999999997983137	0.000000001304141
903	2.000000000029570	19.081091898046854	0.001000000000114	0.999999999997722	2.999999999590861	0.000000000857717
904	2.000000000043606	16.677154754765095	0.001000000000529	0.999999999997380	2.999999999940223	0.000000000142662
905	2.000000000028157	20.096266642754063	0.001000000000156	0.999999999999942	2.999999999993502	0.000000000029278
906	2.000000000064755	11.865699768854151	0.001000000000003	0.999999999999904	2.999999999990302	0.000000000001471
907	2.000000000015553	10.685419950527919	0.001000000000159	0.999999999999916	2.999999999999439	0.000000000181167
908	2.000000000000565	1.344526978589959	0.001000000000023	0.999999999999563	2.999999999943916	0.000000000033777
909	2.000000000000711	17.050056047859947	0.001000000000141	0.999999999986976	2.999999999742940	0.000000000093615
910	2.000000000003329	15.359993649410770	0.001000000000012	0.999999999999657	2.999999999758193	0.000000000084209
911	2.000000000984723	15.625548597360575	0.001000000000074	0.999999999999794	2.999999999622534	0.000000000675759
912	2.000000000007143	20.785955981368716	0.001000000000003	0.999999999999903	2.999999999995623	0.000000000143254
913	2.000000000129668	20.314763763089683	0.001000000000738	0.999999999999236	2.999999998868620	0.000000000117654
914	2.000000000001911	20.217289955037927	0.001000000000196	0.999999999992195	2.999999999955826	0.000000000077882
915	2.000000000099978	20.557865991155804	0.001000000000001	0.999999999998974	2.999999998894436	0.000000002533405
916	2.000000000066438	19.914707703864245	0.001000000000676	0.999999999999748	2.999999999949472	0.000000000185916
917	2.000000000025147	0.951154307010030	0.001000000000014	0.999999999999997	2.999999999997594	0.000000000720934
918	2.000000000043908	1.872364050262448	0.001000000000091	0.999999999999996	2.999999999544694	0.000000000384918
919	2.000000000100352	10.683531920025626	0.001000000000004	0.999999999999382	2.999999999866356	0.000000000000128
920	2.000000000000434	17.422610140510290	0.001000000000000	0.999999999999985	2.999999999953318	0.000000000480040
921	2.000000000155138	4.354690480330338	0.001000000000322	0.999999999999864	2.999999999993615	0.000000005068813
922	2.000000000000114	17.124890299254691	0.001000000000002	0.999999999999793	2.999999999975817	0.000000001352743
923	2.000000000018179	5.193754685752817	0.001000000000021	0.999999999999992	2.999999999754524	0.000000000002343
924	2.000000000042585	20.316486578463387	0.001000000000281	0.999999999999800	2.999999999971059	0.000000000060491
925	2.000000000049913	20.268156001211224	0.001000000000825	0.999999999999899	2.999999999549276	0.000000000024400
926	2.000000000034127	15.268165902736392	0.001000000000066	0.999999999999921	2.999999999855589	0.000000001064229
927	2.000000000229067	7.299600554534313	0.001000000000001	0.999999999999045	2.999999999993859	0.000000000487601
928	2.000000000021240	20.212663143072415	0.001000000000007	1.000000000000000	2.999999999998892	0.000000000851444

929	2.000000000020436	1.874783365725943	0.001000000000040	0.999999999999152	2.999999999817360	0.000000000134221
930	2.000000000064346	6.490395183734591	0.001000000000000	0.999999999999804	2.999999999948949	0.000000000039389
931	2.000000000006502	19.425548740887564	0.001000000000029	0.999999999999905	2.999999999722791	0.000000000267052
932	2.000000000010507	19.624227347315358	0.001000000000001	1.000000000000000	2.999999999678365	0.000000001602921
933	2.000000000141199	0.952476230342684	0.001000000000059	0.999999999999987	2.999999999910053	0.000000000035278
934	2.000000000139545	7.299565912368973	0.001000000000066	0.999999999999932	2.999999999128995	0.000000000148091
935	2.000000000001491	20.540834814816503	0.001000000000060	0.999999999998868	2.999999999722271	0.000000000000093
936	2.000000000000002	9.284224254229679	0.001000000000003	0.999999999999998	2.999999999886444	0.000000000248891
937	2.000000000002487	4.652089680768934	0.001000000000296	0.999999999999748	2.999999999980603	0.000000000111973
938	2.000000000000901	2.676261472868217	0.001000000000009	0.999999999998819	2.999999999943896	0.000000000203360
939	2.000000000000118	0.408850433046796	0.001000000000010	0.999999999999795	2.999999998567619	0.000000000089681
940	2.000000000003118	10.877403598708121	0.001000000000001	0.999999999998991	2.999999999966342	0.000000000025882
941	2.000000000007006	19.207907416777115	0.001000000000013	0.999999999999776	2.999999999054915	0.000000000003730
942	2.000000000001291	1.717927589392222	0.001000000000002	0.999999999999980	2.999999999999916	0.000000000017782
943	2.000000000032941	15.267449145860731	0.001000000000151	0.999999999999638	2.999999999733401	0.000000000317875
944	2.000000000211048	18.330998063817233	0.001000000000058	0.999999999994224	2.999999999797285	0.000000000001386
945	2.000000000219481	17.137358718463453	0.001000000000000	0.999999999996949	2.999999999419268	0.000000000347836
946	2.000000000009159	20.580410110518027	0.001000000000000	0.999999999999951	2.999999999999812	0.000000002228573
947	2.000000000285726	19.795097023301675	0.001000000000457	0.999999999998417	2.999999999999612	0.000000000050426
948	2.000000000010497	19.878760306710241	0.001000000000075	0.999999999999609	2.999999999993622	0.000000000566745
949	2.000000000018179	5.193754685752817	0.001000000000021	0.999999999999992	2.999999999754524	0.000000000002343
950	2.000000000129858	20.546846177245545	0.001000000000096	0.999999999999827	2.999999999941862	0.000000000201909
951	2.000000000007056	18.207142358615712	0.001000000000000	0.999999999999890	2.999999999976293	0.000000000016368
952	2.000000000053997	11.086402005250331	0.001000000000196	0.999999999998686	2.999999999993065	0.000000000001606
953	2.000000000018179	5.193754685752817	0.001000000000021	0.999999999999992	2.999999999754524	0.000000000002343
954	2.000000000019681	19.943328815591080	0.001000000000054	0.999999999999937	2.999999999337880	0.000000000345561
955	2.000000000000715	20.248615731023442	0.001000000000061	0.999999999999885	2.999999999821420	0.000000002448483
956	2.000000000018179	5.193754685752817	0.001000000000021	0.999999999999992	2.999999999754524	0.000000000002343
957	2.000000000007056	18.207142358615712	0.001000000000000	0.999999999999890	2.999999999976293	0.000000000016368
958	2.000000000000690	14.835939782361516	0.001000000000025	0.999999999999454	2.999999999961473	0.000000000202126
959	2.000000000002487	4.652089680768948	0.001000000000296	0.999999999999748	2.999999999980603	0.000000000111973
960	2.000000000401579	19.794821883080896	0.001000000000332	0.999999999997646	2.999999999965958	0.000000000160312
961	2.000000000009963	10.519232407837649	0.001000000000599	0.999999999997554	2.999999999754730	0.000000000276021
962	2.000000000096411	4.651997056588666	0.001000000000196	0.999999999999854	2.999999999998066	0.000000000003854
963	2.000000000100352	10.683531920025626	0.001000000000004	0.999999999999382	2.999999999866356	0.000000000000128
964	2.000000000004305	18.758487338682102	0.001000000000000	0.999999999991014	2.999999999764739	0.000000002374342
965	2.000000000140426	10.541718584772882	0.001000000000013	0.999999999994739	2.999999999999711	0.000000000495474
966	2.000000000000219	20.350171293899113	0.001000000000183	0.999999999999996	2.999999999812399	0.000000001516437
967	2.000000000066438	19.914707703864245	0.001000000000676	0.999999999999748	2.999999999949472	0.000000000185916
968	2.000000000036541	15.899837002660513	0.001000000000000	0.999999999999505	2.999999999964678	0.000000000284854
969	2.000000000036782	20.180220377404620	0.001000000000036	0.999999999999852	2.999999999993544	0.000000000346092
970	2.000000000984723	15.625548597360575	0.001000000000074	0.999999999999794	2.999999999622534	0.000000000675759
971	2.000000000196651	20.316515172223319	0.001000000000008	1.000000000000000	2.999999999684933	0.000000001900140
972	2.000000000029570	19.081091898046854	0.001000000000114	0.999999999997722	2.999999999590861	0.000000000857717
973	2.000000000095888	19.409831119682146	0.001000000000365	0.999999999998774	2.999999999952614	0.000000000415913
974	2.000000000051033	14.967739908397757	0.001000000000157	0.999999999997471	2.999999999996174	0.000000000024102
975	2.000000000010950	7.524312534032691	0.001000000000009	0.999999999999702	2.999999999936333	0.000000000447521
976	2.000000000056077	18.912266429264790	0.001000000000509	0.999999999999450	2.999999999971411	0.000000000563897
977	2.000000000006733	18.210452615704192	0.001000000000001	0.999999999998990	2.999999999972370	0.000000000148522
978	2.000000000000576	8.891002145278884	0.001000000000029	0.999999999999997	2.999999999856162	0.000000000066813
979	2.000000000007799	18.207037675117377	0.001000000000006	0.999999999999892	2.999999999926201	0.000000000049519
980	2.000000000031551	19.081481403652138	0.001000000000272	0.999999999999199	2.999999999999362	0.000000001362649
981	2.000000000002432	11.621859093519907	0.001000000000114	0.999999999999987	2.999999999808187	0.000000000074552
982	2.000000000056712	4.359935625908421	0.001000000000011	0.999999999999932	2.999999999999881	0.000000000234285
983	2.000000000034930	19.927496902206290	0.001000000000101	0.999999999998343	2.999999999627009	0.000000001146941
984	2.000000000062471	15.971162664501518	0.001000000000004	0.999999999999553	2.999999999951459	0.000000000079821
985	2.000000000001160	20.260456842081897	0.001000000000057	0.999999999999611	2.999999999988244	0.000000000165552
986	2.000000000008662	13.164931859512604	0.001000000000001	0.999999999999857	2.999999999997881	0.000000000381985
987	2.000000000025147	0.951154307010030	0.001000000000014	0.999999999999997	2.999999999997594	0.000000000720934

988	2.000000000984723	15.625548597360575	0.001000000000074	0.999999999999794	2.999999999622534	0.000000000675759
989	2.000000001083014	17.107039814043482	0.001000000000055	0.999999999999835	2.999999999492968	0.000000000248052
990	2.000000000124884	20.137961357147979	0.001000000000214	0.999999999999904	2.999999999854041	0.000000000000047
991	2.000000000262075	19.230583512458939	0.001000000000164	0.999999999999936	2.999999999037744	0.000000001650368
992	2.000000000096411	4.651997056588666	0.001000000000196	0.999999999999854	2.999999999998066	0.000000000003854
993	2.000000000029405	13.459905524990791	0.001000000000000	1.000000000000000	2.999999999953210	0.000000000413310
994	2.000000000032477	18.161253172995785	0.001000000000115	0.999999999998670	2.999999999999966	0.000000000004968
995	2.000000000028635	1.874496394763732	0.001000000000000	0.999999999999406	2.999999999839794	0.000000000687123
996	2.000000000034127	15.268165902736392	0.001000000000066	0.999999999999921	2.999999999855589	0.000000001064229
997	2.000000000000023	6.460611441143363	0.001000000000006	0.999999999998314	2.999999999768991	0.000000000298454
998	2.000000000000846	4.978400024668479	0.001000000000027	0.999999999999990	2.999999999245653	0.000000000006698
999	2.000000000205513	20.604827751952246	0.001000000000625	0.999999999999170	2.999999998453449	0.000000000214359
1000	2.000000000984723	15.625548597360575	0.001000000000074	0.999999999999794	2.999999999622534	0.000000000675759

Table A.4: The results of optimisations for 1000 rounds of Nelder-Mead simplex algorithm for high LET IR using 1000 bootstrap data sets.

A.5 Parameter estimation using Simulated Annealing algorithm (see section 4.8)

A.5.1 Simulated Annealing algorithm

```
function [estimates,model] = parameterfitting_newALLPARAMETERS3SA(xdata, ydata,i)


model = @LQfun; %the model describes in LQfun function
%Random starting values
start_point=[7.6732   11.9704    0.0022    0.1564    0.7285    1.8870;
    11.7853    1.2689    0.0075    0.8555    2.7523    1.0801;
    33.9473    4.9023    0.0020    0.6448    0.8072    3.9520;
    11.6627    7.3601    0.0069    0.3763    2.2965    4.7465;
    32.9428   17.0776    0.0054    0.1909    0.5660    1.6378;
    11.2539    0.3475    0.0080    0.4283    0.8625    3.3563;
    37.3120    0.9210    0.0074    0.4820    0.2733    2.1932;
    15.2994    3.5363    0.0091    0.1206    1.7286    4.1675;
    9.4706   13.5048    0.0090    0.5895    2.0501    3.8443;
    11.5412   15.2199    0.0040    0.2262    1.6398    0.8363;
    25.4097   13.4764    0.0073    0.3846    1.2772    4.3099;
    19.9850    9.3899    0.0028    0.5830    1.9333    4.9494;
    15.3631   11.3849    0.0013    0.2518    1.9429    2.5721;
```

33.5715	6.1800	0.0077	0.2904	2.0371	4.4214;
24.2400	15.4892	0.0055	0.6171	1.9074	2.9401;
22.8895	3.9508	0.0053	0.2653	2.8355	0.7738;
36.8534	14.2867	0.0091	0.8244	0.6268	0.9993;
12.8619	3.8378	0.0065	0.9827	2.1278	2.0348;
30.7736	7.6783	0.0066	0.7302	0.7087	3.7435;
30.6417	13.0170	0.0087	0.3439	0.3582	4.1279;
16.4569	16.2270	0.0082	0.5841	1.8219	3.9498;
23.5772	1.7121	0.0062	0.1078	1.3504	1.5926;
4.8825	19.3239	0.0026	0.9063	1.3762	2.6703;
4.0501	16.1333	0.0032	0.8797	1.9858	0.4498;
22.1703	10.1346	0.0090	0.8178	2.3109	0.5585;
31.6084	9.0771	0.0013	0.2607	1.0507	0.6815;
37.4924	9.3040	0.0054	0.5944	1.9860	3.3933;
6.9364	6.3882	0.0025	0.0225	1.2485	2.4759;
23.6153	10.5855	0.0098	0.4253	2.5258	0.9486;
19.8368	10.6325	0.0074	0.3127	2.4988	2.4750;
2.4523	17.0035	0.0055	0.1615	0.7693	0.7380;
14.8107	16.5302	0.0052	0.1788	1.8404	0.2749;
15.6941	11.5831	0.0058	0.7475	0.4454	0.8435;
9.1740	11.0184	0.0097	0.7485	1.8594	3.7585;
2.0455	17.2600	0.0020	0.5433	0.7819	1.8418;
14.0239	17.8575	0.0015	0.3381	1.3370	4.7091;
28.5854	16.4098	0.0037	0.8323	2.5320	0.0859;
25.7597	6.6266	0.0062	0.5526	0.5886	4.1453;
22.6364	9.4166	0.0058	0.9575	0.9116	3.1330;
18.6834	15.6457	0.0091	0.8928	1.4499	2.6937;
12.9222	2.3087	0.0059	0.3565	1.0134	3.2525;
21.0630	2.3062	0.0049	0.5464	2.3955	3.6331;
30.9388	5.6311	0.0059	0.3467	2.9625	0.4724;
30.9715	10.9204	0.0074	0.6228	0.4771	4.3879;
23.8901	20.2222	0.0012	0.7966	0.7106	0.0718;
30.4112	14.7774	0.0082	0.7459	2.1067	1.4715;
26.5303	6.5026	0.0023	0.1255	1.1264	0.8996;
6.6823	6.0790	0.0053	0.8224	2.9211	4.6315;

21.1671	17.6831	0.0033	0.0252	2.9169	0.3409;
15.1959	18.9556	0.0043	0.4144	1.9311	2.9055;
5.5016	13.3005	0.0070	0.7314	2.5803	3.1858;
7.6183	5.3298	0.0025	0.7814	1.2057	3.2563;
9.5304	1.8686	0.0035	0.3673	1.8958	4.3231;
27.5463	17.4318	0.0028	0.7449	2.9557	0.2798;
18.3974	12.1678	0.0028	0.8923	1.6784	4.0843;
28.3873	19.7126	0.0039	0.2426	2.8008	2.6446;
11.7578	1.2948	0.0089	0.1296	2.1610	3.4718;
2.3708	12.1662	0.0052	0.2251	1.4521	1.0620;
22.2268	5.9472	0.0046	0.3500	1.9171	2.7164;
12.6169	17.2133	0.0026	0.2871	2.6629	3.5126;
37.9567	3.9930	0.0097	0.9275	0.5962	4.7822;
36.4448	9.2156	0.0047	0.0513	1.1861	2.2227;
16.9220	8.1958	0.0086	0.5927	2.9765	0.4270;
2.9445	17.1893	0.0065	0.1629	1.2071	0.2867;
27.5146	14.0811	0.0044	0.8384	1.9766	3.1473;
33.8125	4.3380	0.0089	0.1676	2.7040	3.9809;
38.9170	6.6323	0.0081	0.5022	2.9861	3.4560;
4.1634	2.8059	0.0052	0.9993	1.9595	1.7265;
19.1123	13.9688	0.0083	0.3554	0.3253	4.7341;
24.1339	11.8828	0.0091	0.0471	0.1083	2.6010;
28.0922	3.5525	0.0049	0.2137	1.8543	4.7691;
29.3384	3.0934	0.0040	0.3978	1.7014	0.3680;
26.7015	9.9122	0.0064	0.3337	2.8859	1.0352;
29.6228	18.8820	0.0091	0.2296	2.2383	3.8751;
16.2062	11.4921	0.0073	0.9361	1.9875	4.5709;
24.1001	0.7116	0.0044	0.6832	1.5699	3.9128;
6.4125	1.1460	0.0076	0.9621	0.7797	1.4777;
4.1909	16.7427	0.0096	0.4380	2.8860	0.7592;
39.2311	9.3993	0.0059	0.9403	1.6206	4.2396;
12.8233	7.9723	0.0059	0.0058	0.0908	3.9243;
24.6090	16.4225	0.0038	0.6103	2.0889	1.3542;
38.5621	7.5911	0.0016	0.8011	1.5591	1.1391;
9.0596	11.0805	0.0026	0.2330	0.1771	1.6051;

9.3355	14.8033	0.0018	0.9325	2.6701	4.1478;
14.9825	18.1216	0.0052	0.7633	0.9906	4.1109;
37.4501	6.8521	0.0011	0.8264	0.6891	2.8534;
16.8454	13.5256	0.0092	0.5735	0.3418	2.8591;
12.3822	20.2675	0.0068	0.7926	0.9328	1.4301;
7.7740	1.6050	0.0010	0.3290	0.6853	3.4957;
17.0901	12.2156	0.0013	0.2235	1.9560	3.9813;
16.2395	8.6209	0.0029	0.3124	0.1985	2.2079;
6.9824	6.4461	0.0051	0.5845	0.8263	2.2311;
18.5315	5.5055	0.0021	0.8299	0.8455	2.3283;
5.4775	15.7814	0.0011	0.2905	2.6402	1.3952;
25.3558	20.6907	0.0075	0.4026	1.3330	3.3769;
2.4172	3.9014	0.0042	0.8621	2.2677	4.5183;
23.7839	16.2461	0.0080	0.6147	1.8099	4.5426;
32.0097	4.0929	0.0049	0.9912	2.3498	3.7360;
10.9439	20.6314	0.0049	0.2037	0.3418	1.3026;
19.0247	16.6845	0.0014	0.8272	2.9357	3.4482;
23.6356	8.8356	0.0014	0.6759	2.5458	0.6592;
4.3333	15.1606	0.0018	0.2489	0.1519	0.6175;
20.8590	10.3747	0.0063	0.4758	1.3986	0.9545;
26.4080	16.8242	0.0032	0.3991	0.9770	0.7287;
10.4081	7.4296	0.0086	0.5994	1.8906	2.9252;
33.8081	1.5484	0.0087	0.8005	0.6909	0.3668;
38.9009	12.2980	0.0097	0.1051	1.7397	4.1116;
34.1622	18.9253	0.0054	0.8214	1.8095	3.6145;
21.2280	4.0507	0.0030	0.8411	1.7996	4.6293;
12.5973	9.0046	0.0030	0.3545	1.3453	2.4632;
30.3715	15.5820	0.0058	0.4301	0.1063	3.2744;
11.0034	0.8413	0.0079	0.5722	1.5414	4.4506;
38.3791	19.6756	0.0041	0.7008	1.2232	2.6926;
25.5699	15.8833	0.0052	0.7425	0.3241	1.4110;
24.8100	11.6301	0.0068	0.7579	1.3796	4.8798;
8.5590	3.8447	0.0093	0.3891	1.3526	0.1821;
5.4332	10.3663	0.0025	0.4293	1.6534	1.6312;
11.7000	10.7794	0.0074	0.9563	2.4162	4.8651;

34.6257	20.6705	0.0062	0.5730	2.1026	1.8252;
36.6205	17.7764	0.0049	0.8497	2.6167	1.5457;
28.5861	20.0094	0.0090	0.2763	0.1566	0.6046;
29.5569	14.1241	0.0045	0.6223	0.6590	4.5788;
10.7357	8.4053	0.0026	0.5884	1.3789	0.6774;
23.8900	19.4400	0.0067	0.9635	2.8756	1.6606;
32.8039	9.9829	0.0066	0.0859	2.3701	4.4874;
17.3460	4.8402	0.0040	0.5005	1.3556	2.4982;
39.5607	8.2556	0.0082	0.5216	1.0003	3.0764;
5.4200	14.6667	0.0100	0.0902	0.1773	2.9157;
14.1958	11.6247	0.0098	0.9047	2.2227	3.4913;
21.4335	15.7371	0.0021	0.8844	1.5204	0.1467;
4.3030	20.6962	0.0031	0.4390	0.5998	2.6394;
29.5761	20.0100	0.0012	0.7817	1.2816	0.1604;
32.9595	3.3950	0.0068	0.4229	1.7467	4.2536;
36.4201	16.5189	0.0044	0.0942	1.6222	2.8028;
6.8255	6.4892	0.0083	0.5985	2.6098	4.6480;
36.7083	11.0013	0.0058	0.4709	0.7943	3.4833;
26.0297	3.4669	0.0042	0.6959	0.9542	2.9140;
5.7065	12.5262	0.0095	0.6999	0.3576	4.0770;
12.5829	5.4876	0.0089	0.6385	2.8195	4.3951
22.7815	13.6079	0.0060	0.0336	1.9367	4.9446;
38.3853	14.3374	0.0066	0.0688	1.4384	0.0026;
38.6658	15.5610	0.0063	0.3196	1.9180	4.3272;
7.9893	9.3820	0.0029	0.5309	1.6341	3.0628;
38.8825	1.7680	0.0037	0.6544	1.9419	4.9498;
38.3723	4.7818	0.0052	0.4076	1.6317	2.6384;
20.4443	18.9907	0.0031	0.8200	2.1631	2.3976;
32.4107	3.1914	0.0086	0.7184	1.5675	4.0067;
7.3917	17.1736	0.0028	0.9686	2.9811	1.1392;
18.0269	11.2049	0.0030	0.5313	0.6560	2.4905;
36.7979	20.7097	0.0025	0.3251	0.3174	4.5043;
32.1039	1.6508	0.0030	0.1056	0.3291	2.8733;
38.4607	9.2187	0.0049	0.6110	0.1908	4.2259;
26.9181	2.2421	0.0038	0.7788	1.2137	3.6932;

3.3570	19.9989	0.0093	0.4235	1.3451	2.9299;
34.2669	0.1239	0.0049	0.0908	1.0974	1.2337;
37.4917	16.1166	0.0027	0.2665	2.2905	3.3321;
27.7919	16.9968	0.0091	0.1537	1.8837	0.4174;
30.7941	18.0638	0.0098	0.2810	2.3159	3.1298;
30.2390	1.7808	0.0049	0.4401	2.7986	3.3047;
16.9046	8.3281	0.0020	0.5271	2.9182	3.6488;
26.9082	5.4232	0.0033	0.4574	0.5761	4.4538;
8.5051	16.6390	0.0047	0.8754	0.4166	4.9115;
28.8298	8.9848	0.0064	0.5181	2.0888	3.8451;
3.2096	18.9348	0.0034	0.9436	0.2815	2.9072;
12.5231	3.8033	0.0064	0.6377	1.5762	4.6416;
3.7545	5.5049	0.0074	0.9577	1.5910	2.9005;
5.6910	3.0494	0.0030	0.2407	2.5834	0.0849;
33.2914	2.8528	0.0021	0.6761	1.4546	0.6043;
28.4035	18.0762	0.0037	0.2891	1.1804	4.3136;
14.0498	12.0637	0.0039	0.6718	2.0143	2.4215;
38.1084	11.4441	0.0048	0.6951	2.2238	4.2243;
3.3090	3.0373	0.0056	0.0680	1.5602	1.0470;
18.6723	17.7386	0.0018	0.2548	1.0431	2.7615;
16.4992	12.9430	0.0034	0.2240	0.4500	3.1494;
31.0896	7.3143	0.0082	0.6678	1.7583	0.1600;
32.2176	10.6839	0.0013	0.8444	0.7864	3.0736;
9.1012	8.3702	0.0094	0.3445	0.1334	1.8121;
20.6110	1.6049	0.0076	0.7805	2.2648	0.2477;
18.9323	5.0089	0.0054	0.6753	0.7284	2.4478;
26.5599	2.5881	0.0062	0.0067	1.3272	0.9626;
28.9559	3.8460	0.0031	0.6022	2.0634	0.6154;
30.6781	5.0097	0.0051	0.3868	1.0777	1.0275;
12.4890	8.6911	0.0097	0.9160	2.2090	0.7326;
27.8287	1.0586	0.0059	0.0012	1.1841	0.9454;
26.8937	18.7702	0.0057	0.4624	2.0502	0.2133;
8.1792	19.6437	0.0031	0.4243	2.1121	3.1760;
6.5219	10.2192	0.0054	0.4609	1.3269	1.4093;
20.9378	10.1857	0.0066	0.7702	0.0587	2.6930;

38.4703	7.0395	0.0071	0.3225	0.9926	3.4758;
14.9347	18.7149	0.0046	0.7847	1.2729	2.4956;
24.2402	7.6941	0.0043	0.4714	0.8108	2.6790;
10.5049	2.3365	0.0099	0.0358	0.5912	2.2259;
30.5481	16.2275	0.0013	0.1759	2.4652	0.6197;
11.6936	8.1196	0.0090	0.7218	1.2898	2.4518;
21.2264	5.0458	0.0092	0.4735	2.6633	4.2650;
28.5649	8.4138	0.0082	0.1527	1.1735	4.3696;
35.8543	2.0303	0.0019	0.3411	2.3073	1.3515;
38.4531	2.7678	0.0034	0.6074	1.1904	1.0423;
22.7942	19.5868	0.0040	0.1917	2.4255	2.8249;
7.2677	19.8793	0.0071	0.7384	2.2652	3.2016;
7.6732	11.9704	0.0022	0.2428	1.1322	2.0851;
11.7853	1.2689	0.0075	0.9174	0.6481	1.0299;
33.9473	4.9023	0.0020	0.2691	2.3712	4.7397;
11.6627	7.3601	0.0069	0.7655	2.8479	0.4104;
32.9428	17.0776	0.0054	0.1887	0.9827	0.5285;
11.2539	0.3475	0.0080	0.2875	2.0138	0.7102;
37.3120	0.9210	0.0074	0.0911	1.3159	0.8323;
15.2994	3.5363	0.0091	0.5762	2.5005	3.1048;
9.4706	13.5048	0.0090	0.6834	2.3066	2.8685;
11.5412	15.2199	0.0040	0.5466	0.5018	0.2604;
25.4097	13.4764	0.0073	0.4257	2.5859	4.6560;
19.9850	9.3899	0.0028	0.6444	2.9696	3.6433;
15.3631	11.3849	0.0013	0.6476	1.5433	3.6892;
33.5715	6.1800	0.0077	0.6790	2.6528	0.3170;
24.2400	15.4892	0.0055	0.6358	1.7641	4.3022;
22.8895	3.9508	0.0053	0.9452	0.4643	4.6720;
36.8534	14.2867	0.0091	0.2089	0.5996	4.9220;
12.8619	3.8378	0.0065	0.7093	1.2209	4.2947;
30.7736	7.6783	0.0066	0.2362	2.2461	3.9278;
30.6417	13.0170	0.0087	0.1194	2.4768	2.5669;
16.4569	16.2270	0.0082	0.6073	2.3699	0.8880;
23.5772	1.7121	0.0062	0.4501	0.9556	1.9929;
4.8825	19.3239	0.0026	0.4587	1.6022	0.6697;

```
   4.0501   16.1333    0.0032    0.6619    0.2699    0.1544;
  22.1703   10.1346    0.0090    0.7703    0.3351    4.6957;
  31.6084    9.0771    0.0013    0.3502    0.4089    1.5065;
  37.4924    9.3040    0.0054    0.6620    2.0360    1.4777;
   6.9364    6.3882    0.0025    0.4162    1.4855    1.6647;
  23.6153   10.5855    0.0098    0.8419    0.5691    2.3353;
  19.8368   10.6325    0.0074    0.8329    1.4850    3.2410;
   2.4523   17.0035    0.0055    0.2564    0.4428    0.1261;
  14.8107   16.5302    0.0052    0.6135    0.1649    4.2110];

SP=start_point(i,:)
lb=[2 0.0277 0.001 0 0 0];ub=[40 20.79 0.01 1 3 5];
%*********using SIMULANNEALBND BUILT-IN PACKAGE IN MATLAB***********

options=saoptimset('ObjectiveLimit',0,'MaxFunEval',10000,'TolFun',0.001,
'MaxIter',500,'TemperatureFcn',
@temperaturefast,'InitialTemperature',100,'PlotFcns',
{@saplotbestf,@saplottemperature,@saplotf,@saplotbestx});
%options = saoptimset('InitialTemperature',100);
[estimates,fval] = simulannealbnd(model,SP,lb,ub,options);

%*********************************************************************
                 The model
%*********************************************************************
    function [fval, FittedCurve ] = LQfun(params)
        gamma = params(1);
        alpha1 = params(2);
        alpha2 = params(1);
        p = params(4);
        Vmax = params(5);
        Km=params(6);
npoints=7;
num=100;
%initial condition of model
%*******************************
```

```
for j=1:1:8
for k=1:1:21
ic(k,j)=((((gamma*xdata(j,1))^(k-1))*exp(-gamma*xdata(j,1)))/factorial(k-1))*num;
end
end
%*******************************
for i=1:1:npoints+1
Kmax=20;T=24;
for m=1:1:Kmax+1
for k=1:1:Kmax+1
V(k,:)=(k-1)*(1-p)*Vmax/(Km+(k-1));
if (m-1)+(k-1)<=Kmax
K=k-1;M=m-1;
d6(k,m)=(-alpha1*(m-1)-alpha2*((k-1)^2))-((Vmax*(k-1))/(Km+k-1));
G(k,m)=(k-1)*p*Vmax/(Km+k-1);
else
continue
end
end
end
s=Kmax+1;
V=V(1:Kmax+1,1);
for l=1:1:Kmax
l;
s=s+(Kmax+1-l);
end
s;
t=0;
A=zeros(s);
for r=1:1:Kmax
n=s-(Kmax-(r-1));
if r-1==0
v1=[V;zeros(n-length(V),1)];
A=A+diag(v1,-(Kmax-(r-1)));
continue
```

```
else
r-1;
t;
t=t+(Kmax+1-(r-2));
v2=zeros(t,1);
v4=V(1:Kmax+1-(r-1),1);
v3=[v2;v4];
v1=[v3;zeros(n-length(v3),1)];
A=A+diag(v1,-(Kmax-(r-1)));
end
end
size(A);
x=[d6(1:Kmax+1,1)];
for m=1:1:Kmax
x=[x;d6(1:Kmax+1-m,m+1)];
end
x;
A1=diag(x);
size(A1);
matrix=A+A1;
G;
GG=[G(2:Kmax+1,1)];
for m=1:1:Kmax
GG=[GG;G(1:Kmax+1-m,m+1)];
end
A3=diag(GG,1);
system=A+A1+A3;%SYSTEM OF ODE
NN=ic(:,i);NNN=NN(1:Kmax+1,1);
Nnew=[NNN;zeros(s-length(NNN),1)];
%******************
%simulation results
%******************
solution=expm(system*T)*Nnew;
Sol=sum(solution);
S(:,i)=Sol/num;
```

```
%*****************
end
%*******************
%Objective function values (SSE)
%*********************
    S_log=log10(S*100)'; FittedCurve=S_log;
    Fitted=FittedCurve'; %compare this data with the real/experimental data
    ErrorVector =FittedCurve-ydata;
    fval= sum(ErrorVector.*ErrorVector); %This is the cost function
    end
    end
```

A.5.2 Results of parameter estimation using low LET IR survival data for $\xi = 150$

	Column 1						Column 2							Column 3	Column 4
	Initial guesses						Estimated parameter values							$\alpha_{exp} = 0.0598$	$\beta_{exp} = 0.0158$
Run	δ	α_1	α_2	p	V_{max}	K_M	δ	α_1	α_2	p	V_{max}	K_M	SSE	α_{model}	β_{model}
1	7.6732	11.9704	0.0022	0.1564	0.7285	1.8870	2.0000	6.2194	0.0011	0.99999	2.9974	0.00021	35.5698	1.2165	0.0340
2	11.7853	1.2689	0.0075	0.8555	2.7523	1.0801	2.0000	9.4877	0.0078	0.99980	3.0000	0.00253	35.5808	1.2168	0.0340
3	33.9473	4.9023	0.0020	0.6448	0.8072	3.9520	2.0000	7.6534	0.0095	0.99999	2.9987	0.00032	35.5644	1.2164	0.0340
4	11.6627	7.3601	0.0069	0.3763	2.2965	4.7465	2.0000	3.8419	0.0100	1.00000	3.0000	0.00014	35.5563	1.2163	0.0340
5	32.9428	17.0776	0.0054	0.1909	0.5660	1.6378	2.0000	5.4462	0.0010	1.00000	2.9999	0.00008	35.5562	1.2163	0.0340
6	11.2539	0.3475	0.0080	0.4283	0.8625	3.3563	2.0000	4.4432	0.0013	1.00000	2.9978	0.00023	35.5678	1.2165	0.0340
7	37.3120	0.9210	0.0074	0.4820	0.2733	2.1932	2.0000	8.3287	0.0100	0.99556	2.9250	0.02895	36.2662	1.2321	0.0332
8	15.2994	3.5363	0.0091	0.1206	1.7286	4.1675	2.0000	20.7899	0.0010	0.99985	3.0000	0.00024	35.5606	1.2164	0.0340
9	9.4706	13.5048	0.0090	0.5895	2.0501	3.8443	2.0000	20.6491	0.0085	0.99999	2.9976	0.00035	35.5697	1.2166	0.0340
10	11.5412	15.2199	0.0040	0.2262	1.6398	0.8363	2.0053	0.5218	0.0090	0.99423	2.7679	0.11712	38.2300	1.2714	0.0314
11	25.4097	13.4764	0.0073	0.3846	1.2772	4.3099	2.0000	14.3145	0.0032	1.00000	2.9792	0.00005	35.6556	1.2183	0.0339
12	19.9850	9.3899	0.0028	0.5830	1.9333	4.9494	2.0000	10.2479	0.0100	1.00000	2.9997	0.00001	35.5570	1.2163	0.0340
13	15.3631	11.3849	0.0013	0.2518	1.9429	2.5721	2.0004	6.6293	0.0011	0.99941	2.9985	0.00012	35.6029	1.2171	0.0340
14	33.5715	6.1800	0.0077	0.2904	2.0371	4.4214	2.0001	5.9524	0.0014	0.99999	2.9998	0.00003	35.5618	1.2164	0.0340
15	24.2400	15.4892	0.0055	0.6171	1.9074	2.9401	2.0000	14.9496	0.0096	1.00000	2.9994	0.00159	35.5712	1.2166	0.0340
16	22.8895	3.9508	0.0053	0.2653	2.8355	0.7738	2.0000	17.3398	0.0011	0.99998	3.0000	0.00006	35.5564	1.2163	0.0340
17	36.8534	14.2867	0.0091	0.8244	0.6268	0.9993	2.0000	10.0119	0.0012	0.99999	2.9995	0.00159	35.5743	1.2167	0.0340
18	12.8619	3.8378	0.0065	0.9827	2.1278	2.0348	2.0000	9.7628	0.0010	1.00000	2.9985	0.00109	35.5722	1.2167	0.0340
19	30.7736	7.6783	0.0066	0.7302	0.7087	3.7435	2.0000	1.3691	0.0026	0.99966	2.9997	0.00088	35.5721	1.2166	0.0340
20	30.6417	13.0170	0.0087	0.3439	0.3582	4.1279	2.0000	17.6068	0.0075	0.99890	2.9851	0.00232	35.6729	1.2188	0.0339
21	16.4569	16.2270	0.0082	0.5841	1.8219	3.9498	2.0000	17.5566	0.0098	0.99916	2.9964	0.00065	35.5972	1.2172	0.0339
22	23.5772	1.7121	0.0062	0.1078	1.3504	1.5926	2.0000	9.9101	0.0044	0.99998	2.9997	0.00000	35.5573	1.2162	0.0340
23	4.8825	19.3239	0.0026	0.9063	1.3762	2.6703	2.0000	19.2823	0.0010	0.99997	3.0000	0.00001	35.5563	1.2163	0.0340
24	4.0501	16.1333	0.0032	0.8797	1.9858	0.4498	2.0000	9.9975	0.0028	1.00000	3.0000	0.00005	35.5577	1.2163	0.0340
25	22.1703	10.1346	0.0090	0.8178	2.3109	0.5585	2.0000	18.4630	0.0017	0.99996	2.9989	0.14335	36.7281	1.2452	0.0323
26	31.6084	9.0771	0.0013	0.2607	1.0507	0.6815	2.0000	10.8062	0.0010	1.00000	2.9974	0.00012	35.5686	1.2165	0.0340
27	37.4924	9.3040	0.0054	0.5944	1.9860	3.3933	2.0000	2.7421	0.0098	1.00000	3.0000	0.00000	35.5552	1.2162	0.0340
28	6.9364	6.3882	0.0025	0.0225	1.2485	2.4759	2.0000	11.5805	0.0097	1.00000	2.9989	0.00005	35.5609	1.2164	0.0340
29	23.6153	10.5855	0.0098	0.4253	2.5258	0.9486	2.0000	12.5407	0.0010	1.00000	3.0000	0.00019	35.5568	1.2163	0.0340
30	19.8368	10.6325	0.0074	0.3127	2.4988	2.4750	2.0000	1.6404	0.0010	1.00000	3.0000	0.00000	35.5553	1.2162	0.0340

31	2.4523 17.00350.00550.16150.76930.7380	2.0001 2.5057 0.00850.999952.99990.00075	35.5676	1.2165	0.0340
32	14.810716.53020.00520.17881.84040.2749	2.0000 8.5743 0.00100.999952.99990.00004	35.5572	1.2163	0.0340
33	15.694111.58310.00580.74750.44540.8435	2.0000 8.5957 0.00541.000003.00000.00000	35.5553	1.2163	0.0340
34	9.1740 11.01840.00970.74851.85943.7585	2.000019.52230.00241.000002.99660.00003	35.5736	1.2166	0.0340
35	2.0455 17.26000.00200.54330.78191.8418	2.000917.40370.00110.995152.99770.06681	36.2960	1.2336	0.0330
36	14.023917.85750.00150.33811.33704.7091	2.000012.90200.00991.000002.99920.00001	35.5590	1.2164	0.0340
37	28.585416.40980.00370.83232.53200.0859	2.000217.60810.00110.999842.99460.05802	52.1402	1.5643	0.0151
38	25.7597 6.6266 0.00620.55260.58864.1453	2.0000 8.1070 0.00320.999992.99900.00007	35.5605	1.2163	0.0340
39	22.6364 9.4166 0.00580.95750.91163.1330	2.000013.39350.00980.999442.99930.00001	35.5731	1.2166	0.0340
40	18.683415.64570.00910.89281.44992.6937	2.0000 4.2629 0.00960.999933.00000.00044	35.5605	1.2164	0.0340
41	12.9222 2.3087 0.00590.35651.01343.2525	2.0000 6.8721 0.01000.999943.00000.00139	35.5681	1.2166	0.0340
42	21.0630 2.3062 0.00490.54642.39553.6331	2.0000 2.5189 0.01000.999992.99990.00029	35.5584	1.2163	0.0340
43	30.9388 5.6311 0.00590.34672.96250.4724	2.0000 2.3938 0.00990.999952.99820.00349	35.5949	1.2172	0.0339
44	30.971510.92040.00740.62280.47714.3879	2.000120.34600.01000.999452.99140.00037	35.6212	1.2176	0.0339
45	23.890120.22220.00120.79660.71060.0718	2.0000 1.0157 0.01000.999973.00000.00000	35.5559	1.2163	0.0340
46	30.411214.77740.00820.74592.10671.4715	2.000013.45410.00961.000002.99840.00001	35.5628	1.2164	0.0340
47	26.5303 6.5026 0.00230.12551.12640.8996	2.0000 3.3243 0.01000.999943.00000.00002	35.5566	1.2163	0.0340
48	6.6823 6.0790 0.00530.82242.92114.6315	2.0000 1.4633 0.00901.000002.99670.00266	35.5931	1.2172	0.0339
49	21.167117.68310.00330.02522.91690.3409	2.000013.30930.00970.999883.00000.00036	35.5644	1.2164	0.0340
50	15.195918.95560.00430.41441.93112.9055	2.000014.62720.00270.999992.99990.00012	35.5567	1.2163	0.0340
51	5.5016 13.30050.00700.73142.58033.1858	2.0000 6.3874 0.00110.999992.99740.00021	35.5698	1.2165	0.0340
52	7.6183 5.3298 0.00250.78141.20573.2563	2.000011.52380.00780.999803.00000.00253	35.5808	1.2169	0.0339
53	9.5304 1.8686 0.00350.36731.89584.3231	2.000013.03990.00150.999632.99820.00040	35.5755	1.2167	0.0340
54	27.546317.43180.00280.74492.95570.2798	2.000010.08670.01001.000003.00000.00067	35.5610	1.2164	0.0340
55	18.397412.16780.00280.89231.67844.0843	2.000010.53790.00990.999973.00000.00000	35.5560	1.2163	0.0340
56	28.387319.71260.00390.24262.80082.6446	2.000017.58610.00980.999992.99940.00088	35.5657	1.2165	0.0340
57	11.7578 1.2948 0.00890.12962.16103.4718	2.000017.09230.01001.000003.00000.00000	35.5552	1.2163	0.0340
58	2.3708 12.16620.00520.22511.45211.0620	2.000018.83580.00320.995702.96700.98135	52.0881	1.5633	0.0152
59	22.2268 5.9472 0.00460.35001.91712.7164	2.000011.75150.00850.999992.99730.00037	35.5714	1.2166	0.0340
60	12.616917.21330.00260.28712.66293.5126	2.000019.58490.01001.000003.00000.00000	35.5552	1.2162	0.0340
61	37.9567 3.9930 0.00970.92750.59624.7822	2.000018.24110.00670.999932.99970.00011	35.5593	1.2163	0.0340
62	36.4448 9.2156 0.00470.05131.18612.2227	2.000016.09570.01000.999872.99970.00317	35.5861	1.2170	0.0339
63	16.9220 8.1958 0.00860.59272.97650.4270	2.000019.87760.00111.000002.99980.00010	35.5571	1.2163	0.0340
64	2.9445 17.18930.00650.16291.20710.2867	2.000018.80800.00141.000002.99930.00003	35.5592	1.2163	0.0340
65	27.514614.08110.00440.83841.97663.1473	2.000019.00840.00961.000002.99940.00177	35.5730	1.2166	0.0340
66	33.8125 4.3380 0.00890.16762.70403.9809	2.0003 1.4216 0.00301.000002.99990.00005	35.5795	1.2165	0.0340
67	38.9170 6.6323 0.00810.50222.98613.4560	2.0000 9.9380 0.00361.000002.99930.00013	35.5599	1.2163	0.0340
68	4.1634 2.8059 0.00520.99931.95951.7265	2.0000 4.4709 0.00101.000002.99970.00002	35.5566	1.2163	0.0340
69	19.112313.96880.00830.35540.32534.7341	2.000013.55820.00260.999212.99960.00097	35.5834	1.2169	0.0339
70	24.133911.88280.00910.04710.10832.6010	2.000019.50280.00991.000003.00000.00000	35.5552	1.2163	0.0340
71	28.0922 3.5525 0.00490.21371.85434.7691	2.000012.75900.00980.999092.99610.00071	35.6010	1.2173	0.0339
72	29.3384 3.0934 0.00400.39781.70140.3680	2.0000 1.0501 0.01001.000003.00000.00000	35.5553	1.2162	0.0340
73	26.7015 9.9122 0.00640.33372.88591.0352	2.000020.58450.00960.999992.95640.00069	35.7712	1.2207	0.0338
74	29.622818.88200.00910.22962.23833.8751	2.000016.17460.00991.000002.99930.00000	35.5586	1.2164	0.0340
75	16.206211.49210.00730.93611.98754.5709	2.000020.40010.00130.999823.00000.00058	35.5645	1.2165	0.0340
76	24.1001 0.7116 0.00440.68321.56993.9128	2.000318.50350.00291.000002.99810.00011	35.5839	1.2167	0.0340
77	6.4125 1.1460 0.00760.96210.77971.4777	2.0000 1.4503 0.00981.000003.00000.00002	35.5554	1.2163	0.0340
78	4.1909 16.74270.00960.43802.88600.7592	2.000019.68980.00971.000002.99880.00006	35.5615	1.2164	0.0340
79	39.2311 9.3993 0.00590.94031.62064.2396	2.000020.31730.00131.000002.99670.22614	37.3854	1.2610	0.0314
80	12.8233 7.9723 0.00590.00580.09083.9243	2.000011.15670.00100.999982.99970.00006	35.5582	1.2164	0.0340
81	24.609016.42250.00380.61032.08891.3542	2.000015.14510.00100.999903.00000.00000	35.5575	1.2163	0.0340
82	38.5621 7.5911 0.00160.80111.55911.1391	2.000011.26690.01000.999842.99970.00150	35.5737	1.2168	0.0340
83	9.0596 11.08050.00260.23300.17711.6051	2.000012.18850.00550.999953.00000.00002	35.5566	1.2163	0.0340
84	9.3355 14.80330.00180.93252.67014.1478	2.0000 0.0874 0.01001.000002.99990.00000	35.5564	1.2163	0.0340
85	14.982518.12160.00520.76330.99064.1109	2.0002 6.9865 0.00110.999632.99870.00625	35.6330	1.2180	0.0339
86	37.4501 6.8521 0.00110.82640.68912.8534	2.0000 6.4768 0.00991.000002.99690.00004	35.5704	1.2166	0.0340
87	16.845413.52560.00920.57350.34182.8591	2.000013.65530.00820.997972.99790.00459	35.6527	1.2185	0.0339
88	12.382220.26750.00680.79260.93281.4301	2.000113.56920.00990.971062.54910.01047	38.6676	1.2809	0.0309
89	7.7740 1.6050 0.00100.32900.68533.4957	2.000017.88290.00980.999422.99920.00001	35.5735	1.2167	0.0340

90	17.0901	12.2156	0.0013	0.2235	1.9560	3.9813	2.0000	1.7156	0.0096	0.99993	3.0000	0.00045	35.5606	1.2165	0.0340
91	16.2395	8.6209	0.0029	0.3124	0.1985	2.2079	2.0002	0.4312	0.0096	0.99927	2.9994	0.00045	35.5900	1.2170	0.0339
92	6.9824	6.4461	0.0051	0.5845	0.8263	2.2311	2.0001	3.0685	0.0011	0.99986	2.9995	0.00000	35.5657	1.2164	0.0340
93	18.5315	5.5055	0.0021	0.8299	0.8455	2.3283	2.0000	19.0151	0.0086	1.00000	2.9999	0.00000	35.5559	1.2163	0.0340
94	5.4775	15.7814	0.0011	0.2905	2.6402	1.3952	2.0000	3.2265	0.0091	0.99995	2.9965	0.00009	35.5740	1.2166	0.0340
95	25.3558	20.6907	0.0075	0.4026	1.3330	3.3769	2.0000	11.7366	0.0046	1.00000	2.9953	0.00003	35.5788	1.2167	0.0340
96	2.4172	3.9014	0.0042	0.8621	2.2677	4.5183	2.0000	20.6103	0.0010	0.99996	2.9996	0.00000	35.5587	1.2163	0.0340
97	23.7839	16.2461	0.0080	0.6147	1.8099	4.5426	2.0000	12.9775	0.0083	0.99999	2.9917	0.00000	35.5956	1.2171	0.0339
98	32.0097	4.0929	0.0049	0.9912	2.3498	3.7360	2.0000	9.3979	0.0081	0.99981	2.9994	0.00047	35.5667	1.2165	0.0340
99	10.9439	20.6314	0.0049	0.2037	0.3418	1.3026	2.0000	12.9624	0.0019	1.00000	2.9999	0.00002	35.5558	1.2162	0.0340
100	19.0247	16.6845	0.0014	0.8272	2.9357	3.4482	2.0003	18.3529	0.0050	0.99996	2.9109	0.05597	36.4751	1.2368	0.0329
101	23.6356	8.8356	0.0014	0.6759	2.5458	0.6592	2.0001	3.4804	0.0011	0.9999	2.9930	0.0001	35.6000	1.2170	0.0340
102	4.3333	15.1606	0.0018	0.2489	0.1519	0.6175	2.0000	15.9362	0.0078	0.9998	3.0000	0.0025	35.5805	1.2168	0.0340
103	20.8590	10.3747	0.0063	0.4758	1.3986	0.9545	2.0000	11.5642	0.0081	0.9997	2.9990	0.0070	35.6249	1.2180	0.0339
104	26.4080	16.8242	0.0032	0.3991	0.9770	0.7287	2.0000	9.3688	0.0100	0.9999	3.0000	0.0008	35.5632	1.2165	0.0340
105	10.4081	7.4296	0.0086	0.5994	1.8906	2.9252	2.0000	13.4045	0.0099	1.0000	3.0000	0.00001	35.5560	1.2163	0.0340
106	33.8081	1.5484	0.0087	0.8005	0.6909	0.3668	2.0000	17.2845	0.0065	0.9989	2.9999	0.0017	35.5957	1.2173	0.0339
107	38.9009	12.2980	0.0097	0.1051	1.7397	4.1116	2.0000	20.0822	0.0067	0.9999	2.9998	0.0001	35.5583	1.2164	0.0340
108	34.1622	18.9253	0.0054	0.8214	1.8095	3.6145	2.0000	16.8697	0.0010	1.0000	2.9950	0.0003	35.5813	1.2167	0.0340
109	21.2280	4.0507	0.0030	0.8411	1.7996	4.6293	2.0000	20.3461	0.0019	1.0000	2.9995	0.0001	35.5597	1.2163	0.0340
110	12.5973	9.0046	0.0030	0.3545	1.3453	2.4632	2.0000	7.2996	0.0100	1.0000	3.0000	0.00001	35.5552	1.2162	0.0340
111	30.3715	15.5820	0.0058	0.4301	0.1063	3.2744	2.0000	17.5770	0.0096	1.0000	3.0000	0.00001	35.5555	1.2163	0.0340
112	11.0034	0.8413	0.0079	0.5722	1.5414	4.4506	2.0000	3.2139	0.0100	0.9998	2.9997	0.0021	35.5774	1.2168	0.0340
113	38.3791	19.6756	0.0041	0.7008	1.2232	2.6926	2.0000	20.1259	0.0011	1.0000	2.9998	0.0001	35.5570	1.2163	0.0340
114	25.5699	15.8833	0.0052	0.7425	0.3241	1.4110	2.0000	11.8455	0.0014	1.0000	2.9994	0.0003	35.5622	1.2164	0.0340
115	24.8100	11.6301	0.0068	0.7579	1.3796	4.8798	2.0000	18.1059	0.0096	1.0000	2.9994	0.0016	35.5715	1.2167	0.0340
116	8.5590	3.8447	0.0093	0.3891	1.3526	0.1821	2.0000	3.8935	0.0011	1.0000	3.0000	0.0001	35.5564	1.2163	0.0340
117	5.4332	10.3663	0.0025	0.4293	1.6534	1.6312	2.0000	15.4698	0.0010	1.0000	2.9997	0.0002	35.5597	1.2164	0.0340
118	11.7000	10.7794	0.0074	0.9563	2.4162	4.8651	2.0000	16.1480	0.0026	0.9993	2.9997	0.0009	35.5582	1.2163	0.0340
119	34.6257	20.6705	0.0062	0.5730	2.1026	1.8252	2.0000	19.1169	0.0099	1.0000	2.9985	0.0200	35.5817	1.2169	0.0339
120	36.6205	17.7764	0.0049	0.8497	2.6167	1.5457	2.0000	17.4892	0.0020	0.9993	2.9944	0.0100	35.7287	1.2206	0.0337
121	28.5861	20.0094	0.0090	0.2763	0.1566	0.6046	2.0000	15.1838	0.0044	1.0000	2.9997	0.00001	35.6811	1.2193	0.0338
122	29.5569	14.1241	0.0045	0.6223	0.6590	4.5788	2.0000	7.6860	0.0010	1.0000	3.0000	0.00001	35.5573	1.2163	0.0340
123	10.7357	8.4053	0.0026	0.5884	1.3789	0.6774	2.0001	7.4401	0.0073	1.0000	2.9826	0.0034	35.5563	1.2163	0.0340
124	23.8900	19.4400	0.0067	0.9635	2.8756	1.6606	2.0000	12.2375	0.0014	0.9997	2.9994	0.0312	35.6757	1.2187	0.0339
125	32.8039	9.9829	0.0066	0.0859	2.3701	4.4874	2.0000	1.1576	0.0034	0.9997	2.9992	0.0006	35.8243	1.2229	0.0336
126	17.3460	4.8402	0.0040	0.5005	1.3556	2.4982	2.0000	6.9122	0.0098	1.0000	3.0000	0.00001	35.5723	1.2166	0.0340
127	39.5607	8.2556	0.0082	0.5216	1.0003	3.0764	2.0000	16.3675	0.0019	0.9995	2.9999	0.0047	35.5554	1.2163	0.0340
128	5.4200	14.6667	0.0100	0.0902	0.1773	2.9157	2.0000	4.4375	0.0010	1.0000	3.0000	0.0002	35.6073	1.2176	0.0339
129	14.1958	11.6247	0.0098	0.9047	2.2227	3.4913	2.0000	4.5205	0.0010	1.0000	3.0000	0.00001	35.5568	1.2163	0.0340
130	21.4335	15.7371	0.0021	0.8844	1.5204	0.1467	2.0000	20.7573	0.0010	0.9997	2.9986	0.00001	35.5553	1.2163	0.0340
131	4.3030	20.6962	0.0031	0.4390	0.5998	2.6394	2.0000	19.7968	0.0085	1.0000	2.9876	0.0009	35.5699	1.2166	0.0340
132	29.5761	20.0100	0.0012	0.7817	1.2816	0.1604	2.0000	19.6115	0.0054	1.0000	3.0000	0.00001	35.6230	1.2177	0.0339
133	32.9595	3.3950	0.0068	0.4229	1.7467	4.2536	2.0000	8.2176	0.0100	1.0000	2.9999	0.0044	35.5553	1.2162	0.0340
134	36.4201	16.5189	0.0044	0.0942	1.6222	2.8028	2.0000	11.0065	0.0100	1.0000	2.9981	0.0001	35.5925	1.2172	0.0339
135	6.8255	6.4892	0.0083	0.5985	2.6098	4.6480	2.0000	0.2773	0.0099	1.0000	2.9993	0.00001	35.5653	1.2165	0.0340
136	36.7083	11.0013	0.0058	0.4709	0.7943	3.4833	2.0003	2.8201	0.0081	0.9990	2.9906	0.0018	35.5587	1.2163	0.0340
137	26.0297	3.4669	0.0042	0.6959	0.9542	2.9140	2.0000	10.7524	0.0098	1.0000	2.9996	0.0006	35.6585	1.2183	0.0339
138	5.7065	12.5262	0.0095	0.6999	0.3576	4.0770	2.0000	19.5660	0.0098	0.9995	2.9993	0.00001	35.5621	1.2164	0.0340
139	12.5829	5.4876	0.0089	0.6385	2.8195	4.3951	2.0000	11.4957	0.0096	0.9999	3.0000	0.0004	35.5720	1.2167	0.0340
140	22.7815	13.6079	0.0060	0.0336	1.9367	4.9446	2.0002	17.4180	0.0081	0.9999	2.9977	0.0007	35.5601	1.2164	0.0340
141	38.3853	14.3374	0.0066	0.0688	1.4384	0.0026	2.0000	12.9494	0.0098	0.9670	2.8711	0.0001	35.5881	1.2168	0.0340
142	38.6658	15.5610	0.0063	0.3196	1.9180	4.3272	2.0000	19.1591	0.0100	0.9999	2.9996	0.0004	52.9402	1.5775	0.0145
143	7.9893	9.3820	0.0029	0.5309	1.6341	3.0628	2.0001	8.9999	0.0098	0.9993	2.9991	0.0002	35.5616	1.2164	0.0340
144	38.8825	1.7680	0.0037	0.6544	1.9419	4.9498	2.0000	10.5831	0.0100	1.0000	3.0000	0.00001	35.5851	1.2168	0.0340
145	38.3723	4.7818	0.0052	0.4076	1.6317	2.6384	2.0000	1.3133	0.0100	1.0000	2.9927	0.0001	35.5559	1.2163	0.0340
146	20.4443	18.9907	0.0031	0.8200	2.1631	2.3976	2.0000	6.8798	0.0100	0.9999	3.0000	0.00001	35.5920	1.2170	0.0340
147	32.4107	3.1914	0.0086	0.7184	1.5675	4.0067	2.0000	20.6464	0.0058	0.9981	2.7399	0.0023	35.5565	1.2163	0.0340
148	7.3917	17.1736	0.0028	0.9686	2.9811	1.1392	2.0000	16.1798	0.0097	0.9999	3.0000	0.0003	36.9241	1.2442	0.0327

149	18.0269	11.2049	0.0030	0.5313	0.6560	2.4905	2.0000	4.3074	0.0029	1.0000	2.9998	0.00001	35.5629	1.2163	0.0340
150	36.7979	20.7097	0.0025	0.3251	0.3174	4.5043	2.0000	14.6272	0.0027	1.0000	2.9999	0.00012	35.5579	1.2163	0.0340

Table A.5: The results of optimisations for 150 rounds of Simulated Annealing using low LET IR. Columns 3 and 4 are the value of LQ parameters α_{model} and β_{model} for each run with the value of LQ parameters for the experimental data $\alpha_{exp} = 0.2790$ Gy^{-1} and $\beta_{exp} = 0.0357$ Gy^{-2}.

A.5.3 Results of parameter estimation using high LET IR survival data for $\xi = 150$

	Column 1						Column 2							Column 3	Column 4
	Initial guesses						Estimated parameter values							$\alpha_{exp} = 0.0598$	$\beta_{exp} = 0.0158$
Run	δ	α_1	α_2	p	V_{max}	K_M	δ	α_1	α_2	p	V_{max}	K_M	SSE	α_{model}	β_{model}
1	7.6732	11.9704	0.0022	0.1564	0.7285	1.8870	2.0000	5.5692	0.0088	0.9905	2.9947	0.1161	2.32	1.0582	0.0809
2	11.7853	1.2689	0.0075	0.8555	2.7523	1.0801	2.0070	7.9445	0.0016	0.9631	2.4083	0.1748	3.1113	1.1826	0.0688
3	33.9473	4.9023	0.0020	0.6448	0.8072	3.9520	2.0004	0.1487	0.0011	0.9711	2.4635	0.0052	2.6755	1.1119	0.0766
4	11.6627	7.3601	0.0069	0.3763	2.2965	4.7465	2.0067	2.3688	0.0034	0.9979	2.9984	0.0531	2.2478	1.0388	0.0841
5	32.9428	17.0776	0.0054	0.1909	0.5660	1.6378	2.0000	12.164	0.0088	0.9935	2.8603	3.1436	5.6394	1.526	0.0288
6	11.2539	0.3475	0.0080	0.4283	0.8625	3.3563	2.0000	9.4274	0.0099	0.9995	2.9877	0.0000	2.1209	1.0173	0.086
7	37.312	0.9210	0.0074	0.4820	0.2733	2.1932	2.0000	11.5854	0.0097	0.9998	2.658	0.7302	3.445	1.2474	0.059
8	15.2994	3.5363	0.0091	0.1206	1.7286	4.1675	2.0000	2.2955	0.0012	0.9999	2.9989	0.0011	2.1128	1.0159	0.0862
9	9.4706	13.5048	0.0090	0.5895	2.0501	3.8443	2.0002	20.7896	0.0011	0.9964	2.9879	0.0745	2.2431	1.0425	0.0829
10	11.5412	15.2199	0.0040	0.2262	1.6398	0.8363	2.0000	0.4287	0.0093	0.9910	2.9616	0.0001	2.173	1.0273	0.0849
11	25.4097	13.4764	0.0073	0.3846	1.2772	4.3099	2.0000	1.3646	0.0014	1.0000	2.9991	0.0079	2.1225	1.018	0.0859
12	19.985	9.3899	0.0028	0.5830	1.9333	4.9494	2.0000	13.5035	0.0029	0.9980	2.6767	0.0014	2.3694	1.0599	0.082
13	15.3631	11.3849	0.0013	0.2518	1.9429	2.5721	2.0000	7.5185	0.0016	0.9984	2.998	0.0092	2.1312	1.0197	0.0857
14	33.5715	6.1800	0.0077	0.2904	2.0371	4.4214	2.0003	1.2708	0.0086	0.9998	2.9999	0.0022	2.1159	1.0163	0.0861
15	24.24	15.4892	0.0055	0.6171	1.9074	2.9401	2.0006	9.4257	0.0091	0.9991	2.9058	0.0631	2.2801	1.0478	0.0826
16	22.8895	3.9508	0.0053	0.2653	2.8355	0.7738	2.0014	11.739	0.0014	0.9936	2.9797	0.2917	2.5803	1.1072	0.075
17	36.8534	14.2867	0.0091	0.8244	0.6268	0.9993	2.0000	1.9149	0.0012	0.9452	2.9935	0.0019	2.3395	1.0608	0.0808
18	12.8619	3.8378	0.0065	0.9827	2.1278	2.0348	2.0020	3.0476	0.0086	0.9957	2.9927	0.0046	2.1536	1.0226	0.0856
19	30.7736	7.6783	0.0066	0.7302	0.7087	3.7435	2.0033	2.737	0.0099	0.9973	2.8748	0.0047	2.2449	1.0375	0.0844
20	30.6417	13.0170	0.0087	0.3439	0.3582	4.1279	2.0000	15.7789	0.008	1.0000	2.7846	0.5811	3.1151	1.1975	0.0645
21	16.4569	16.2270	0.0082	0.5841	1.8219	3.9498	2.0015	13.6888	0.0044	0.9990	2.9043	0.0021	2.1979	1.03	0.085
22	23.5772	1.7121	0.0062	0.1078	1.3504	1.5926	2.0000	0.4216	0.0085	0.9970	2.9161	0.0304	2.2277	1.0377	0.0838
23	4.8825	19.3239	0.0026	0.9063	1.3762	2.6703	2.0000	17.0833	0.0042	0.9999	2.7943	0.0000	2.2641	1.0419	0.0838
24	4.0501	16.1333	0.0032	0.8797	1.9858	0.4498	2.0111	8.0666	0.0017	0.9182	2.751	0.5527	3.5846	1.2611	0.0588
25	22.1703	10.1346	0.0090	0.8178	2.3109	0.5585	2.0001	6.5105	0.0012	0.9999	2.998	0.0083	2.1242	1.0182	0.0859
26	31.6084	9.0771	0.0013	0.2607	1.0507	0.6815	2.0038	7.6625	0.0017	0.9962	2.9899	0.0084	2.1728	1.0252	0.0855
27	37.4924	9.3040	0.0054	0.5944	1.9860	3.3933	2.0001	0.6229	0.0097	1.0000	2.9239	0.1302	2.3577	1.0642	0.0804
28	6.9364	6.3882	0.0025	0.0225	1.2485	2.4759	2.0001	5.105	0.0011	0.9958	2.9958	0.0147	2.1512	1.0237	0.0852
29	23.6153	10.5855	0.0098	0.4253	2.5258	0.9486	2.0000	12.2303	0.002	0.9979	2.9869	0.0024	2.1315	1.0194	0.0858
30	19.8368	10.6325	0.0074	0.3127	2.4988	2.4750	2.2040	11.2276	0.0012	0.8143	2.8485	0.0157	5.2662	1.3584	0.071
31	2.4523	17.0035	0.0055	0.1615	0.7693	0.7380	2.0000	7.0496	0.001	0.9999	2.9989	0.0560	2.1926	1.0327	0.084
32	14.8107	16.5302	0.0052	0.1788	1.8404	0.2749	2.0050	16.7905	0.0019	0.9956	2.316	0.3972	3.4128	1.2322	0.0626
33	15.6941	11.5831	0.0058	0.7475	0.4454	0.8435	2.0035	3.7663	0.0015	0.9611	2.7387	0.0386	2.556	1.0942	0.078
34	9.174	11.0184	0.0097	0.7485	1.8594	3.7585	2.0001	15.4618	0.0099	1.0000	2.8946	0.0022	2.1912	1.0295	0.0849
35	2.0455	17.2600	0.0020	0.5433	0.7819	1.8418	2.0000	2.6145	0.0097	0.9939	2.9578	0.2837	2.5746	1.1065	0.075
36	14.0239	17.8575	0.0015	0.3381	1.3370	4.7091	2.0002	2.9258	0.0019	0.9993	2.9415	0.0229	2.1906	1.0305	0.0846
37	28.5854	16.4098	0.0037	0.8323	2.5320	0.0859	2.0004	12.7343	0.0099	0.9999	2.9848	0.0009	2.1255	1.0177	0.0861
38	25.7597	6.6266	0.0062	0.5526	0.5886	4.1453	2.0002	17.7825	0.001	0.9992	2.8162	0.0236	2.2874	1.0472	0.083
39	22.6364	9.4166	0.0058	0.9575	0.9116	3.1330	2.0001	12.2106	0.0098	0.9985	2.9026	0.0046	2.1938	1.0302	0.0848
40	18.6834	15.6457	0.0091	0.8928	1.4499	2.6937	2.0001	19.1845	0.0098	0.9995	2.9515	0.0000	2.1475	1.0218	0.0856
41	12.9222	2.3087	0.0059	0.3565	1.0134	3.2525	2.0199	18.7071	0.0079	0.8706	2.4976	0.1589	3.5485	1.2434	0.0631

42	21.063	2.3062	0.0049	0.5464	2.3955	3.6331	2.0000	19.0389	0.0038	0.9254	2.789	1.3705	4.4227	1.3844	0.0434
43	30.9388	5.6311	0.0059	0.3467	2.9625	0.4724	2.0000	8.0444	0.001	0.9994	2.9989	0.0003	2.1139	1.0161	0.0861
44	30.9715	10.9204	0.0074	0.6228	0.4771	4.3879	2.0008	2.9093	0.0031	0.9983	2.9999	0.0007	2.1237	1.0175	0.0861
45	23.8901	20.2222	0.0012	0.7966	0.7106	0.0718	2.0014	20.7865	0.0095	0.9933	2.9963	0.0376	2.2042	1.0337	0.0841
46	30.4112	14.7774	0.0082	0.7459	2.1067	1.4715	2.0000	7.8581	0.0046	1.0000	2.9203	0.0001	2.1679	1.0254	0.0853
47	26.5303	6.5026	0.0023	0.1255	1.1264	0.8996	2.0002	17.687	0.003	1.0000	2.9468	0.0014	2.1518	1.0226	0.0856
48	6.6823	6.0790	0.0053	0.8224	2.9211	4.6315	2.0001	8.2279	0.0081	0.9996	2.9337	0.0059	2.169	1.0258	0.0852
49	21.1671	17.6831	0.0033	0.0252	2.9169	0.3409	2.0004	14.9306	0.0017	0.9994	2.8892	0.0025	2.1997	1.0309	0.0848
50	15.1959	18.9556	0.0043	0.4144	1.9311	2.9055	2.0000	17.7095	0.0015	0.9990	2.9789	0.0536	2.2076	1.0351	0.0838
51	5.5016	13.3005	0.0070	0.7314	2.5803	3.1858	2.0000	5.7372	0.0088	0.9905	2.9947	0.1161	2.32	1.0582	0.0809
52	7.6183	5.3298	0.0025	0.7814	1.2057	3.2563	2.0070	4.6211	0.0016	0.9631	2.4085	0.1921	3.1398	1.1874	0.0682
53	9.5304	1.8686	0.0035	0.3673	1.8958	4.3231	2.0066	9.5593	0.0098	0.9974	2.9632	0.0283	2.2387	1.036	0.0846
54	27.5463	17.4318	0.0028	0.7449	2.9557	0.2798	2.0231	10.7168	0.0099	0.9983	2.9533	0.0025	2.3306	1.0415	0.0861
55	18.3974	12.1678	0.0028	0.8923	1.6784	4.0843	2.0004	0.9247	0.0073	0.9815	2.8878	0.3114	2.727	1.1322	0.0722
56	28.3873	19.7126	0.0039	0.2426	2.8008	2.6446	2.0000	4.2634	0.0012	0.9495	2.9821	0.0202	2.3574	1.0642	0.0804
57	11.7578	1.2948	0.0089	0.1296	2.1610	3.4718	2.0000	2.7849	0.0078	0.9966	2.9388	0.0017	2.1701	1.0262	0.0852
58	2.3708	12.1662	0.0052	0.2251	1.4521	1.0620	2.0058	5.323	0.0022	0.9917	2.9106	0.0063	2.2612	1.0397	0.0843
59	22.2268	5.9472	0.0046	0.3500	1.9171	2.7164	2.0000	18.7718	0.0059	0.9965	2.9759	0.0086	2.154	1.0238	0.0853
60	12.6169	17.2133	0.0026	0.2871	2.6629	3.5126	2.0000	8.1045	0.001	0.9992	2.9993	0.0010	2.1152	1.0162	0.0861
61	37.9567	3.9930	0.0097	0.9275	0.5962	4.7822	2.0048	13.8843	0.0095	0.9998	2.9016	0.0501	2.2944	1.0472	0.0832
62	36.4448	9.2156	0.0047	0.0513	1.1861	2.2227	2.0000	2.455	0.0029	0.9980	2.6826	0.0013	2.3643	1.0591	0.0821
63	16.922	8.1958	0.0086	0.5927	2.9765	0.4270	2.0026	18.7459	0.0099	1.0000	2.9998	0.0039	2.1351	1.0186	0.0862
64	2.9445	17.1893	0.0065	0.1629	1.2071	0.2867	2.0008	4.2303	0.0035	0.9999	2.9968	0.0039	2.1244	1.0176	0.0861
65	27.5146	14.0811	0.0044	0.8384	1.9766	3.1473	2.0000	17.5991	0.0077	0.9831	2.6555	1.6079	4.5698	1.4023	0.0416
66	33.8125	4.3380	0.0089	0.1676	2.7040	3.9809	2.0011	17.0845	0.0099	0.9675	2.3784	0.0532	2.8649	1.1435	0.0731
67	38.917	6.6323	0.0081	0.5022	2.9861	3.4560	2.0035	19.3365	0.006	0.9852	2.9277	0.0002	2.2477	1.0389	0.0841
68	4.1634	2.8059	0.0052	0.9993	1.9595	1.7265	2.0000	7.6674	0.001	0.9999	2.994	0.0114	2.1313	1.0196	0.0857
69	19.1123	13.9688	0.0083	0.3554	0.3253	4.7341	2.0000	7.4328	0.0071	0.9847	2.86	0.0090	2.2874	1.048	0.0828
70	24.1339	11.8828	0.0091	0.0471	0.1083	2.6010	2.0000	0.8458	0.0099	1.0000	2.8836	0.0000	2.1951	1.03	0.0849
71	28.0922	3.5525	0.0049	0.2137	1.8543	4.7691	2.0009	19.4849	0.01	0.9968	2.98	0.0056	2.152	1.0228	0.0855
72	29.3384	3.0934	0.0040	0.3978	1.7014	0.3680	2.0054	0.4045	0.0015	0.9992	2.6621	0.0075	2.4301	1.0674	0.0819
73	26.7015	9.9122	0.0064	0.3337	2.8859	1.0352	2.0004	17.7205	0.0095	0.9999	2.1483	2.5474	6.0712	1.5662	0.0259
74	29.6228	18.8820	0.0091	0.2296	2.2383	3.8751	2.0006	8.8131	0.0096	0.9320	2.988	4.3689	6.547	1.6159	0.0206
75	16.2062	11.4921	0.0073	0.9361	1.9875	4.5709	2.0023	9.7434	0.0011	0.9994	2.9929	0.0078	2.1461	1.0209	0.0859
76	24.1001	0.7116	0.0044	0.6832	1.5699	3.9128	2.0007	7.3933	0.0012	0.9985	2.925	0.0049	2.1828	1.028	0.0851
77	6.4125	1.1460	0.0076	0.9621	0.7797	1.4777	2.0000	2.2351	0.0011	0.9977	2.7972	0.0000	2.2705	1.0432	0.0836
78	4.1909	16.7427	0.0096	0.4380	2.8860	0.7592	2.0000	13.714	0.0011	0.9973	2.9974	0.0065	2.1323	1.0198	0.0857
79	39.2311	9.3993	0.0059	0.9403	1.6206	4.2396	2.0063	6.6353	0.001	0.9998	2.9927	0.0019	2.166	1.022	0.0862
80	12.8233	7.9723	0.0059	0.0058	0.0908	3.9243	2.0026	1.0355	0.0093	0.9724	2.8765	0.0590	2.421	1.0727	0.08
81	24.609	16.4225	0.0038	0.6103	2.0889	1.3542	2.0000	18.9414	0.001	0.9999	2.9989	0.0492	2.1827	1.0306	0.0843
82	38.5621	7.5911	0.0016	0.8011	1.5591	1.1391	2.0257	5.8508	0.0087	0.9895	2.6431	0.0175	2.6704	1.0969	0.0809
83	9.0596	11.0805	0.0026	0.2330	0.1771	1.6051	2.0000	17.7293	0.001	0.9984	3	0.0022	2.1196	1.0172	0.086
84	9.3355	14.8033	0.0018	0.9325	2.6701	4.1478	2.0007	10.1641	0.0011	0.9995	2.9994	0.0034	2.1221	1.0172	0.0861
85	14.9825	18.1216	0.0052	0.7633	0.9906	4.1109	2.0003	0.5027	0.001	0.9810	2.9524	0.0810	2.3413	1.061	0.0808
86	37.4501	6.8521	0.0011	0.8264	0.6891	2.8534	2.0002	10.7709	0.0019	0.9995	2.8881	0.0175	2.2215	1.0356	0.0842
87	16.8454	13.5256	0.0092	0.5735	0.3418	2.8591	2.0001	19.5868	0.0051	0.9789	2.9973	0.0200	2.2254	1.0386	0.0834
88	12.3822	20.2675	0.0068	0.7926	0.9328	1.4301	2.0059	19.2927	0.0015	0.9970	2.979	0.0001	2.1808	1.025	0.0859
89	7.774	1.6050	0.0010	0.3290	0.6853	3.4957	2.0057	18.7625	0.01	0.9996	2.9928	0.0051	2.1663	1.0225	0.0861
90	17.0901	12.2156	0.0013	0.2235	1.9560	3.9813	2.0001	0.2194	0.0098	0.9996	2.9591	0.0000	2.1416	1.0209	0.0857
91	16.2395	8.6209	0.0029	0.3124	0.1985	2.2079	2.0000	18.5612	0.01	1.0000	2.9995	0.0006	2.1112	1.0155	0.0862
92	6.9824	6.4461	0.0051	0.5845	0.8263	2.2311	2.0048	11.9976	0.0091	0.9979	2.849	0.0261	2.3061	1.0483	0.0833
93	18.5315	5.5055	0.0021	0.8299	0.8455	2.3283	2.0000	11.3849	0.0093	0.9996	2.9936	0.0129	2.1349	1.0204	0.0856
94	5.4775	15.7814	0.0011	0.2905	2.6402	1.3952	2.0066	3.234	0.0085	0.9640	2.7625	1.7608	4.7699	1.4239	0.0399
95	25.3558	20.6907	0.0075	0.4026	1.3330	3.3769	2.0006	7.8191	0.0095	0.9957	2.9974	0.0375	2.188	1.031	0.0843
96	2.4172	3.9014	0.0042	0.8621	2.2677	4.5183	2.0000	6.7374	0.0086	0.9866	2.8892	0.0201	2.2744	1.0461	0.0829
97	23.7839	16.2461	0.0080	0.6147	1.8099	4.5426	2.0085	12.7028	0.0028	0.9964	2.3655	0.0102	2.7481	1.1172	0.0773
98	32.0097	4.0929	0.0049	0.9912	2.3498	3.7360	2.0000	16.8683	0.001	0.9898	2.4727	0.1183	2.7754	1.1315	0.0739
99	10.9439	20.6314	0.0049	0.2037	0.3418	1.3026	2.0003	16.6714	0.0017	0.9995	2.9077	0.0107	2.1975	1.0311	0.0847
100	19.0247	16.6845	0.0014	0.8272	2.9357	3.4482	2.0031	18.3441	0.0047	0.9590	2.738	0.0397	2.5634	1.0959	0.0778

101	23.6356	8.8356	0.0014	0.6759	2.5458	0.6592	2.0007	7.4847	0.0029	0.9954	2.9398	0.0011	2.178	1.0274	0.0851
102	4.3333	15.1606	0.0018	0.2489	0.1519	0.6175	2.0021	11.8435	0.0011	0.9996	2.9987	0.0171	2.1533	1.0227	0.0856
103	20.859	10.3747	0.0063	0.4758	1.3986	0.9545	2.0027	9.0561	0.0014	0.9834	2.9752	0.0230	2.2477	1.0408	0.0835
104	26.408	16.8242	0.0032	0.3991	0.9770	0.7287	2.0061	9.5454	0.0034	0.9981	2.9986	0.0486	2.2352	1.0366	0.0843
105	10.4081	7.4296	0.0086	0.5994	1.8906	2.9252	2.0000	4.9188	0.0035	0.9990	2.6766	0.8145	3.5403	1.2622	0.0572
106	33.8081	1.5484	0.0087	0.8005	0.6909	0.3668	2.0000	3.095	0.0079	0.9938	2.6305	0.3496	2.9626	1.1686	0.0686
107	38.9009	12.2980	0.0097	0.1051	1.7397	4.1116	2.0000	19.4234	0.0078	0.9969	2.9583	0.0014	2.1543	1.0234	0.0854
108	34.1622	18.9253	0.0054	0.8214	1.8095	3.6145	2.0000	5.2534	0.0012	0.9999	2.9989	0.0011	2.1128	1.0158	0.0862
109	21.228	4.0507	0.0030	0.8411	1.7996	4.6293	2.0002	19.6919	0.001	0.9921	2.6228	0.0355	2.4949	1.0829	0.0794
110	12.5973	9.0046	0.0030	0.3545	1.3453	2.4632	2.0000	3.4832	0.001	0.9992	2.9994	0.0009	2.1149	1.0162	0.0861
111	30.3715	15.5820	0.0058	0.4301	0.1063	3.2744	2.0000	11.2342	0.0082	0.9998	2.8395	0.0009	2.2306	1.0362	0.0843
112	11.0034	0.8413	0.0079	0.5722	1.5414	4.4506	2.0000	13.2877	0.001	0.9993	2.9959	0.0240	2.1506	1.0238	0.0852
113	38.3791	19.6756	0.0041	0.7008	1.2232	2.6926	2.0001	3.9364	0.0098	0.9976	2.5934	0.0011	2.4421	1.072	0.0809
114	25.5699	15.8833	0.0052	0.7425	0.3241	1.4110	2.0000	14.8349	0.0084	1.0000	2.9066	0.0726	2.2857	1.0493	0.0823
115	24.81	11.6301	0.0068	0.7579	1.3796	4.8798	2.0054	5.8712	0.0076	0.9974	2.6452	0.0143	2.4624	1.0732	0.0812
116	8.559	3.8447	0.0093	0.3891	1.3526	0.1821	2.0007	12.1896	0.0066	0.9995	2.8875	0.0046	2.2066	1.032	0.0847
117	5.4332	10.3663	0.0025	0.4293	1.6534	1.6312	2.0053	1.635	0.0017	0.9914	2.9984	0.0007	2.1855	1.0267	0.0855
118	11.7	10.7794	0.0074	0.9563	2.4162	4.8651	2.0008	13.8239	0.0012	1.0000	2.9852	0.0007	2.1274	1.0179	0.0861
119	34.6257	20.6705	0.0062	0.5730	2.1026	1.8252	2.0051	14.6823	0.0084	0.9182	2.8867	0.0841	2.707	1.1234	0.0742
120	36.6205	17.7764	0.0049	0.8497	2.6167	1.5457	2.0161	18.0136	0.0015	0.9989	2.4758	0.0484	2.7588	1.1166	0.0778
121	28.5861	20.0094	0.0090	0.2763	0.1566	0.6046	2.0011	7.7282	0.0044	0.9993	2.9902	0.0015	2.1304	1.0184	0.086
122	29.5569	14.1241	0.0045	0.6223	0.6590	4.5788	2.0025	17.239	0.0045	0.9920	2.8424	0.0492	2.3521	1.059	0.0817
123	10.7357	8.4053	0.0026	0.5884	1.3789	0.6774	2.0000	16.8945	0.0042	0.9999	2.7977	0.0000	2.2615	1.0415	0.0838
124	23.89	19.4400	0.0067	0.9635	2.8756	1.6606	2.0002	11.5715	0.01	0.9886	2.1596	0.6012	3.9026	1.3058	0.0539
125	32.8039	9.9829	0.0066	0.0859	2.3701	4.4874	2.0019	12.8671	0.0011	0.9995	2.9943	0.0063	2.1391	1.0197	0.086
126	17.346	4.8402	0.0040	0.5005	1.3556	2.4982	2.0081	20.2866	0.0046	0.9977	2.641	0.1529	2.7079	1.1178	0.0759
127	39.5607	8.2556	0.0082	0.5216	1.0003	3.0764	2.0016	0.6487	0.0026	0.9836	2.2939	0.6143	3.7862	1.2904	0.0554
128	5.42	14.6667	0.0100	0.0902	0.1773	2.9157	2.0006	20.5942	0.0094	0.9869	2.9883	2.1825	4.7523	1.4273	0.0385
129	14.1958	11.6247	0.0098	0.9047	2.2227	3.4913	2.0000	13.7894	0.002	0.9980	2.9876	0.0022	2.1301	1.0192	0.0858
130	21.4335	15.7371	0.0021	0.8844	1.5204	0.1467	2.0000	8.294	0.001	1.0000	2.6687	0.0108	2.3829	1.0625	0.0817
131	4.303	20.6962	0.0031	0.4390	0.5998	2.6394	2.0000	18.1643	0.0011	0.9998	2.8493	0.0045	2.2288	1.0361	0.0843
132	29.5761	20.0100	0.0012	0.7817	1.2816	0.1604	2.0017	16.3963	0.0012	0.9974	2.9696	0.0448	2.2208	1.0363	0.0839
133	32.9595	3.3950	0.0068	0.4229	1.7467	4.2536	2.0001	4.6535	0.0012	1.0000	2.9634	0.0132	2.1568	1.024	0.0853
134	36.4201	16.5189	0.0044	0.0942	1.6222	2.8028	2.0001	15.0432	0.0099	1.0000	2.9138	0.0018	2.1761	1.0269	0.0851
135	6.8255	6.4892	0.0083	0.5985	2.6098	4.6480	2.0125	12.5136	0.0023	0.9950	2.9829	0.3035	2.6829	1.1179	0.0751
136	36.7083	11.0013	0.0058	0.4709	0.7943	3.4833	2.0002	15.386	0.0019	0.9995	2.9434	0.0171	2.1795	1.0283	0.0849
137	26.0297	3.4669	0.0042	0.6959	0.9542	2.9140	2.0000	4.3735	0.01	0.9979	2.6448	0.0025	2.3984	1.0649	0.0815
138	5.7065	12.5262	0.0095	0.6999	0.3576	4.0770	2.0059	9.2136	0.0015	0.9970	2.9788	0.0013	2.183	1.0254	0.0858
139	12.5829	5.4876	0.0089	0.6385	2.8195	4.3951	2.0001	8.3325	0.0095	0.9824	2.9807	0.0030	2.1983	1.0327	0.0842
140	22.7815	13.6079	0.0060	0.0336	1.9367	4.9446	2.0001	3.8034	0.0098	0.9995	2.9565	0.0000	2.1436	1.0212	0.0857
141	38.3853	14.3374	0.0066	0.0688	1.4384	0.0026	2.0000	18.931	0.0093	1.0000	2.9052	0.0299	2.2237	1.0366	0.0839
142	38.6658	15.5610	0.0063	0.3196	1.9180	4.3272	2.0001	4.6344	0.0015	0.9076	2.4817	0.9524	4.3531	1.3712	0.0457
143	7.9893	9.3820	0.0029	0.5309	1.6341	3.0628	2.0002	6.5787	0.0086	0.9999	2.9997	0.0004	2.1125	1.0157	0.0862
144	38.8825	1.7680	0.0037	0.6544	1.9419	4.9498	2.0003	0.6389	0.0075	0.9990	2.9193	0.0039	2.1808	1.0278	0.0851
145	38.3723	4.7818	0.0052	0.4076	1.6317	2.6384	2.0229	18.8619	0.0081	0.9559	2.6823	0.3406	3.2786	1.2049	0.067
146	20.4443	18.9907	0.0031	0.8200	2.1631	2.3976	2.0000	16.6219	0.0086	0.9823	2.8916	0.0210	2.2907	1.0493	0.0825
147	32.4107	3.1914	0.0086	0.7184	1.5675	4.0067	2.0166	19.6381	0.0028	0.9938	2.8344	0.0287	2.4326	1.0637	0.083
148	7.3917	17.1736	0.0028	0.9686	2.9811	1.1392	2.0033	19.9138	0.0081	0.9996	2.9627	0.1661	2.4058	1.0723	0.0796
149	18.0269	11.2049	0.0030	0.5313	0.6560	2.4905	2.0003	9.6956	0.0017	0.9995	2.9063	0.0075	2.1937	1.0301	0.0848
150	36.7979	20.7097	0.0025	0.3251	0.3174	4.5043	2.0139	9.82	0.0016	0.9497	2.7849	1.5948	4.7231	1.4143	0.0417

Table A.6: The results of optimisations for 150 rounds of Simulated Annealing using high LET IR. Columns 3 and 4 are the value of LQ parameters α_{model} and β_{model} for each run with the value of LQ parameters for the experimental data $\alpha_{exp} = 0.8$ Gy^{-1} and $\beta_{exp} = 0.01$ Gy^{-2}.

A.6 Nelder-Mead Simplex and SA algorithm performance

Dose (Gy)	log(survival rate)
0	2
1	1.8634
2	1.6957
4	1.2675
6	0.7152
8	0.0390
10	−0.7612

Table A.7: The simulation data for low LET IR are generated for the parameter values $\delta = 2$, $\alpha 1 = 11.4775$, $\alpha 2 = 0.0082$, $p = 0.9011$, $V_{max} = 2.3076$, and $K_M = 5$ to check the consistency of the NM simplex and SA algorithm performance to the parameter estimation procedure.

Dose (Gy)	log(survival rate)
0	2
0.5	1.8298
1	1.6568
1.5	1.4812
2.25	1.2126
3	0.9376
3.5	0.7514
4	0.5622

Table A.8: The simulation data for high LET IR are generated for the parameter values $\delta = 3.6703$, $\alpha 1 = 18.9733$, $\alpha 2 = 0.001$, $p = 0.7942$, $V_{max} = 2.9387$, and $K_M = 3.7560$ to check the consistency of the NM simplex and SA algorithm performance to the parameter estimation procedure.

A.7 Results of two-fraction survival data for low LET IR

	Column 1		Column 2	
	Low LET IR		High LET IR	
Run	α	β	α	β
1	0.2095	0.0203	0.7614	0.0061
2	0.2075	0.0251	0.76	0.009
3	0.2112	0.0256	0.7476	0.0103
4	0.2115	0.025	0.7599	0.0095
5	0.2086	0.0254	0.753	0.0091
6	0.2063	0.0258	0.751	0.0094
7	0.2038	0.0254	0.7605	0.0095
8	0.2083	0.0259	0.7609	0.009
9	0.2121	0.026	0.7605	0.0096
10	0.21	0.0259	0.7598	0.0095
11	0.2149	0.0254	0.7499	0.0093
12	0.2176	0.025	0.755	0.009
13	0.2153	0.0249	0.7471	0.01
14	0.2118	0.026	0.7449	0.011
15	0.2166	0.0259	0.7452	0.0113
16	0.2142	0.0258	0.7601	0.009
17	0.2094	0.026	0.7516	0.0095
18	0.2092	0.0259	0.7538	0.0095
19	0.2132	0.026	0.7628	0.0094
20	0.2129	0.0256	0.7537	0.0094
21	0.2107	0.025	0.7482	0.0097
22	0.208	0.0261	0.7549	0.0089
23	0.2108	0.0261	0.755	0.0092
24	0.2114	0.0259	0.7508	0.0094
25	0.2167	0.0256	0.7544	0.0098
26	0.2084	0.0255	0.7475	0.0094
27	0.2096	0.0253	0.7514	0.0093
28	0.2079	0.0255	0.7557	0.009
29	0.2201	0.026	0.7496	0.0103
30	0.2079	0.0254	0.7552	0.0094
31	0.2073	0.0258	0.7562	0.0095
32	0.2104	0.0254	0.7588	0.0092
33	0.212	0.0257	0.7539	0.0092
34	0.2171	0.0254	0.7525	0.0092
35	0.2068	0.0255	0.7617	0.0096
36	0.2077	0.0254	0.7582	0.0091
37	0.2065	0.0258	0.7615	0.0094

38	0.2124	0.0258	0.7534	0.009
39	0.2123	0.0248	0.7584	0.0093
40	0.2164	0.0261	0.7547	0.0092
41	0.2082	0.0255	0.7512	0.0094
42	0.2124	0.0258	0.7612	0.0092
43	0.2048	0.0261	0.7555	0.0094
44	0.2126	0.0258	0.7471	0.0103
45	0.2089	0.0263	0.7543	0.0092
46	0.2128	0.0255	0.7515	0.009
47	0.2066	0.0259	0.7591	0.0091
48	0.2034	0.0259	0.7513	0.009
49	0.2116	0.0255	0.751	0.0088
50	0.209	0.0254	0.7528	0.0093
51	0.2134	0.0264	0.7447	0.01
52	0.2076	0.0255	0.754	0.0094
53	0.2084	0.0263	0.7583	0.0094
54	0.2083	0.0255	0.7559	0.0093
55	0.2089	0.0261	0.7484	0.01
56	0.2114	0.0262	0.75	0.0096
57	0.2052	0.0251	0.7539	0.0094
58	0.2125	0.0257	0.7668	0.0094
59	0.211	0.0253	0.7526	0.0091
60	0.2122	0.0258	0.7556	0.0096
61	0.2103	0.0261	0.7521	0.0092
62	0.2146	0.0257	0.7574	0.009
63	0.2137	0.0257	0.7588	0.0091
64	0.2101	0.0252	0.7617	0.0094
65	0.2221	0.0262	0.757	0.0095
66	0.214	0.0254	0.7569	0.0092
67	0.212	0.0259	0.7579	0.0095
68	0.2076	0.0255	0.7643	0.0095
69	0.2046	0.0259	0.7539	0.0098
70	0.2154	0.0254	0.7569	0.0092
71	0.2111	0.0261	0.754	0.0094
72	0.2196	0.0256	0.7458	0.01
73	0.2176	0.0261	0.742	0.01
74	0.2101	0.0261	0.7507	0.0094
75	0.2093	0.0262	0.7545	0.0089
76	0.2141	0.0254	0.7465	0.01
77	0.2023	0.0253	0.7606	0.0091
78	0.2106	0.0261	0.754	0.0095
79	0.2103	0.0258	0.7643	0.0095
80	0.2166	0.025	0.7621	0.0092
81	0.217	0.026	0.7514	0.0094

82	0.2124	0.0257	0.7533	0.0093
83	0.2163	0.0253	0.7515	0.0095
84	0.2039	0.0263	0.7576	0.0091
85	0.2087	0.0253	0.7493	0.0091
86	0.2098	0.0262	0.7522	0.009
87	0.208	0.0255	0.7433	0.01
88	0.2158	0.0264	0.7558	0.0091
89	0.2106	0.0255	0.752	0.0092
90	0.209	0.0256	0.7602	0.0087
91	0.2094	0.0254	0.7514	0.0089
92	0.214	0.0256	0.751	0.01
93	0.2175	0.0259	0.746	0.01
94	0.2065	0.0257	0.7546	0.0089
95	0.2159	0.0262	0.75	0.0095
96	0.2185	0.0259	0.7582	0.009
97	0.2148	0.0262	0.7539	0.0093
98	0.2151	0.0261	0.7541	0.0091
99	0.2114	0.0261	0.757	0.0091
100	0.2154	0.0253	0.7575	0.0093
101	0.2076	0.0254	0.7577	0.0093
102	0.2085	0.0264	0.7555	0.0095
103	0.2066	0.0255	0.7608	0.0091
104	0.2111	0.025	0.7515	0.0095
105	0.2128	0.0256	0.7679	0.0093
106	0.2153	0.0261	0.7572	0.0097
107	0.211	0.0259	0.7499	0.01
108	0.2127	0.0259	0.7548	0.0086
109	0.2126	0.0249	0.7558	0.009
110	0.2091	0.0251	0.7571	0.0091
111	0.2098	0.0262	0.7616	0.0092
112	0.2171	0.026	0.7582	0.0094
113	0.2109	0.0262	0.7549	0.0095
114	0.2048	0.0255	0.7528	0.0091
115	0.216	0.0262	0.7528	0.0095
116	0.2076	0.0254	0.7527	0.009
117	0.2076	0.0257	0.7578	0.0094
118	0.2114	0.0258	0.7575	0.0092
119	0.2082	0.0263	0.7535	0.0091
120	0.2108	0.026	0.7559	0.0092
121	0.2034	0.0254	0.7615	0.009
122	0.2104	0.0251	0.7534	0.0088
123	0.2099	0.0259	0.7603	0.0094
124	0.2047	0.0261	0.7538	0.0095
125	0.2022	0.0261	0.7527	0.0094

126	0.2087	0.0255	0.7582	0.0095
127	0.2145	0.0254	0.7511	0.0091
128	0.21	0.026	0.7531	0.0093
129	0.2061	0.0258	0.7599	0.0091
130	0.2175	0.0258	0.7481	0.01
131	0.2117	0.0248	0.752	0.0091
132	0.2078	0.0245	0.7599	0.0093
133	0.2129	0.0258	0.743	0.01
134	0.206	0.0258	0.7456	0.0091
135	0.2102	0.0264	0.7545	0.0093
136	0.214	0.0264	0.743	0.0089
137	0.2063	0.0256	0.7622	0.0095
138	0.2156	0.0263	0.7646	0.0091
139	0.2129	0.0257	0.7589	0.0092
140	0.2096	0.025	0.7646	0.0095
141	0.2105	0.0259	0.7486	0.0094
142	0.2076	0.0262	0.7467	0.01
143	0.2206	0.0263	0.756	0.0092
144	0.2114	0.0258	0.7675	0.0095
145	0.2118	0.0261	0.7602	0.0096
146	0.2069	0.0257	0.7595	0.0093
147	0.2108	0.0259	0.7545	0.0089
148	0.213	0.0257	0.7645	0.0095
149	0.2109	0.0262	0.7494	0.0091
150	0.2147	0.0255	0.7595	0.009

Table A.9: Results of two-fraction survival data for low and high LET IR

Appendix B

Analysis of the structurally unstable bistable system using MAPLE (see chapter 6)

B.1 Using resultants

```
> restart;
> with(plots, implicitplot,PolynomialTools,DEtools);
> a1 := 1; a2 := 1; b1 := 200; b2 := 10; g1 := 4;
> g2 := 4; K1 := 30; K2 := 1;
> dotx1 := a1*(a/d-x1)-b1*x1*y1^g1/(K1+y1^g1)-d*x1;
> doty1 := a2*(1-y1)-b2*y1*x1^g2/(K2+x1^g2);
> simplify(dotx1);
> simplify(doty1);
> dotx1 := numer(dotx1);
> doty1 := numer(doty1);
> r1 := resultant(dotx1, doty1, y1);
> r2 := diff(r1, x1);
> r3 := resultant(r1, r2, x1);
> r3 := evalf(%);
```

```
#parameters a and d are very small. Let us assume that a=eA and d=eD,
#where A,D=O(1) and 0<e<<1.
#In the perturbation technique, after substitung A and D in the equation for r3,
#the equation becomes r6(A,delta)+r7(A,delta)e+Higher Order Terms (HOT)=0.
#Which means that
> r5 := subs(a = e*A, d = e*delta, r3);
#we use delta=D, we could not have used D because D is a special function in MAPLE.
> coeffs(r5, e, 'k');
> k;
> maxse := max(k);
#This syntax provides the smallest and the largest exponent of e
> r5rescaled := expand(r5/e^33);#e^33 is the smallest one
> coeffsr5 := coeffs(r5rescaled, e, 't');
#**********************************************
#r6(A,delta)+r7(A,delta)e+Higher Order Term(HOT)=0.
#**********************************************
#r6 is taken from r5rescaled
> r6 := -6.874031960*10^147*A^20*delta^13+2.501077087*10^147*A^8*delta^25+5.898600220
*10^148*A^16*delta^17+2.787004386*10^148*A^12*delta^21-2.098048254*10^123*A^32*delta-
1.045562823*10^147*delta^33-9.343386656*10^131*A^28*delta^5-2.634193844*10^147*A^4
*delta^29-1.387446145*10^140*A^24*delta^9;

#Next, after zoom-in (see chapter 6), in the A, D region, we expect that
#there is a line which passes through the origin and this line is given by A=mD.

> r6 := subs(A = m*delta, r6);
> coeffs(r6, delta, 's');
> s;
> r7 := simplify(r6/delta^33);#r7 is polynomial in 'm'.
> m := solve(r7);
#The above solution shows that m=0.7567928014 and m= 1.733670494.
#These values correspond to the slopes of the lines in the A,D region.
```

B.2 Using Sturm's theorem

```
##################################################################
> #sturms_theorem_cauchy_criterion.mw;
###################################################################
> restart;
>with(RealDomain)
##################################################################
>#                  Region II: a=d=0.001
##################################################################
> r1 := 31.-231.031*x1+1324.*x1^4-2125.324*x1^5+21786.*x1^8-23007.786*x1^9+1.59724*10^5*x1^12-
1.60683724*10^5*x1^13+4.39231*10^5*x1^16-4.39870231*10^5*x1^17;
> sturmr1 := sturmseq(r1, x1);
> P[0] := 0.7047533071e-4-0.5252253590e-3*x1+0.3009978641e-2*x1^4-0.4831706831e-2*x1^5
+0.4952824371e-1*x1^8-0.5230584927e-1*x1^9+.3631161846*x1^12-.3652980190*x1^13
+.9985467737*x1^16-1.000000000*x1^17;
> P[1] := -0.3089560935e-4+0.7082302682e-3*x1^3-0.1421090245e-2*x1^4+0.2330740881e
-1*x1^7-0.2769133196e-1*x1^8+.2563173068*x1^11-.2793455439*x1^12+.9398087282*x1^15
-1.000000000*x1^16;
> P[2] := -0.1243794183e-2+0.8954839007e-2*x1-0.4018432483e-1*x1^4+0.6178370302e-1*x1^5-
0.4455285137*x1^8+.4458947493*x1^9-1.637437090*x1^12+1.557038753*x1^13-0.7535897965e
-3*x1^3-0.2480016210e-1*x1^7-.2727334820*x1^11-1.000000000*x1^15;
> P[3] := -0.6203846900e-2*x1+0.2468344451e-1*x1^4-0.6310002754e-1*x1^5+.2707721660*x1^8
-.5552747414*x1^9+.9925827010*x1^12-1.991444140*x1^13-6.422447727*10^(-12)*x1^7
+6.422447727*10^(-11)*x1^11+0.5751198543e-2*x1^2+0.3968026030e-1*x1^6+.2863735719*x1^10
+1.000000000*x1^14+0.7705808450e-3;
> P[4] := 0.1856476587e-2*x1-.2395347635*x1^12+1.000000000*x1^13-0.6334696202e-2*x1^4
+0.2767423326e-1*x1^5-0.6616103421e-1*x1^8+.2747662310*x1^9-0.3706566029e-2*x1^2
-0.1124182747e-1*x1^6-0.1060720938e-1*x1^10-0.3528815738e-2*x1^3-0.1050684985e-1*x1^7
-0.9631279041e-2*x1^11-0.2053161366e-3;
> P[5] := 0.4713851277e-2*x1-1.000000000*x1^12-0.2937745440e-1*x1^4+0.1421729836e-1*x1^5
-.2838640123*x1^8+0.1329996481e-1*x1^9+0.4460995820e-2*x1^2+0.1319777124e-1*x1^6
+0.1197370154e-1*x1^10+0.4249439598e-2*x1^3+0.1229931456e-1*x1^7+0.1075563486e-1*x1^11
-0.7052972668e-3;
> P[6] := -.6152497814*x1-39.20502994*x1^4+41.91261032*x1^5-93.70964827*x1^8
```

```
+102.6750878*x1^9+.1124596794*x1^2+.3713030311*x1^6+.3939164329*x1^10+.3383139179*x1^3
+1.039434332*x1^7+1.000000000*x1^11+.3717692646;
> P[7] := -0.6100378676e-2*x1-.1577537014*x1^4+.5476734604*x1^5-.3772372210*x1^8
+1.319118135*x1^9+0.6401181026e-2*x1^2-.4074564304*x1^6-1.000000000*x1^10
+0.1969914732e-3*x1^3+0.3611483651e-3*x1^7+0.1474235758e-2;
> P[8] := 0.5970164101e-2*x1+.3775439665*x1^4-.4083209867*x1^5+.9024265726*x1^8-
1.000000000*x1^9-0.1122106917e-2*x1^2-0.2113568562e-2*x1^6-0.3579795980e
-2-0.3300121002e-2*x1^3-0.6050223899e-2*x1^7;
> P[9] := 0.6781266534e-2*x1-.5913092788*x1^4+0.2974492284e-2*x1^5-1.000000000*x1^8
+0.3597415262e-2+0.7542607477e-2*x1^2+0.3332249736e-2*x1^6+0.1156168520e-1*x1^3
+0.9565650672e-2*x1^7;
> P[10] := -10.01270932*x1+192.4425668*x1^4-220.5642888*x1^5+.4369895516
+1.388742543*x1^2+2.510253782*x1^6+.6175183343*x1^3+1.000000000*x1^7;
> P[11] := -.1131579363*x1+2.137168347*x1^4-3.297808554*x1^5+0.4837388337e
-2+0.5952119897e-1*x1^2+1.000000000*x1^6+0.6863809827e-3*x1^3;
> P[12] := 0.4598589868e-1*x1-.8844569605*x1^4+1.000000000*x1^5-0.2008835968e
-2-0.5680232840e-2*x1^2-0.2721774405e-2*x1^3;
> P[13] := 0.3137862600e-1*x1-1.000000000*x1^4+0.1975881910e-2+0.3214755262e
-1*x1^2+0.3751222043e-1*x1^3;
> P[14] := -9.119753673*x1+1.570276951+.6519435935*x1^2+1.000000000*x1^3;
> P[15] := -.8272251562*x1+.1133113368+1.000000000*x1^2;
> P[16] := 1.000000000*x1-.1751267209;
> P[17] := 1;
> sturm(sturmr1, x1, -2, 2);
                                       3
> sturm(sturmr1, x1, -2, 0);
                                       0
> sturm(sturmr1, x1, 0, 2);
                                       3
> sturm(sturmr1, x1, 0, .5);
                                       1
> sturm(sturmr1, x1, .5, 1);
                                       2
> sturm(sturmr1, x1, 1, 1.5);
                                       0
```

```
> sturm(sturmr1, x1, 1.5, 1.99855);
                                      0
> sturm(sturmr1, x1, 0, .1);
                                      0
> sturm(sturmr1, x1, .1, .2);# There is one root in this range
                                      1
> sturm(sturmr1, x1, .2, .3);
                                      0
> sturm(sturmr1, x1, .3, .4);
                                      0
> sturm(sturmr1, x1, .4, .5);
                                      0
> sturm(sturmr1, x1, .5, .6); #There is one root in this range
                                      1
> sturm(sturmr1, x1, .6, .7);
                                      0
> sturm(sturmr1, x1, .7, .8);
                                      0
> sturm(sturmr1, x1, .8, .9);
                                      0
> sturm(sturmr1, x1, .9, 1); #There is one root in this range
                                      1
> solve(r1);# 0.1357108811, 0.5059157713, 0.9936728609,
            # These are the roots of polynomial using MAPLE.
            # This is only to check that the theorem gives a similar answer to
            # the one given by MAPLE.

#####################################################################################
>#              Region I: a/d=0.5, a:=0.0005,d:=0.001
#####################################################################################
> r3 := -0.155e-1-.231031*x1+.6620*x1^4-2.125324*x1^5+10.8930*x1^8-23.007786*x1^9
+79.8620*x1^12-160.683724*x1^13+219.6155*x1^16-439.870231*x1^17;
> sturmr3 := sturmseq(r3, x1);
> P[0] := 0.3523766536e-4-0.5252253590e-3*x1+0.1504989320e-2*x1^4-0.4831706831e
-2*x1^5+0.2476412185e-1*x1^8-0.5230584927e-1*x1^9+.1815580923*x1^12
```

```
-.3652980190*x1^13+.4992733868*x1^16-1.000000000*x1^17;
> P[1] := -0.3089560935e-4+0.3541151341e-3*x1^3-0.1421090245e-2*x1^4+0.1165370440e
-1*x1^7-0.2769133196e-1*x1^8+.1281586534*x1^11-.2793455439*x1^12+.4699043641*x1^15
-1.000000000*x1^16;
> P[2] := -0.2487588370e-2+6.228155020*x1^13-3.274874185*x1^12+1.783579000*x1^9
-.8910570286*x1^8+.2471348124*x1^5-0.8036864970e-1*x1^4+0.3581935608e-1*x1
-1.000000000*x1^15-.2727334819*x1^11-0.2480016209e-1*x1^7-0.7535897961e-3*x1^3;
> P[3] := -0.3101923451e-2*x1+0.1926452113e-3+0.6170861123e-2*x1^4-0.3155001376e
-1*x1^5+0.6769304151e-1*x1^8-.2776373707*x1^9+.2481456752*x1^12-.9957220700*x1^13
-3.211223859*10^(-14)*x1^3+0.5751198544e-2*x1^2+0.3968026030e-1*x1^6
+.2863735720*x1^10+1.000000000*x1^14;
> P[4] := -0.6002610492e-2*x1+.5520290517*x1^12-1.000000000*x1^13+0.1353261184e
-1*x1^4-0.4045527292e-1*x1^5+.1501691636*x1^8-.2871228487*x1^9-0.4785322276e
-3*x1^2-0.1451364068e-2*x1^6-0.1369432398e-2*x1^10-0.9111679354e-3*x1^3
-0.2712951143e-2*x1^7-0.2486871894e-2*x1^11+0.4185660861e-3;
> P[5] := 0.2755279314e-1*x1-1.000000000*x1^12+1.023736298*x1^4+0.9304759687e
-1*x1^5+2.266969256*x1^8+.1014669070*x1^9+0.5374251080e-1*x1^2+.1801738049*x1^6
+.1947697202*x1^10+.1020851314*x1^3+.3404698301*x1^7+.3657364547*x1^11
-0.9528008962e-2;
> P[6] := -0.6705472153e-1*x1-.7912013505*x1^4+8.107469246*x1^5-1.796888592*x1^8
+19.63397274*x1^9+.1395533681*x1^2+.4719074415*x1^6+.5154185510*x1^10
+.2759855751*x1^3+.9251652999*x1^7+1.000000000*x1^11+0.1050498881e-1;
> P[7] := -0.5013961149e-2*x1-.1030676807*x1^4+.4047618757*x1^5-.2464813289*x1^8
+.9804597672*x1^9+0.7033977918e-2*x1^2-.4062962875*x1^6-1.000000000*x1^10
+0.7987639444e-4*x1^3+0.1464167828e-3*x1^7+0.9695453312e-3;
> P[8] := 0.3528577647e-2*x1+0.4532904193e-1*x1^4-.4128617201*x1^5
+.1038378116*x1^8-1.000000000*x1^9-0.6955999272e-2*x1^2-0.1289429874e
-1*x1^6-0.5732823648e-3-0.1357711416e-1*x1^3-0.2489136623e-1*x1^7;
> P[9] := 0.1032027013e-1*x1+.3810724243*x1^4+0.1907742605e-1*x1^5+1.000000000*x1^8
-0.3576754427e-2+0.1985533678e-1*x1^2+0.3628881221e-1*x1^6+0.3727015819e-1*x1^3
+0.6724395025e-1*x1^7;
> P[10] := 16.98819188*x1-163.0145728*x1^4+328.3124121*x1^5-.3618618409
+.3054781558*x1^2+.2362761796*x1^6+.9180856159*x1^3+1.000000000*x1^7;
> P[11] := -0.9882317082e-2*x1+0.8558389094e-1*x1^4-.6657676368*x1^5+0.1972453711e
-3+0.5153819616e-1*x1^2+1.000000000*x1^6+0.3443311383e-3*x1^3;
```

```
> P[12] := -0.5168945761e-1*x1+.4959809539*x1^4-1.000000000*x1^5
+0.1101002493e-2-0.8176653719e-3*x1^2-0.2634320836e-2*x1^3;
> P[13] := 0.4069349354e-2*x1+1.000000000*x1^4-0.8173366710e-2
+0.9856389000e-2*x1^2+0.2066103255e-1*x1^3;
> P[14] := 17.94902622*x1-1.542080432+.5331362904*x1^2+1.000000000*x1^3;
> P[15] := -.6082085148*x1+0.4519719592e-1+1.000000000*x1^2;
> P[16] := -1.000000000*x1+0.8569016123e-1;
> P[17] := -1.000000000;
> sturm(sturmr3, x1, -infinity, infinity);
                                      1
> sturm(sturmr3, x1, -.4992733868, .4992733868);
                                      1
> sturm(sturmr3, x1, -infinity, -.4992733868);
                                      0
> sturm(sturmr3, x1, -.4992733868, 0);
                                      0
> sturm(sturmr3, x1, 0, .4992733868);
                                      1
> sturm(sturmr3, x1, .4992733868, infinity);
                                      0
> sturm(sturmr3, x1, 0, .1);
                                      1
> sturm(sturmr3, x1, .1, .2);
                                      0
> sturm(sturmr3, x1, .2, .3);
                                      0
> sturm(sturmr3, x1, .3, .4);
                                      0
> sturm(sturmr3, x1, .4, .4993);
                                      0
> sturm(sturmr3, x1, 0, 0.1e-1);
                                      0
> sturm(sturmr3, x1, 0.1e-1, 0.2e-1);
                                      0
> sturm(sturmr3, x1, 0.2e-1, 0.3e-1);
```

```
                                       0
> sturm(sturmr3, x1, 0.3e-1, 0.4e-1);
                                       0
> sturm(sturmr3, x1, 0.4e-1, 0.5e-1);
                                       0
> sturm(sturmr3, x1, 0.5e-1, 0.6e-1);
                                       0
> sturm(sturmr3, x1, 0.6e-1, 0.7e-1); #There is one root in this range
                                       1
> sturm(sturmr3, x1, 0.7e-1, 0.8e-1);
                                       0
> sturm(sturmr3, x1, 0.8e-1, 0.9e-1);
                                       0
> sturm(sturmr3, x1, 0.9e-1, .1);
                                       0
> solve(r3);# 0.06713624576
            # This is the root of polynomial using MAPLE.
            # This is only to check that the theorem gives a similar answer to the
            # one given by MAPLE.
```

Bibliography

[1] B. Abbasi, A. H. E. Jahromi, J. Arkat, and M. Hosseinkouchack. Estimating the parameters of Weibull distribution using simulated annealing algorithm. *Applied Mathematics and Computation*, 183(1):85–93, 2006.

[2] N. Albright. A Markov formulation of the repair-misrepair model of cell survival. *Radiation Research*, 118(1):1–20, 1989.

[3] U. Alon. *An Introduction to Systems Biology: Design Principles of Biological Circuits.* Taylor and Francis Group, 2006.

[4] D. Angeli, J. E. Ferrell, and E. D. Sontag. Detection of multistability, bifurcations, and hysteresis in a large class of biological positive-feedback systems. *Proc. Natl. Acad. Sci. USA*, 101:1822–1827, 2004.

[5] N. Aravindan, S. Mohan, T. S. Herman, and M. Natarajan. Nitric oxide-mediated inhibition of NF-κB regulates hyperthermia-induced apoptosis. *Journal of Cellular Biochemistry*, 106:999–1009, 2009.

[6] C. J. Bakkenist and M. B. Kastan. DNA damage activates ATM through intermolecular autophosphorylation and dimer dissociation. *Nature*, 421:499–506, 2003.

[7] F. Ballarini. From DNA radiation damage to cell death: Theoretical approaches. *Journal of Nucleic Acids*, 3:7–15, 2010.

[8] H. Barreto and F. M. Howland. *Introductory Econometrics: Using Monte Carlo Simulation with Microsoft Excel.* Cambridge University Press, 2006.

[9] R. Baskar. Emerging role of radiation induced bystander effects: Cell communications and carcinogenesis. *Genome Integrity*, 1(13):1–8, 2010.

[10] S. Bhatti, S. Kozlov, A. A. Farooqi, A. Naqi, M. Lavin, and K. K. Khanna. ATM protein kinase: The linchpin of cellular defenses to stress. *Cell. Mol. Life Sci.*, DOI 10.1007/s00018-011-0683-9:1–30, 2011.

[11] M. T. Borisuk. *Bifurcation analysis of a model of the frog egg cell cycle*. PhD thesis, Mathematics department, Virginia Polytechnic Institute and State University, May 1997.

[12] D. W. A. Bourne. Least squares criteria. Website, May 2010. `http://www.boomer.org/c/p3/c06/c0607.html`.

[13] J. R. Bradley, A. J. Giaccia, D. Johnson, and B. Pober. *Medical genetics*. Blackwell Publishing Ltd., 2006.

[14] D. J. Brenner, L. R. Hlatky, P. J. Hahnfeldt, Y. Huang, and R. K. Sachs. The linear-quadratic model and most other common radiobiological models result in similar predictions of time-dose relationships. *Radiation Research*, 150:83–91, 1998.

[15] G. P. Bromfield, A. Meng, P. Warde, and R. G. Bristow. Cell death in irradiated prostate epithelial cells: Role of apoptotic and clonogenic cell kill. *Prostate Cancer and Prostatic Diseases*, 6:73–85, 2003.

[16] N. E. Buchler, U. Gerland, and T. Hwa. Nonlinear protein degradation and the function of genetic circuits. *Proc. Natl. Acad. Sci. USA*, 102:9559–9564, 2005.

[17] S. Burdak-Rothkamm, K. Rothkamm, and K. M. Prise. ATM acts downstream of ATR in the DNA damage response signaling of bystander cells. *Cancer Research*, 103:149–161, 2008.

[18] M. Carlone, D. Wilkins, and P. Raaphorst. The modified linear-quadratic model of Guerrero and Li can be derived from a mechanistic basis and exhibits linear-quadratic-linear behaviour. *Phys. Med. Biol.*, 50:L9–L15, 2005.

[19] K. H. Chadwick and H. P. Leenhout. A molecular theory of cell survival. *Phys. Med. Biol.*, 18(1):78–87, 1973.

[20] D. E. Chang, S. Leung, M. R. Atkinson, A. Reifler, D. Forger, and A. J. Ninfa. Building biological memory by linking positive feedback loops. *Proc. Natl. Acad. Sci. USA*, 107(1):175–180, 2010.

[21] E. Choi. Resultant and discriminant of linear combination of polynomials. *Journal of the ChungCheong Mathematical Society*, 23(4):663–677, 2010.

[22] C. H. Chou, P. J. Chen, P. H. Lee, A. L. Cheng, H. C. Hsu, and J. C. H. Cheng. Radiation-induced hepatitis B virus reactivation in liver mediated by the bystander effect from irradiated endothelial cells. *Clinical Cancer Research*, 13(3):851–857, 2007.

[23] D.P. Clark and N. Pazdernik. *Biotechnology: Academic Cell Update*. Elsevier, 2010.

[24] M. Cohn and K. Horibata. Analysis of the differentiation and of the heterogeneity within a population of Escherichia Coli undergoing induced 13-galactosidase synthesis. *J. Bacteriol*, 78:601–612, 1957.

[25] M. Colasanti and T. Persichini. Nitric oxide: An inhibitor of NF-κB/Rel system in glial cells. *Brain Research Bulletin*, 52(3):155–161, 2000.

[26] G. M. Cooper and R. E. Hausman. *The cell: A molecular approach, Fifth Edition*. ASM PRESS, 2009.

[27] G. Craciun, Y. Tang, and M. Feinberg. Understanding bistability in complex enzyme-driven reaction networks. *Proc. Natl. Acad. Sci. USA*, 103:8697–8702, 2006.

[28] J. Cui, C. Chen, H. Lu, T. Sun, and P. Shen. Two independent positive feedbacks and bistability in the Bcl-2 apoptotic switch. *PLOS One*, 3(1):e1469, 2008.

[29] S. B. Curtis. Lethal and potentially lethal lesions induced by radiation - A unified repair model. *Radiation Research*, 106:252–270, 1986.

[30] S. B. Curtis. Mechanistic models. *Journal of Basic Life Sciences*, 58:367–382, 1991.

[31] J. M. Cushing. An introduction to structured population dynamics. In *CBMS-NSF Regional Conference Series in Applied Mathematics*. SIAM, Philadelphia, PA, 1987.

[32] C. Price D. Byatt, I. Coope. 40 years of the Nelder-Mead algorithm. *Univ. of Canterbury, New Zealand*, 2003.

[33] G.K. Dasika, S.C.J. Suh-Chin Lina, S. Zhaoa, P. Sung, A. Tomkinson, and E.Y.H.P. Lee. DNA damage-induced cell cycle checkpoints and DNA strand break repair in development and tumorigenesis. *Oncogene*, 18(55):7883–7899, 1999.

[34] A. Dawson and T. Hillen. Derivation of the tumor control probability (TCP) from a cell cycle. *Computational and Mathematical Methods in Medicine*, 7:121–142, 2006.

[35] F. A. Derheimer and M. B. Kastan. Multiple roles of ATM in monitoring and maintaining DNA integrity. *FEBS Lett.*, 584(17):3675–3681, 2010.

[36] J. S. Dickey, B. J. Baird, C. E. Redon, M. V. Sokolov, O. A. Sedelnikova, and W. M. Bonner. Intercellular communication of cellular stress monitored by γ-H2AX induction. *Carcinogenesis*, 30(10):1686–1695, 2009.

[37] L. E. Dickson. *First Course in the Theory of Equations (Classic Reprint Series)*. Forgotten Books, 2010.

[38] B. Dieriks, D. V. Winnok, D. Hanane, B. Sarah, and V. O. Patrick. Medium-mediated DNA repair response after ionizing radiation is correlated with the increase of specific cytokines in human fibroblasts. *Mutation Research*, 687(1-2):40–48, 2010.

[39] M. R. Domingo-Sananes and B. Novak. Different effects of redundant feedback loops on a bistable switch. *Chaos*, 20(4):045120(1)–045120(11), 2010.

[40] B. Efron and Tibshirani R.J. *An Introduction to the Bootstrap*. Chapman and Hall New York, 1993.

[41] R.J. Epstein. *Human molecular biology: an introduction to the molecular basis of health and disease*. Cambridge University Press, 2003.

[42] D. Eriksson, P. Lofroth, L. Johansson, K. A. Riklund, and T. Stigbrand. Cell cycle disturbances and mitotic catastrophes in HeLa Hep2 cells following 2.5 to 10 *Gy* of ionizing radiation. *Clinical Cancer Research*, 13:5501s–5508s, 2007.

[43] A. Facoetti, F. Ballarini, R. Cherubini, S. Gerardi, R. Nano, A. Ottolenghi, K. M. Prise, K. R. Trott, and C. Zilio. Gamma ray-induced bystander effect in tumour glioblastoma cells: A specific study on cell survival, cytokine release and cytokine receptors. *Radiat. Protection Dosimetry*, 122(1-4):271–274, 2006.

[44] W. Feller. *An Introduction to Probability Theory and Its Applications, Vol. 1, 3rd Edition*. John Wiley and Sons, 1968.

[45] J. E. Ferrell and W. Xiong. Bistability in cell signaling: How to make continuous processes discontinuous, and reversible processes irreversible. *Current Opinion in Cell Biology*, 11:227–236, 2001.

[46] J. E. Jr. Ferrell, J. R. Pomerening, S. Y. Kim, N. B. Trunnell, W. Xiong, C. Y. Huang, and E. M. Machleder. Simple, realistic models of complex biological processes: Positive feedback and bistability in a cell fate switch and a cell cycle oscillator. *FEBS Lett.*, 583(24):3999–4005, 2009.

[47] Jr. J. E. Ferrell, Y. T. Tony Tsai, and Q. Yang. Modeling the cell cycle: Why do certain circuits oscillate? *Proc. Natl. Acad. Sci. USA*, 144(6):874–885, 2011.

[48] T. Finkel and Holbrook N. J. Oxidants, oxidative stress and the biology of ageing. *Nature*, 408(6809):239–247, 2000.

[49] M. Foss and T. Farine. *Science in nursing and health*. Pearson Education Ltd., 2007.

[50] A. K. Freeman and A. N. A. Monteiro. Phosphatases in the cellular response to DNA damage. *Cell Communication and Signaling*, 8(27):1–12, 2010.

[51] T. Fujiwara. A novel molecular therapy using bioengineered Adenovirus for human gastrointestinal cancer. *Acta Med. Okayama*, 62(3):151–162, 2011.

[52] S. Fulda and K. M. Debatin. Extrinsic versus intrinsic apoptosis pathways in anticancer chemotherapy. *Oncogene*, 25:4798–4811, 2006.

[53] M. D. Garrett. Cell cycle control and cancer. *Current Science*, 81(5):515–522, 2001.

[54] S. A. Ghandhi, B. Yaghoubian, and S. A. Amundson. Global gene expression analyses of bystander and alpha particle irradiated normal human lung fibroblasts: Synchronous and differential responses. *Radiation Protection Dosimetry*, 1:63:1–14, 2008.

[55] D. M. Gibson, J. H. Steinrauf, and R. A. Parker. Synthesis and degradation of interconvertible enzymes. Kinetic equations of a model system. *Journal of Bioenergetics and Biomembranes*, 16:433–439, 1984.

[56] A. Goldbeter. A minimal cascade model for the mitotic oscillator involving cyclin and Cdc2 kinase. *Proc. Natl. Acad. Sci. USA*, 88:9107–3111, 1991.

[57] M. D. Gow. *Examination of Bystander Cell Death Following Low-LET Irradiation*. PhD thesis, Medical Physics, McMaster University, Hamilton, Ontario, July 2011.

[58] B.P. Griffin, C.M. Rimmerman, and E.J. Topol. *The Cleveland Clinic Cardiology Board Review*. Lippincott Williams and Wilkins, 2006.

[59] M. Grinfeld and S. D. Webb. Structural instability in an autophosphorylating kinase switch. *Mathematical Biosciences*, 219:92–96, 2009.

[60] E. Gudowska-Nowak, M. Kraemer, G. Kraft, and G. Taucher-Scholz. Compound Poisson statistics and models of clustering of radiation induced DNA double strand breaks. Preprint, 2000. `http://arxiv.org/abs/physics/0011071`.

[61] M. Guerrero and X. A. Li. Extending the linear-quadratic model for large fraction doses pertinent to stereotactic radiotherapy. *Phys. Med. Biol.*, 50(10):L9–L13, 2004.

[62] A. Gunnlaugsson, P. Nilsson, E. Elisabeth Kjellen, and A. Johnsson. The effect on the small bowel of 5-FU and oxaliplatin in combination with radiation using a microcolony survival assay. *Radiation Oncology 2009*, 4(61):1–7, 2009.

[63] P. Hahnfeldt, R. K. Sachs, and L. R. Hlatky. Evolution of DNA damage in irradiated cells. *J. Math. Biol.*, 30:493–511, 1992.

[64] E. J. Hall and A. J. Giaccia. *Radiobiology for the Radiologist*. Lippincott, Williams and Wilkins, 2006.

[65] W. Han, S. Chen, K. N. Yu, and L. Wu. Nitric oxide mediated DNA double strand breaks induced in proliferating bystander cells after alpha-particle irradiation. *Mutation Research*, 684:81–89, 2010.

[66] L. Hanin, O. Hyrien, J. Bedford, and A. Yakovlev. A comprehensive stochastic model of irradiated cell populations in culture. *Journal of Theoretical Biology*, 239:401–416, 2006.

[67] L. Hanin and M. Zaider. Cell survival probability at large doses: An alternative to the linear-quadratic model. *Phys. Med. Biol.*, 55:4687–4702, 2010.

[68] T. K. Hei. Cyclooxygenase-2 as a signaling molecule in radiation-induced bystander effect. *Molecular Carcinogenesis*, 45:455–460, 2006.

[69] T. K. Hei, H. Zhou, V. N. Ivanov, M. Hong, B. H. Lieberman, D. J. Brenner, S. A. Amundson, and C. R. Geard. Mechanism of radiation-induced bystander effects: A unifying model. *Journal of Pharmacy and Pharmacology*, 60:943–950, 2008.

[70] D. Heinrich. 100 *Great Problems of Elementary Mathematics*. Dover Publications, 1965.

[71] T. Hillen, G. De Vries, J. Gong, and C. Finlay. From cell population models to tumor control probability: Including cell cycle effects. *Acta Oncologica*, 00:1–9, 2010.

[72] C. Y. Ho and H. Y. Li. DNA damage during mitosis invokes a JNK-mediated stress response that leads to cell death. *J. Cell. Biochem.*, 1:725–731, 2010.

[73] M. Hong, A. Xu, H. Zhou, L. Wu, G. Randers-Pehrson, R. M. Santella, Z. Yu, and T. K. Hei. Mechanism of genotoxicity induced by targeted cytoplasmic irradiation. *British Journal of Cancer*, 103:1263–1268, 2010.

[74] H.H. Hoos and T.G. Stutzle. *Statistic local search; foundation and application*. Morgan Khaufmann Publishers, 2005.

[75] R. S. Hotchkiss, A. Strasser, J. E. McDunn, and P. E. Swanson. Mechanisms of disease: Cell death. *The New England Journal of Medicine*, 361:1570–1583, 2009.

[76] P. Hughes and E. Ferrett. *Introduction to Health and Safety in Construction (3rd Edition)*. Elsevier Ltd., 2008.

[77] F. Ianzini, A. Bertoldo, E. A. Kosmacek, S. L. Phillips, and M. A. Mackey. Lack of p53 function promotes radiation-induced mitotic catastrophe in mouse embryonic fibroblast cells. *Cancer Cell International*, 6:11:1–8, 2006.

[78] L. Ingber and A. Petraglia. *Stochastic global optimization and its applications with fuzzy adaptive*. Springer Heidelberg New York Dordrecht London, 2012.

[79] V. N. Ivanov, H. Zhou, S. A. Ghandhi, T. B. Karasic, B. Yaghoubian, S. A. Amundson, and T. K. Hei. Radiation-induced bystander signaling pathways in human fibroblasts: A role for interleukin-33 in the signal transmission. *Cellular Signaling*, 22(7):1076–1087, 2010.

[80] H. Jakubowski. Transport and kinetics. Website, August 2010. `http://employees.csbsju.edu/hjakubowski/classes/ch331/transkinetics/olcomplicatedenzyme.html`.

[81] M. Joiner and A. van der Kogel. *Basic Clinical Radiobiology, Fourth Edition.* Hodder Arnold, 2009.

[82] L. Joseph and C. Reinhold. Fundamentals of clinical research for radiologist: Introduction to probability theory and sampling distributions. *A. J. R.*, 180:917–923, 2003.

[83] Burke E. K. and G. Kendall. *Search Methodologies: Introductory Tutorials in Optimization and Decision Support Techniques.* Springer, 2005.

[84] M. Kan'O, T. Kawata, H. Ito, N. Shigematsu, C. Liu, T. Uno, K. Isobe, H. Kawakami, F. Cucinotta, K. George, and A. Kubo. Repair of potential lethal damage in normal cells and ataxia telangiectasia; consideration of non-homologous end-joining. *J. Radiat. Res.*, 48:31–38, 2007.

[85] O. Kapuy, D. Barik, M. R. Sananes, J. J. Tyson, and B. Novak. Bistability by multiple phosphorylation of regulatory proteins. *Prog. Biophys. Mol. Biol.*, 100(1-3):47–56, 2010.

[86] A. M. Kellerer and H. D. Rossi. Theory of dual radiation action. *Curr. Top. Radiat. Res.*, 8(2):85–158, 1972.

[87] A. M. Kellerer and H. H. Rossi. A generalized formulation of dual radiation action. *Radiation Research*, 75:471–488, 1978.

[88] L.J. Kenneth. *Numerical Method in Economics.* Massachusetts Institute of Technology, 1998.

[89] S. Y. Kim and J. E. Ferrell. Substrate competition as a source of ultrasensitivity in the inactivation of Wee1. *Cell*, 128:1133–1145, 2007.

[90] S. Kok and C. Sandrock. Locating and characterizing the stationary points of the extended Rosenbrock function. *Evol. Comput.*, 17(3):437–453, 2009.

[91] S. Kozlov, N. Gueven, K. Keating, J. Ramsay, and M. F. Lavin. ATP activates ataxia-telangiectasia mutated (ATM) in vitro. Importance of autophosphorylation. *J. Biol. Chem.*, 278(11):9309–9317, 2003.

[92] E.B. Kramer. *A system for studying the molecular genetics of translational accuracy.* ProQuest, 2008.

[93] H. Le, S. Algaze, and E. Tan. Michaelis-Menten kinetics. Website, March 2011. `http://chemwiki.ucdavis.edu/Biological_Chemistry/Catalysts/Enzymatic_Kinetics/Michaelis-Menten_Kinetics`.

[94] S. Legewie, B. Schoeberl, N. Blthgen, and H. Herzel. Competing docking interactions can bring about bistability in the MAPK cascade. *Biophysical Journal*, 93:2279–2288, 2007.

[95] B. Lewin, J.E. Krebs, E.S. Goldstein, and S.T. Kilpatrick. *Lewin's genes 10.* Jones and Bartlett Publishers, 2009.

[96] Y. Li and D. Yang. The ATM inhibitor KU-55933 suppresses cell proliferation and induces apoptosis by blocking Akt in cancer cells with overactivated Akt. *Mol. Cancer. Ther.*, 9:113–125, 2010.

[97] P. Lirk, G. Georg Hoffmann, and J. Josef Rieder. Inducible Nitric Oxide Synthase: Time for reappraisal. *Current Drug Targets - Inflammation and Allergy*, 1:89–108, 2002.

[98] J. E. Lisman. A mechanism for memory storage insensitive to molecular turnover: A bistable autophosphorylating kinase. *Proc. Nat. Acad. Sci. USA*, 82:3055–3057, 1985.

[99] M. Lobrich, B. Rydberg, and P. K. Cooper. Repair of x-ray-induced DNA double strand breaks in specific Not I restriction fragments in human fibrolasts: Joining of correct and incorrect ends. *Proc. Natl. Acad. Sci. USA*, 92:12050–12054, 1995.

[100] M. Lobrich, A. Shibata, A. Beucher, A. Fisher, M. Ensminger, A. A. Goodarzi, O Barton, and P. A. Jeggo. γ-H2AX foci analysis for monitoring DNA double-strand break repair strengths, limitations and optimization. *Cell Cycle*, 9(4):662–669, 2010.

[101] U.S. Department of Energy Low Dose Radiation Research Program. Glossary: Absorbed Dose. Website, March 2011. `http://lowdose.energy.gov/glossary.aspx`.

[102] L. Ma, J. Wagner, J.J. Rice, W. Hu, A. J. Levine, and G.A. Stolovitzky. A plausible model for the digital response of p53 to DNA damage. *Proc. Natl. Acad. Sci. USA*, 40(102):14266–14271, 2005.

[103] A.G. Marangoni. *Enzyme Kinetics: A Modern Approach.* John Wiley and Sons, 2003.

[104] J. H. Mathews and K. K. Fink. *Numerical method using MATLAB.* Prentice Hall Inc., 2004.

[105] MathWorks. R2010b documentation MATLAB - fminsearch. Website, 2011. http://www.mathworks.com/help/techdoc/ref/fminsearch.html.

[106] F. P. Miller, A. F. Vandome, and J. McBrewster. *Hill Equation.* Betascript Publishing, 2010.

[107] G. T. Miller and S. E. Spoolman. *Sustaining the earth: An integrated approach.* Yolanda Cossio, 2008.

[108] P. Miller, A. M. Zhabotinsky, J. E. Lisman, and X. J. Wang. The stability of a stochastic CaMKII switch: Dependence on the number of enzyme molecules and protein turnover. *PLoS Biology*, 3:0705–0717, 2005.

[109] D. K. Mishra, K. D. Dolan, and L. Yang. Bootstrap Confidence Intervals for the Kinetic Parameters of Degradation of Anthocyanins in Grape Pomace. *Journal of Food Process Engineering*, 34:1220 – 1233, 2011.

[110] S. Miyamoto. Nuclear initiated NF-κB signaling: NEMO and ATM take center stage. *Cell. Research*, 21:116–130, 2011.

[111] D.O. Morgan. *The cell cycle: principles of control.* New Science Press Ltd, 2007.

[112] W.F. Morgan. Is there a common mechanism underlying genomic instability, bystander effects and other nontargeted effects of exposure to ionizing radiation? *Oncogene*, 22:7094–7099, 2003.

[113] C. Mothersill and C. B. Seymour. Radiation-induced bystander effects and the DNA paradigm: An out of field perspective. *Mutation Research*, 597:5–10, 2006.

[114] K. Mouri, J. C. Nacher, and T. Akutsu. A mathematical model for the detection mechanism of DNA double-strand breaks depending on autophosphorylation of ATM. *PLoS One*, 4(4):1–14, 2009.

[115] E. M. Myasnikova, S. T. Rachev, and A. Y. Yakovlev. Queueing models of potentially lethal damage repair in irradiated cells. *Mathematical Biosciences*, 135(1):85–109, 1996.

[116] Y. Nourani and B. Andresen. A comparison of simulated annealing cooling strategies. *J. Phys. A: Math. Gen.*, 31:8373 – 8385, 1998.

[117] B. Novak, J. C. Sible, and J. J. Tyson. Checkpoints in the cell cycle. Encyclopedia of Life Sciences. Website, 2002. http://www.els.net/WileyCDA/ElsArticle/refId-a0001355.html.

[118] A. Novick and M. Weiner. Enzyme induction as an all-or-none-phenomenon. *Proc. Natl. Acad. Sci. USA*, 43:553566, 1957.

[119] M. Ojima, A. Furutani, N. Ban, and M. Kai. Persistence of DNA double-strand breaks in normal human cells induced by radiation-induced bystander effect. *Radiation Research*, 175(1):90–96, 2011.

[120] S.M. Oliveira, N.J. Teixeira, and L Fernandes. What do we know about the α/β? for prostate cancer? *Med. Phys.*, 39(6):3189–3201, 2012.

[121] S. F. C. O'Rourke, H. McAneney, and T. Hillen. Linear quadratic and tumor control probability modelling in external beam radiotherapy. *J. Math. Biol.*, 58:799–817, 2009.

[122] A. Oshima, K. Tani, Y. Hiroaki, Y. Fujiyoshi, and G. E. Sosinsky. Three-dimensional structure of a human connexin26 gap junction channel reveals a plug in the vestibule. *Proc. Natl. Acad. Sci. USA*, 104(24):10034–10039, 2007.

[123] M.P. Pall. *Explaining 'Unexplained Illnesses': Disease Paradigm for Chronic Fatigue Syndrome, Multiple Chemical Sensitivity, Fibromyalgia, Post-Traumatic Stress Disorder, and Gulf War Syndrome.* Informa Healthcare New York, 2007.

[124] J. Partouche. Stochastic modelling of the cell killing effects of low and high radiation. Master's thesis, Health Physics, Texas A and M University, December 2004.

[125] G.A. Petsco and D. Ringe. *Protein Structure and Function.* New Science Press, 2004.

[126] A. N. Pisarchik, R. Jaimes-Reategui, J. R. Villalobos-Salazar, J. H. Garcia-Lopez, and S. Boccaletti. Synchronization of chaotic systems with coexisting attractors. *Physical Review Letters*, 96:244102(1)–244102(4), 2006.

[127] J. R. Pomerening, E. D. Sontag, and J. E. Ferrell. Building a cell cycle oscillator: Hysteresis and bistability in the activation of Cdc2. *Nat. Cell. Biol.*, 5:346–351, 2003.

[128] J. Portugal, M. Bataller, and S. Mansilla. Cell death pathways in response to antitumor therapy. *Tumori*, 95:409–421, 2009.

[129] K. M. Prise and J. M. O'Sullivan. Radiation-induced bystander signalling in cancer therapy. *Nat. Rev. Cancer*, 9(5):351–360, 2009.

[130] L. Qiao, R. B. Nachbar, I. G. Kevrekidis, and S. Y. Shvartsman. Bistability and oscillations in the Huang-Ferrell model of MAPK signaling. *PLoS Computational Biology*, 3:353–359, 2007.

[131] C.R. Reeves. *Modern heuristic techniques for combinatorial problems.* Halsted Press, 1993.

[132] K. Rothkamm and S. Horn. γ-H2AX as protein biomarker for radiation exposure. *Ann. Ist. Super. Sanita*, 45(3):265–271, 2009.

[133] K. Rothkamm, I. Kruger, L. H. Thompson, and M. Lobrich. Pathways of DNA double strand break repair during the mammalian cell cycle. *Moleculer And Cellular Biology*, 23:5706–5715, 2003.

[134] K. Rothkamm and M. Lobrich. Evidence for a lack of DNA double-strand break repair in human cells exposed to very low x-ray doses. *Proc. Natl. Acad. Sci. USA*, 100:50575062, 2003.

[135] C. E. Rube, S. Grudzenski, M. Kuhne, X. Dong, N. Rief, M. Lobrich, and C. Rube. DNA double-strand break repair of blood lymphocytes and normal tissues analysed in a preclinical mouse model: Implications for radiosensitivity testing. *Clin. Cancer Res.*, 14(20):6546–6555, 2008.

[136] R. K. Sachs, P. Chen, P. Hahnfeldt, D. Lai, and L. R. Hlatky. DNA damage in non-proliferating cells subjected to ionizing radiation at high or low dose rates. *J. Math. Biol.*, 31:291–315, 1993.

[137] R. K. Sachs, P. Hahnfeldt, and D. J. Brenner. The link between low-LET dose-response relations and the underlying kinetics of damage production/repair/misrepair. *Int. J. Radiat. Biol.*, 72:351–374, 1997.

[138] R. K. Sachs, L. Hlatky, P. Hahnfeldt, and P. L. Chen. Incorporating dose-rate effects in Markov radiation cell survival models. *Radiation Research*, 124:216–226, 1990.

[139] R. K. Sachs, L. R. Hlatky, and P. Hahnfeldt. Simple ODE models of tumor growth and anti-angiogenic or radiation treatment. *Math. Comp. Model.*, 33:1297–1305, 2001.

[140] D. Schulte-Frohlinde, F. Mark, and Y. Ventur. Transformation frequency of gamma-irradiated plasmid DNA and the enzymatic double strand break formation by incubation in a protein extract of Escherichia Coli. *Radiat Prot Dosimetry*, 52(1-4):283–289, 1994.

[141] M.K. Sen and P.L. Stoffa. *Global optimization methods in geophysical inversion*. Cambridge University Press, 2012.

[142] A. Shibata, S. Conrad, J. Birraux, V. Geuting, O. Barton, A. Ismail, A. Kakarougkas, K. Meek, G. Taucher-Scholz, M. Lobrich, and P. A. Jeggo. Factors determining DNA double-strand break repair pathway choice in G2 phase. *The EMBO Journal*, 30:1079–1092, 2011.

[143] S. N. Sivanandam and S. N. Deepa. *Introduction to genetic algorithms.* Berlin; New York:Springer, 2007.

[144] S. So, A. J. Davis, and D. J. Chen. Autophosphorylation at Serine 1981 stabilizes ATM at DNA damage sites. *The Journal of Cell Biology*, 187(7):977–990, 2009.

[145] S. T. Sonis. The biologic role for NF-κB in disease and its potential involvement in mucosal injury associated with anti-neoplastic therapy. *Critical Reviews in Oral Biology and Medicine*, 13(5):380–389, 2002.

[146] W. Sontag. A cell survival model with saturable repair after irradiation. *Radiat. Environ. Biophys.*, 26:63–79, 1987.

[147] W. Sontag. Comparison of six different models describing survival of mammalian cells after irradiation. *Radiation and Environmental Biophysics*, 29:185–201, 1990.

[148] R. D. Stewart. Two-lesion kinetic model of double-strand break rejoining and cell killing. *Radiation Research*, 156:365–378, 2001.

[149] K. Takahashi, S. Tanase-Nicola, and P. R. ten Wolde. Spatio-temporal correlations can drastically change the response of a MAPK pathway. *Proc. Natl. Acad. Sci. USA*, 107(6):2473–2478, 2010.

[150] P. Thorne. Year of radiotherapy: A lot can change in 100 years. Website, July 2011. `http://scienceblog.cancerresearchuk.org/2011/07/29/100-years-radiotherapy/`.

[151] C. A. Tobias. The repair-misrepair model in radiobiology: Comparison to other models. *Radiation Research*, 104:S77–S95, 1985.

[152] M. Tubiana, J. Dutreix, and A. Wambersie. *Introduction to Radiobiology.* Taylor and Francis, 1990.

[153] S. Tuljapurkar and H. Calwell. *Structured-population models in marine, terrestrial, and freshwater systems.* International Thomson Publishing, 1997.

[154] J. J Tyson, B. Novak, G. M. Odell, K. Chen, and C. D. Thron. Chemical kinetic theory: Understanding the cell-cycle regulation. *Trends Biochem. Sci.*, 21:89–96, 1996.

[155] J.J. Tyson, K.C. Chen, and B. Novak. Sniffers, buzzers, toggles and blinkers: dynamics of regulatory and signaling pathways in the cell. *Current Opinion in Cell Biology*, 15:221231, 2003.

[156] G. J. M. J. Van Den Aardweg, E. Kilic, A. De Klein, and G. P. M. Luyten. Dose fractionation effects in primary and metastatic human uveal melanoma cell lines. *Investigative Ophthalmology and Visual Science*, 44:4660–4664, 2003.

[157] J. Wang, R. Li, C. Guo, C. Fournier, and W. K-Weyrather. The influence of fractionation on cell survival and premature differentiation after carbon ion irradiation. *L. Radiat. Res.*, 49:391–398, 2008.

[158] J. Wang, N. Pabla, C. Y. Wang, W. Wang, P. V. Schoenlein, and Z. Dong. Caspase-mediated cleavage of ATM during cisplatin-induced tubular cell apoptosis: Inactivation of its kinase activity toward p53. *AJP - Renal Physiol*, 291(6):F1300–F1307, 2006.

[159] L. Wang, B. L. Walker, S. Iannaccone, D. Bhatt, P. J. Kennedy, and W. T. Tse. Bistable switches control memory and plasticity in cellular differentiation. *Proc. Natl. Acad. Sci. USA*, 106(16):6638–6643, 2009.

[160] X. Wang, N. Hao, H. G. Dohlman, and T. C. Elstonz. Bistability, stochasticity, and oscillations in the mitogen-activated protein kinase cascade. *Biophysical Journal*, 90:19611978, 2006.

[161] P. J. Welch and J. Y. Wang. Coordinated synthesis and degradation of cdc2 in the mammalian cell cycle. *Proc. Natl. Acad. Sci. USA*, 89(7):3093 – 3097, 1992.

[162] Y. Xu, F. Fang, D. K. St Clair, S. Josson, P. Sompol, I. Spasojevic, and W. H. St Clair. Suppression of RelB-mediated manganese superoxide dismutase expression reveals a primary mechanism for radiosensitization effect of 1α,25-dihydroxyvitamin D3 in prostate cancer cells. *Molecular Cancer Therapeutics*, 6(7):2048–2056, 2007.

[163] H. Yang, N. Asaad, and K. D. Held. Medium-mediated intercellular communication is involved in bystander responses of x-ray-irradiated normal human fibroblasts. *Oncogene*, 24:2096–2103, 2005.

[164] T. C. Yang, L.M. Craise, M.T. Mei, and C.A. Tobias. Neoplastic cell transformation by heavy charged particles in research and medicine. *Radiation Research*, 8:S177–S187, 1985.

[165] G. G. Yao, C. Tan, M. West, J. R. Nevins, and L. You. Origin of bistability underlying mammalian cell cycle entry. *Molecular Systems Biology*, 7(485):1–10, 2011.

[166] M. Zaider and G. N. Menarbo. Tumor control probability: A formulation applicable to any temporal protocol of dose delivery. *Phys. Med. Biol.*, 45:279–293, 2000.

[167] X. Zhang. *Development and validation of a nanodosimetry-based cell survival model for mixed high- and low-LET radiations*. PhD thesis, Woodruff School of Mechanical Engineering, Georgia Institute of Technology, June 2006.

[168] X. P. Zhang, F. Liu, and W. Wang. Coordination between cell cycle progression and cell fate decision by the p53 and E2F1 pathways in response to DNA damage. *The Journal of Biological Chemistry*, 285:31571–31580, 2010.

[169] X. P. Zhang, F. Liu, and W. Wang. Two-phase dynamics of p53 in the DNA damage response. *Proc. Natl. Acad. Sci. USA*, 108(22):8990–8995, 2011.

[170] Z. Zhi Guo, S. Kozlov, M. F. Lavin, M. D. Person, and T. T. Paull. ATM activation by oxidative stress. *Science*, 330(6003):517–521, 2010.

[171] H. Zhou, M. Hong, Y. Chai, and T. K. Hei. Consequences of cytoplasmic irradiation: Studies from microbeam. *Journal of Radiation Research*, 50:A59–A65, 2009.

[172] H. Zhou, V. N. Ivanov, J. Gillespie, C. R. Geard, S. A. Amundson, D. J. Brenner, Z. Yu, H. B. Lieberman, and T. K. Hei. Mechanism of radiation-induced bystander effect: Role of the cyclooxygenase-2 signaling pathway. *Proc. Natl. Acad. Sci. USA*, 102(41):14641–14646, 2005.

[173] H. Zhou, V. N. Ivanov, Y. C. Lien, M. Davidson, and T. K. Hei. Mitochondrial function and NF-κB-mediated signaling in radiation-induced bystander effects. *Cancer Research*, 68(7):2233–2240, 2008.